

FREQUENCY HOPPING WAVEFORM SYNTHESIS  
BASED ON CHIRP MIXING  
USING SURFACE ACOUSTIC WAVE DEVICES

A THESIS SUBMITTED TO THE FACULTY OF SCIENCE OF  
THE UNIVERSITY OF EDINBURGH, FOR THE DEGREE  
OF DOCTOR OF PHILOSOPHY

BY

E W PATTERSON, BSc

UNIVERSITY OF EDINBURGH

1982



## ABSTRACT

Frequency hopping (FH) waveform synthesis provides a useful method for generating spread spectrum (SS) signals. A summary of SS techniques and applications is presented.

Techniques for frequency synthesis based on direct, indirect and digital "look-up" methods are described and their limitations for fast FH applications discussed. Surface acoustic wave (SAW) technology and applications are introduced and a comparison of synthesis techniques using SAW oscillators, filter banks and mixing linear frequency modulated (FM) (chirp) waveforms is presented. In particular, SAW chirp mixing is shown to be attractive for coherent, wideband, multi-frequency fast FH.

A theoretical analysis of the chirp mixing process defines the synthesiser performance in terms of the chirp parameters. The design and construction of a prototype sum frequency equipment is described and performance is reported for continuously generated FH and CW signals.

Error mechanisms arising from the chirp mixing process and component tolerances are identified. An analysis of ideal CW operation provides a method for quantifying the effects of individual errors. Computer simulation of typical errors using Fourier series and fast Fourier transform (FFT) techniques demonstrate the performance limitations. The degradation of synthesiser performance due to temperature variation is also reported.

The synthesiser performance is discussed in relation to similar equipment used in FH mode and topics for further study are suggested.

## DECLARATION

I hereby declare that this thesis has been composed entirely by myself and that the work described herein is my own.

## ACKNOWLEDGEMENTS

The financial support of the Procurement Executive of the UK Ministry of Defence (DCVD Contract RU5-7) and the UK Science Research Council during the period of this study is gratefully acknowledged.

I wish to thank Dr J M Hannah for his continued guidance, encouragement and supervision throughout the period of study. Thanks are also due to Dr P M Grant for helpful discussions and provision of background information. I am indebted to Professor J H Collins for supplying the research facilities, and to R C Corner and A S M Dods for technical assistance.

Thanks are due to Dr B J Darby and Dr M B N Butler for providing useful background information. Thanks are also due to Linda Halstead for her care and efficiency in typing the manuscript.

Finally, I would like to thank my parents for their unfailing support, and my fiancée, Doreen, for her patience, help and encouragement during the preparation of this thesis.



## CONTENTS

Title Page	(i)
Abstract	(ii)
Declaration	(iii)
Acknowledgements	(iv)
Contents	(v)
List of Symbols and Abbreviations	(viii)
 CHAPTER 1 : INTRODUCTION	 1
 CHAPTER 2 : SPREAD SPECTRUM COMMUNICATIONS	 5
2.1 Introduction	5
2.2 Code Generation and Selection	8
2.3 Spectral Spreading Techniques	10
2.3.1 Direct Sequence	10
2.3.2 Frequency Hopping	14
2.3.3 Chirp Modulation	16
2.3.4 Time Hopping	17
2.3.5 Hybrid Techniques	18
2.4 Information Transmission and Retrieval	19
2.4.1 DS Data Modulation	20
2.4.2 FH Data Modulation	21
2.4.3 Chirp Data Modulation	22
2.5 Synchronisation and Tracking	22
2.5.1 Synchronisation Acquisition	23
2.5.2 Tracking	26
2.6 Summary and Applications	27
 CHAPTER 3 : FREQUENCY SYNTHESIS	 42
3.1 Introduction	42
3.2 Traditional Frequency Synthesis	43
3.2.1 Direct Synthesis	43
3.2.2 Indirect Synthesis	47
3.2.3 Digital "Look-up" Synthesis	51

3.3	SAW Technology and Applications	53
3.3.1	Introduction to SAW Technology	53
3.3.2	The SAW Chirp Filter	57
3.3.3	SAW Device Applications	60
3.4	SAW Techniques for Frequency Synthesis	65
3.4.1	SAW Filter Banks	65
3.4.2	SAW Oscillators	67
3.4.2.1	Single Mode Oscillators	67
3.4.2.2	Multimode Oscillators	68
3.4.2.3	Discriminator Oscillator	69
3.4.2.4	Mode Locked Oscillator	70
3.4.2.5	Multimode Oscillator and Filter Bank	71
3.4.3	Chirp Synthesis Technique	72
3.4.3.1	Introduction	72
3.4.3.2	SAW Chirp Mixing	73
3.4.3.3	Discrete Chirp ROM	76
3.4.3.4	Tapped Delay Line	76
3.4.4	Comparison of SAW Synthesis Techniques	77

#### CHAPTER 4 : THE DESIGN, CONSTRUCTION AND PERFORMANCE OF A SAW CHIRP MIXING SYNTHESISER

4.1	Frequency Synthesis Based on Chirp Mixing	91
4.2	Design Aspects	96
4.2.1	SAW Devices for Chirp Mixing	96
4.2.2	System Configuration	98
4.3	Constructional Aspects	99
4.3.1	Digital Section	99
4.3.1.1	Master Control Board	100
4.3.1.2	Programmable Pulse Generator Boards	100
4.3.1.3	PN Code Generator	101
4.3.1.4	Manual Switch Network	101
4.3.2	RF Section	102
4.3.2.1	Impulser Circuit	102
4.3.2.2	Chirp Filters	103
4.3.2.3	Amplifier/Mixer Circuits	103
4.3.2.4	Summing, Limiting and Filtering Components	104

4.4	Performance of a Prototype SAW Chirp Mixing Synthesiser	104
4.4.1	Experimental Results	104
4.4.2	Discussion of Results	106
CHAPTER 5 :	EVALUATION OF SYNTHESISER DESIGN AND PERFORMANCE	119
5.1	Waveform Analysis and Error Sources	119
5.1.1	Error Sources	121
5.1.2	Analysis Technique	124
5.2	Fourier Series Analysis	128
5.2.1	Mathematical Derivation	128
5.2.2	Graphical Interpretation	133
5.2.3	Discussion of the Synthesised Waveform	135
5.2.4	Calculated Error Levels	137
5.3	Computer Simulation	140
5.3.1	Difference Frequency Simulation	140
5.3.2	Sum Frequency Simulation	143
5.4	Temperature Dependence of Synthesiser Operation	145
5.5	Discussion of Results	149
CHAPTER 6 :	SUMMARY AND CONCLUDING REMARKS	177
	References	184
	Appendices	

LIST OF SYMBOLS AND ABBREVIATIONS

AMF	Analog Matched Filter
B	Chirp Bandwidth
$\text{Bi}_{12}\text{GeO}_{20}$	Bismuth Germanium Oxide
CCD	Charge Coupled Device
CDMA	Code Division Multiple Access
CPSM	Continuous Phase Shift Modulation
CW	Continuous Wave
DAC	Digital to Analog Conversion (/Convertor)
DC	Direct Current
DDL	Dispersive Delay Line
DFT	Discrete Fourier Transform
DLL	Delay Locked Loop
DS	Direct Sequence
DSSS	Direct Sequence Spread Spectrum
EM	Electro-Magnetic
EMAS	Edinburgh Multi-Access System
$\mathcal{F}$	Forward Fourier Transformation symbol
FDM	Frequency Division Multiplex
FDMA	Frequency Division Multiple Access
FFH	Fast Frequency Hopping
FFT	Fast Fourier Transform
FH	Frequency Hopping
FHSS	Frequency Hopping Spread Spectrum
FM	Frequency Modulation
FSK	Frequency Shift Keying
FT	Fourier Transform
HF	High Frequency

IDT	Interdigital Transducer
IF	Intermediate Frequency
LC	L-Inductance, C-Capacitance
LED	Light Emitting Diode
$\text{LiNbO}_3$	Lithium Niobate
$\text{LiTaO}_3$	Lithium Tantalate
LO	Local Oscillator
LSI	Large Scale Integration
MFSK	Multiple Frequency Shift Keying
MOSFET	Metal-on-Silicon Field Effect Transistor
MSK	Minimum Shift Keying
PD	Phase Detector
PG	Processing Gain
PIN	P-Type, Intrinsic, N-Type (semiconductor device)
PLL	Phase Locked Loop
PN	Pseudo Noise
PPG	Programmable Pulse Generator
PSK	Phase Shift Keying
RAC	Reflective Array Compressor
RF	Radio Frequency
ROM	Read Only Memory
SAW	Surface Acoustic Wave
$\text{Sa}(x)$	Sampling Waveform $\equiv \sin x/x$
SHF	Super High Frequency
Si	Silicon
SNR	Signal to Noise Ratio
SOS	Silicon-on-Sapphire
SS	Spread Spectrum

SSB	Single Side Band
SSMA	Spread Spectrum Multiple Access
$T_o$	Chirp Duration
TB(P)	Time Bandwidth (Product)
TDMA	Time Division Multiple Access
TH	Time Hopping
TTL	Transistor-Transistor-Logic
$\mu$	Chirp Dispersive Slope
UHF	Ultra High Frequency
VCO	Voltage Controlled Oscillator
VDL	Variable Delay Line
VHF	Very High Frequency
ZnO	Zinc Oxide

## CHAPTER 1 : INTRODUCTION

Spread spectrum (SS) communications systems<sup>1,2</sup> employ a wideband (10 to 500 MHz) synthesiser in each transmitter which spreads narrow-band information from the subscriber into a common wideband channel. The remote receiver employs an identical synthesiser, synchronised to the incoming signal, with integration over the data bit interval to demodulate the wideband transmission for information recovery. Interference protection is provided by the use of characteristic pseudo noise (PN) coded signals with low cross correlation properties which result in enhanced signal to noise ratio (SNR), or processing gain at the receiver, determined to first order by the ratio of transmitted-to-information bandwidth. The two favoured spreading techniques are frequency hopping (FH) and phase shift keying (PSK).<sup>1,2</sup>

PN-PSK, commonly known as direct sequence spread spectrum (DSSS), equipments achieve spectral spreading through direct modulation of the carrier by a fast bit rate PN code. The simplicity of PN code generation through digital shift register techniques combined with the availability of wideband phase modulators makes this an attractive system, but wideband performance is currently limited to <100 MHz by the capabilities of high speed digital circuits. The major restriction on the use of this technique is the delay time required to achieve synchronisation between received and local codes when long duration code sequences are required.

FH modulation is achieved by multiple frequency shift keying (MFSK) where the required SS bandwidth is divided into a large number of contiguous subchannels (or slots). Individual frequencies are

selected under PN code control, and orthogonality between adjacent slots is ensured if the dwell time on each frequency equals the reciprocal of the slot separation. Thus for a given RF bandwidth (ie, a defined processing gain) the PN code rate for an FH system can be very much slower than for its DS equivalent. This has significant advantage in reducing synchronisation delay, but is achieved at the expense of additional complexity in the form of a wideband, fast switching frequency synthesiser.

Conventional techniques for frequency synthesis are based on direct or indirect methods.<sup>3</sup> Direct iterative synthesisers combine a number of coherent reference sources through a process of repetitive mix-filter-divide operations. This provides a fast switching, high resolution output, but at the expense of size, weight and power consumption when wideband operation is required. Indirect synthesis, based on phase locked loop techniques, potentially offers an excellent low power, compact solution but the associated switching speed is generally too slow for fast FH applications. For this reason, DSSS systems have predominated in recent years, but advances in technology and future systems requirements continue to stimulate interest in FH techniques.

Of particular importance in this respect has been the emergence of a number of novel techniques for direct synthesis based on surface acoustic wave (SAW) components.<sup>4</sup> The three principal approaches which have been proposed are : (1) substitution of SAW bandpass filters into conventional direct synthesisers;<sup>5</sup> (2) use of SAW delay lines in programmable oscillators;<sup>6</sup> and (3) mixing linear frequency modulated (FM) (chirp) waveforms generated by timed impulsing of SAW chirp filters.<sup>7</sup> This thesis is primarily concerned



with the SAW chirp mixing approach which has the capability of providing a large number of hops ( $<4000$ ) over a wide bandwidth ( $<500$  MHz) with minimal size, weight and power requirement. Operating under direct digital control, this synthesiser can be configured to produce a continuous output of either continuous-wave (CW) or FH form.

The main purpose of the thesis has been to report the design and construction of a prototype SAW chirp mixing synthesiser and to present a detailed theoretical analysis of the synthesised waveform. The information thus obtained permits a fuller understanding of the fundamental limitations associated with this technique and provides a basis for quantitative assessment of performance degradation due to practical design and manufacturing tolerances.

An introduction to Spread Spectrum communications is presented in Chapter 2, including a review of the common techniques used for coding, modulation, information transmission, synchronisation and tracking. Chapter 3 covers traditional techniques for frequency synthesis, an introduction to SAW devices and applications, and a review of recent SAW techniques for frequency synthesis. SAW chirp filter design and performance characteristics in particular are discussed in this Chapter and the review of SAW based synthesisers illustrates the relative merits of the chirp mixing technique.

The design theory of chirp mixing is described in Chapter 4 and expressions are derived for hop duration, bandwidth and number of hops in terms of the chirp parameters. A detailed description of the design and construction of a prototype sum frequency synthesiser with 63 hops over a 25 MHz bandwidth at 120 MHz centre frequency is presented,

and performance of this unit is reported operating in both CW and FH modes. Comparison of performance with published results for similar equipments providing 127 hops over a 50 MHz bandwidth centred on 360 MHz concludes this Chapter.

A more detailed analysis of the synthesised waveform in Chapter 5 describes analytic and computer aided techniques for quantifying the degradation attributable to practical limitations in the synthesiser hardware. Computer simulations are reported which define the CW performance under predicted operational conditions. CW operation in particular was chosen for this analysis as the spectral distortion attributable to individual error mechanisms is most clearly illustrated.

Finally, Chapter 6 contains a summary of the work described in this thesis and discusses the implications of these results on the potential performance of SAW chirp mixing synthesisers operating in both CW and FH modes. A report of experimental work carried out in this area subsequent to completion of the work reported here is included in this Chapter, along with suggestions for further study.

## CHAPTER 2 : SPREAD SPECTRUM COMMUNICATIONS

### 2.1 INTRODUCTION

The historic development of radio communication is based on frequency division multiplexing (FDM) where individual subscribers are allocated specific channels within a given operating band.<sup>8,9</sup> To handle the increasing volume of communications traffic, systems design effort has concentrated on improving the spectral efficiency of existing bands and expanding the useful radio frequency (RF) spectrum. This optimisation process is fundamentally limited by :

- (1) the minimum bandwidth required for acceptable communication;
- (2) the maximum useful RF spectrum.

The former is dependent upon the type of communication (eg, voice, TV, data), the modulation technique and the fidelity of the link. The latter is primarily related to atmospheric effects, equipment size, complexity and cost for a particular application. To minimise the disruption caused in congested sections of the spectrum (ie, HF, VHF, UHF) international cooperation via regulatory bodies is required to plan and allocate band usage.<sup>8</sup>

This approach to spectral occupancy can be attributed to the technology available during early developments in radio communication, rather than to fundamental principles of physics, and in some situations does not present the optimum solution. In 1949, Shannon's publication<sup>10</sup> "Communications in the Presence of Noise" proposed wideband coded signals as an effective method for

communication in a high noise (or low signal) environment. He described the process mathematically in a channel capacity theorem, (Equation (2.1)) which states that the channel capacity (C) can be maintained under low signal (S) to noise (N) conditions by increasing the channel bandwidth (W).

$$C = W \log_2(1 + \frac{S}{N}) \quad \dots (2.1)$$

In essence, this equation contradicts the objectives of FDM systems design and lays the foundation for spread spectrum (SS) communications, the techniques for which are described in the remainder of this chapter.

Spread spectrum communications systems<sup>1, 2</sup> employ a common wideband channel to accommodate a large number of subscribers through the use of selective addressing techniques. A typical SS link, Figure 2.1, employs a transmitted signal bandwidth many times larger than the information bandwidth to achieve some or all of multipath/interference rejection, low density signal transmission, message privacy, high resolution ranging, multiple and selective accessing capabilities.

The favoured signal waveforms for spread spectrum applications are phase shift keying (PSK)<sup>1, 11</sup> and frequency hopping (FH)<sup>1, 12</sup>, although time hopping (TH)<sup>11, 12</sup> and linear frequency modulation (FM or chirp)<sup>13</sup> are alternatives often combined with PSK and FH to form hybrid solutions.<sup>1, 12</sup> Irrespective of the waveform, spectral spreading is normally achieved under the control of a pseudo noise (PN)<sup>11, 14</sup> code. These codes are conveniently generated by digital shift register techniques and are particularly suited to SS

techniques due to their ease of implementation, abundance of combinations, and attractive auto- and cross-correlation properties (see Section 2.2). In the case of PSK-SS, the wideband signal is generated by direct modulation of the carrier by the PN code, resulting in the nomenclature Direct Sequence Spread Spectrum (DSSS) for this configuration. The FH waveform alternatively is achieved indirectly by multiple Frequency Shift Keying (FSK) under the control of a PN code, and is known simply as PN-FHSS.

In the SS receiver<sup>12</sup>, a replica of the spreading code and waveform is available along with synchronisation, tracking and demodulation circuitry. Following initial synchronisation of the received and local codes, the narrowband data is retrieved from the wideband noise signal by active or passive correlation, integration over the data bit period and subsequent detection. Discrimination<sup>11,33</sup> against multipath reflections and other cochannel signals is achieved in the correlation process. The resultant processing gain (PG) or signal to noise ratio (SNR) improvement, is an important figure of merit for an SS link, and can be expressed as

$$PG = \frac{B_s}{R} \quad \dots (2.2)$$

where  $B_s$  is the spreading bandwidth and  $R$  the information bandwidth or data rate. Careful selection of PN codes with optimal<sup>16</sup> auto- and cross-correlation properties is necessary in a multi-access net to ensure a high level of receiver discrimination.

The remainder of the chapter reviews the major functions within a SS system. Codes and code generation are discussed in Section 2.2,

leading into a more detailed description of the common spectral spreading techniques in Section 2.3. Information transmission and retrieval are discussed in Section 2.4 and synchronisation and tracking in Section 2.5. Finally, the chapter is summarised in Section 2.6 with a discussion of SS techniques and applications.

## 2.2 CODE GENERATION AND SELECTION

Independent of the SS modulation format, the wideband signal is predominantly generated or controlled by a pseudo noise (PN) code, which can be attributed to a number of unique properties:

- (1) ease of implementation;
- (2) abundance of variable length code combinations;
- (3) low auto- and cross-correlation properties.

The PN codes normally employed are linear maximal length sequences (m-sequences).<sup>14,15</sup> These are conveniently produced by digital shift register techniques<sup>14,15</sup> which implement a feedback function comprising modulo-2 addition of specified register states as illustrated in Figure 2.2. In this form, the sequence generated has the maximal length ( $L = 2^{n-1}$ ) possible from the available number ( $n$ ) of shift register bits. Tabular data<sup>15</sup> is available for the feedback functions required to generate m-sequences with values of  $n \leq 34$ .

In an operating system, codes may be selected as disjoint subsequences from a very long m-sequence or by modulo-2 addition of two separate m-sequences.<sup>16</sup> In the latter case individual subscribers

can be allocated a discrete address according to the relative delay between two common m-sequences.

In direct sequence systems, spectral spreading and subsequent correlation is achieved with PN-PSK waveforms. The main attraction of PN coding for this application relates to its two state auto-correlation function<sup>14</sup> (Figure 2.3) which exhibits a sharp peak when the received and local codes are accurately aligned. Outside  $\pm 1$  bit of synchronism the response is minimal, and a set of time sidelobes can be observed<sup>14</sup> with peak amplitude  $\frac{1}{N}$  relative to the correlation peak, where  $N$  is the number of chips in the correlator (ie, its time-bandwidth (TB) product). In situations where a short burst of code is transmitted a similar correlation response is obtained but the peak time sidelobe level in this case is approximately  $2/\sqrt{N}$ .<sup>17</sup>

In addition to the autocorrelation performance of a PN code, consideration must be given in an uncoordinated code division multiple access (CDMA) system<sup>18</sup> to the ratio of cross- to auto-correlation products<sup>20</sup> of the codes selected. In general, the cross-correlation function between different m-sequences may be relatively large.<sup>16</sup> This can result in false synchronisation acquisition when a receiver attempts to lock onto a peak due to cross-correlation between the reference code and that of an unintended cochannel user. Gold<sup>16</sup> has reported the existence of non-maximal length sequences which exhibit bounded cross-correlation properties at the expense of minor degradation of the auto-correlation performance.

Other sequences of significance in SS systems are the Barker<sup>21</sup> and Reed-Solomon<sup>22</sup> codes. The Barker codes are used as short

(< 13 bit) synchronisation codes whilst the Reed-Solomon codes provide error detection and correction capability.

## 2.3 SPECTRAL SPREADING TECHNIQUES

### 2.3.1 Direct Sequence

Systems which employ direct modulation of the RF carrier by a PN code sequence are known as direct sequence spread spectrum (DSSS). Currently this is the most common SS technique and can be found in systems such as SKYNET<sup>23</sup> and NAVSTAR<sup>24</sup>, the satellite based Global Positioning System (GPS).

The format of a DS communication link is shown in Figure 2.4, along with the constituent time and frequency domain waveforms. The transmitter comprises a data source, encoder, PN code generator, RF source and wideband modulator. Although any one of the amplitude or angle modulation techniques applicable to digital signalling<sup>8</sup> can be used, biphasic or quadriphase PSK<sup>1</sup> is favoured due to the availability of wideband phase modulators. The resultant PN-PSK waveform has an amplitude spectrum<sup>11</sup> bounded by a  $\sin x/x$  function, where  $x = \omega\tau/2$  and  $\tau$  is the duration of a code chip (or bit). The nominal bandwidth ( $B_s = \frac{2}{\tau}$ ) of this signal is defined to the first nulls of the  $\sin x/x$  function and hence the processing gain of a DS signal is defined as

$$PG_{DS} = \frac{2}{\tau R} = T_r B_s \quad \dots (2.3)$$

where  $R$  is the information rate and  $T_r$  the duration of a data bit.



In practice the  $\sin x/x$  envelope exists outside the first nulls with a first sidelobe pair at a level of -13 dB with respect to the main lobe. Subsequent sidelobe levels decrease in amplitude at a rate of 6 dB per octave.<sup>25</sup> This results in undesirable energy spillage causing interference to adjacent channel users. It has recently been shown<sup>25</sup> that continuous phase shift modulation (CPSM), or minimum shift keying (MSK) can be employed to reduce this effect. The MSK spectrum has a first sidelobe level of -23 dB with respect to the main lobe and subsequent sidelobes decreasing in amplitude at the rate of 12 dB per octave. Surface acoustic wave (SAW) bandpass filters<sup>26</sup> can be used to generate the MSK waveform<sup>25</sup> from a standard PSK signal, and to provide matched filtering in the receiver.<sup>25</sup>

The DS receiver contains a replica of the transmitted PN coded signal, a correlator, synchroniser, tracking circuit and data demodulator. Following initial synchronisation the incoming signal is correlated with a stored replica and integrated over the data bit period to remove the wideband modulation for data recovery. This process is the key feature of a DS system and provides the signal enhancement, interference rejection and selective addressing capabilities of the link. Correlation can be achieved actively in a sliding correlator<sup>1,2</sup>, or passively in a matched filter.<sup>27</sup> The choice of method is determined by the application<sup>32</sup> and is related to the processing gain (ie, time bandwidth product), required in the receiver. The constraints associated with the physical or economic implementation of the equipment may also be considered.

DS transmission can take place in either continuous or burst modes. Continuous signalling is achieved by the repetitive transmission of short codes (typical periodicity of milliseconds or seconds) or by the use of code lengths in excess of the link duration. In a multi access environment, this leads to simultaneous cochannel transmissions where discrimination between signals is provided by the correlation properties (see Section 2.2) of the unique subscriber codes. Communication in this form is known as code division multiple accessing<sup>18</sup> and is attractive for large geographic coverage systems such as those employed in a satellite repeater.<sup>23</sup> As an alternative, subscribers can transmit information in short PN coded bursts, which permits the use of uncoordinated or conventional time domain multiple accessing according to operational requirements.<sup>28</sup>

Continuous transmission DS systems predominantly use active correlation to demodulate the wideband PN waveform as this provides maximum flexibility and processing gain (ie, TB's in excess of  $10^4$ ) in the receiver. Due to the long code lengths and continuous transmission employed in this configuration, slow synchronisation, data preambles and repetition can be used to ensure acceptable communication. In comparison burst systems require the use of matched filters as these synchronise immediately to the short bursts of received signal to decode the transmitted data. SAW<sup>29</sup> and charge coupled device (CCD)<sup>30</sup> technology provide suitable time bandwidth products<sup>31</sup> (up to 1000) over a convenient frequency range<sup>31</sup> (1 MHz - 1 GHz) for this application (see Section 2.5).<sup>29</sup>

DS receivers reject interference as illustrated in Figure 2.5.

The incoming signal is compressed to a narrow bandwidth by the correlation process, whilst the interference signal is in effect spread spectrum modulated by the receiver code. A narrowband post correlation filter can then extract the narrowband information and limit the system noise bandwidth.<sup>11</sup> However, a strong colocated transmitter may overcome the processing gain of a receiver which is decoding a weak or distant transmission<sup>11</sup> irrespective of the CDMA properties. This effect is known as the near-far problem<sup>11</sup> and limits the application of DSSS techniques in dense communications systems such as mobile radio networks.

The main constraints on the maximum available PG are :

- (1) the maximum available code rate ( $1/\tau$ );
- (2) the minimum information rate.

The former is limited by high speed digital circuit capabilities (typically 100 M bps), and the latter by clock instabilities between transmit and receive clocks (typically 10 baud). Although this implies a PG of 70 dB, 30 dB to 40 dB is more typical for an active correlator and 20 dB to 30 dB for a fixed coded AMF.<sup>32</sup> One major advantage of high code rate transmission other than for increased PG, is the improved range resolution available.<sup>34</sup> However, the associated penalties are increased size, weight and power consumption. In addition, the long codes required to avoid range ambiguity, increase the time uncertainty between received and local codes, leading to long synchronisation acquisition delays.

The problem of synchronisation is one of the major drawbacks in a DSSS system. Techniques for reducing acquisition time in DS

systems are discussed in Section 2.4, but improved performance can also be achieved by using frequency hopping techniques which achieve similar PG's with lower code rates. There is considerable advantage associated with a combination of these techniques.<sup>1,2</sup>

### 2.3.2 Frequency Hopping

A PN frequency hopped (FH) waveform consists of a train of RF pulses, where the frequency of each individual pulse is selected under PN code control.<sup>12</sup> The format of a PNFH link is illustrated in Figure 2.6 along with the constituent time and frequency domain waveforms.

In comparison with the PN-PSK system of Figure 2.4, the FH equipment differs only by the inclusion of a wideband frequency synthesiser. Encoded data is modulated by the FH waveform at an IF frequency convenient to synthesiser implementation and subsequently up converted for transmission. Conventional synthesisers<sup>3</sup> are based on direct or indirect methods, and in principle can be designed to produce a large number of output frequencies with arbitrary bandwidth and resolution.<sup>3</sup> In practice several hundred hops is typical<sup>3,64</sup> with bandwidth and resolution dependent on application.

The FH spectrum consists of a number of overlapping sin x/x responses, each at a centre frequency dictated by the individual hop, and each with a bandwidth determined by the hop period. Orthogonality between adjacent frequency slots is achieved by defining the hop period (or dwell time) to be the reciprocal of the slot separation.<sup>12</sup> The resultant RF bandwidth ( $B_s$ ) and processing gain ( $B_s/R$ ) are determined primarily by the number of available hops

and are independent of the PN code rate. Hence, for a given PG, the hop rate of an FH synthesiser can be much reduced in comparison to an equivalent DS equipment. The data rate ( $R$ ) can be greater than, equal to or less than the code rate depending on the system design and performance criteria.<sup>35,36,60</sup> Current systems have been designed with  $B_s > 100 \text{ MHz}$ <sup>41</sup> and  $R < 1 \text{ kbaud}$ <sup>35</sup> to provide a PG capability of 50 dB, but 20 dB to 30 dB is more typical.<sup>60</sup>

The FH receiver<sup>11</sup> operates in a conventional heterodyne mode where the LO is replaced by a code controlled synthesiser identical to and synchronised with the incoming signal. In this way, the wideband SS signal is demodulated to allow recovery of the baseband information. Protection from multipath reflection and other co-channel transmissions is achieved by the frequency diversity inherent in the FH waveform. However, in dense transmission environments, and situations where short delay multipath signals exist, any interference signal of identical frequency and significant power which is present at the receive antennae may result in data corruption. This possibility can be minimised by increasing the number of available frequencies (or decreasing the number of co-channel users) and reducing the hop duration. Some form of redundancy or error detection/correction coding can also be employed.<sup>1,15</sup> The penalty incurred by increasing the synthesiser bandwidth and switching speed is one of size, weight, power consumption and cost where conventional techniques are concerned.

The complexity of fast switching phase coherent, wideband frequency synthesisers as compared to the relatively simple wideband phase modulator employed in DS systems has discouraged the use of

pure FHSS in many applications. However, the reduced PN code rate required in a FH system for a given PG, provides a significant advantage over the DS equivalent in terms of the reduced delay to synchronisation and acquisition. This factor has stimulated research into novel techniques for frequency synthesis as described in Chapter 3.

### 2.3.3 Chirp Modulation

Chirp or pulsed frequency modulation (FM) is a SS technique commonly applied in modern radar systems.<sup>13,37</sup>

Spectral spreading is achieved by the generation of a swept frequency pulse of duration  $T$  and bandwidth  $B_s$  as illustrated in Figure 2.7. To maintain precise control of the sweep characteristic this is often carried out at a suitable IF prior to upconversion for transmission. In the receiver, the transmitted pulse is down converted for correlation in a matched filter having equal but opposite frequency sweep characteristic. This process is commonly known as pulse compression<sup>13</sup> and provides a processing gain expressed as

$$PG = \frac{T}{\tau} = TB_s \quad \dots (2.4)$$

where  $\tau$  is the -4 dB bandwidth of the compressed pulse.

SAW technology is particularly suited to the generation and detection of chirp signals<sup>37</sup>, due to the precise definition and repeatability of the sweep characteristic. Time bandwidth products of up to 1000<sup>95</sup> are currently available with this technique.

Although commonly used in radar systems, chirp modulation has not found such widespread application in SS communications systems. However, some applications have been proposed.<sup>39</sup> where it can provide extra processing gain when combined with other SS waveforms. It will also be shown in Chapters 3 and 4 that the SAW chirp filter has a significant application in the field of fast frequency synthesis for SS applications.<sup>7</sup>

#### 2.3.4 Time Hopping

Time hopping (TH) is seldom used as an independent SS technique<sup>12</sup> but can often be employed with other SS methods to incorporate a level of TDMA in the transmission.

The DS transmitter illustrated in Figure 2.4, can be altered to represent the TH equivalent by replacing the wideband phase modulator by a code controlled on/off switch. Data is stored for high speed transmission during the switch "on" period, which occurs at a time selected by the PN control code. A similar time synchronised facility is available in each receiver along with data storage and demultiplexing equipment.

The basic TH system operates on a single carrier frequency, and hence is susceptible to inference from high power cochannel transmissions. For this reason it is common to find TH combined with FH or DS to provide some added interference protection.<sup>40</sup> As with conventional TDMA equipment, the need for accurate time synchronisation between transmitter and receiver is essential to ensure reliable communication. The use of SAW fixed coded AMF's in the receiver circumvent this problem for DS burst transmission due to their

asynchronous operation.<sup>32</sup>

### 2.3.5 Hybrid Techniques

In most applications, a hybrid spread spectrum signal processing system would prove optimum not only in combining the attractive qualities of each technique, but also in reducing the performance required (and hence complexity) of each individual method.<sup>12,35,40</sup>

A combined PN/FH/TH configuration such as proposed for the Joint Tactical Information Distribution System (JTIDS)<sup>41</sup>, allocates a transmission time for individual users, and provides DS modulation followed by FH spreading within each time slot. In this way, full use can be made of the advantages associated with each type :

DS : High accuracy ranging.

Multipath tolerance by discrimination.

Maximum processing gain.

FH : Low speed PN code generation.

Rapid synchronisation acquisition.

Multiple access by orthogonal frequency slots.

Multipath tolerance by frequency diversity.

TH : Multiple access by non-overlapping time slots.

High bandwidth efficiency of TDMA available.

Pulsed transmitter operation.



Chirp modulation is less commonly used but would normally be combined with FH to provide a measure of frequency diversity in the link.<sup>39</sup> Its chief attraction is due to the simple, compact format of chirp generators and receivers available in SAW technology.

## 2.4 INFORMATION TRANSMISSION AND RETRIEVAL

The modulation techniques used<sup>12</sup> for transmitting information via a SS link are determined primarily by the format of the spreading waveform. Maximum flexibility is obtained where the spreading and data modulation are achieved independently, but this can lead to increased hardware requirements and reduction of the inherent message privacy associated with the wideband signal.<sup>12</sup>

Both analog and digital modulation are possible<sup>12</sup>, but digital techniques are favoured due to compatibility with the predominantly digital SS systems. Suppressed carrier modulation<sup>7</sup> is used where possible to optimise the transmitter efficiency and maintain the characteristic low power noise-like spectrum.

In the receiver data demodulation is achieved following removal of the wideband SS signal. Here it has been assumed that synchronisation between received and local codes has been acquired and an effective tracking loop is in operation.

The following subsections describe the data modulation and demodulation techniques used with the common spreading waveforms.

### 2.4.1 DS Data Modulation

Direct PN-PSK modulation of an RF carrier results in the  $\sin x/x$  spectrum illustrated in Figure 2.3. The use of analog<sup>1</sup> or non-coherent digital modulation<sup>12,42</sup> in such a system results in superposition of the modulation spectrum on that of the SS waveform, destroying the noise-like properties of the spectrum and permitting information retrieval without detailed knowledge of the spreading code.

As a result, SS code modification is the preferred method for data modulation in a DS system. Two basic techniques exist :

- (1) Code rate modulation;
- (2) Code modification.

The former is less common due to the requirement for wide deviation high stability oscillators in the transmit and receive equipments. The latter is achieved by coherent modulo-2 addition of the data and spreading codes prior to modulation of the RF carrier. This technique is suitable for both continuous and burst mode transmission and represents the most common method of DS data modulation. It incorporates the advantages of simple modulo-2 addition techniques along with a minimum component count resulting from shared use of the RF modulator by the data and SS codes.

In the receiver, demodulation of both the DS and data coding is achieved by conventional PSK double sideband suppressed carrier techniques.<sup>43</sup> In this respect DS demodulation results in the most

complex SS receiver, and a considerable amount of literature has been published on the subject.<sup>43,44</sup>

#### 2.4.2 FH Data Modulation

The FH spectrum illustrated in Figure 2.4 differs fundamentally from its DS equivalent as the associated multiple accessing, message privacy and interference protection facilities are provided by frequency diversity rather than code correlation techniques. The resultant method used for information transmission is therefore less critical than for a DS system and is normally chosen for ease of implementation.

The FH process itself can be viewed as a form of wideband multiple frequency shift keying (MFSK) so it is common to find information modulation in the form of binary or MFSK. Analog modulation can be used in slow hopping ( $f_m \tau \gg 1$ ,  $f_m$  = information bandwidth,  $\tau$  = hop period) systems, but it has been shown<sup>45</sup> that for fast hopping ( $f_m \tau \ll 1$ ) the self-noise generated by the hopping process in conjunction with analog FM is dominant.

FSK data modulation can be achieved by standard single sideband techniques<sup>8</sup>, or by code modification as in DS systems. For simple binary FSK, the latter technique assigns mark and space data to an individual code selected hop and its inverse respectively. The receiver then has prior knowledge of the two specific frequency slots which require examination for decision purposes. Where M-ary transmission is required, the number of hops and the resolution required can increase the synthesiser complexity to a stage where SSB techniques are preferable.

Demodulation in the receiver is most conveniently achieved by standard integrate and dump filters.<sup>8</sup> The receiver complexity is dictated by the number of signalling levels used and the overall performance required from the system.<sup>12,64</sup>

It should be noted that FH is used in conjunction with DS, TH and chirp modulation in many SS systems to provide additional interference protection through frequency diversity. In these situations information is normally incorporated in one of the other spreading codes prior to the hopping process.<sup>41,64</sup>

### 2.4.3 Chirp Data Modulation

Chirp techniques transmit information in binary form by the use of contradirected waveforms.<sup>39</sup> Each transmitter generates an up chirp (positive FM) to represent a binary '1' and a down chirp (negative FM) to represent a binary '0'.

In the receiver the incoming signal is split and fed into two channels containing down and up chirps respectively to decode the '1' and '0' data states. A comparison of the compression filter outputs allows a data decision to be made.

## 2.5 SYNCHRONISATION AND TRACKING

Throughout the previous sections, it was assumed that the received and local codes were in synchronism and that an effective code tracking loop was in operation. In practice, this represents one of the major problems encountered in a SS system and in terms of overall system complexity, one which is not found in

conventional communications systems.

The effect is most noticeable in DS systems where high bit rate, long duration codes are necessary to satisfy system performance requirements, such as range resolution, multipath tolerance and large PG. Alternatively, FH systems can achieve similar performance levels, in terms of processing gain, with much slower code rates at the expense of reduced multipath tolerance and range resolution. Thus a combination of these techniques leads to a desirable compromise between performance criteria and hardware complexity.

The following subsections describe common techniques for synchronisation acquisition and code tracking.

### 2.5.1 Synchronisation Acquisition

The prime uncertainties in a received SS signal are the carrier frequency and code phase. To permit demodulation of the SS waveform, the received and local codes must be aligned to within  $\frac{1}{2}$  chip length as described in Section 2.2, and the carrier frequency offset must fall within the bandwidths of the post correlation and tracking loop filters.<sup>59</sup>

The use of high stability oscillators in both transmitter and receiver can reduce the frequency offset to that of the predicted Doppler shift for any given application. The misalignment of received and local codes by more than  $\frac{1}{2}$  chip length, however, causes a much greater problem as there is no measure as to the extent of the misalignment. In the worst case this must be assumed to be the entire code length, although in cases where

transmitter and receiver codes have previously achieved synchronisation or have been initiated simultaneously, the error can be reduced to one of clock drift and range uncertainty.<sup>24</sup>

The simplest form of synchronisation acquisition is achieved by the serial search technique (sliding correlation)<sup>48</sup> where a number of trials are conducted with a  $\frac{1}{2}$  chip variation of the local code timing between trials. For long code sequences, this can be a time consuming process as integration over millisecond periods is necessary when the input signal to noise ratio is in the range -30 dB to -40 dB. In general, the acquisition time of the sliding correlator is equal to the receiver time uncertainty multiplied by its processing gain.<sup>12</sup> For moderate code lengths (<10,000 chips) the acquisition time is typically between 2 and 10 seconds for this technique.<sup>12</sup>

A number of sequential estimation techniques have been proposed<sup>49,50</sup> which provide fast synchronisation methods for relatively high input signal to noise ratios (typically >-10 dB),<sup>49</sup> and for long PN codes.

An alternative method for reducing the acquisition delay is based on the use of matched filtering techniques,<sup>27</sup> as discussed for the demodulation of burst mode DS transmissions. In particular, SAW and CCD AMF's provide suitable TB products for this application.

The AMF can be used to detect a suitably chosen subsequence of a long PN code or alternatively a preamble sequence transmitted specifically for synchronisation purposes. Either approach provides an asynchronous time reference for the receiver code generator. Where the subsequence or preamble are short (<1000 chips), the AMF

can be fixed coded.<sup>32</sup> However, when the PN code duration is necessarily long and the use of preambles excluded, a programmable AMF,<sup>51</sup> can be set to detect a subsequence in advance of the known time uncertainty.

SAW programmable AMF's incorporating diode, transistor or MOSFET integrated tap switches have been developed,<sup>52</sup> but there is a preference to using SAW convolvers for this signal processing function. Examples of SAW degenerate acoustic<sup>53</sup> and semiconductor<sup>54</sup> convolvers have been demonstrated, the latter being more efficient but also more complex to fabricate. It is worth noting that the convolver does not exhibit the same intrinsic asynchronous performance of the fixed coded devices, as convolution depends on the incoming and reference signals being present in the device at essentially coincident times.

For systems which require matched filtering of large (>1000) TB signals, a number of options are available. The simplest technique involves cascading devices by connecting several individual matched filters in series through wideband delay lines. The alternatives are based on the use of a programmable AMF or convolver combined with a recirculating delay line integrator<sup>56</sup> and more recently on SAW acousto-electric storage correlators.<sup>55</sup>

Matched filtering techniques such as described above have been shown<sup>55,56</sup> to provide an improvement in acquisition time some two orders of magnitude over current active correlators.

### 2.5.2 Tracking

Following initial synchronisation acquisition, two forms of tracking loop are required. The first prevents further code slippage due to clock instabilities or Doppler shift, and the second ensures sub-carrier tracking for coherent demodulation.

Code tracking is commonly achieved with a delay locked loop (DLL)<sup>57</sup> or a tau-dither loop.<sup>58</sup> The DLL multiplies the incoming code with two identical versions of the reference code offset in time by one chip period. The two resultant correlation peaks are separated by one chip period and can be subtracted to produce a discriminator response as illustrated in Figure 2.8. The resultant output signal is low pass filtered and used to control the VCO which provides the clock increment for the PN code reference generator. The tau-dither loop achieves the same purpose by means of a single correlator acting alternatively on delayed and undelayed signals. The advantage of this method over the DLL is the reduced hardware count, but an associated SNR loss of approximately 3 dB is incurred.<sup>58</sup>

Carrier tracking is achieved by a Costas<sup>44</sup> (Figure 2.9) or squaring loop<sup>44</sup> when coherent demodulation of biphase data is required. The relative position of the carrier and delay lock loops in a system is determined by the overall operating conditions, and both coherent and non-coherent PN coded systems have been demonstrated.<sup>59</sup>



## 2.6 SUMMARY AND APPLICATIONS

The preceding sections have described the prime functions associated with a spread spectrum communications system. Section 1 introduced the topic of spread spectrum communication in relation to conventional FDM systems. PN code generation techniques were presented in Section 2 and the common forms of spectral spreading, DS, FH, chirp and TH were described in Section 3. The methods for information transmission via an SS link were discussed in Section 4, and finally synchronisation and tracking techniques presented in Section 5.

The techniques which are encompassed by the term SS provide a unique combination of system characteristics :

- Selective addressing
- Code division multiple access
- Low density signal transmission
- Inherent message privacy/security
- High resolution ranging
- Interference rejection.

Although these are not all attributable to each individual SS technique, suitable combinations of DS, FH, TH and chirp modulation present an optimum hybrid solution for most requirements (see Section 2.3.5).

The penalties associated with an SS link are that of increased receiver complexity (as described in Sections 2.4 and 2.5) and problematic frequency allocation. Despite these problems spread

spectrum techniques have found application in ground-to-ground,<sup>60</sup> ground-air-ground,<sup>41</sup> communications<sup>23</sup> and navigation systems<sup>24</sup> as will be described in the following paragraphs. Table 2.1 presents a summary of these systems highlighting the SS modulation technique employed.

In satellite communications SSMA techniques provide an alternative to conventional FDMA and TDMA systems. FDMA represents the simplest option in terms of ground equipment complexity and system coordination. However, the nonlinearities associated with a hard limiting satellite receiver generate intermodulation products which reduce the efficiency of the down link transmission and require uplink power coordination.<sup>61</sup> TDMA systems avoid this problem by multiplexing individual users through the satellite receiver according to a preconceived time plan. In this way only one user accesses the repeater at a given instant of time, allowing saturation of the down link transmitter without power loss and removing the need for up link power coordination. This improvement in efficiency is achieved at the expense of increased system complexity where a high degree of ground equipment synchronisation is required along with high peak power transmission capacity.<sup>28</sup> In addition time guard bands are required to allow for transmission delay uncertainty and long delays can result for subscriber access to the link.

In comparison SSMA techniques use a common wideband channel for transmission and achieve mutual interference protection by CDMA. The number of potential users in a CDMA system is dictated by the available number of unique code addresses whilst inter user interference is governed by the code cross correlation properties. The advantages associated with CDMA are that no timing coordination is

required, simultaneous random accessing is possible, satellite repeater bandwidth is efficiently used (ie, no guardbands) and simultaneous ranging and communication facilities can be achieved.<sup>47</sup> It should be noted that the number of simultaneous users in a CDMA link is considerably less (typically 0.1) than a comparable FDMA or TDMA link, but where a large number of potential users is combined with a low individual activity factor, CDMA can provide the most efficient multi-access technique (see Figure 2.1(b)).

Message privacy is an additional attraction for SSMA in tactical and commercially secure applications. The use of a SS uplink with demodulation in the satellite prevents unauthorised use of the satellite and ensures that uplink noise is removed prior to conventional down link transmission.<sup>63</sup> The TATS (Tactical Transmission System) described by Drouilhet and Bernstein<sup>64</sup> is an example of a SSMA system which uses Reed-Solomon data encoding followed by MFSK modulation and SS bandspreading by means of fixed pattern FH.<sup>65</sup>

The ranging capabilities of fast chip rate DSSS systems has been utilised in several space programs, notably Mariner, Apollo and Voyager. Tracking systems for space applications<sup>34,66</sup> operate by interrogating a transponder which either directly re-transmits or acquires and regenerates the received code sequence. In the receiver, the returned code is acquired and compared with the transmitted version to provide a measure of the two-way range. Alternatively, passive navigation can be achieved by DS techniques where the time difference measured between codes originating from spatially displaced but time synchronised platforms (eg, satellite transmitters) enables calculation of latitude, longitude, altitude

and velocity. An example of this technique is the NAVSTAR satellite based Global Positioning System.<sup>24</sup>

The application of SS techniques to ground mobile communications has received a considerable amount of study.<sup>67,68,71</sup> A number of early papers predicted very high spectral efficiency with virtually unlimited user addressing facility.<sup>68,69</sup> More recent publications by Matthews and Drury<sup>70</sup> and Shipton and Ormondroyd<sup>71</sup> have shown that in practice, performance differs little from current narrowband SSB or FM techniques, and incurs the penalty of increased receiver complexity. However, due to the low power noise-like spectrum associated with a DS transmission, it has been shown<sup>71</sup> that band-sharing with existing TV transmissions can yield added communication capacity which would otherwise have been unavailable. The technique of slow FH has been proposed for ground tactical applications, examples of which are the JAGUAR-V<sup>60</sup> and SYNCGARS<sup>72</sup> equipment.

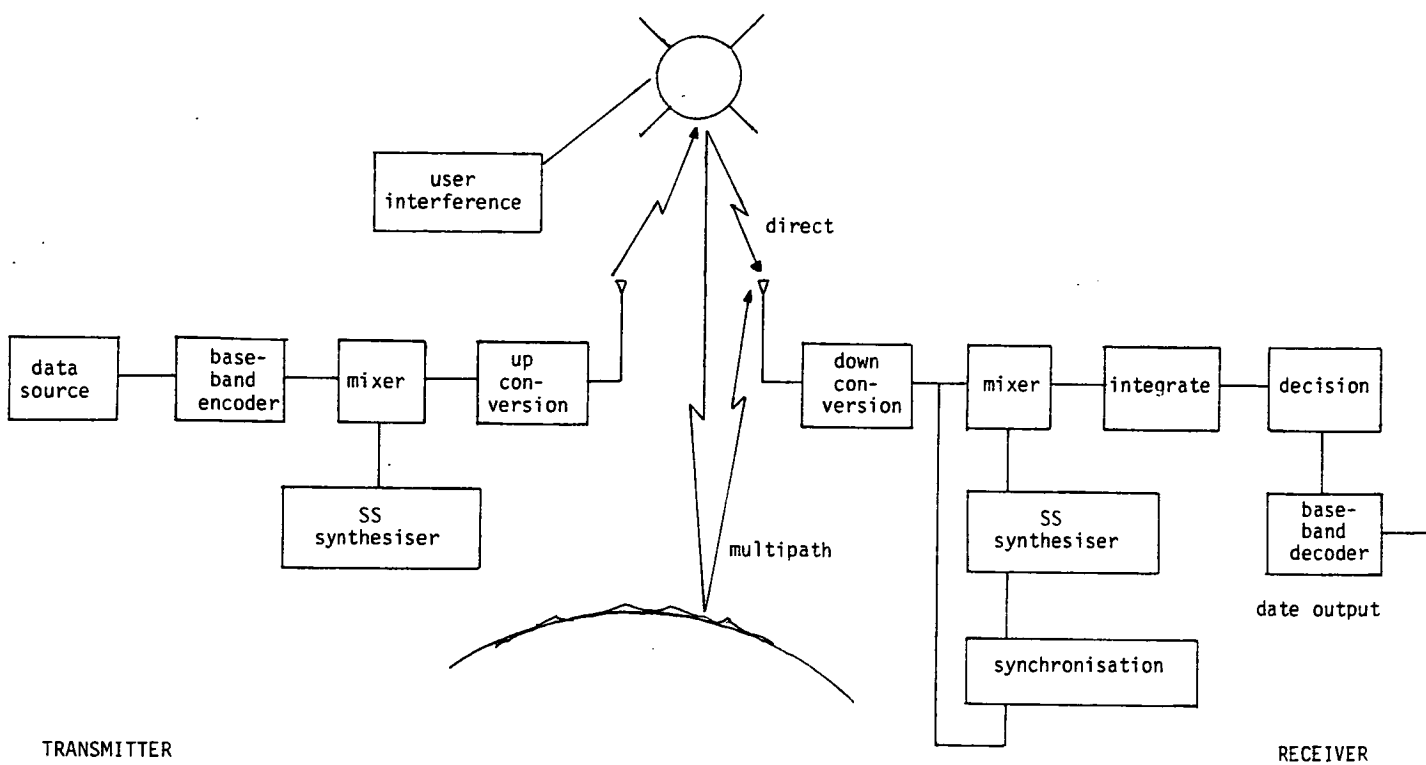
Finally, an excellent example of a hybrid SS system is presented in the Joint Tactical Information Distribution System (JTIDS)<sup>41</sup> for ground-air-ground communication. This system shares the 960-1215 MHz band with existing identification and ranging facilities and employs a combination of coordinated TH, FH and DSSS modulation techniques. Message coding is performed by a Reed-Solomon encoder to provide error detection and correction, prior to spectral spreading by a 5 MHz chip rate MSK code. This code burst is then frequency hopped into the 255 MHz band and the transmission time allocated according to a pre-determined time plan.

The systems described in this section illustrate the variety of applications where SS communications are effective. The main

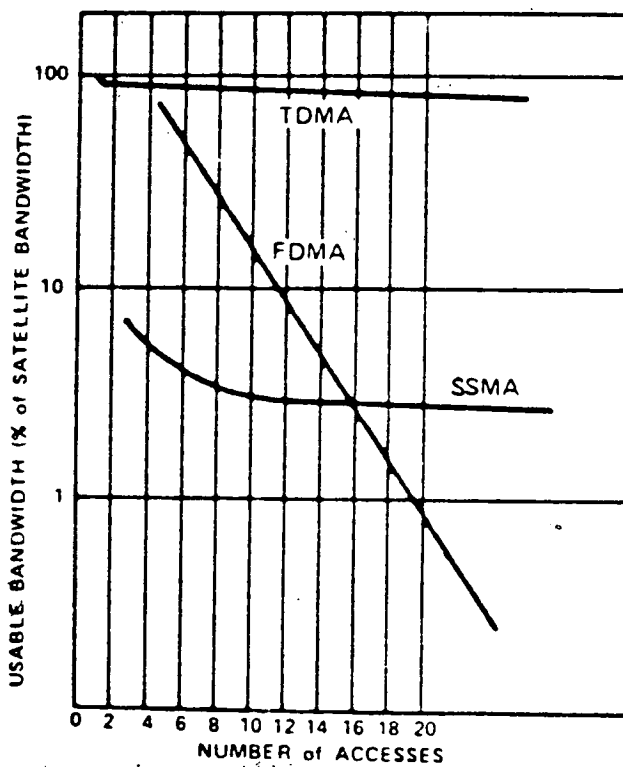
limitations on widespread use of SS techniques can be attributed to the implementational complexity of the transmit/receive equipment by comparison with conventional techniques. Recent advances in SAW and CCD technology have reduced the synchronisation problems associated with DSSS and similar advances in techniques in frequency synthesis should improve the capabilities of FH equipment.

SCENARIO	FREQUENCY ALLOCATION	CODING FORMAT	SYSTEM
Ground-Ground	VHF/UHF	FH	JAGUAR SYNCGARS
Ground-Air-Ground	L Band	DS/FH	JTIDS
Ground/Air-Satellite- -Ground/Air	L Band UHF/SHF	DS DS/FH	SKYNET NAVSTAR/GPS TDRSS TATS

Table 2.1 Examples of Spread Spectrum Systems

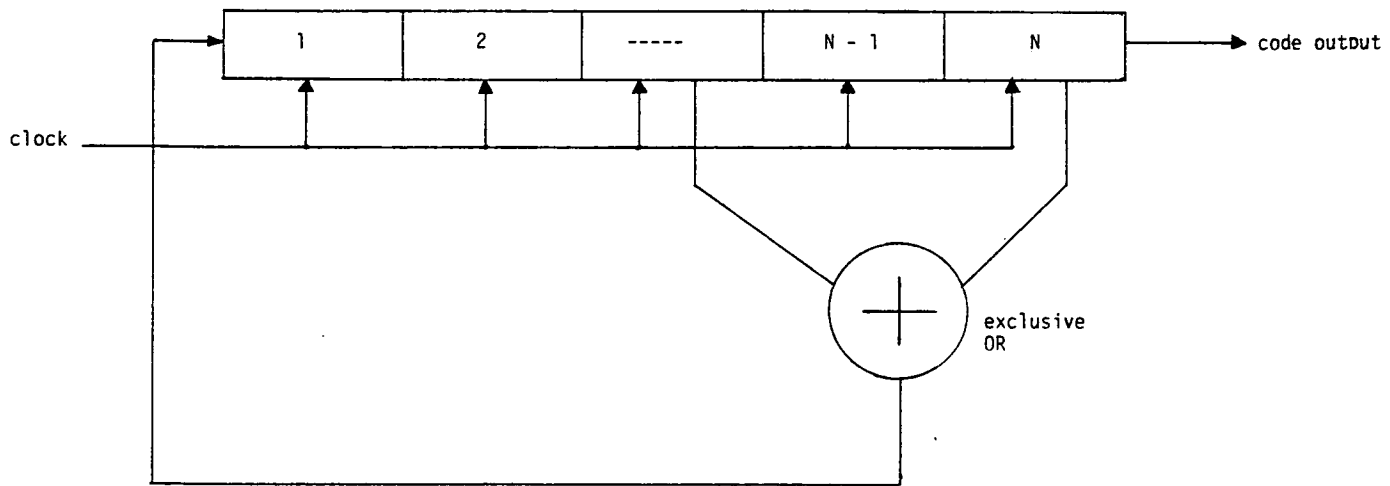


(a) Typical Spread Spectrum System

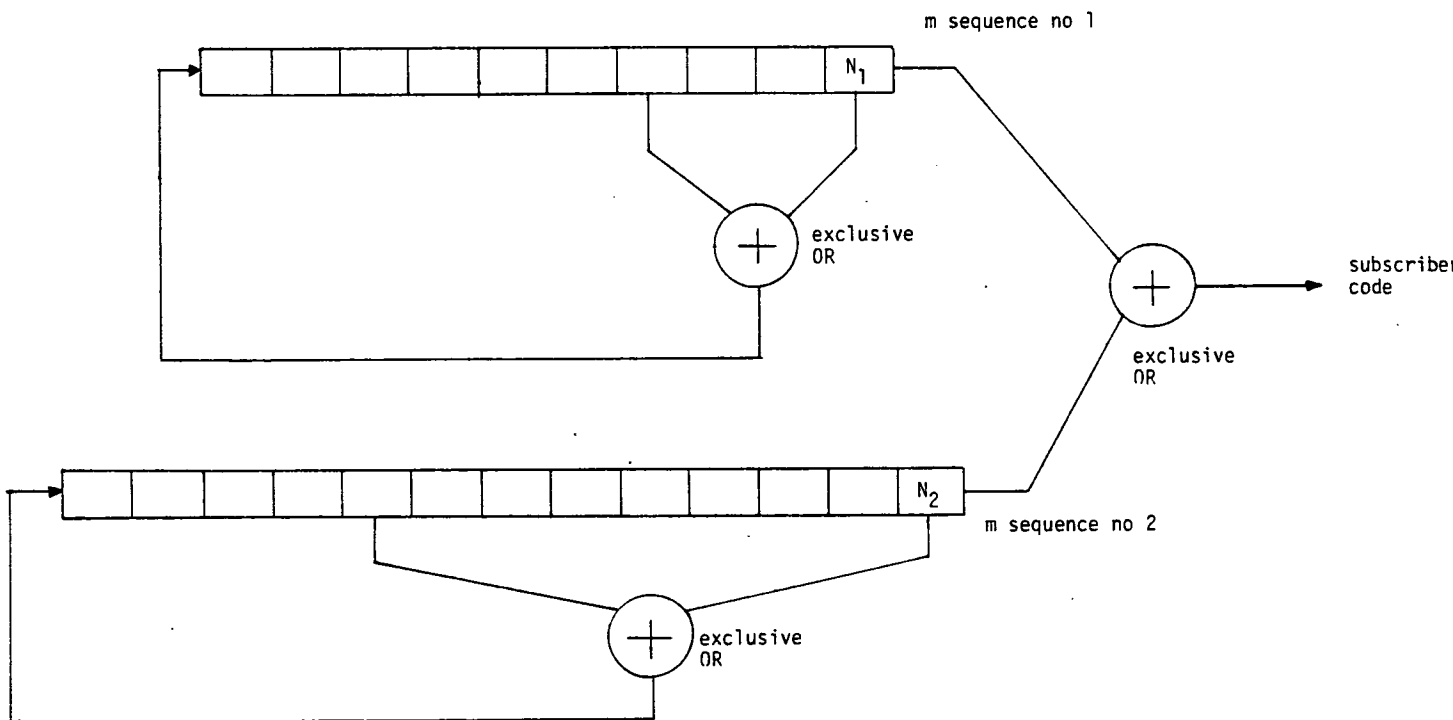


(b) Comparison of Multiple Access Techniques

Figure 2.1 Spread Spectrum Systems

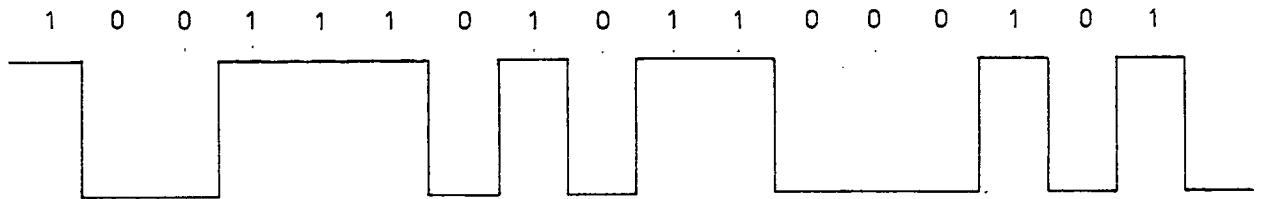


(a) Digital Shift Register PN Code Generator

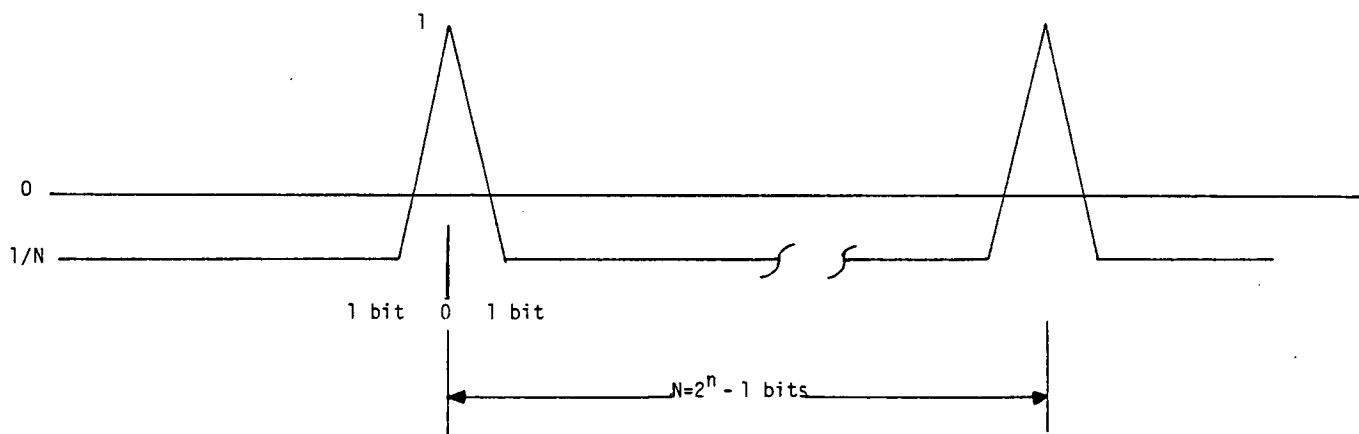


(b) Multiple Code Generation by Modulo-2 Addition



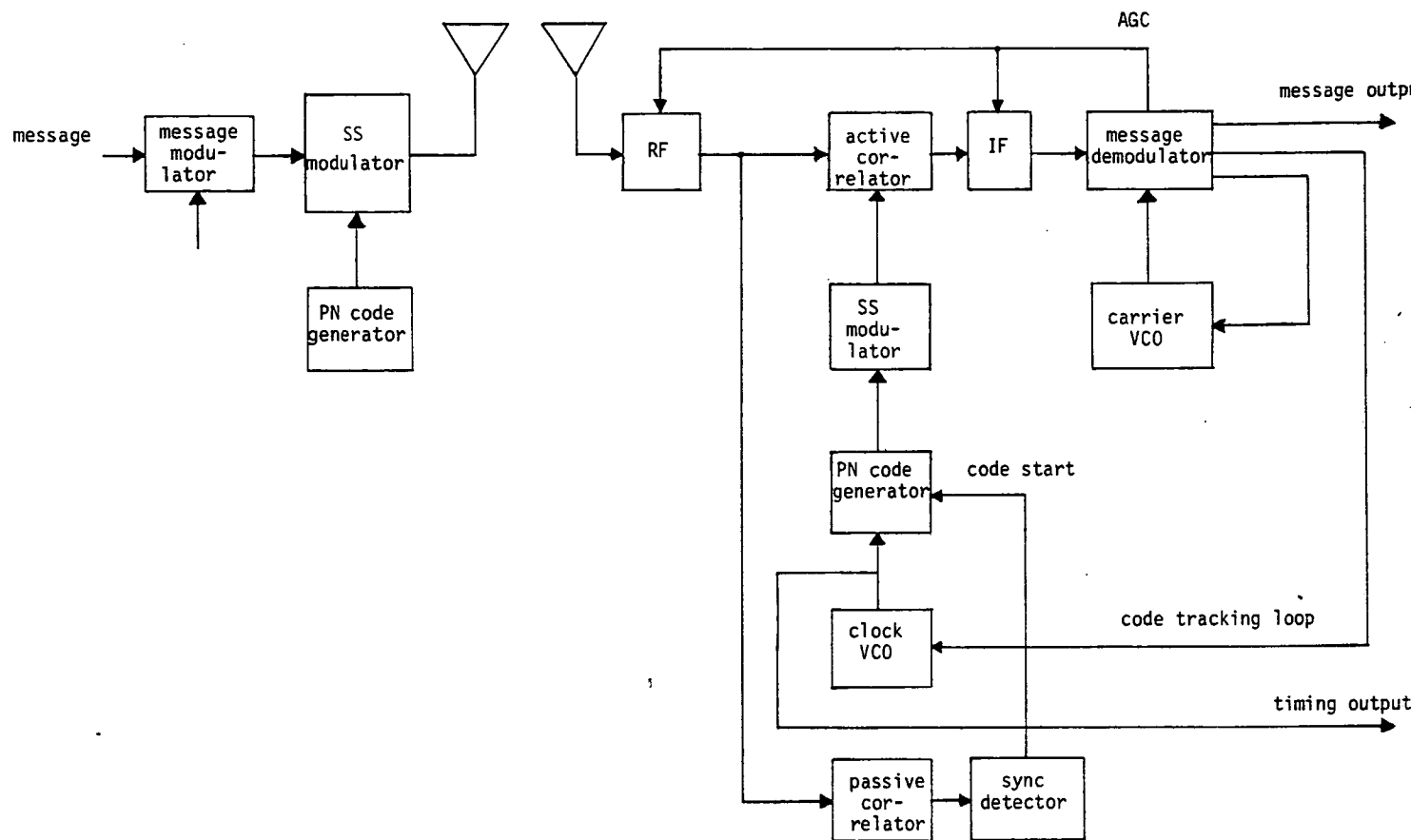
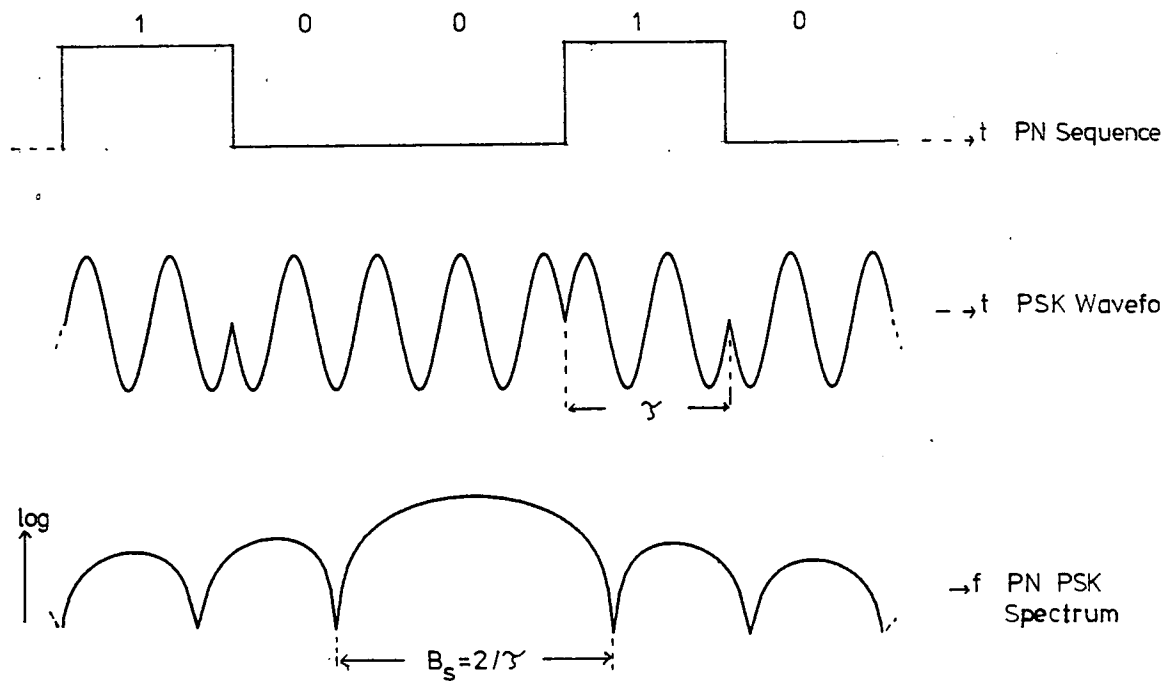



(a) PN Code Sequence



(b) Auto Correlation Function

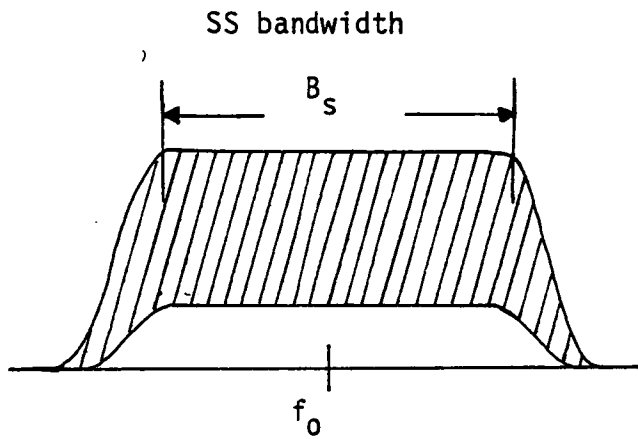
Figure 2.3 PN Code Waveforms

(a) Generic Transmit/Receive Configuration(b) DS Time/Frequency Domain Waveforms**Figure 2.4** Direct Sequence Spread Spectrum Link

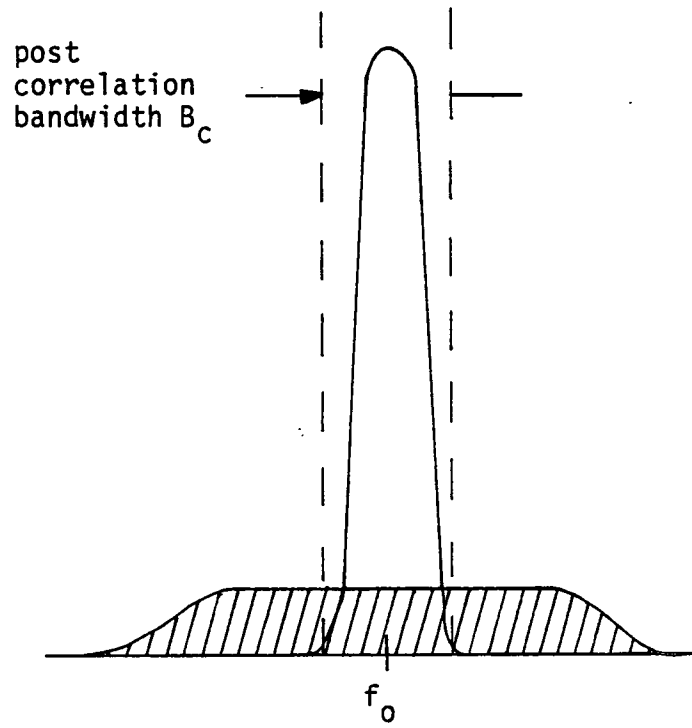
 interference

 desired signal

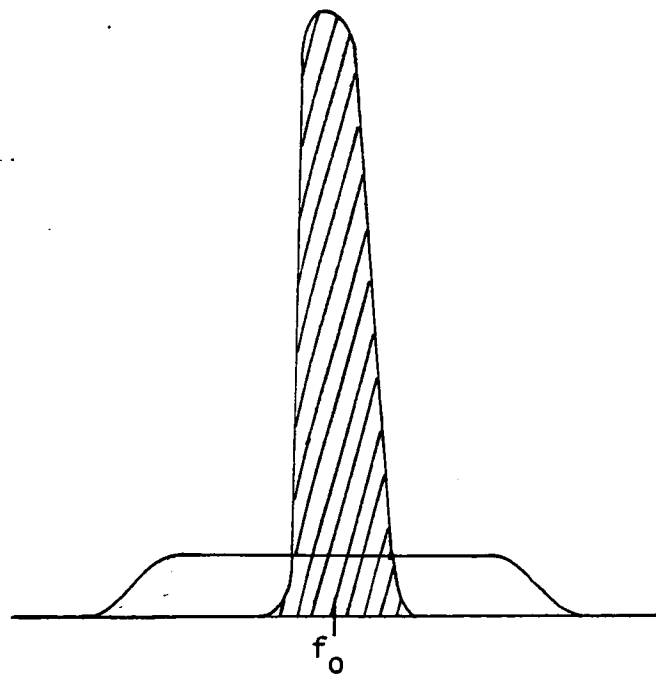
processing gain =  $\frac{B_s}{B_c}$



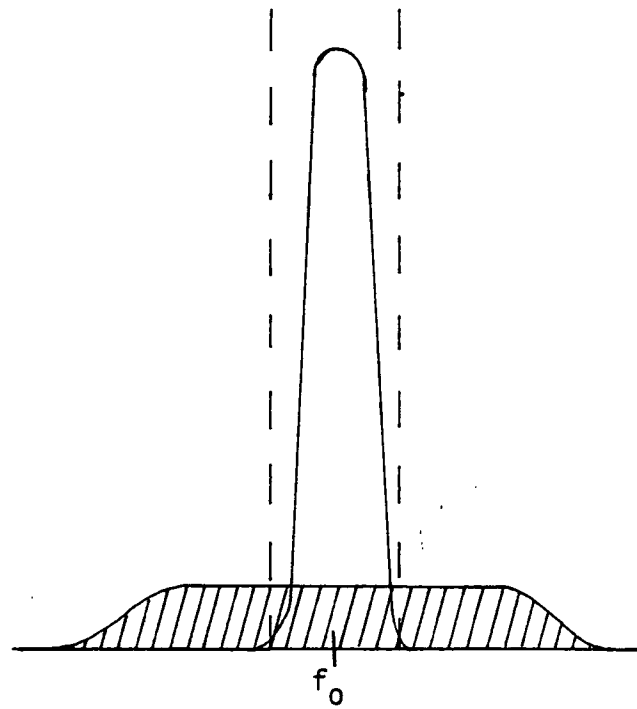
(a) Received Signal Plus Wideband Interference



(b) Correlator Output

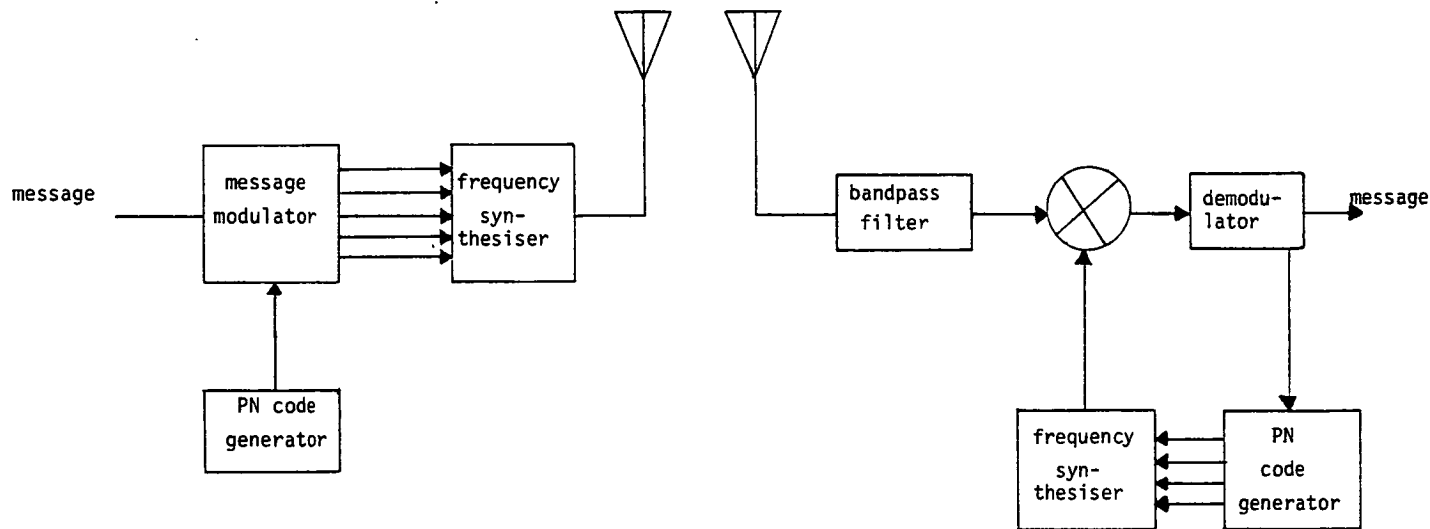


(c) Received Signal Plus Narrowband Interference

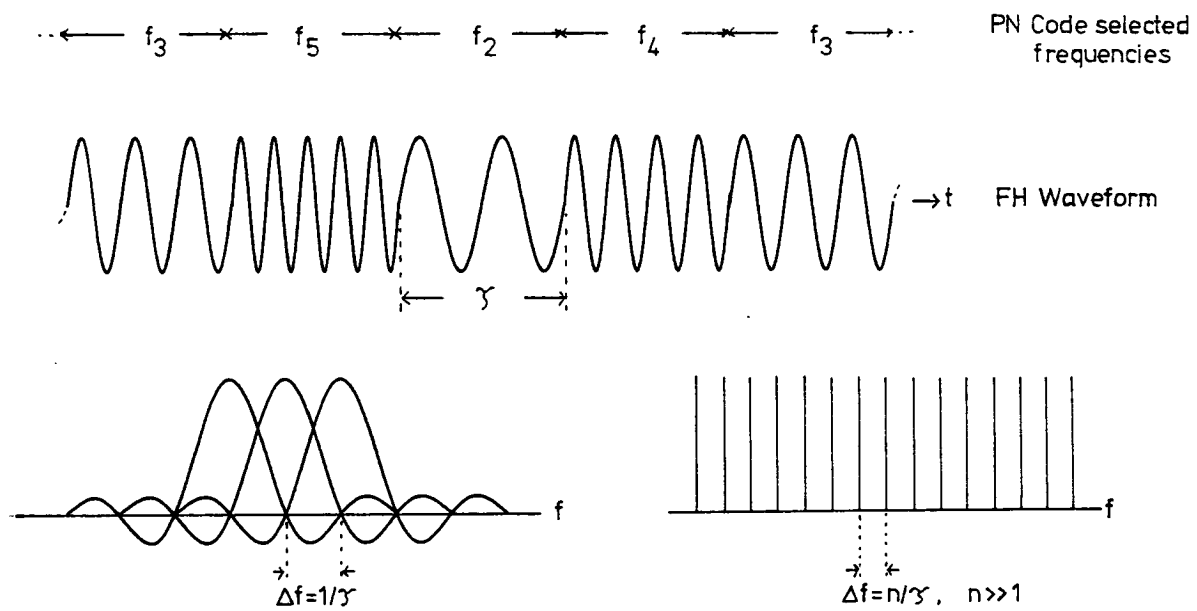


(d) Correlator Output

Figure 2.5 Interference Rejection in a DSSS Link

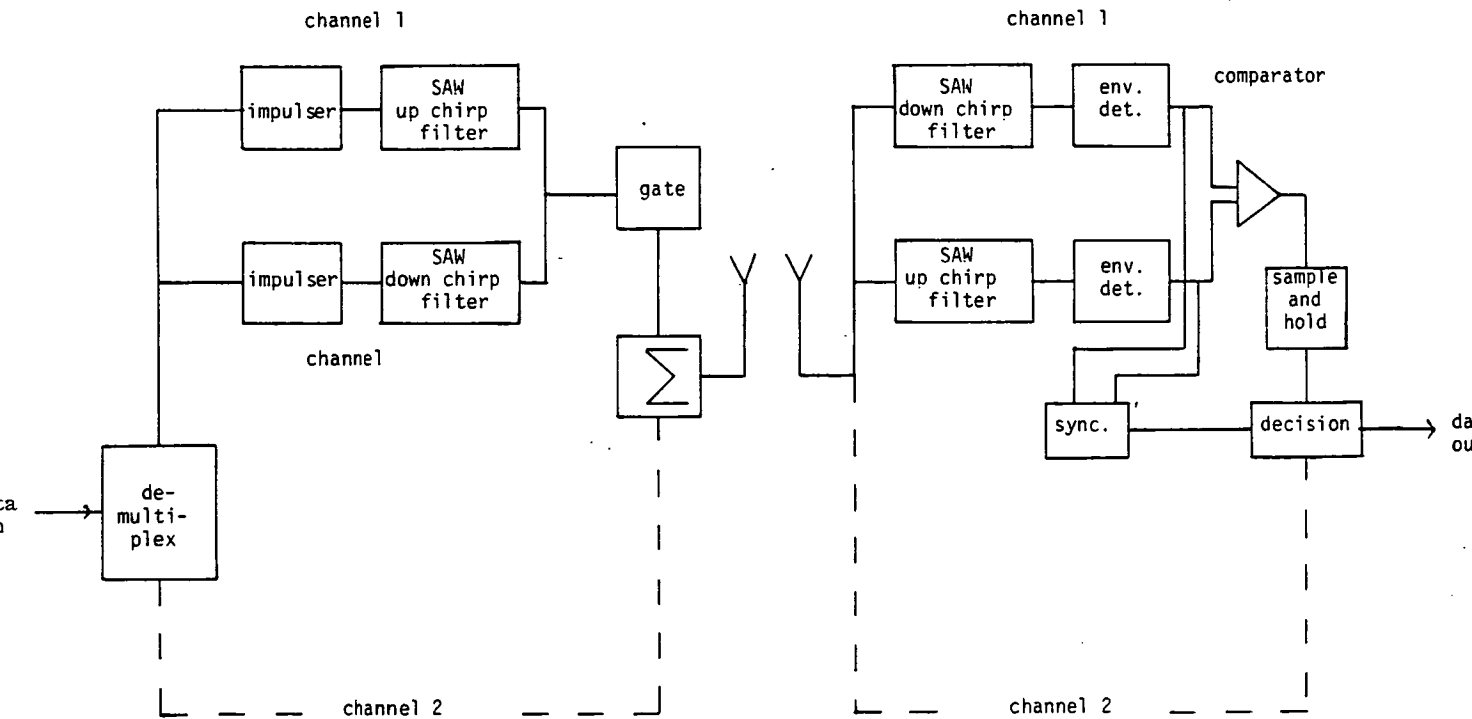


(a) Generic Transmit/Receive Configuration

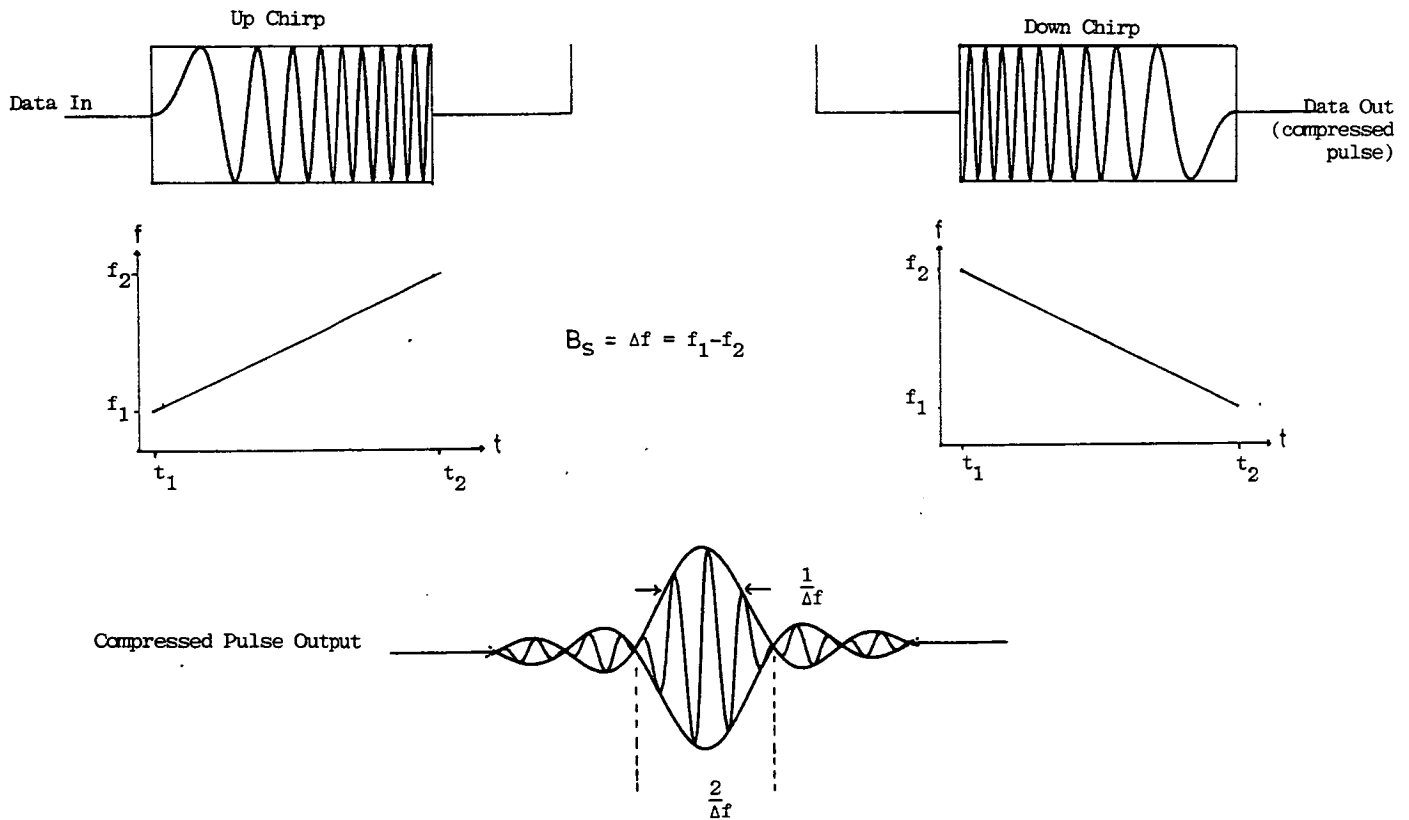


(b) Time/Frequency Domain Waveforms

**Figure 2.6** Frequency Hop Spread Spectrum Link

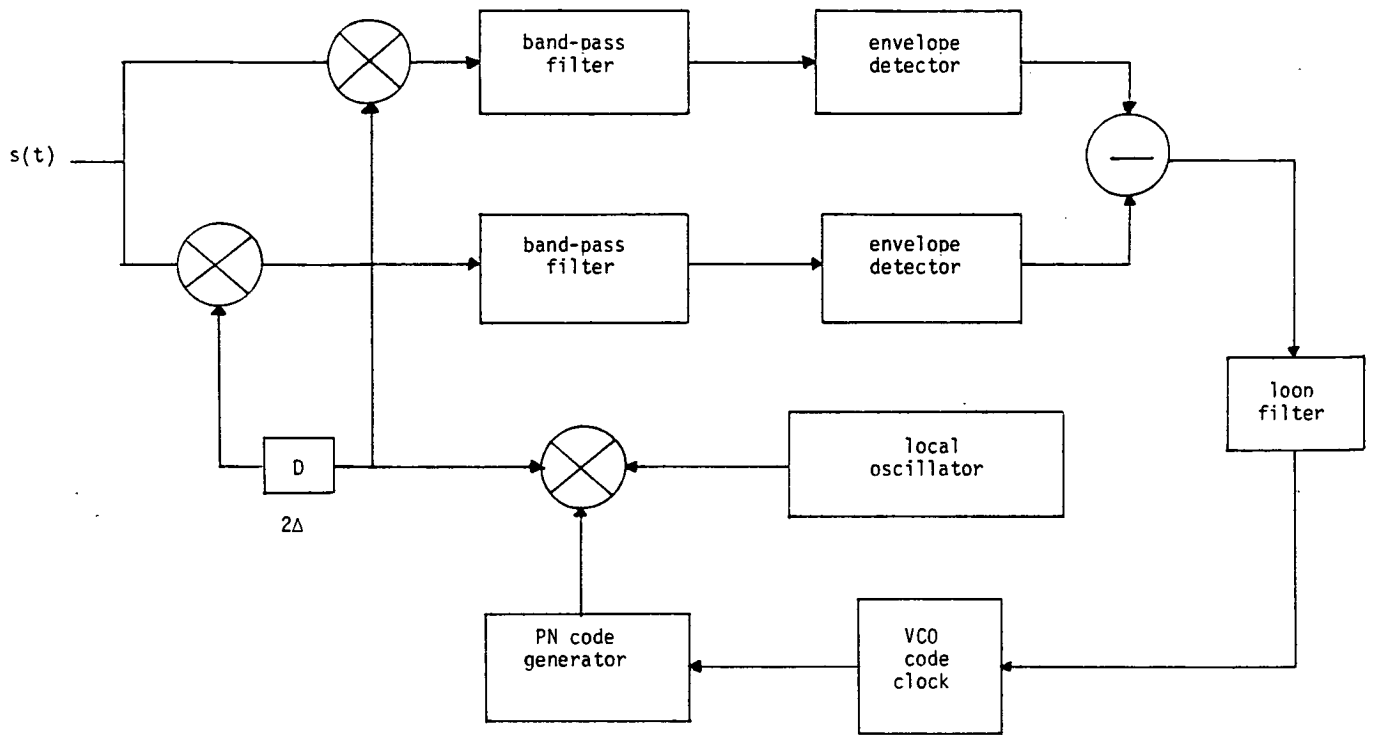
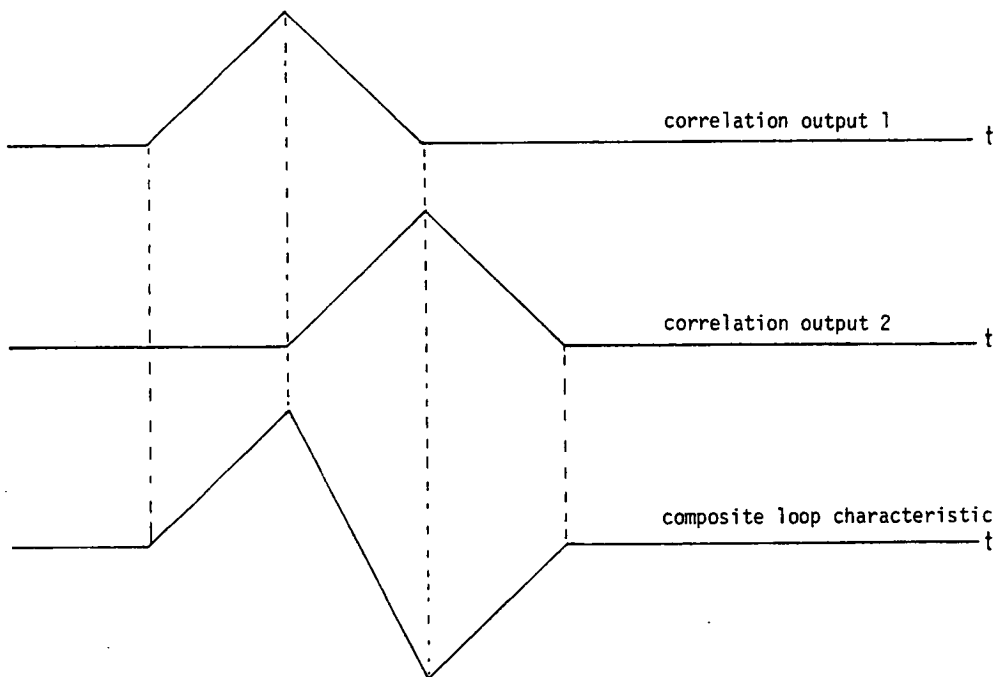


(a) Typical Chirp Spread Spectrum Data Link



(b) Time Domain Chirp Waveforms and Compressed Pulse Output

Figure 2.7 Chirp Spread Spectrum Link

(a) Loop Configuration(b) Discriminator Characteristic**Figure 2.8** Delay Locked Loop for Code Tracking

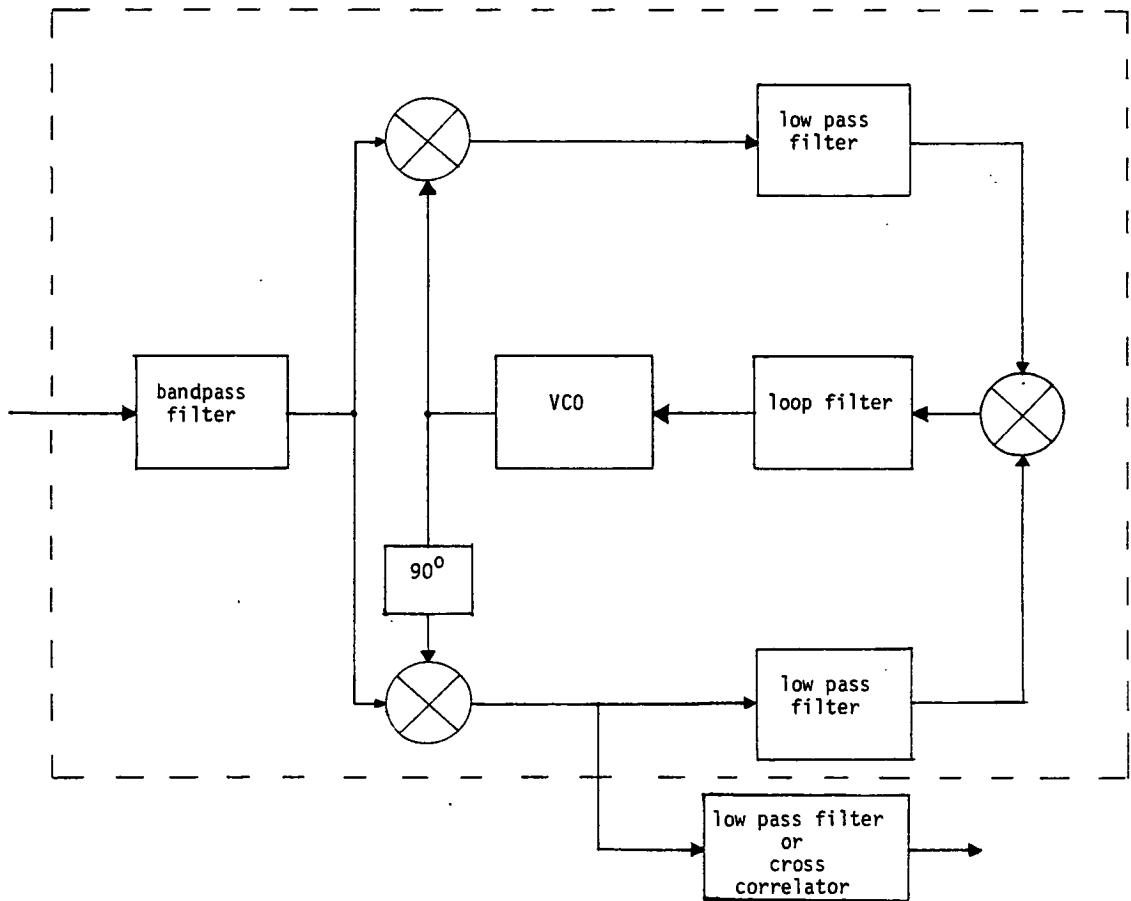


Figure 2.9 Costas Suppressed Carrier Tracking Loop

#### COMPARISON OF PSK AND FH WAVEFORM PARAMETERS

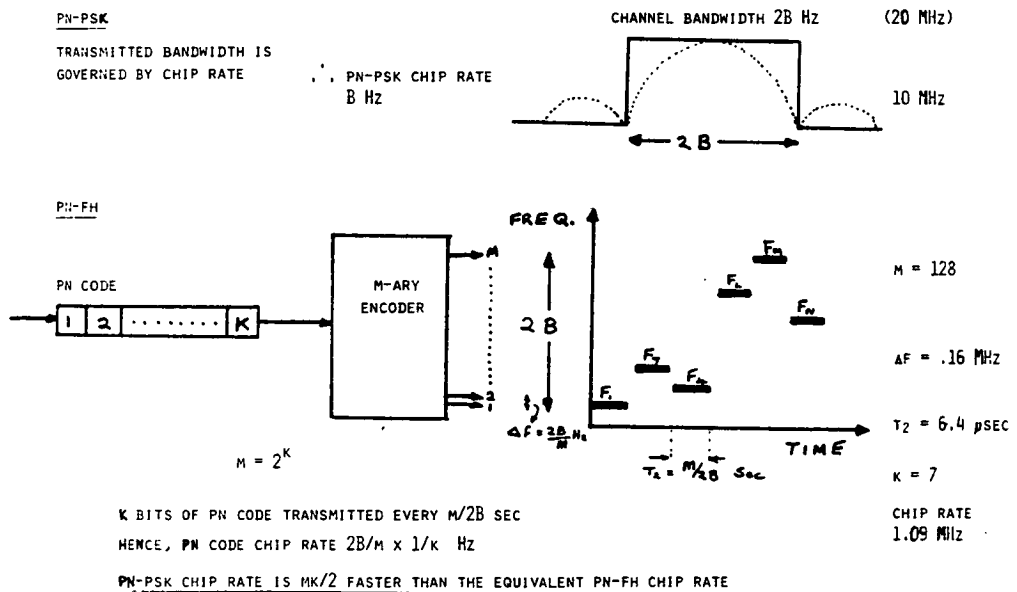


Figure 2.10 Comparison of PSK and FH Waveform Parameters

## CHAPTER 3 : FREQUENCY SYNTHESIS

### 3.1 INTRODUCTION

Techniques for frequency synthesis were developed during the 1950's and 1960's to meet the requirements of multichannel communications systems.<sup>3</sup> During this period the increasing demand for communications capacity appeared to be outpacing the available RF spectrum in HF, VHF and UHF bands, so a great deal of design effort was allocated to improving spectral efficiency.

Crystal controlled oscillators provided a significant advance over previous manually tuned equipments as their high stability performance reduced the need for guard bands between channels, and encouraged single sideband transmission without a tracking carrier.<sup>3</sup> By combining a number of such oscillators through mixing and filtering, a much larger range of output frequencies could be generated. This technique is known as incoherent direct synthesis<sup>1</sup> and is limited in accuracy and stability by the number of oscillators and switchable filters required. Subsequent development of this method replaced the individual crystal oscillators by a comb of frequencies derived from a single reference source. Coherent operation could now be achieved in a compact low cost equipment which, in addition to its high stability performance, could provide fast, accurate adaption to varying propagation and interference conditions with a minimum level of operator skill.<sup>73</sup>

Alternative techniques for frequency synthesis include indirect (or phase locked loop)<sup>3</sup> and digital "look-up" synthesis.<sup>3,74</sup> All



these equipments can be used in a variety of applications<sup>3</sup> including mobile communication, radio and television broadcasting, automatic test and measurement systems and spread spectrum (SS) communications systems. In particular, recent interest in SS communications has increased the search for coherent, wideband, fast switching, multi-frequency synthesisers as discussed in Chapter 2. This has led to the investigation of a number of novel surface acoustic wave (SAW) techniques which will be described in this Chapter.

The three conventional techniques for frequency synthesis, direct, indirect and digital "look-up", are reviewed in Section 3.2, and this is followed by a general introduction to SAW technology and applications in Section 3.3. Section 3.4 discusses a variety of SAW techniques for frequency synthesis and finally concludes the Chapter with a review of the techniques discussed.

## 3.2 TRADITIONAL FREQUENCY SYNTHESIS

### 3.2.1 Direct Synthesis

Direct, or iterative, synthesis<sup>3</sup> is a modular system comprising a number of identical stages as illustrated in Figure 3.1.

Each individual stage requires  $K$  input frequencies, spaced by  $\Delta f$ , with a centre frequency  $f_c(K-1/K)$ , where  $f_c$  is the reference source and  $K$  is an integer with typical value between 4 and 10.<sup>3,64,75</sup> A single frequency is selected from the input comb in an RF switching network and is combined in a balanced mixer with  $f_c/K$  or the output from the previous stage as applicable. The sum product generated in the mixer is then selected in a bandpass filter, divided by  $K$  and low pass

filtered to remove harmonics. This signal serves as the input to the following stage and this process is continued for the remaining  $(N-1)$  stages in the synthesiser. In practice the desired output is taken from the bandpass filter in the final stage, as this provides a more useful frequency range for communications applications.

Coherent operation is achieved if the  $K$  frequencies input to each stage are derived from a single reference oscillator. This can be achieved by harmonic multiplication of a stable source with filter selection of individual comb frequencies, or by indirect phase locked loop techniques. The phase noise of the direct synthesiser is therefore closely related to that of the reference source which can be selected to meet a particular requirement.

Spurious signal suppression is much harder to define as this is primarily determined by the circuit layout and package design. The on/off ratio of the frequency select switches provides the fundamental limitation, and for high frequency operation ( $f_c > 50$  MHz) frequency conversion techniques are often employed to allow RF switching at low frequencies where improved on/off ratios can be obtained. Typical values for spurious suppression are in the range 60 dB to 70 dB, but through the use of careful design and fabrication techniques, suppression levels of 80 dB to 100 dB have been achieved.<sup>3,76</sup>

The operating parameters for a direct synthesiser consisting of a chain of  $N$  stages are given as follows :

$$\text{Number of output frequencies} = K^N \quad \dots (3.1)$$

$$\text{Bandwidth (B)} = K.(\Delta f) \quad \dots (3.2)$$

$$\text{Minimum resolution} = B/(K^N) \quad \dots (3.3)$$

Fine resolution is readily achieved in an iterative synthesiser by increasing the number of stages (N). The percentage bandwidth however is limited by filtering constraints at the mixer output where the bandpass filter must select all sum products yet reject any direct feedthrough from the mixer input. It can be shown<sup>3</sup> that with ideal filter characteristics the maximum percentage bandwidth is  $200/(2K-1)$  and by assuming a filter stopband/passband ratio of 2:1, this formula yields approximately 5% and 14% bandwidth for values of  $K=10$  and 4 respectively. In practice, the choice of  $K$  is determined by the minimum values dictated by the level of inband mixer spurs (typically  $K \geq 4$ ) and the maximum value acceptable for system complexity (typically  $K \leq 16$ ). Multiples of  $K=2$  are often used where direct digital control of the synthesiser is expected,<sup>64</sup> whereas  $K=10$  is favoured for manually operated equipment.<sup>75</sup>

Synthesiser switching time is predominantly determined by the cumulative envelope delays of the bandpass and low pass filters in each stage. Assuming typical filter characteristics and values of  $K \geq 4$ , the approximate switching time per stage is

$$T_s = \frac{2.5(K-1)}{f_c} \quad \dots (3.4)$$

From this it can be seen that the overall switching time ( $NT_s$ ) is reduced by increasing  $f_c$  or decreasing  $K$ . To maintain a constant

number of output frequencies,  $N$  must be increased as  $K$  decreases.

Hence,  $NT_s$  is in fact proportional to  $K/\log_2 K$  rather than  $K$ .

Typical values<sup>1,3</sup> of  $f_c$  lie between 1 MHz and 100 MHz with  $\Delta f$  in the range 10 kHz to 1 MHz. Based on Equation (3.4), the maximum switching time for a synthesiser with  $f_c = 50$  MHz and  $K = N = 10$  is  $4.8 \mu s$ , which is representative of practical performance.<sup>3</sup> Where possible individual stages in the synthesiser are designed to operate at frequencies below 100 MHz. This is due partially to the difficulty in reducing spurious signals caused by RF crosstalk and mixer spurs, and partially to the increased cost and power consumption of digital dividers at these frequencies.

As high frequency operation is desirable to maximise the absolute bandwidth and minimise the synthesiser switching time, a design trade-off exists between performance, complexity, size, power consumption and cost. If wideband operation is a prime consideration, frequency multiplication ( $\times M$ ) can be used to expand the synthesised bandwidth at the expense of spurious and noise performance which is degraded by  $20 \log_{10} M$ . Alternatively, for wideband operation at low frequencies, down conversion can be applied.

Due to its modular construction, the iterative direct synthesiser is a versatile equipment which can provide fast switching, wideband, high resolution, coherent operation with excellent spurious suppression and phase noise characteristics. From the foregoing discussion, it can be seen that all of these features can only be met simultaneously at the expense of high system complexity, size, power consumption and cost. Table 3.1 presents a list of typical performance parameters in comparison with an equivalent indirect synthesiser.

### 3.2.2 Indirect Synthesis

Indirect synthesis<sup>3</sup> is based on the phase locked loop (PLL) technique<sup>78</sup> illustrated in Figure 3.2. This system is a closed loop electronic servo consisting of a voltage controlled oscillator (VCO), programmable divider ( $\div N$ ), phase detector (PD) and loop filter.

The operation of the loop is such that the VCO output is divided prior to phase comparison with a stable reference source. The resultant error signal is filtered to remove unwanted harmonics and used to complete the feedback loop which adjusts the VCO output frequency so as to reduce the error signal. The loop is said to be in lock when the output from the phase detector is constant and the output frequency ( $f_o$ ) is related to the reference ( $f_r$ ) by the ratio :

$$f_o = N f_r \quad \dots (3.5)$$

By varying the division ratio ( $N$ ), the output frequency can be selected, with minimum resolution  $f_r$ , across the operating range of the VCO. When the loop is in lock, any phase change in either reference or VCO output results in an error correction voltage at the PD output which adjusts the VCO to track the reference signal.

Phase lock loop design is commonly approached using Laplace transform techniques,<sup>78</sup> which are only valid for positive real time linear parameters. As the PLL contains both linear and non-linear functions, this must be justified by restricting the analysis to situations where the loop bandwidth is small in comparison with the reference frequency and small signal operation is considered.<sup>78</sup> Considerable information is available in the literature<sup>78,79,80</sup>

concerning PLL analysis, and hence this will not be reported in detail here.

PLL's are commonly categorised by type and order, where type refers to the number of pure integrations in the loop, and order refers to the highest degree polynomial in the characteristic equation. Due to the inherent integral relationship between phase and frequency,<sup>78</sup> the basic loop is type 1, and in this case a constant phase error at the PD output tunes the VCO to its lock frequency. For frequency synthesis applications, type 2 loops are favoured,<sup>78</sup> where the addition of an integration in the loop filter reduces this phase error to zero, providing coherent operation for all output frequencies.

Practical PLL design involves considerable trade-off between performance parameters for a given application. Bandwidth, resolution, switching speed and noise performance are all inter-related and must be considered separately for each individual case. For a given application, the two most important functions in the loop are the phase detector<sup>80</sup> and loop filter.<sup>78</sup> The common phase detector characteristics are sinusoidal, triangular and saw tooth responses. The first two are suitable for situations where  $f_r$  is relatively close to  $f_o/N$  (ie,  $\theta_e \ll \pm \frac{\pi}{2}$ ) but for wideband frequency synthesis where  $f_r$  differs considerably from  $f_o/N$ , the saw tooth response is preferred. In this case the phase error determines the polarity of the error signal and ensures that the VCO control voltage is changed in the correct direction to minimise the error signal. It is common to find digital phase detectors<sup>3,85</sup> in modern indirect synthesisers.

The loop filter is the prime factor which governs the type and order of the loop transfer function and hence is a critical factor in determining the loop dynamic response and performance. Type 2 operation is normally achieved through use of an integrate and lead loop filter.<sup>78</sup> The filter is required to reject any harmonic signals at the PD output and to provide smoothing of any dc ripple content on the VCO control signal. The integrator provides a short term memory capacity to store the VCO control signal during phase lock which enables rapid relocking following any phase transients at the PD output. The filter is normally designed to be narrowband with a sharp cut-off and high rejection. This reduces the effects of noise sidebands external to the loop (ie, on the reference waveform), but increases the loop sensitivity to internal noise such as microphonic effects.<sup>3</sup> For frequency synthesis, it also has the effect of reducing the loop switching speed and hence for fast switching applications, a design trade-off between switching speed and noise performance must be accepted.

For narrowband applications, the dynamic response of the loop can be determined from its characteristic equation which in the case of the integrate and lead filter is second order. The normalised form for this equation defines two important terms in PLL design, the damping ratio ( $\zeta$ ) and the natural frequency ( $\omega_n$ ). Families of curves are available<sup>78</sup> which graph the output phase or frequency response caused by input phase or frequency steps for values of  $\zeta$  between 0.1 and 2.0. For a particular loop,  $\omega_n$  and  $\zeta$  can be defined in terms of the circuit parameters, and with reference to these graphs, the optimum circuit parameters selected to achieve the required dynamic response. To yield optimum overshoot and noise

performance  $\tau$  is typically selected between 0.5 and 1.0.

For wideband applications, the above analysis is unrepresentative as the large value frequency steps cannot be analysed by conventional Laplace techniques. In this case, the loop switching speed is restricted by the maximum output from the PD and the slew rate of the amplifiers and VCO components in the loop.<sup>85</sup> An empirical figure quoted for PLL switching is typically 20 to 30 times the period of the reference signal.<sup>3</sup> This can vary from milliseconds to seconds for common designs.<sup>83,85</sup> A technique often used to improve switching speed involves decoding the input frequency control word in a digital to analog converter (DAC) and feeding this information directly to the VCO.<sup>3</sup> This pretunes the VCO to the point where normal phase locking can be effected. A number of techniques have been suggested for increasing the PLL resolution without increasing the switching speed or reducing the noise performance excessively. These include digiphase switching, direct loop combination, vernier loop combination and digital "look up"/PLL combination.<sup>3,80,86</sup>

The difficulty in implementing a PLL is increased when high frequency operation is required. When digital division and phase detection are used, the VCO output is normally reduced to a suitable frequency by standard down conversion or prescaling techniques.<sup>3</sup> Prescaling is normally favoured as this results in the minimum component count and reduces the need for a second input signal to the loop. This is limited to VCO frequencies below 1 GHz at present, but development of gigabit logic should extend this in the future.



In general terms, the PLL synthesiser represents a considerable improvement over the direct synthesiser in terms of component count, size, weight and power consumption. For many applications such as airborne and manpack equipments, these features are highly desirable and the associated penalty of slow switching speed is accepted as a design trade-off. Typical performance figures for PLL synthesis are listed in Table 3.1, and a description of design procedures for a number of applications can be found in the reference list.<sup>3,82,83</sup>

### 3.2.3 Digital "Look-Up" Synthesis

This technique represents a modern approach to frequency synthesis based on the use of digital read only memory (ROM) and digital to analog converters (DAC).<sup>3,74</sup> The design and manufacture of this equipment can be attributed to recent advances in digital large scale integration (LSI) which have increased both the capacity and availability of memory devices. Although this technique does not presently provide high frequency wideband operation, the operating principle is described below for completeness.

Tabulated values of sine and cosine functions are stored in ROM and selected values read out sequentially to form a sampled signal of the desired frequency. This in turn is converted into analog form in a DAC. The sampling interval ( $t_s$ ) is chosen to be  $1/f_r$  (where  $f_r$  is the system reference clock), and the desired trigonometric value is calculated from



$$\theta_0 = 2 \cdot \pi \cdot f_0 \cdot t \quad \dots (3.6)$$

where

$f_0$  = output frequency

$t = Nt_s, \quad N = 0, 1, 2, \dots$

The maximum value for  $f_0$  is restricted to  $f_r/2$  by the Nyquist sampling criterion<sup>8</sup> but  $f_r/4$  is accepted as a practical limit for operational systems. At present,  $f_r$  is limited by the finite access time of the ROM (10 - 100 kHz for MOS devices), the multiplication process required and the maximum operating speeds of DAC's. Improved frequency resolution requires an increase in the number of tabulated trigonometric values, and the accuracy of these values governs the spectral purity of the output. The consequence of the latter two factors is to increase the ROM storage required, and although economies can be made due to the symmetry of the sinusoidal waveform<sup>74</sup>, this, coupled with the associated memory access time, limits the performance of the system.

Following DAC the signal is low pass filtered to remove unwanted harmonics. The envelope delay of this filter is the governing factor in the synthesiser switching speed, and typical figures of 1 to 10  $\mu$ s have been reported<sup>3</sup> for filters of varying complexity. The maximum operating frequency is dependent on the logic family used and can vary from 200 kHz for CMOS to 12 MHz for ECL.<sup>3</sup> However, it should be noted that power consumption can increase by a factor of 40 and noise performance degrade by 40 dB between these extremes.<sup>3</sup> Techniques have been suggested for increasing the synthesiser centre frequency by single sideband modulation, up conversion and filtering or harmonic selection.<sup>3</sup>

Although this filter does not provide the high frequency, wide-band operating capacity of the iterative or PLL synthesisers, it is a useful technique for synthesis of frequencies below 1 MHz.<sup>74,87</sup> As digital circuit operating speeds continue to increase, the digital look-up synthesiser may find wider application.

### 3.3 SAW TECHNOLOGY AND APPLICATIONS

#### 3.3.1 Introduction to SAW Technology

In the field of electronics and signal processing, the surface acoustic wave (SAW) is associated with a longitudinal wave propagating in a piezoelectric material with a velocity some five orders of magnitude lower than the velocity of electromagnetic radiation. This wave, sometimes known as a Rayleigh wave,<sup>88</sup> is non-dispersive and typically has more than 95% of its energy content confined within a depth equal to one wavelength. Due to this latter feature and the comparatively low velocity of the SAW (typically  $3 \times 10^5 \text{ ms}^{-1}$  for quartz) a large number of wavelengths can be contained within a relatively small (less than 250 mm) device, and the waveform can be sampled or otherwise modified during propagation. Practical implementation of SAW devices became possible with the development of the interdigital transducer,<sup>89</sup> which permits efficient transduction of electric and acoustic energy, and this has proven to be a highly reproducible structure using photolithographic replication techniques pioneered in the semiconductor industry.

The interdigital transducer (IDT) consists of a set of interleaved electrodes made from a metal film deposited on a highly polished piezoelectric substrate. The diagram in Figure 3.3

illustrates a basic SAW delay line with identical, uniform input and output transducers. This simple IDT structure has a constant pitch ( $L$ ) and aperture ( $W$ ) over the transducer length. Its impedance as seen at the electrical input port can be represented by a series equivalent circuit,<sup>89</sup> with a reactance which in practice is predominantly capacitive. In the device passband, the transducer can be electrically matched by an inductor to cancel the reactive component so that all incident electrical energy is converted to acoustic energy. The value of electrode overlap required to make the resonant impedance of the device equal to  $50\Omega$  ( $W_{50}$ ) can be easily calculated.<sup>89</sup>

When a sinusoidal voltage applied to the electrical port approaches the resonant frequency of the IDT, strong coupling of electric to acoustic energy occurs and surface waves are launched in both directions normal to the IDT. At the design stage, it is possible to select the device operating frequency by varying the electrode pitch ( $L$ ), and similarly the amplitude contribution of an electrode pair (to a first approximation) can be controlled by varying the electrode aperture ( $W$ ). Maximum values for  $L$  and  $W$  are dictated by substrate size and cost while fabrication techniques and diffraction effects limit minimum dimensions.

The bidirectionality of the SAW leads to a minimum theoretical device insertion loss of 6 dB for ideally tuned and matched transducers and the reflection coefficient<sup>89</sup> of -6 dB gives rise to a triple transit signal (corresponding to three transits between transducers) appearing at the output 2 delay periods after the input signal, with a comparative level of -12dB. In the simple device

shown in Figure 3.3, unwanted surface waves travelling away from, or passing under, the output transducer are absorbed by wax or adhesive tape, or alternatively scattered by angling the ends of the crystal. Improved triple transit suppression can be gained at the expense of increased insertion loss or by the use of special design techniques.<sup>90,91</sup> In situations where low insertion loss is a critical requirement, IDT geometries<sup>92</sup> comprising more than 2 transducers can be used to reduce the loss to less than 2 dB.

In most piezoelectric materials, the periodic structure of the IDT also excites bulk or volume acoustic waves which reflect off the end and reverse faces of the substrate. In most cases these waves have velocities between 1.5 and 2 times greater than the desired surface wave, and can lead to undesirable out of band responses. Elaborate fabrication and design techniques can be employed to reduce bulk waves by as much as 50 → 60 dB.<sup>93</sup>

Although necessary for energy conversion, the IDT loads the material substrate due to its finite mass and the piezoelectric coupling effect. Both these effects tend to reduce the surface wave velocity relative to that on the free surface of the material. The relative contribution of these two perturbations is dependent on the operating frequency and the substrate material.<sup>94</sup>

In a complex SAW device, IDT structures with between 50 and 10,000<sup>95</sup> elements may be used. This can result in undesirable interelectrode reflections which degrade the device performance. Figure 3.4 shows three forms of transducer structure commonly used. The simple  $\lambda/4$  structure used to illustrate the IDT in Figure 3.3 creates a particular problem since each finger edge reflects an

incident SAW in phase at the fundamental frequency. For transducer structures with a large number of elements, this reflection severely impairs performance, and the  $\lambda/8$  or "split finger" electrode configuration must be used.<sup>96</sup> This reduces the finger width for a given centre frequency and hence limits the maximum device operating frequency due to photolithographic fabrication constraints. For high frequency operation, the  $\lambda/6$  structure provides a useful compromise between reflection suppression and fabrication complexity.

The above description has been confined to uniform transducers, but in practice, many SAW devices are designed with a non-uniform IDT where the periodicity or the aperture (or both) are allowed to vary. Such devices belong to the general class of transversal filters (Figure 3.5)<sup>97</sup> and can be used to perform functions such as frequency filtering, correlation and dispersive delay. In the context of this manuscript, the SAW dispersive delay line (DDL) is of major importance, and is more fully discussed in Section 3.3.2. The general application of SAW devices in radar and communications systems is discussed in Section 3.3.3.

A range of piezoelectric substrate material is available for SAW device fabrication, and the choice is mainly governed by the device type, its operating frequency, bandwidth, time delay and environment. The most commonly used are quartz and lithium niobate ( $\text{LiNbO}_3$ ). ST-X quartz is the only readily available material with a zero temperature coefficient of delay at a convenient and selectable temperature. A typical characteristic for 42 degree rotated ST-X cut is shown in Figure 3.6. The null point of this parabola can be varied over 25 to 100 degrees centigrade by a 10 degree variation of

the crystal orientation.<sup>98</sup> The disadvantage of quartz substrates is their low coupling coefficient which leads to high insertion loss and narrowband (<4%) operation in uniform bandpass and simple delay structures. Lithium niobate has a much higher coupling coefficient allowing bandwidths in excess of 20% for tuned uniform transducers, and exhibits a velocity anisotropy which substantially reduces beam spreading due to diffraction. The high coupling can lead to spurious signals and reflections as discussed previously. The temperature coefficient of lithium niobate is approximately 90 ppm/degree centigrade, which may necessitate temperature control for some applications. Other materials of significance are  $\text{LiTaO}_3$ ,  $\text{Bi}_{12}\text{GeO}_{20}$  and  $\text{ZnO}$  on  $\text{Si}$ .<sup>98</sup>

From the above discussion, it can be seen that trade-offs exist when selecting a material for a particular application. The main factors which must be taken into consideration are : percentage bandwidth, acoustic velocity, temperature coefficient of velocity and delay, spurious signal rejection, acoustic loss, availability and cost of material. Table 3.2 presents the parameters of some available substrate materials, and details optimum uniform IDT design considerations. Further information regarding SAW fabrication and design techniques can be found in References 4 and 94.

### 3.3.2 The SAW Chirp Filter

A dispersive delay line (DDL) has a group delay characteristic which is a specified function of the instantaneous frequency of the input signal. This can be achieved in SAW technology by two distinct approaches : the first based on the IDT,<sup>99</sup> and the second

on the reflective array compressor (RAC).<sup>100</sup> The former is historically the more proven technique and is of particular relevance to this manuscript, but for completeness, some reference is given to RAC techniques at the end of the section.

Frequency dispersion is achieved in an IDT structure by varying the interelectrode pitch ( $L$ ) across the length of the transducer. The desired amplitude characteristic is independently realised by varying the aperture ( $W$ ) of the electrodes, a process commonly known as apodisation. In this way it is possible to design either linear or non-linear dispersive filters with or without amplitude weighting. In this case the device of interest is the linear frequency modulated (FM) filter, most commonly known as the "chirp" filter from its application in radar pulse compression systems.<sup>13</sup>

The simplest chirp filter design combines a wideband non-dispersive IDT with a dispersive IDT as in Figure 3.7 (a). The main disadvantage of this configuration is the inherent bandwidth limitation of the non-dispersive transducer. The use of a double dispersion design as in Figure 3.7(b), circumvents this problem by sharing the dispersion between transducers, such that each transducer covers the required bandwidth in one half the dispersive delay. As discussed in Section 3.3.1, spurious signals caused by the SAW travelling under the metalised IDT structure can degrade performance, hence the double dispersive inclined structure illustrated in Figure 3.7(c) is an attempt to minimise this interaction. High performance devices also make use of split finger techniques to minimise the effect of inter-electrode reflections.<sup>99</sup>



A prime figure of merit for a chirp filter is its time bandwidth (TB) product, which refers to the device time delay in  $\mu\text{s}$  multiplied by its bandwidth in MHz. Also of interest to the system designer is the operating frequency, the insertion loss, the group delay variation, the amplitude ripple and the level of time domain spurious signals. Table 3.3 lists current and projected performance bounds for IDT based SAW chirp filters.

The alternative approach to SAW chirp filter design, the RAC, is based on an earlier bulk acoustic wave device, the IMCON.<sup>101</sup> Input and output transduction is achieved by conventional IDT design, whilst frequency selection relies on a reflective array of etched grooves with graded periodicity. The SAW normally propagates at approximately 45 degrees to the groove and the combination of two such arrays as shown in Figure 3.8 results in a compact U shaped structure which allows a given time dispersion to be realised in approximately half the size of a conventional filter. The array grooves are fabricated using sophisticated ion-beam etching techniques,<sup>102</sup> and introduce virtually no propagation loss and negligible dispersion.<sup>94</sup> Amplitude weighting is achieved by varying the groove depth as the reflectivity varies linearly with depth for shallow grooves.

In addition to increasing the available delay, measured phase errors can be compensated for by loading the substrate with a variable width metallisation between the two reflective arrays. Since the frequency dispersion occurs spatially down the length of the crystal, the metallisation can be varied to achieve accurate phase compensation at any point in the band. The RAC structure greatly reduces spurious bulk waves and does not suffer from the surface loading

effects encountered in IDT devices. This allows optimal matching of input and output transducers to minimise insertion loss.

The present and projected future capabilities of SAW RAC devices are tabulated in Table 3.3, alongside the figures for IDT designs. Although the RAC can achieve much higher time-bandwidth products, these filters cannot meet the stability of IDT structures manufactured on quartz, since they normally use a high coupling material such as lithium niobate.

### 3.3.3 SAW Device Applications

SAW components can be used to perform a variety of signal processing functions, examples of which include frequency filters, resonators, dispersive and non-dispersive delay lines, phase coded and tapped delay lines and convolvers. Application of these devices has been reported<sup>103,4</sup> in both radar and communications systems, but the most significant areas of impact have been in pulse compression radars<sup>38</sup>, television IF filtering,<sup>104</sup> compressive receivers<sup>105</sup> and spread spectrum synchronisation.<sup>4</sup> Table 3.4 presents a list of potential systems applications for SAW devices along with the associated properties which make this technology an attractive option.

Pulse compression radar systems<sup>13</sup> commonly employ a linear FM, or chirp, transmit pulse combined with matched filtering in the receiver to provide increased range detection without loss of resolution in a peak power limited system. The processing gain associated with pulse compression is equal to the TB product of the transmitted signal and the resulting compressed pulse has a  $\sin x/x$  envelope with time sidelobes commencing at -13 dB with respect to

the main lobe. As this sidelobe pattern is undesirable in many applications, it is common to employ spectral weighting in the receiver to reduce the level of sidelobes at the expense of pulse broadening and loss of compression gain.<sup>13</sup>

SAW dispersive delay lines provide a convenient and reproducible method for generating and detecting the chirp signals used in pulse compression radars.<sup>38</sup> The DDL characteristics described in Table 3.3 illustrate that pulses with bandwidths of 10 MHz to 100 MHz and time delays of 1  $\mu$ s to 100  $\mu$ s can be achieved at suitable IF frequencies (30 to 300 MHz). For linear FM systems spectral weighting<sup>99</sup> in the compressor can be applied to achieve time sidelobe suppression of 30 to 40 dB.<sup>99</sup> Due to this weighting, the compressor device is no longer a true matched filter and a mismatch loss of approximately 1.2 to 1.4 dB is experienced.

The use of non-linear FM coding<sup>106</sup> avoids the mismatch problem by sharing the spectral weighting function between transmit and receive filters. This results in a close approximation to true matched filtering, and devices have been reported<sup>107</sup> which exhibit sidelobe suppression of 45 dB with a mismatch loss of less than 0.2 dB. The major disadvantage of the non-linear system is its increased sensitivity to Doppler shifts in the returned signal, and hence its use is restricted to applications where the expected Doppler shift is less than 1% of the centre frequency.

To achieve low time sidelobe performance, amplitude and phase errors within the loop are required to be of the order of 0.1 dB and 1 degree respectively.<sup>99</sup> Recent work<sup>107</sup> in multi-channel systems has led to examination of device matching by noise cancellation

techniques. Typical cancellation levels of  $>30$  dB were found in devices with bandwidths in the range 2 to 30 MHz and time delays in the range 2 to 40  $\mu$ s.

Other applications for SAW DDL's include variable delay modules,<sup>108</sup> Fourier transform processors<sup>108</sup> and frequency synthesisers.<sup>7</sup> The FT processor reduces the standard Fourier integral to a series of multiplications and convolutions using linear FM waveforms. A number of SAW DDL FT processor configurations have been reported<sup>109</sup> but the best known of these is the compressive (or microscan) receiver<sup>105</sup> which provides a broad band, high resolution, instantaneous signal detection facility. Table 3.5 illustrates the performance capabilities of compressive receivers using IDT, RAC and IMCON devices. SAW spectrum analyser equipments are available<sup>110</sup> which provide : (1) 100 point spectral resolution of analog or digital signals within a 6 MHz bandwidth in 50  $\mu$ s, and (2) 500 point spectral resolution within a 25 MHz bandwidth in 40  $\mu$ s.

The output of a FT processor for a CW input signal is a single time domain impulse (a narrow  $\sin x/x$  response with suppressed side-lobes in practice) whose position in time is determined by the input frequency. Conversely, an inverse FT processor should produce a CW output burst for an input impulse function, where the frequency of the output signal is controlled by the relative timing of the input pulse. This method for frequency synthesis was initially postulated by Atzeni<sup>7</sup> and is the subject of more detailed investigation in Section 3.4.3, Chapters 4 and 5.

The variable delay module utilises the dispersive characteristic of the SAW DDL to offer differential delays to signals of varying

centre frequency. Figure 3.9 illustrates a suitable variable delay line (VDL) configuration which has demonstrated<sup>111</sup> continuously variable delay between 10 and 20  $\mu$ s for signals with 15 MHz bandwidth and 100 MHz centre frequency.

SAW bandpass filters have many applications in radar and communications equipment, but their impact has been most noticeable in the field of TV IF filtering.<sup>104</sup> Due to the transversal nature of SAW filters, complex amplitude and group delay functions such as illustrated in Figure 3.10 can be realised. However, the most significant factor in this application for the TV manufacturer is the availability of small size, low cost components which reduce the complexity of the IF strip and need no elaborate setting up procedures. These devices are currently produced at a rate of millions per annum using mass production techniques similar to those of the semiconductor industry. The response shown in Figure 3.10 is produced by a filter manufactured on lithium niobate and mounted in a T08 can with a selling price of approximately 75 pence for large quantities.

Other uses for SAW bandpass filters are in noise and bandwidth reduction applications.<sup>26</sup> Table 3.6 lists the current and projected performance levels available for these devices along with that of the SAW resonator. The SAW resonator<sup>112</sup> is a reflective device which offers a potentially higher Q-factor ( $>10,000$ ) than the conventional transversal filter. It has the advantage of lower insertion loss (3 dB to 6 dB) than IDT designs but suffers from poor out of band rejection (typically  $<30$  dB).

A more recent use of SAW bandpass filters has been in the generation and detection of MSK waveforms<sup>25</sup> for spread spectrum communications as discussed in Chapter 2.

Non-dispersive SAW delay lines and resonator structures can be incorporated in the feedback loop of a high gain amplifier to realise a SAW oscillator.<sup>113</sup> This and other SAW techniques for frequency synthesis are reviewed in more detail in Section 3.4 due to their particular relevance to this thesis.

Phase coded tapped delay lines<sup>52</sup> and convolvers<sup>53</sup> were discussed in Chapter 2 due to their significance in spread spectrum communications where they can provide fast synchronisation acquisition or code correlation for short duration burst transmissions. 13-bit Barker code devices have been produced<sup>114</sup> which exhibit correlation side-lobes of -21 dB with respect to the peak response. The maximum number of taps predicted<sup>32</sup> for a fixed coded device is 1024, whilst the added complexity of switching networks reduces this number to approximately 128 for programmable devices. In situations where programmability is essential, the SAW convolver provides the best option with time bandwidth products in the range 500-1000. Techniques for recirculating delay lines have been demonstrated<sup>56</sup> which yield an increase of  $10^3$  in the available TB, and more recent investigations<sup>55</sup> into acousto electric convolvers have reported techniques for further improvement.

### 3.4 SAW TECHNIQUES FOR FREQUENCY SYNTHESIS

SAW technology has introduced a mixture of novel and conventional techniques into the field of frequency synthesis. These are of particular interest for fast frequency hopping (FFH) applications (see Chapter 2) where they combine the advantages of wideband, fast switching performance with low power operation and rugged, compact construction.

Three main groups can be defined for ease of description : filter banks, oscillators and chirp techniques. Each of these are described in the following sections, and their relative merits discussed in Section 3.4.4.

#### 3.4.1 SAW Filter Banks

SAW bandpass filters can be designed to exhibit a  $\sin x/x$  frequency response as illustrated in Figure 3.11. The associated time domain impulse response of this filter is a rectangular burst of sinusoid with frequency  $f_0$ , where  $f_0$  is the centre frequency of the filter, and duration  $\tau$ , where  $\frac{1}{\tau}$  is the null spacing of the  $\sin x/x$  envelope. By impulsing such a filter with a short duration, high energy pulse, a rectangular burst signal is generated, and by repetitive impulsing at a rate equal to  $\frac{1}{\tau}$ , a CW waveform is obtained.<sup>116</sup> When this technique is employed for frequency synthesis, a separate filter is required for each individual output frequency (unless individual outputs are combined as in the direct synthesis technique described in Section 3.2.1).

Using SAW filter design techniques, it is possible to design a bank of filters with identical frequency responses, each separated in

centre frequency by  $\frac{1}{\tau}$ . In this way an impulse train with repetition period  $\tau$  can be fed in parallel to the filter bank and the desired output selected in an appropriate switching network. Since the desired output has a response null coincident with all adjacent filter peaks, high spurious signal suppression is potentially available.

Considerable investigation of this technique<sup>115-124</sup> has been made, but perhaps the most significant of all is that by Carr et al.<sup>117-123</sup> They have demonstrated a synthesiser which comprises a 16-channel SAW filterbank with a 16-input/1-output silicon-on-sapphire (SOS) PIN diode switch array. The individual filters have a response of the form

$$\frac{\sin(x)}{(x)} \cdot \frac{\sin(2x)}{(2x)}$$

where  $x = \pi(f - f_0)/f_c$

$f$  = applied frequency

$f_0$  = filter pass frequency

$f_c$  = null separation = reference clock frequency

This is a combination of 2 filter responses, one with nulls at  $f_c$ , the other with nulls at  $f_c/2$ , resulting in an overall response with very deep nulls spaced by  $f_c$ . Frequency selection is achieved in the SOS diode array, and on/off ratios in excess of 50 dB have been observed, with a switching time of less than 5 ns. Considerable care must be taken during the design and packaging of this unit to minimise spurious signals generated both in the SAW device and due to electromagnetic breakthrough.



This technique provides a coherent, fast switched output with stability dependent on the external reference clock. It does, however, suffer from complex fabrication problems both in relation to the switch network and the difficulty of multiplexing the pulse train into the filter bank when a large number of output frequencies or wide bandwidth operation is required. In view of these factors it would appear that the SAW filter bank synthesiser is best suited to operation over bandwidths of 50 MHz - 100 MHz with between 10 - 20 available output frequencies. A recent paper by Zaken et al<sup>124</sup> demonstrated the combination of a 10 channel filter bank with direct synthesis techniques to provide 100 output frequencies spaced by 1 MHz in the range 420 MHz to 519 MHz. A switching speed of 3  $\mu$ s was measured which was primarily due to filter response times in the direct synthesiser IF section.

### 3.4.2 SAW Oscillators

#### 3.4.2.1 Single Mode Oscillators :

The single mode oscillator,<sup>113</sup> illustrated in Figure 3.12, incorporates a VHF/UHF SAW delay line in the feedback loop of a high gain amplifier. This configuration can support a comb of  $n$  frequencies  $w_n$  when the condition

$$w_n \tau_d + \theta_e = 2n\pi$$

where  $\tau_d$  = SAW delay -  $\mu$ s

$\theta_e$  = electrical phase shift of  
magnitude  $\ll w_n \cdot \tau_d$

$n$  = integer

is satisfied. A single mode is selected from this comb by the frequency response of the SAW delay line, which is designed to have nulls at all other comb frequencies. This produces an output with high short term stability (ie, good spectral purity or single sideband noise performance) but with poorer medium and long term characteristics. in comparison to a conventional crystal oscillator. By including a variable phase network ( $\theta_e$ ) in the feedback loop, the oscillator can be tuned over a bandwidth which is related to the Q or number of wavelengths in the SAW filter. With values of  $\theta_e$  in the range  $+\pi/2$  to  $-\pi/2$  the bandwidth ( $\Delta f$ ) is expressed by  $\pm \frac{f_0}{4L}$  where L is the delay line length <sup>measured as</sup> the total number of wavelengths at the centre frequency.

Bale et al <sup>6</sup> have demonstrated a method for repetitively defining the starting phase of a SAW oscillator. This entails impulsing the oscillator with sufficient energy at the frequency of interest to allow the subsequent build-up of oscillation. The loop settling time is found to be equivalent to approximately 10 recirculations (or  $10 \tau_d$ ) which limits this technique to slow switching applications. Faster switching over the same bandwidth could be made possible by two or more identical oscillators, arranged such that one only was connected to the output whilst the other(s) switched frequency. Alternatively, a number of similar oscillators with varying centre frequency could be combined as in a direct synthesiser (see Section 3.2.1) to increase the operating band and the number of output frequencies.

### 3.4.2.2 Multimode Oscillators :

The same configuration as the single mode oscillator (Figure 3.12) can be used with a wideband SAW delay line in the feedback loop, hence

permitting oscillation at a large number of the available modes. Once again, Bale et al<sup>6</sup> have demonstrated such a system where individual modes are selected by injecting a narrowband pulse at the desired frequency to excite oscillation at the corresponding mode. They have reported a system using a 2.3  $\mu$ s SAW delay line with a centre frequency of 70 MHz and demonstrated selection of modes spaced by 435 kHz between 54 MHz and 92 MHz. Coherent operation between frequencies is possible provided the associated excitation pulses are also coherent.

It was also shown that not all possible modes could be excited and that in some cases several modes appeared to be supported simultaneously (a feature known as multimoding). Recent theoretical and experimental work,<sup>125</sup> has indicated that these problems arise primarily as a function of the delay line frequency response, and it is hoped that these can be reduced by suitable SAW device design.

As with the single mode oscillator, frequency switching requires approximately 10 recirculations of the feedback loop, and hence fast switching operation requires a number of oscillators in parallel.

#### 3.4.2.3 Discriminator Oscillator :

A variation on the single mode oscillator is the discriminator oscillator<sup>126</sup> illustrated in Figure 3.13. This follows the principle of indirect synthesis (as described in Section 3.2.2), where the output from a conventional VCO is input to a SAW frequency discriminator and the subsequent output used to control the VCO frequency. The length of the SAW delay line governs the discriminator response and hence the tuning range of the oscillator,

and to maintain high spectral purity, a delay line of long duration (ie,  $100 \lambda$ ) is required. To increase the available tuning range without reducing the stability, a double loop system can be used, with a short duration ( $\sim 10 \lambda$ ) delay line for coarse tuning, and the original delay line for fine tuning (as illustrated in Figure 3.14 (a) and (b)).

In this configuration it is common to divide the VCO output prior to the SAW discriminator. This has the advantage of increasing the fundamental operating frequency at the expense of reduced stability. The maximum operating frequency is currently limited by digital division technology to  $\sim 1.5$  GHz. A SAW discriminator oscillator of this type has been reported<sup>127</sup> with an operating frequency of 1.425 GHz, and direct VCO modulation capability of 1 MHz.

Like the single mode oscillator this technique is most suited to slow (ms) switching applications over 1% - 5% bandwidths. Performance for FH applications can be improved by suitable combination of a number of identical oscillators as before.

#### 3.4.2.4 Mode Locked Oscillator :

This technique, reported by Gilden et al,<sup>128</sup> is a variant of the multimode oscillator, and is based on the block diagram of Figure 3.12. In this case, the feed back loop contains a non-linear element known as an amplitude expander, which maintains the circulation of a narrow RF pulse which contains the Fourier components of all the possible modes. The time domain output takes the form of an RF pulse train with repetition rate equal to the

reciprocal of the SAW device delay,  $\tau_d$  and pulse width approximately equal to the reciprocal of the SAW device bandwidth (B). The equivalent frequency domain output comprises a comb spectrum of  $n$  frequencies spaced by  $1/\tau_d$  over a bandwidth, B. The oscillation can be self starting<sup>129</sup> or alternatively can be induced by a synchronised trigger pulse as in the multimode oscillator of Section 3.4.2.2.

Gilden et al<sup>128</sup> reported a mode locked oscillator operating at 100 MHz with 20 MHz bandwidth, and 556 kHz resolution. It should be noted however that this device is not directly capable of generating FH waveforms, but can be used as a comb generator for direct frequency synthesis or filter bank techniques as described in the following section.

#### 3.4.2.5 Multimode Oscillator and Filter Bank :

Adkins<sup>130</sup> has reported a combination of the mode locked oscillator and the SAW filter bank to achieve fast frequency hopping. This system combines additional transducers on the substrate of the oscillator delay line which are designed to select individual frequencies from the generated comb spectrum.

Each output transducer has a  $\sin x/x$  response with null separation equal to the comb spacing. In this way the adjacent comb frequencies are suppressed and the required output can be selected by a PIN diode switch array. Experimental results for a 140 MHz oscillator with 10 MHz mode spacing and two mode selection transducers at 130 MHz and 140 MHz have been reported.<sup>130</sup> The diode switches were stated to have an isolation of 60 dB and

switching time of 2 ns, but due to high electromagnetic breakthrough and SAW insertion loss the spectral purity was only 20 dB.

This technique is limited in bandwidth by the capabilities of the SAW oscillator, and the number of potential output frequencies is limited by the resultant complexity of the SAW device design.

### 3.4.3 Chirp Synthesis Techniques

#### 3.4.3.1 Introduction :

Chirp synthesis is based on mixing two time delayed but overlapping linear FM waveforms. Figure 3.15 illustrates the two useful system configurations known as difference and sum frequency modes respectively.

In the difference frequency mode, two chirp waveforms with identical start frequency ( $\omega_1 = \omega_2$ ), dispersive slope  $\mu$ , and time separation  $\tau$ , are combined in a mixer and the difference product (or lower sideband) selected in a low pass filter. The resultant output is a pulse of frequency  $(\omega_1 - \omega_2 + \mu\tau)$  existing for  $\tau < t < T$ , where  $T$  is the duration of the chirps. During the periods  $0 < t < \tau$  and  $T < t < T + \tau$ , unmixed portions of the chirp waveforms can be removed by a suitable time gate.

The waveforms used in sum frequency generation again have dispersive slopes of equal magnitude, but this time differing in sign (ie,  $|\mu_1| = |\mu_2|$  but  $\mu_1 = -\mu_2$ ). In this case, the sum frequency product (or upper sideband) is selected in a bandpass filter following the mixing process. The output pulse has a frequency given by  $(\omega_1 + \omega_2 - \mu\tau)$ , which exists for  $\tau < t < T$ , and again it is possible

to remove unwanted sections of the original waveforms by time gating.

From consideration of the above, it can be seen that the output frequency in each case is dependent on the chirp start frequencies ( $\omega_1$  and  $\omega_2$ ), their dispersive slope ( $\mu$ ), and their time separation ( $\tau$ ). The duration of the output pulse is defined by  $\tau < t < T$ , and it is convenient to define a value for  $\tau_{\max}$  which in turn allows a pulse of constant length  $\tau_{\max} < t < T$  to be selected by time gating. Since  $\omega_1$  and  $\omega_2$  are fixed parameters the synthesiser output frequency is determined by the value of  $\tau$  selected in the range  $0 < \tau < \tau_{\max}$ . In this way the total synthesiser bandwidth is defined by  $\mu\tau_{\max}$  for difference frequency operation and by  $2\mu\tau_{\max}$  (ie, frequencies in the range  $+\mu\tau_{\max}$  to  $-\mu\tau_{\max}$ ) for sum frequency operation. If  $\tau$  is varied in discrete steps under the control of a stable reference clock, a multifrequency wideband synthesiser is produced with accuracy and stability related to that of the reference source and the digital control electronics.

This technique has a variety of implementations which differ mainly in the way in which the chirp waveforms are generated and the variable time delays achieved.

#### 3.4.3.2 SAW Chirp Mixing :

As described in Section 3.3.2, the SAW chirp filter provides a convenient method for linear FM waveform generation. In this approach the chirp waveform is generated by impulsing a SAW dispersive delay line. This impulse can in turn be controlled by a stable reference source, via suitable electronics, to achieve the accurate time delay required between chirp signals.

Atzeni et al<sup>7</sup> first reported this technique using chirp filters with 30 MHz centre frequency and dispersive slope of 100 kHz/ $\mu$ s. Output signals were demonstrated at difference and sum frequencies.

Grant et al<sup>131</sup> reported the development of the technique for use in the generation of continuous output frequency hopped (FH) signals by time interlacing two identical channels. This configuration was also novel in that it used one chirp filter only, fed by an impulse pair separated in time by the desired value of  $\tau$ . The chirp filters used had 60 MHz centre frequency, 25 MHz bandwidth, and 5  $\mu$ s nominal time dispersion. The output from each channel was gated over the period  $2.5 \mu\text{s} < t < 5 \mu\text{s}$  allowing 12.5 MHz bandwidth. The generation of coherent operation was demonstrated by correlation in a SAW degenerate acoustic plate convolver.

Hannah et al<sup>132</sup> extended the work of Grant using two SAW chirps per channel to demonstrate programmable CW difference frequency generation. Phase coherence with a waveform derived from the reference clock was demonstrated to be within 2 degrees at an output frequency of 4.8 MHz. The desired signal to spurious level was -24 dBc, and the SAW filters used were identical to that used by Grant.

Hannah subsequently demonstrated sum frequency operation using the same equipment, but one filter in each channel was replaced by a device identical in characteristic but opposite in dispersive slope. An output signal with 50% duty cycle at 110 MHz was generated with phase coherence of  $<2^\circ$  compared to the reference source. This configuration was capable of hopping over the full chirp bandwidth (25 MHz), with a hop duration of 2.5  $\mu$ s. Switching time between



hops is related to that of the gating signal, which can be as fast as 1 ns, whilst the overall stability is related to the master clock.

Patterson, Dods and Hannah<sup>133</sup> reported a 2-channel PN code controlled chirp mixing synthesiser with a 100% duty cycle operating in both FH and CW modes. A total of 63 hops, each with a duration of 2.5  $\mu$ s, was demonstrated over a 26 MHz band centred on 120 MHz. Selection of a single frequency in the band produced a CW output with spurious signal suppression of >30 dB.

Results from computer simulations showed that this high level of spurious signal could be attributed to amplitude or phase errors in the synthesised waveforms, and careful design and construction techniques could reduce this to >40 dB with available high performance SAW devices.

Finally, Darby et al<sup>134</sup> presented a comparison of two chirp synthesiser equipments, one as described by Patterson et al<sup>133</sup> and the other exhibiting 127 hops each with duration of 2.5  $\mu$ s, operating over a bandwidth of 50 MHz in the frequency range 335 to 385 MHz. This paper includes a discussion of error mechanisms within the chirp mixing process and their effects on the synthesised output. It also discusses the effect of mismatch between transmit and receive signals on FH link performance.

Due to the potential capabilities of this system in comparison to the other SAW frequency synthesis techniques described in this section (see Section 3.4.4), the remainder of this thesis is dedicated to a fuller investigation of this subject.

### 3.4.3.3 Discrete Chirp ROM :

This technique described by Alsup et al<sup>135</sup> is similar to that described in the above section. In this case, however, the continuous SAW chirp filter is replaced by a discrete version. The system configuration is similar to that suggested by Grant<sup>131</sup>, but the discrete filters appear like serial access read-only-memories (ROM's). An alternative method intended to improve performance, suggested the use of a prime sequence filter as an acoustic random access ROM. Both techniques have the disadvantage that the output waveform is of a sampled nature.

### 3.4.3.4 Tapped Delay Line :

The third SAW chirp technique reported by Manes et al<sup>136</sup> and Alsup et al<sup>135</sup> combines two contra-directed chirp waveforms in a SAW tapped delay line. As both chirps are simultaneously launched from opposite ends of the filter, the time delay required between the two signals to generate a particular frequency is achieved by the spatial positioning of the taps on the SAW substrate. In this way the number of output frequencies available is dictated by the number of taps on the SAW substrate. When the two chirp signals are detected at any one tap, they are input to a mixer and the desired product selected by filtering. Either difference or sum operation can take place according to the format of the input chirp signals.

The most attractive feature of this technique lies in the ability to use active chirp generators. This allows the use of long time-duration signals, which in turn allows the generation of long duration bursts of output signal. The number of output frequencies is however,

limited by the number of taps physically realisable on the SAW substrate, and the overall insertion loss of the device.

#### 3.4.4 Comparison of SAW Synthesis Techniques

SAW technology provides a wide variety of synthesis techniques, each of which can be attractive for a particular application. Table 3.7 lists the various techniques and gives a rating of their relative performance in terms of operating frequency, bandwidth, output frequencies, switching speed and spectral purity.

The single mode and discriminator oscillators represent stable frequency sources, but are limited in their application to fast frequency hopping due to their narrow band operation and slow switching speed. The multi mode oscillator is potentially attractive, but there are considerable technological problems in exciting the desired mode and in preventing multimoding. As a single device this approach would still have a slow switching speed, and some form of parallel operation is required for fast switching applications.

The filter bank techniques are much more attractive for FH applications due to the inherently high switching speed. This approach provides high spectral purity with fast (ns) switching speed. At present, however, the SAW/SOS diode fabrication and the device packaging constraints limit the number of available output frequencies to between 20 and 30.

For wideband fast switching multifrequency operation, chirp techniques present the most attractive option from those discussed above. Of the three chirp methods described, chirp mixing using

SAW linear FM filters provides the most flexible solution. The discrete chirp ROM holds no advantage over the continuous version, and has the disadvantage of a sampled output. The tapped delay line technique allows the use of active chirp generation which enables the synthesis of long duration frequency bursts. However, for short duration hops required in fast FH applications, SAW linear FM filters provide a more convenient method for generating the chirp signals, and there would appear to be no advantage in combining these in a SAW tapped delay line. In fact, the extra fabrication complexity would be both costly and limiting in the number of available output frequencies.

For these reasons, SAW chirp mixing appears to be the optimum SAW frequency synthesis technique for generating coherent, wideband, fast switching waveforms when a large number (ie, >100) of output frequencies are required. Current SAW devices can be used to generate waveforms with >100 MHz bandwidth, nanosecond switching speed, and potentially 100's of output frequencies.

PERFORMANCE FEATURE	DIRECT SYNTHESIS	INDIRECT SYNTHESIS
Percentage Bandwidth	<15	octave and wider; limited only by VCO capability
Resolution	<1 Hz	1 to 100 kHz using basic loop; <1 Hz using multiple loop techniques
Switching Speed	1 $\mu$ s - 100 $\mu$ s typ	1 ms to 10 sec typ; normally 20 to 30 times $(\frac{1}{f_{ref}})$
Spurious Suppression	100 dB max 60 dB typ	70 - 100 dB at frequencies offset by >10 loop bandwidths; 50 - 60 dB close in
Relative Complexity	large size, weight; complexity related to number of hops	small size, weight; minimum complexity
Relative Power Consumption	high	low

Table 3.1 Comparison of Direct and Indirect Frequency Synthesis

Material	Crystal Cut and Orientation	Velocity (Km/s)	$k^2$ (%)	$N_{opt}$	$W_{opt}$ (wavelengths)	Optimum Bandwidth (%)	Temp. Coeff of Delay (ppm/ $^{\circ}$ C)	Attenuation at 1 GHz (dB/ $\mu$ s)
LiNbO <sub>3</sub>	Y-Z	3.485	4.8	4	108	25	88	1.07
LiNbO <sub>3</sub>	41 $\frac{1}{2}$ $^{\circ}$ rot. X prop.	4.000	5.5	4	94	26.5	70	1.06
Quartz	Y-X	3.159	0.22	19	43	5.5	-24	2.6
Quartz	ST-X	3.157	0.15	23	35	4.4	$\sim 0$	3.1
Bi <sub>12</sub> GeO <sub>20</sub>	(100) (011)	1.681	1.40	8	26	14	-122	1.6
LiTaO <sub>3</sub>	Z-Y	3.329	1.2	13	31	8	69	1.0
AlN/Al <sub>2</sub> O <sub>3</sub>	X-Z	6.120	0.63	11	60	10	44	1.7*

\* at 200 MHz

Table 3.2 SAW Parameters of Some Common Materials

PARAMETER	IDT		RAC	
	CURRENT	FUT	CURRENT	FUT
Centre frequency (MHz)	10-1200	10-1500	60-1200	60-2000
Bandwidth (MHz)	1-500	1-750	1-500	1-1000
Time dispersion ( $\mu$ s)	05-50	01-80	1-100	05-120
T B	4-800	4-2000	40-16k	10-50k
Amp. ripple (dB p-p)	02	01	05	05
Phase error (deg rms)	05	02	05	05
Sidelobe suppression (dB)	-45	-50	-40	-45

Table 3.3 Current and Projected Performance Bound for SAW IDT and RAC Dispersive Filters

<u>DEVICE</u>	<u>APPLICATIONS</u>
DELAY LINE	Fusing, MTI Radar, Communications Path Length Equaliser, Altimetry, Time Ordering
WIDEBAND DELAY LINE	Recirculating digital storage
BANDPASS FILTER AND RESONATOR	Colour TV, Radar, Communications Satellite Repeaters, ECM, Frequency Synthesis
OSCILLATOR	Stable Source VHF to Microwave - Communications and Radar
TAPPED DELAY LINE	Fourier Transformation, Acoustic Image Scanning, Clutter-reference Radar, SSR, ECM Deception
*DISPERSIVE DELAY LINE ('CHIRP')	Radar Pulse Compression, Variable Delay For Target Simulation, Fourier Transformation (Spectral Analysis). Compressive Receiver, Group Delay Equalisation.
*PSK FILTER	Spread Spectrum Communications, Radar, Military ATC
CONVOLVER	Synchroniser For Spread Spectrum Communications, Fourier Transformation

\* matched filter

Table 3.4 Areas of Application for SAW Devices

	I.D.T		R.A.C		I.M.C.O.N	
	CURRENT	FUTURE	CURRENT	FUTURE	CURRENT	FUTURE
BANDWIDTH (MHz)	250	400	250	500	6	10
RESOLUTION (KHz)	40	20	20	10	0.4	0.15
MAXIMUM NUMBER OF TRANSFORM POINTS	500	2,500	3,600	10,000	6,000	25,000
DYNAMIC RANGE (LIMITED BY CLOSE IN SIDELOBES) (dB)	40	45	35	40	30	35

Table 3.5 Current and Projected Performance Bounds for SAW IDT, RAC and IMCON Compressive Receivers

Parameter	Current	Future
Centre frequency $f_0$ (Hz)	$10^7 - 10^9$	$10^6 - 2 \times 10^9$
3dB bandwidth (Hz)	$5 \times 10^4 - 0.4f_0$	$2 \times 10^4 - 0.8f_0$
Minimum loss (dB)	6	1.5
Minimum shape factor (ratio of bandpass width of 3dB and 40dB)	1.2	1.2
Minimum transition width from bandpass to bandstop (Hz)	$5 \times 10^4$	$2 \times 10^4$
Sidelobe rejection (dB)	55	65
Ultimate rejection (dB)	65	80
Amplitude of bandpass ripple (dB)	0.5	0.2
Linear phase deviation (degrees)	5	2

(a) Band Pass Filters

PARAMETER	CURRENT	PROJECTED
Frequency (MHz)	50 - 400	50 - 1500
Unloaded Q (at 200 MHz)	20,000	40,000
Spurious Suppression (dB)	-25	-40
Temperature Stability $f/f(\tau)$	$\left(\frac{T - T_0}{5.65}\right)^2 \times 10^{-6}$	$\left(\frac{T - T_0}{5.65}\right)^2 \times 10^{-6}$
Ageing (ppm/year)	10	0.5
Complexity	2 port, single pole	2 port, 4 pole

(b) Resonators

Table 3.6 Current and Projected Performance Bounds for SAW (a) Bandpass Filters and (b) Resonators

PERFORMANCE FEATURE	*FILTERBANK	*MULTIMODE OSCILLATOR	CHIRP MIXING
Number of Hops	<500	<500	<4000
Minimum Hop Spacing (kHz)	>50	>50	>50
Maximum Bandwidth (B) (MHz)	<500	<500	<500
Spectral Purity (dBc) CW Output	<-60	<-60	<-40
Switching Speed (ns)	<10	>10 <sup>4</sup>	<10
Clock Frequency	Hop Spacing	Hop Rate	$\frac{B}{2}$
Long Term Stability	Clock Dependent	Clock Dependent	Clock Dependent
Temperature Stability	Clock Dependent	Substrate Dependent	Substrate Dependent
Power Consumption (W)	~10	~10	~10

\* these assume the outputs of several basic synthesisers are combined

Table 3.7 Comparison of SAW FH Synthesiser Performance Capabilities



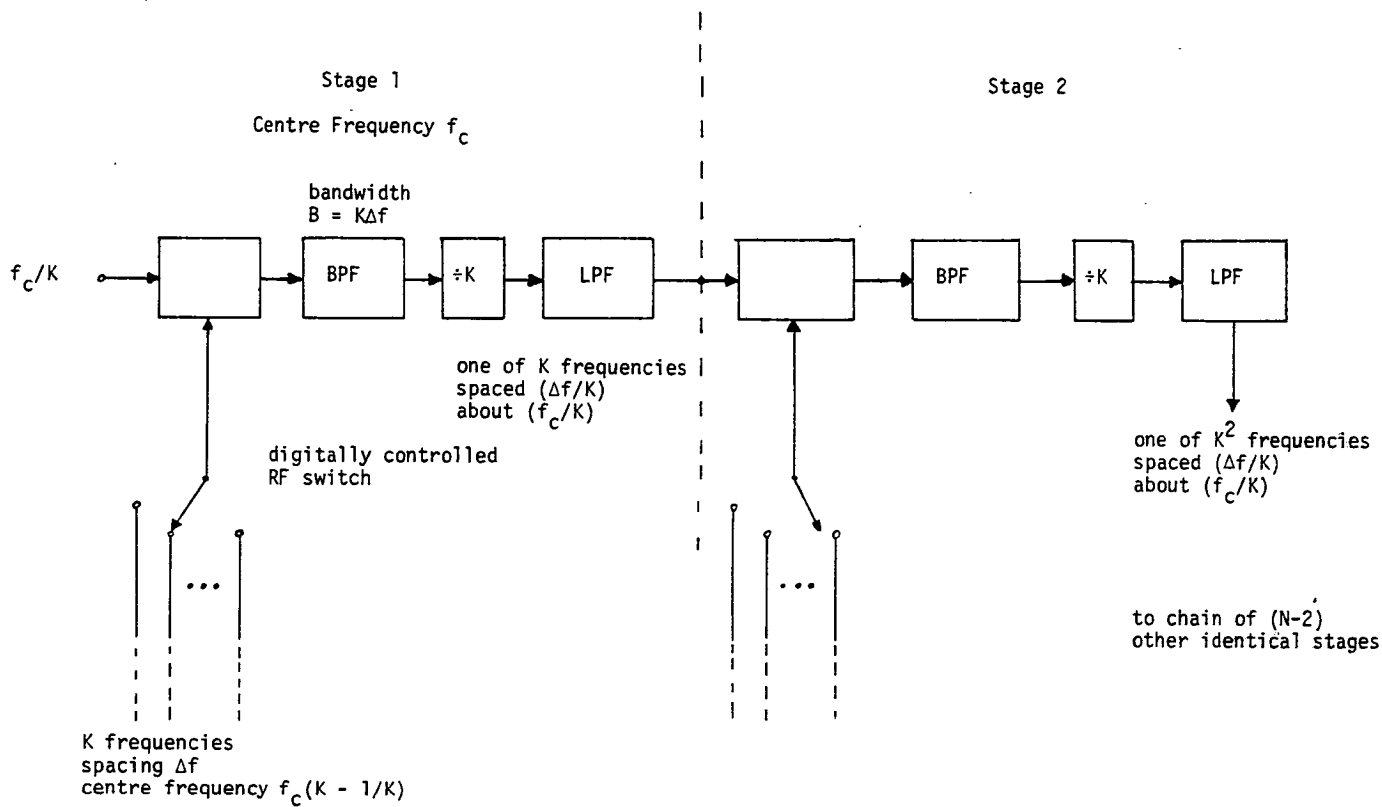


Figure 3.1 Iterative Direct Synthesiser : 2 of  $N$  Stages

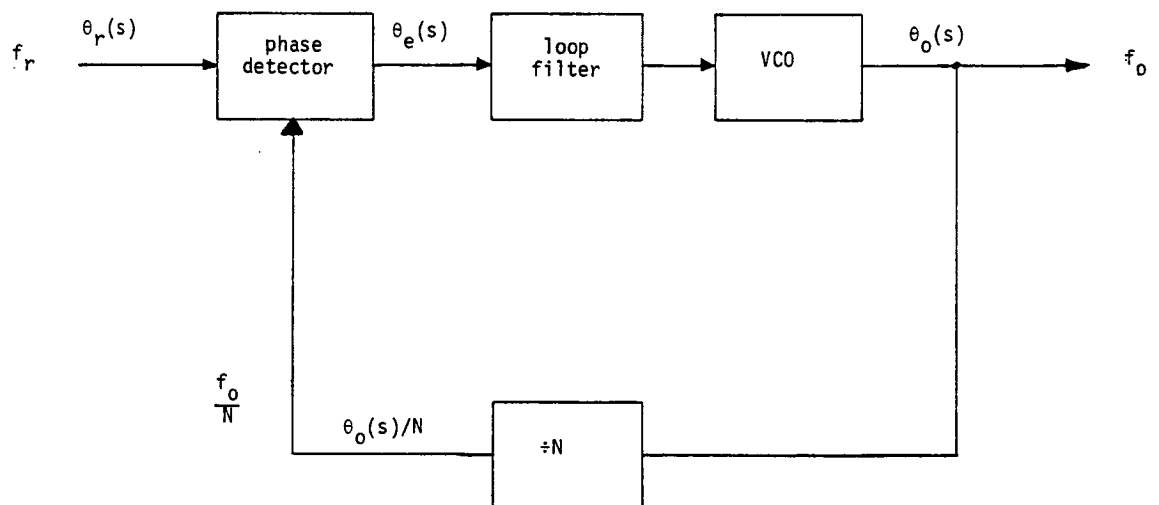


Figure 3.2 Indirect Phase Locked Loop Synthesiser

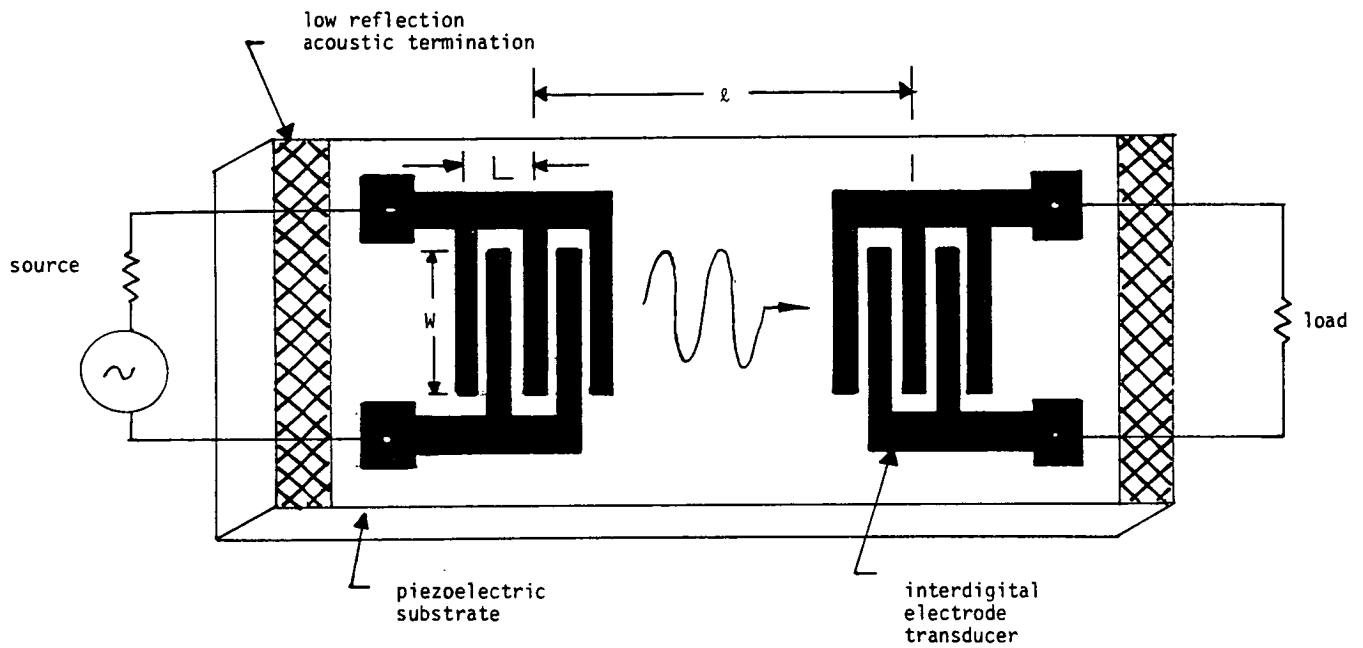


Figure 3.3 Schematic Diagram of a Simple SAW Delay Line

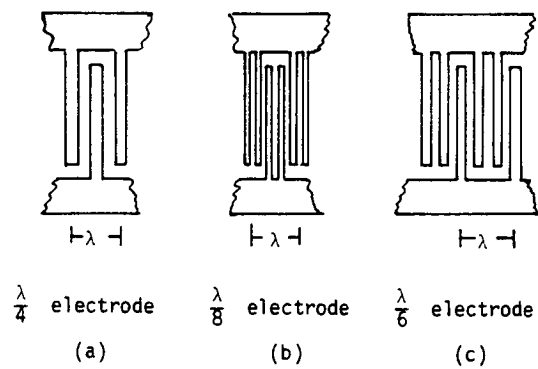


Figure 3.4 Interdigital Transducer Structures

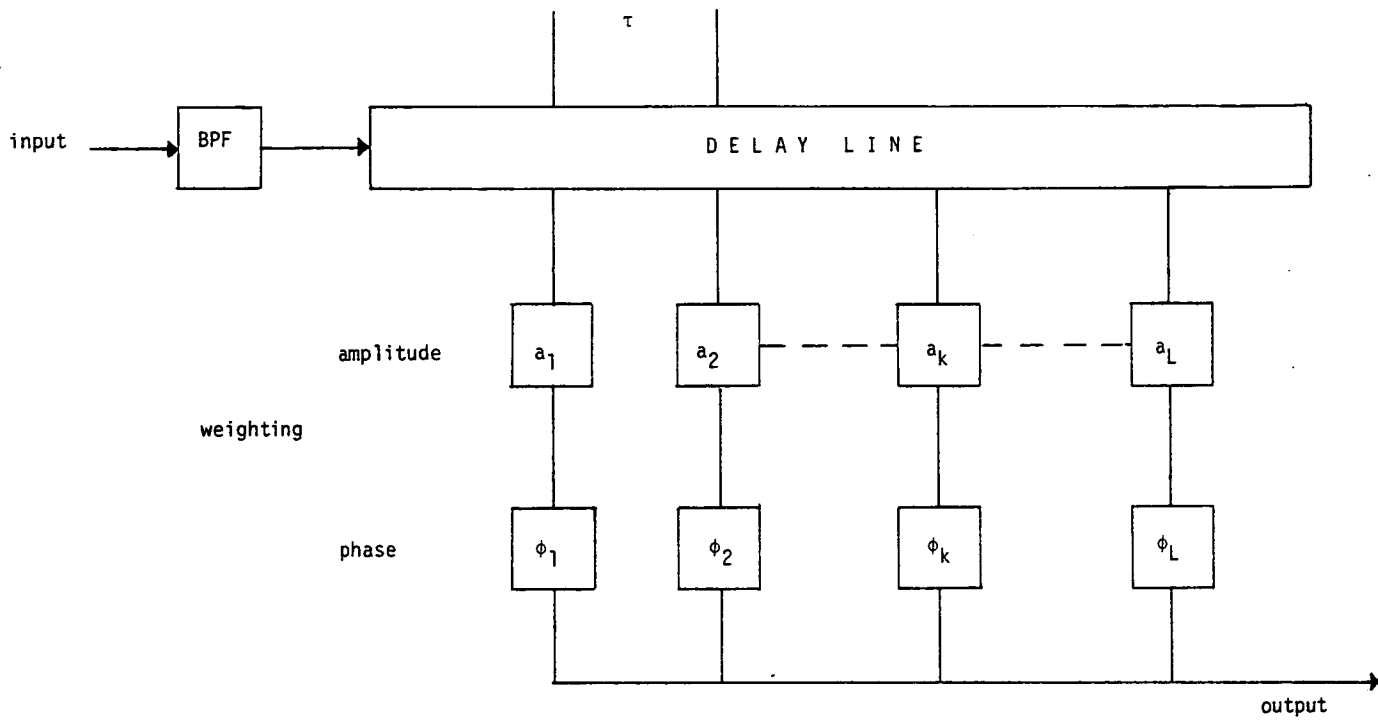


Figure 3.5 Schematic Configuration of Generalised Transversal Filter

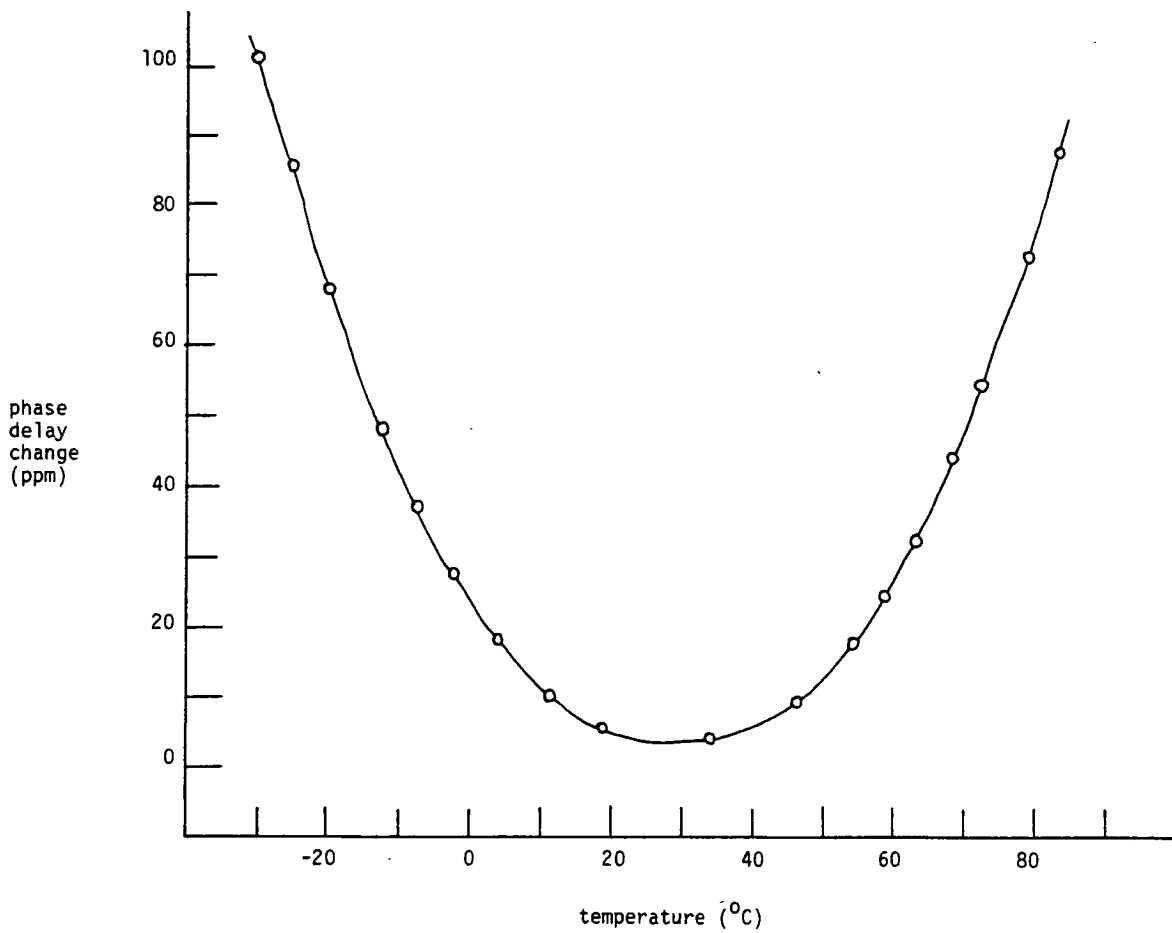


Figure 3.6 Temperature Stability of ST-X Cut Quartz

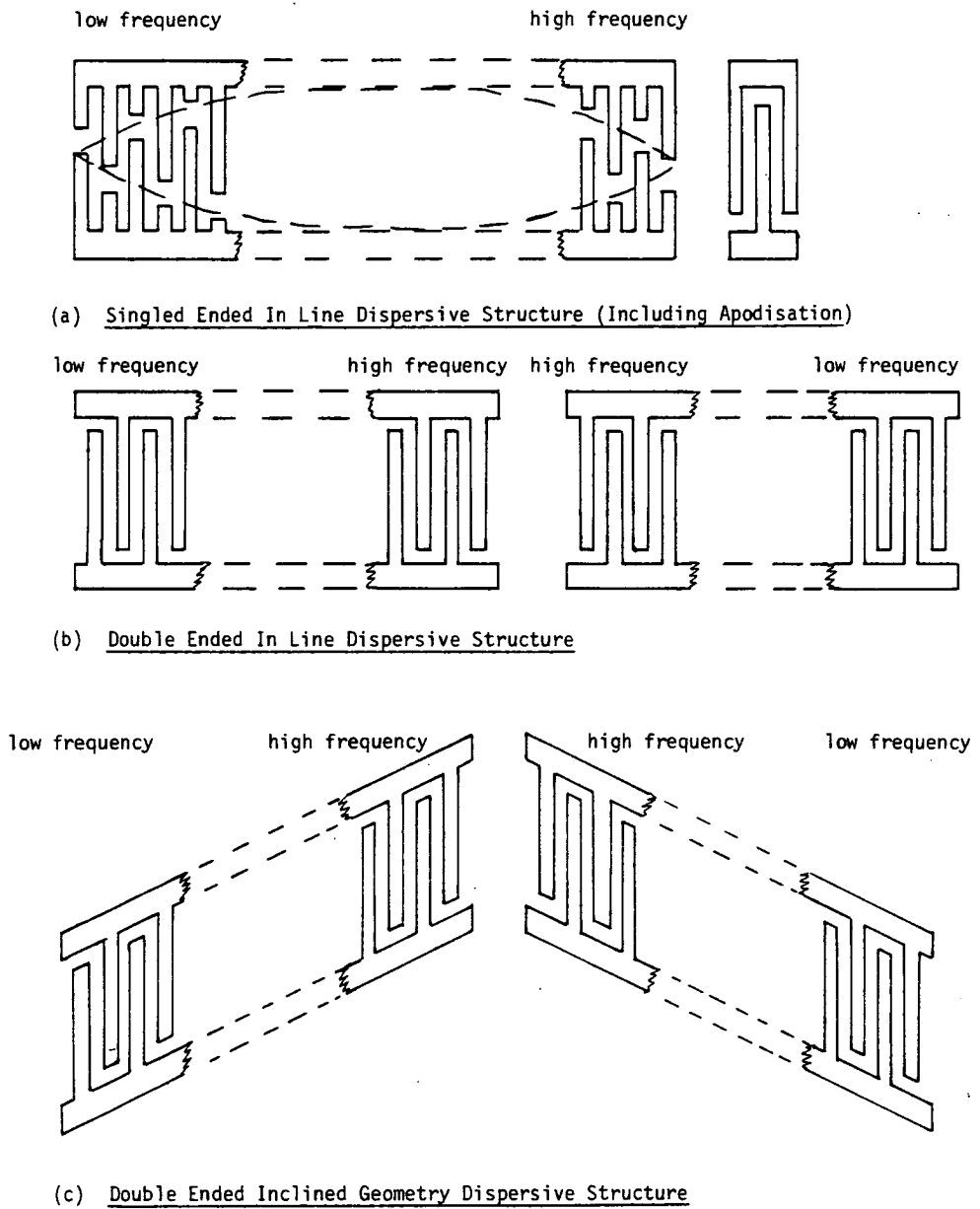


Figure 3.7 SAW Dispersive Delay Lines - Various IDT Structures

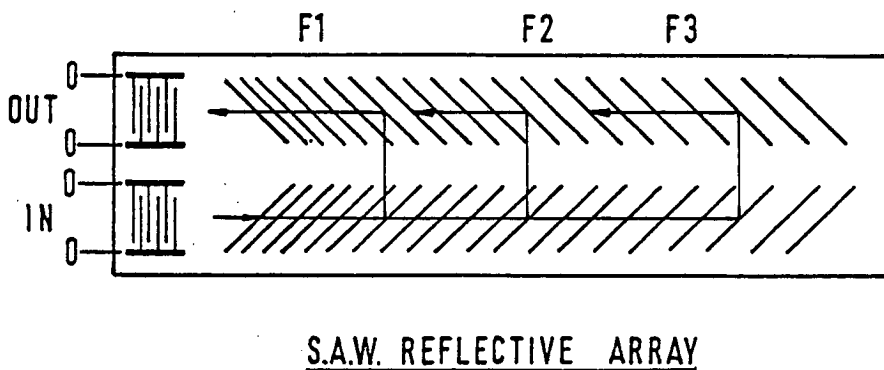


Figure 3.8 SAW Dispersive Delay Line Using RAC Structure

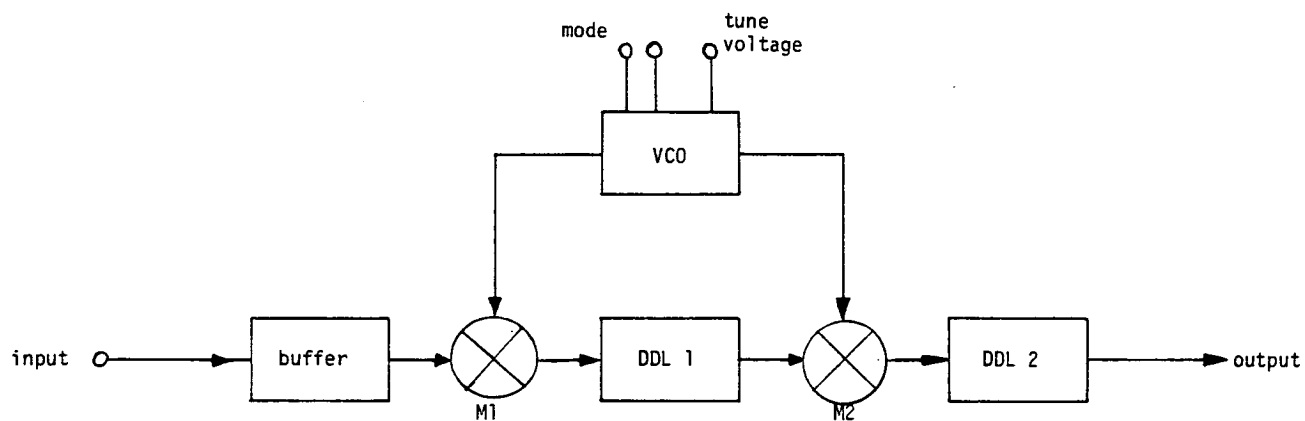


Figure 3.9 SAW Analogue Variable Delay Line

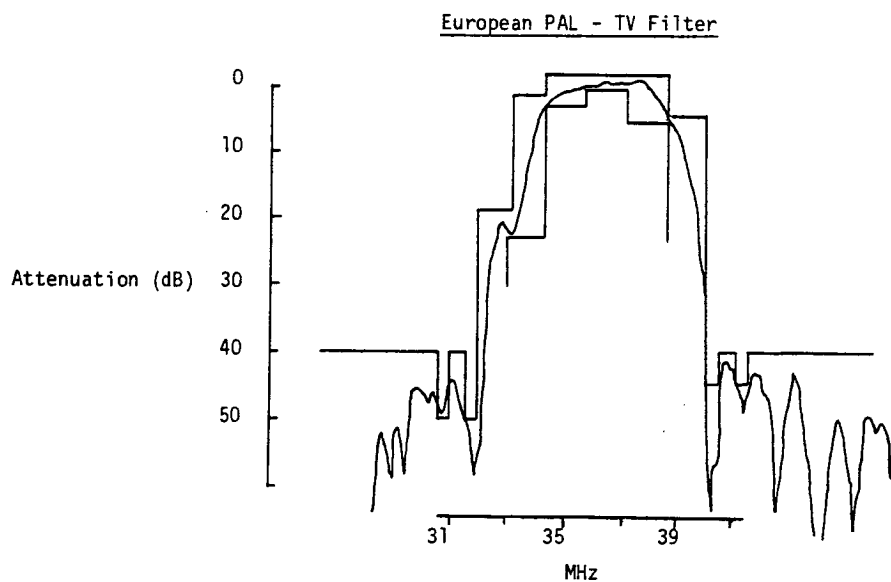


Figure 3.10 Required and Measured Responses of a SAW Filter

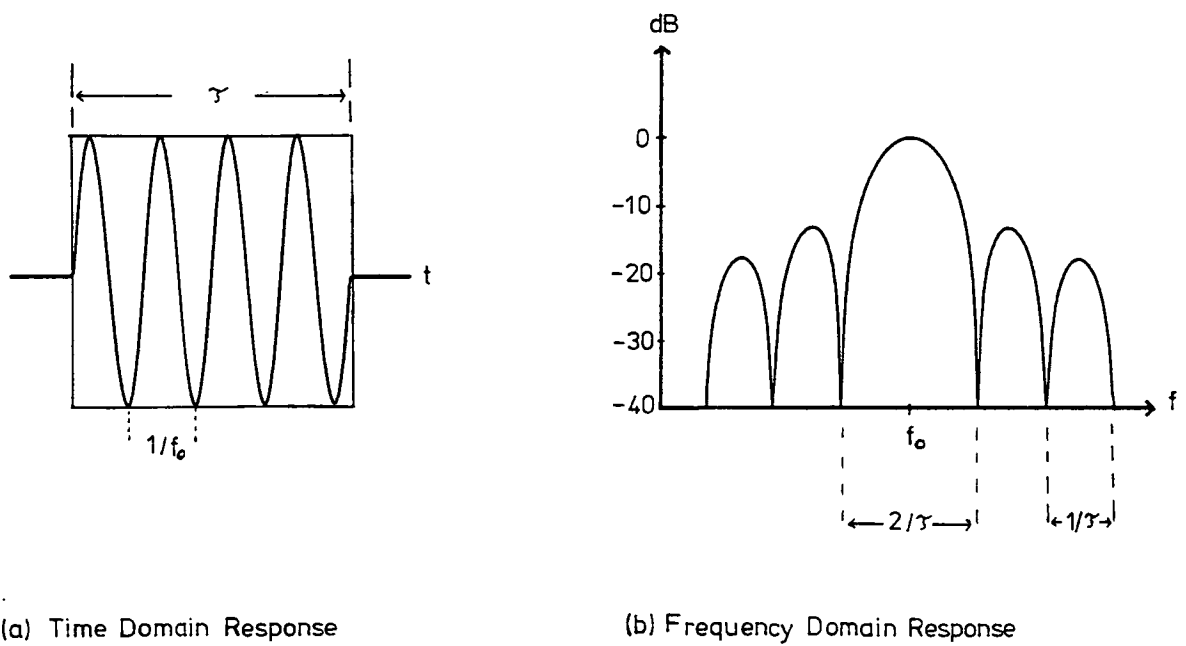


Figure 3.11 Frequency and Time Domain Responses of a Sin  $x/x$  Frequency Filter

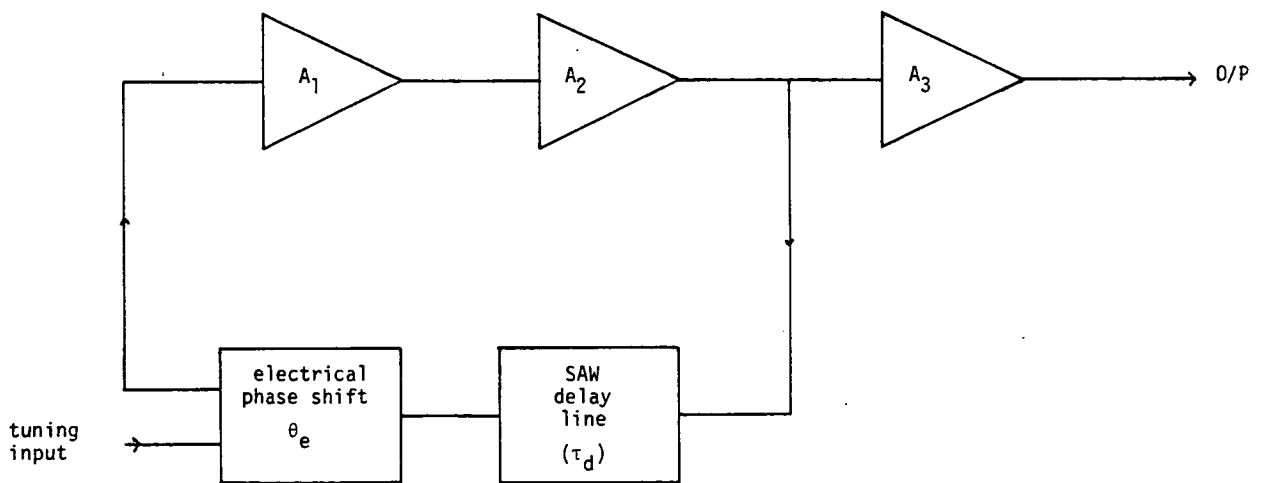


Figure 3.12 Delay Stabilised SAW Oscillator

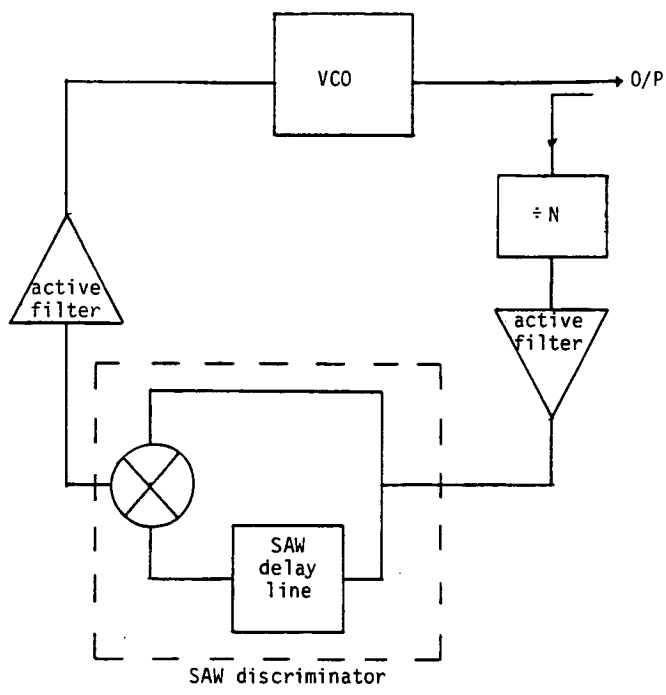


Figure 3.13 SAW Discriminator Oscillator

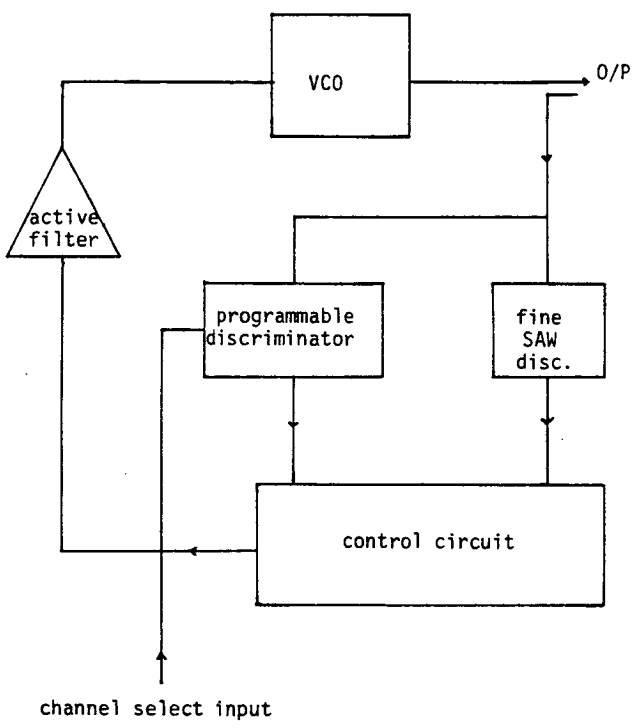


Figure 3.14 (a) Multimode SAW Discriminator Oscillator

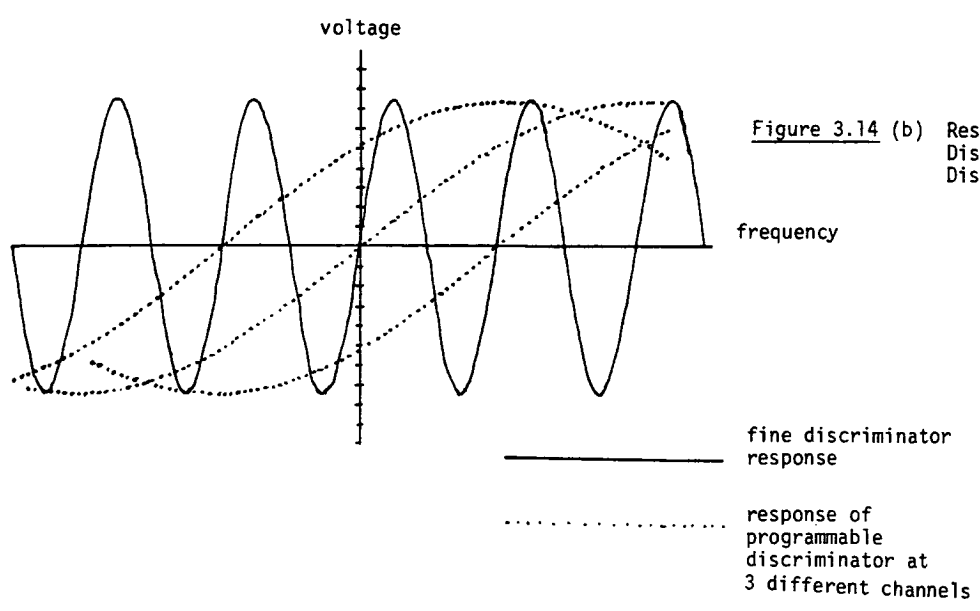
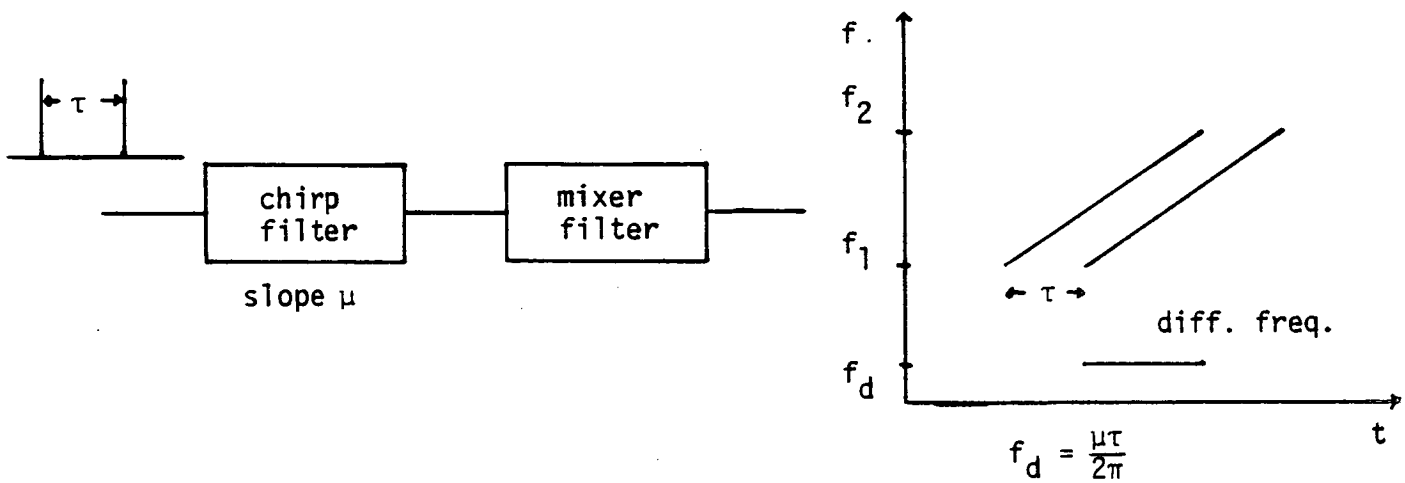
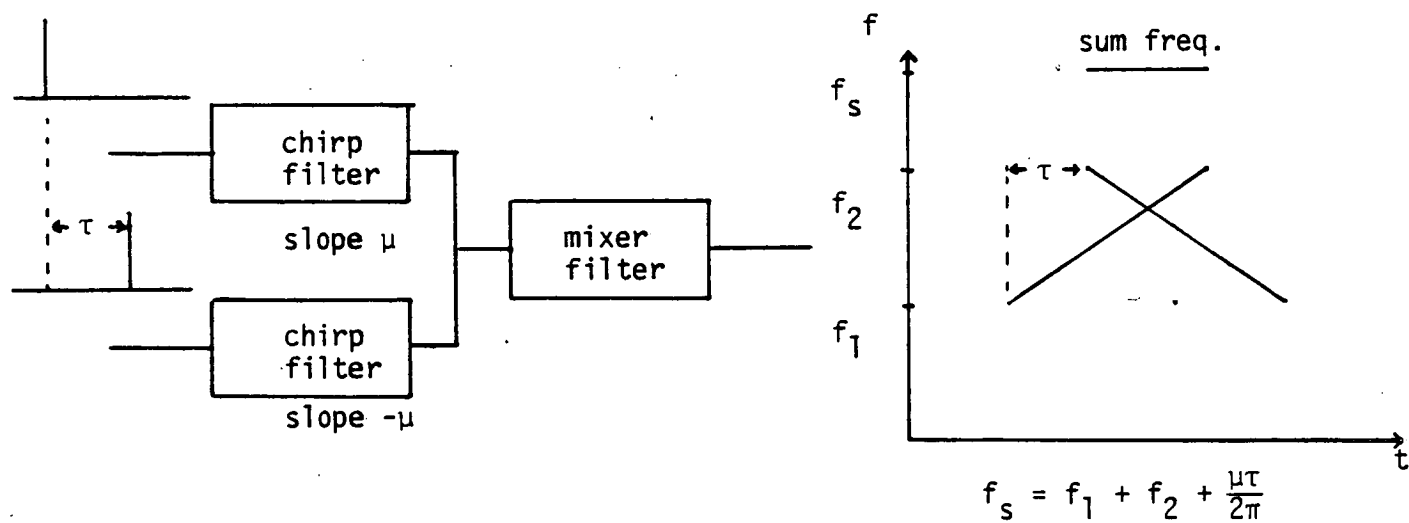


Figure 3.14 (b) Response of Programmable and Fine Discriminator in Multi-Mode SAW Discriminator Oscillator



(a) Difference Frequency Generation (using 1 chirp filter only)



(b) Sum Frequency Generation (can also be used for difference frequency)

Figure 3.15 Chirp Mixing Frequency Synthesis : Sum and Difference Product Generation



## CHAPTER 4 : THE DESIGN, CONSTRUCTION AND PERFORMANCE OF A SAW CHIRP MIXING SYNTHESISER

### 4.1 FREQUENCY SYNTHESIS BASED ON CHIRP MIXING

A variety of SAW techniques for frequency synthesis were described in Section 3.4, but for applications where fast switching, coherent operation is required with a large number of hops (>100) over a wide bandwidth, the chirp mixing technique provides the most attractive solution. The following section describes the theoretical basis for this synthesis technique.

The chirp mixing technique is based on mixing two time delayed but partially overlapping linear FM, or chirp, waveforms. For ideal operation, the two constituent chirp waveforms,  $s_1(t)$  and  $s_2(t)$ , can be expressed as

$$s_1(t) = \cos(\omega_1 t + \frac{1}{2}\mu_1 t^2) \quad 0 < t < T_1 \quad \dots \quad (4.1)$$

$$s_2(t) = \cos\{\omega_2(t - \tau) + \frac{1}{2}\mu_2(t - \tau)^2\} \quad \tau < t < T_2 + \tau \dots \quad (4.2)$$

where  $\omega_1$  and  $\omega_2$  are angular frequencies representing the chirp start frequencies,  $\mu_1$  and  $\mu_2$  are the chirp dispersive slopes,  $T_1$  and  $T_2$  the respective signal durations, and  $\tau$  the time delay between the two signals.

The product of the two waveforms is given by

$$\begin{aligned} s_t(t, \tau) = & \frac{1}{2} \cos \left[ \{(\omega_1 + \omega_2) - \mu_2 \tau\} t - \frac{1}{2} \mu_2 \tau^2 + \frac{1}{2} t^2 (\mu_1 + \mu_2) \right] \\ & + \frac{1}{2} \cos \left[ \{|\omega_1 - \omega_2| + \mu_2 \tau\} t + \omega_2 \tau + \frac{1}{2} \mu_2 \tau^2 + \frac{1}{2} t^2 (\mu_1 - \mu_2) \right] \\ & \text{for } \tau < t < T_1, \text{ if } T_2 \geq T_1 \quad \dots \quad (4.3) \end{aligned}$$

The two cosine terms in this equation represent sum and difference frequency products, which can be selected by bandpass filtering if suitable chirp parameters are selected. The instantaneous frequency associated with each product can be expressed by

$$\omega_s = (\omega_1 + \omega_2) - \mu_2\tau + (\mu_1 + \mu_2)t \quad \dots (4.4)$$

$$\omega_d = (|\omega_1 - \omega_2|) + \mu_2\tau + (\mu_1 - \mu_2)t \quad \dots (4.5)$$

In both these equations the first two terms represent a monotonic angular frequency which is dependent on the value of  $\tau$  for any fixed set of chirp parameters.

The third term in each case represents a residual chirp which can be removed by selection of the chirp parameters as illustrated graphically in Figure 4.1. From this diagram, it can be seen that a constant sum product is achieved by selecting  $|\mu_1| = |\mu_2| = |\mu|$  but  $\mu_2 = -\mu_1$  so that

$$\omega_s = (\omega_1 + \omega_2) - \mu\tau \quad \dots (4.6)$$

Similarly a constant difference product is achieved by selecting  $\mu_1 = \mu_2 = \mu$  so that

$$\omega_d = |\omega_1 - \omega_2| + \mu\tau \quad \dots (4.7)$$

For sum frequency operation the output signal has a centre frequency  $(f_1 + f_2)$  and, allowing for positive and negative variation of  $\tau$ , covers a bandwidth

$$B_s = \frac{\mu}{\pi} \cdot \tau_m \quad \dots (4.8)$$

where  $\tau_m$  represents the maximum permissible value of  $\tau$  (ie,  $\tau_m < T_1$ ).

Difference frequency operation generates an output with centre frequency  $|f_1 - f_2|$ , but due to spectral fold over at 0 Hz, the operating bandwidth is reduced for cases where  $|f_1 - f_2| < |\frac{\mu}{2\pi} \tau_m|$  such that

$$\begin{aligned} B_d &= |f_1 - f_2| + |\frac{\mu}{2\pi} \tau_m|, & |f_1 - f_2| < |\frac{\mu}{2\pi} \tau_m| \\ &= \frac{\mu}{\pi} \tau_m & |f_1 - f_2| \geq |\frac{\mu}{2\pi} \tau_m| \end{aligned} \quad \dots (4.9)$$

It should also be noted that  $B_s \leq f_2 \leq f_1$  to enable selection of the sum or difference product without mutual interference. A value of  $B_s = 0.5 \cdot f_2$  represents a realistic limitation based on practical filter characteristics. From this point onwards, it is assumed that values of  $f_1$  and  $f_2$  have been selected such that  $B_s = B_d = B = \frac{\mu}{\pi} \tau_m$  and  $B \leq 0.5 \cdot f_2$ .

In both cases, as  $\tau$  is varied, the overlap of  $s_1$  and  $s_2$  changes and hence the length of the output pulse varies. For frequency hopping applications, it is desirable to synthesise a mutually orthogonal set of output signals. This means that the frequency spacing of the generated waveforms should be  $1/T_H$ , where  $T_H$  is the hop duration. To achieve this, a constant hop length is necessary and the natural choice is dictated by the minimum possible hop duration which will result from a given maximum value of  $\tau$ ,  $\tau_m$ . By definition

$\tau_m < T_1 < T_2$ , and thus  $T_H$  can be defined as

$$T_H = (T_1 - \tau_m)$$

To maximise the number of orthogonal hops (N) and hence optimise  $\tau_m$ , the following applies :

$$N = \text{Int} \left( \frac{\text{available bandwidth}}{\text{hop bandwidth}} \right) \quad \dots (4.10)$$

where  $\text{Int}(x) \equiv \text{greatest integer } \leq x$

$$\begin{aligned} \Rightarrow N &= \text{Int} \left( \frac{B}{T_H} \right) \\ &= \text{Int} \left( \frac{\mu}{\pi} \tau_m T_H \right) \end{aligned}$$

On substitution for  $T_H$  :

$$N = \text{Int} \left\{ \frac{\mu}{\pi} \tau_m (T_1 - \tau_m) \right\}$$

which for maximum N, implies

$$\tau_m = \frac{T_1}{2} \quad \dots (4.11)$$

$$\Rightarrow T_H = \frac{T_1}{2}$$

$$\Rightarrow N = \text{Int} \left( \frac{\mu}{4\pi} T_1^2 \right) = \text{Int} \left( \frac{BT_1}{2} \right) \quad \dots (4.12)$$

where B represents the chirp bandwidth. From this it is apparent that the maximum available hop bandwidth can be calculated directly from the time-bandwidth product of the constituent SAW filters.

These expressions do not involve  $T_2$  which was initially assumed  $\geq T_1$  (Equation (4.3)). In accordance with the practical constraints of chirp generation,  $T_2$  should be chosen for a minimum time bandwidth (TB) requirement, which results in  $T_1 = T_2 = T_0$ . A consideration of the timing relationships of the chirps (Figure 4.2) shows that under the above conditions it is possible to produce a 50% duty cycle waveform which can be time interlaced with another similar waveform to generate a continuous output.

It should be noted at this point that a continuous output does not necessarily imply phase continuity between hops, as would be required for a CW signal. This situation can only occur when the hop duration,  $T_H$ , is an integral number of cycles of the synthesised frequency. This condition will be satisfied if the synthesised frequency is an exact multiple of the frequency spacing  $(T_H)^{-1}$ .

$$\text{ie, } T_H = \frac{2\pi M}{(\omega_1 + \omega_2) - \mu\tau} \quad \dots (4.13)$$

for sum frequency operation, and

$$T_H = \frac{2\pi M}{(\omega_1 - \omega_2) + \mu\tau} \quad \dots (4.14)$$

for difference frequency operation, where  $M$  represents an integer in each case. The value attributed to  $\tau$  in each case is given by  $\tau_0 + \frac{n 2\pi}{\mu T_H}$ , where  $\tau_0$  is a preset offset delay and  $n$  is an integer in the range  $0 < n < \frac{N}{2}$ .

For CW operation, Equations (4.13) or (4.14), as appropriate, must be satisfied for all allowable values of  $n$ , which is true if valid for any value, say  $n = 0$ . Since  $\omega_1$ ,  $\omega_2$  and  $\mu$  are fixed

parameters for a given chirp waveform, the term  $\tau_0$  has been included to allow selection of  $T_H = \frac{1}{2}T_0$  whilst maintaining the phase continuity required for CW operation.

The required delay term can easily be obtained by digital techniques derived from a stable master clock. The basic timing increment required can be given by

$$\Delta\tau = \frac{\text{range in } \tau}{\text{number of hops}}$$

Referring to Equation (4.12) this can be written as

$$\Delta\tau = \frac{2T_0}{BT_0}$$

Hence the minimum clock frequency must be  $\frac{B}{2}$ .

Consideration of equations (4.4) and (4.5) shows that the starting phase of a given pulse is constant for a given value of  $\tau$ . Thus, by deriving all timing signals for a stable clock, phase coherent operation between two identical synthesisers is obtained.

## 4.2 DESIGN ASPECTS

### 4.2.1 SAW Devices for Chirp Mixing

The most attractive method in practice for generating the waveforms specified in Equations (4.1) and (4.2) is based on impulsing SAW chirp filters. As described in Section 3.2.3, these filters provide an accurately defined linear FM waveform, which can be excited by means of an accurately timed impulse. The required timing relationship between chirp waveforms is achieved by control of the excitation

pulses as illustrated graphically in the timing diagram of Figure 4.2.

The synthesiser described in this section was designed around two readily available chirp filters, with equal but contradirected dispersive slopes. The devices were primarily intended for use as a pulse compression pair and were manufactured on ST-X cut quartz using single finger electrode transducers with doubly dispersive inclined geometries. As is common in pulse compression filters, the down chirp (ie, negative dispersive slope) is unweighted and the up chirp (ie, positive dispersive slope) apodised. <sup>An unweighted up-chirp was designed for the final equipment.</sup> The nominal parameters common to both filters are : centre frequency 60 MHz, bandwidth 25 MHz and time dispersion 5  $\mu$ s.

It can be seen from Equations (4.8) and (4.9) that sum frequency operation offers twice the available system bandwidth compared to difference frequency operation when chirp waveforms with identical centre frequency are considered. This factor, combined with the more attractive output centre frequency of 120 MHz, made sum frequency operation the better choice for practical implementation. The target performance for the synthesiser was calculated from the design rules of Section 4.1 to be :

- centre frequency      120 MHz
- bandwidth              25 MHz
- hop duration            2.5  $\mu$ s
- number of hops        63

#### 4.2.2 System Configuration

A block diagram of the synthesiser is shown in Figure 4.3. Essentially, it can be subdivided into two : the RF section and the digital section.

The RF section comprises two identical channels, each consisting of an up and a down chirp filter with associated impulse generators, RF amplifiers, a mixer, a bandpass filter and a gate. The two channels are time interlaced such that their summed outputs form a continuous signal which is further amplified, passed through an amplitude limiter and finally bandpass filtered to remove harmonic signals generated in the limiting process.

The digital section provides all the control functions necessary for triggering the chirp waveforms, interlacing the channels and timing the appropriate gating signals. The circuitry is driven synchronously from a stable master clock, and consists of two programmable down counters, one for each channel, which are preset by manual switch selection or by PN code control. The counter outputs are decoded and steered digitally to the appropriate impulser which produces a -40V peak, 8 ns baseband impulse to excite the filter. This allows random selection of the relative chirp timing to provide +/- values of  $\tau$ . The digital circuitry also controls the gate timing and duration necessary to select the optimum portion of the synthesised pulse and time interlace the two channels. This signal feeds a transistor drive stage connected to the RF switch.

Figure 4.2 illustrates a timing diagram for one channel of the synthesiser, indicating the relationship required between impulse, chirp and gate timing to obtain input frequencies over the full chirp



bandwidth. To prevent the presence of undesired signals in a gate period it can be seen that a chirp should not be impulsed at a rate greater than  $2/T$  or less than  $2/3T$ . This allows generation of a maximum number of frequencies with no time overlap, and represents the best achievable performance from a minimum amount of hardware.

#### 4.3 CONSTRUCTIONAL ASPECTS

The synthesiser described above can be broken down into two separate sections : the digital control circuitry, and the RF componentry. The unit, pictured in Figure 4.4, is housed in a standard 19 inch ISEP rack,  $5\frac{1}{4}$  inches high and 10 inches deep and weighs approximately 7 kg. The RF section is mounted on an aluminium sheet and placed in a half rack plug-in module whilst each individual circuit board is mounted in a separate plug-in unit. Control signals from the digital section are carried via flexible coaxial conductors to a multiway McMurdo connector on the RF plug-in. External power supplies were used to provide the required 5, 15 and 25V DC regulated voltages with a total power capacity of 15W. The individual sections are described below.

##### 4.3.1 Digital Section

The digital control section comprises three separate boards : two programmable pulse generator (PPG) boards (one for each channel) and one master control board. A fourth board is required for frequency selection, and this was chosen from two plug-ins, one containing a PN code generator and the other a manual switching matrix mounted on the front panel.

#### 4.3.1.1 Master Control Board :

The master control board performs two distinct functions. It provides two time interlaced trigger pulses which initiate the timing cycle for each RF channel, and it also provides the gating waveforms required for selecting the desired output signal.

Figure 4.5 illustrates a schematic diagram of the circuit. A stable external clock (with a nominal value of 12.5 MHz) is input to a 74 series divide-by-63 TTL counter, and the desired trigger pulses (separated by a nominal 2.5  $\mu$ s) are obtained by decoding the '1' and '32' states on the parallel output from the counter. The parallel output is also fed to a PCB mounted dual-in-line switching network and logic circuit which produces the required gate waveform for each channel. This method of gate waveform generation was adopted to allow for the finite delay associated with the RF signal transit through the SAW chirp filters. It also provides a means of adjusting the precise position and duration of each gating signal. As the input impedance of the RF gate was 50 ohms, a push-pull transistor driver stage was included, as illustrated on the circuit schematic of Figure 4.5.

#### 4.3.1.2 Programmable Pulse Generator Boards :

Two PPG boards of identical design and construction are required, each being used to control one RF channel. The two timing pulses required to control the chirp filter excitation, are derived from a 6-bit digital word input from the PN code generator or manual switching network as appropriate. The six-bit word is used to preset a programmable down counter (Type 74193) which is enabled by the trigger

pulse input from the master control board. This trigger pulse acts as the timing signal for the first chirp, and the overflow from the down counter acts as timing signal for the delayed chirp. The down counter is clocked at the master clock rate (12.5 MHz) with a delay increment integrally related to  $\frac{1}{12.5} \mu s$ . As the system is designed to operate with both negative and positive delays, the down counter accepts the five least significant bits of the input control word. The most significant bit is input to a digital 'steering' network which routes the trigger pulse to either filter in a channel and simultaneously routes the delayed timing pulsed of 0-31 clock periods to the other filter resulting in an effective delay variation ranging from -31 to +31 clock periods. This circuit is illustrated schematically in Figure 4.6.

#### 4.3.1.3 PN Code Generator :

The PN code generator is based on a 6-bit digital shift register (Type 74164) with serial input/parallel output facility. As illustrated in Figure 4.7, the output from the register is fed back to the input following combination in exclusive -or gates with the parallel output from bits 5 and 3 respectively. This results in repetitive PN sequence 63 bits in length. A push-button preset facility was incorporated on the front panel to initiate the code sequence.

#### 4.3.1.4 Manual Switch Network :

This facility was provided to enable the selection of a constant output frequency, and to ease frequency selection for evaluation purposes. Six single-pole single-throw switches were used with LED indicators, as indicated in Figure 4.8.

#### 4.3.2 RF Section

The RF section was made up of a number of individually boxed circuits interconnected by 0.085 inch semi-rigid coaxial cable fitted with SMA male connectors. Standard diecast aluminium boxes (dimers) were used where possible, but the chirp filters were mounted in custom designed, milled aluminium packages. All the circuitry was constructed on double sided copper-laminate board and each individual box was fitted with SMA female connectors (except at the input to the impulser which was made by BNC connectors). This modular approach was taken to minimise RF leakage between circuits in an attempt to reduce spurious signals at the output. It also facilitated substitution and modification of individual units during the prototype stage. A block diagram of the RF section is presented in Figure 4.10.

##### 4.3.2.1 Impulser Circuit:

The impulser circuit is illustrated in Figure 4.9. Under normal conditions, the transistor is switched on, until the negative timing pulse of approximately 350  $\mu$ s is applied to the base. This switches the transistor off and generates a back emf of between 100 and 200 volts in the collector circuit. When the transistor is switched on at the end of the timing pulse, avalanche breakdown is initiated in the transistor and a negative pulse of magnitude 40 to 60 volts and duration 6-10 ns is observed.

To achieve the maximum output from the impulser, the transistor should be switched on as the back emf reaches its peak. Care must be taken in selecting the coil and transistor such that the maximum emf is below the inherent avalanche breakdown voltage of the transistor, as control of the exact point of impulse is lost if self avalanche occurs.

#### 4.3.2.2 Chirp Filters :

The chirp filters were manufactured on ST-X cut quartz and were housed in a package with outline dimensions 64 x 38 x 18 mm. The package was designed with separate cavities in base and lid connected by standard feed through connectors. The top cavity was approximately 3 mm in depth, and the crystal was mounted on a layer of RTV adhesive in such a way that the surface was kept very close to the cover plate to minimise EM breakthrough. The base cavity was split into two sections which housed the input and output tuning circuit and the SMA female connectors.

A single resonant coil tuning circuit was used to tune out the capacitive component of the transducer impedance for matching into 50 ohm external circuits. In practice, this was difficult to achieve successfully due to the large percentage bandwidth of the SAW filters.

#### 4.3.2.3 Amplifier/Mixer Circuits :

Each chirp filter had an associated insertion loss of approximately 50 dB, hence amplification was required prior to the mixing process. Avantek sub-miniature thin film amplifiers, type GPD 401, 402 and 403 were cascaded as required to achieve optimum power levels for efficient mixer operation. Considerable care had to be taken in the layout of this circuit when three or more amplifiers were cascaded to prevent spurious oscillation. In some cases, it was found necessary to incorporate a simple filter between stages to reduce this effect.

The mixing process was also performed in one of the amplifier chains using a Minicircuits double balanced mixer type SRA 1.

#### 4.3.2.4 Summing, Limiting and Filtering Components :

The sum product from the mixer was selected in a 4 section LC bandpass filter, commercially manufactured by Telonix. These units were specified with 120 MHz centre frequency and 30 MHz bandwidth.

The final module in the RF section contains a summer (Minicircuits type PSC-1), an amplifier chain as previously described and a limiter (Minicircuits type PLS-1 ) to remove any amplitude variations in the generated waveforms. Finally, a third Telonix filter was used to remove any harmonics generated in the limiting process.

The system output was then taken by a flexible coaxial conductor to a BNC female connector on the back panel of the rack.

### 4.4 PERFORMANCE OF A PROTOTYPE SAW CHIRP MIXING SYNTHESISER

#### 4.4.1 Experimental Results

The synthesiser whose design and construction has been described in the preceding sections operates in the sum frequency mode to give a continuous output comprising either a CW signal under manual switch control or an FH waveform under direct PN code control. The main performance parameters are summarised in Table 4.1.

Figure 4.11 shows the output spectrum generated by the synthesiser when producing an FH waveform under the control of a 63-bit PN code and a hop rate of 400 kHz. The system bandwidth is 25 MHz, at a

centre frequency of 120 MHz, and the individual  $\left( \frac{\sin x}{x} \right)$  spectrum of each individual hop can be seen from the expanded trace shown in Figure 4.12. These spectra illustrate the capability of this synthesis technique for wideband frequency hopping.

Section 4.1 defined conditions which allow CW signal generation. This was achieved in practice by careful matching of the constituent channels and fine tuning of the external master clock frequency to achieve a spectrum of the type illustrated in Figure 4.13. In this case, the output signal is at 122 MHz, and the time domain signal is shown on standard and expanded scales alongside the resultant frequency spectrum. The level of spurious signal in this spectrum is greater than -30 dB with respect to the carrier signal. Further consideration of the CW performance of the system is given in Chapter 5.

Experimental systems had previously shown the excellent phase coherence achieved between a single channel sum frequency synthesiser and the master clock controlling the synthesiser. For FH spread spectrum applications, phase coherence between transmit and receive synthesisers is essential, and as such, these units must have 'identical' performance. Two prototype sum frequency synthesisers were made during this study, and phase coherence between them was measured for CW operation as illustrated in Figure 4.14. The measured coherence, shown in Figure 4.15, is within  $2^\circ$  and is stable from hop to hop over the exposure period ( $20\mu\text{s}$ ). Due to experimental difficulties in maintaining the performance capabilities demonstrated in Figure 4.11 - 4.13, in both synthesisers over any extended period of time, a full analysis of FH modem operation was not possible. In practice, the best SAW devices and ancilliary RF circuitry were

used to optimise the performance of one synthesiser only for CW operation.

#### 4.4.2 Discussion of Results

The results presented here demonstrate a SAW chirp mixing synthesiser operating in both FH and CW modes at a sum frequency of 120 MHz. FH operation under PN code control has shown the generation of 63 hops with 2.5  $\mu$ s duration over a frequency range 107.5 - 132.5 MHz. CW operation was also demonstrated at 122 MHz with peak signal to spurious levels of >30 dB, and phase coherence between synthesisers of  $<2^\circ$ .

These results compare favourably with that of Darby<sup>134</sup> who produced a similar equipment in parallel to, but unknown to this work. Following a similar RF technique with some variations in the digital control section, Darby produced a synthesiser with 127 hops of 2.5  $\mu$ s duration across a frequency range from 335 - 385. This was a dedicated system using a fixed crystal oscillator for a master clock and was used primarily for FH experiments. As the synthesiser described in this Chapter derived its timing from an HP 3200B frequency generator, phase locked to an ovened crystal source, it was more suited for experimental evaluation of CW performance where optimum performance resulted from careful adjustment of the clock frequency. Early experimental results were published by the author along with details of preliminary simulation of performance under practical error conditions.<sup>133</sup> Fuller details of this work are given in Chapter 5.



The conclusion of this experimental work has been to demonstrate the ability of SAW chirp mixing synthesisers to provide coherent, fast switching, wideband FH operation under direct PN code control. Operation in CW mode is possible but the spurious content in the synthesised system is too high for most conventional applications. Techniques for improving this performance for use in CW or slow FH applications by use of a narrow band tracking filter are discussed in the concluding remarks in Chapter 6. It is, however, a valuable feature of this technique that the performance demonstrated was achieved using readily available components at relatively low cost.

PERFORMANCE PARAMETER	THEORETICAL DESIGN		PROTOTYPE PERFORMANCE
	SUM	DIFFERENCE	
Centre Frequency (MHz)	$\frac{1}{2\pi} (\omega_1 + \omega_2)$	$\frac{1}{2\pi}  \omega_1 - \omega_2 $	120
Bandwidth (MHz)	B	B	25
Number of Hops (N)	$\frac{BT_o}{2}$	$\frac{BT_o}{2}$	63
Hop Duration ( $\mu s$ )	$\frac{T_o}{2}$	$\frac{T_o}{2}$	2.5
Slope Requirement (MHz/ $\mu s$ )	$\mu_1 = -\mu_2 = \mu$	$\mu_1 = \mu_2 = \mu$	5
Clock Frequency (MHz)	$\frac{B}{2}$	$\frac{B}{2}$	12.5
CW Restriction (MHz)	$f_s = \frac{2M}{T_o}$	$f_d = \frac{2M}{T_o}$	122

Table 4.1 Chirp Mixing Synthesiser Performance Parameters  
(Theoretical and Experimental)

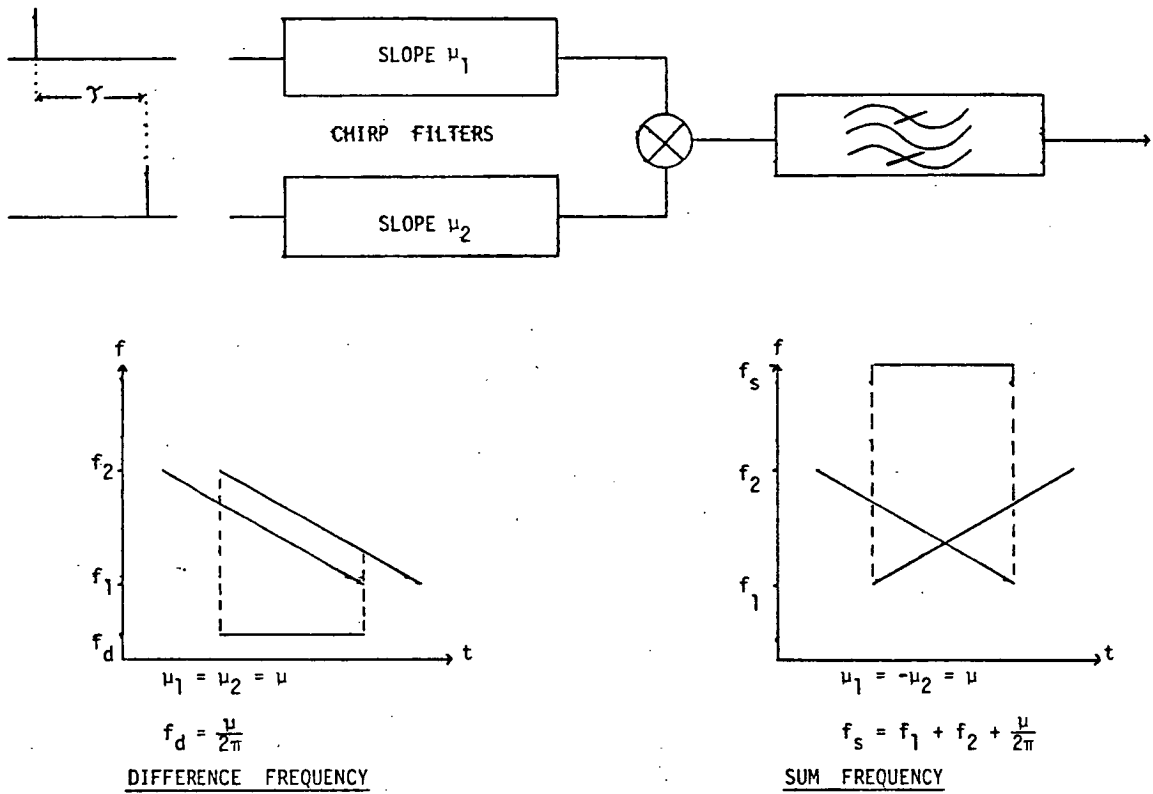


Figure 4.1 SAW Chirp Mixing Synthesis : Sum and Difference Frequency Generation

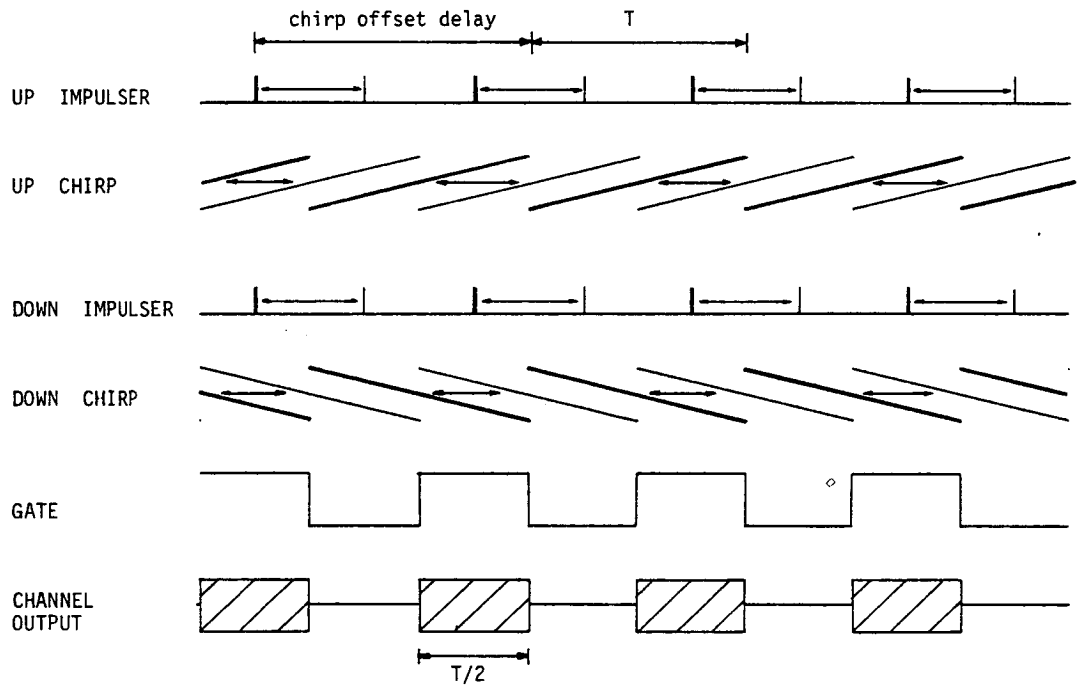


FIGURE 4.2 SYNTHESISER TIMING DIAGRAM

(Range of impulse and chirp timing for output over the full chirp bandwidth. Only one channel shown).

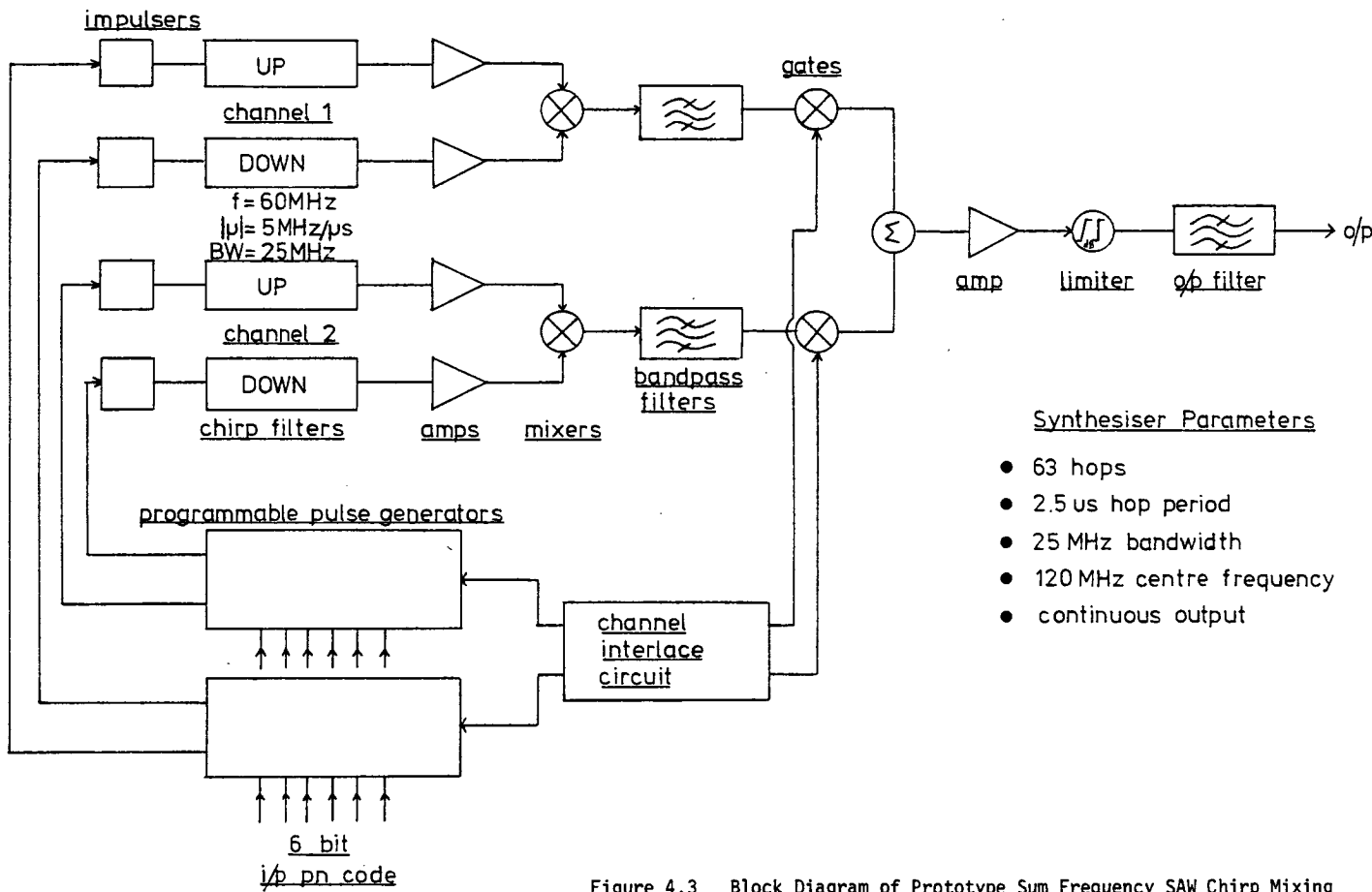


Figure 4.3 Block Diagram of Prototype Sum Frequency SAW Chirp Mixing Synthesiser (Continuous Output)

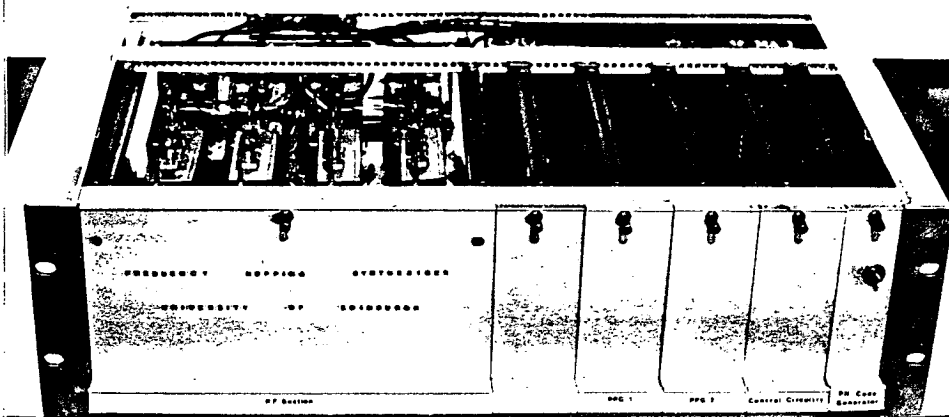


Figure 4.4    Photograph of Prototype Synthesiser Hardware



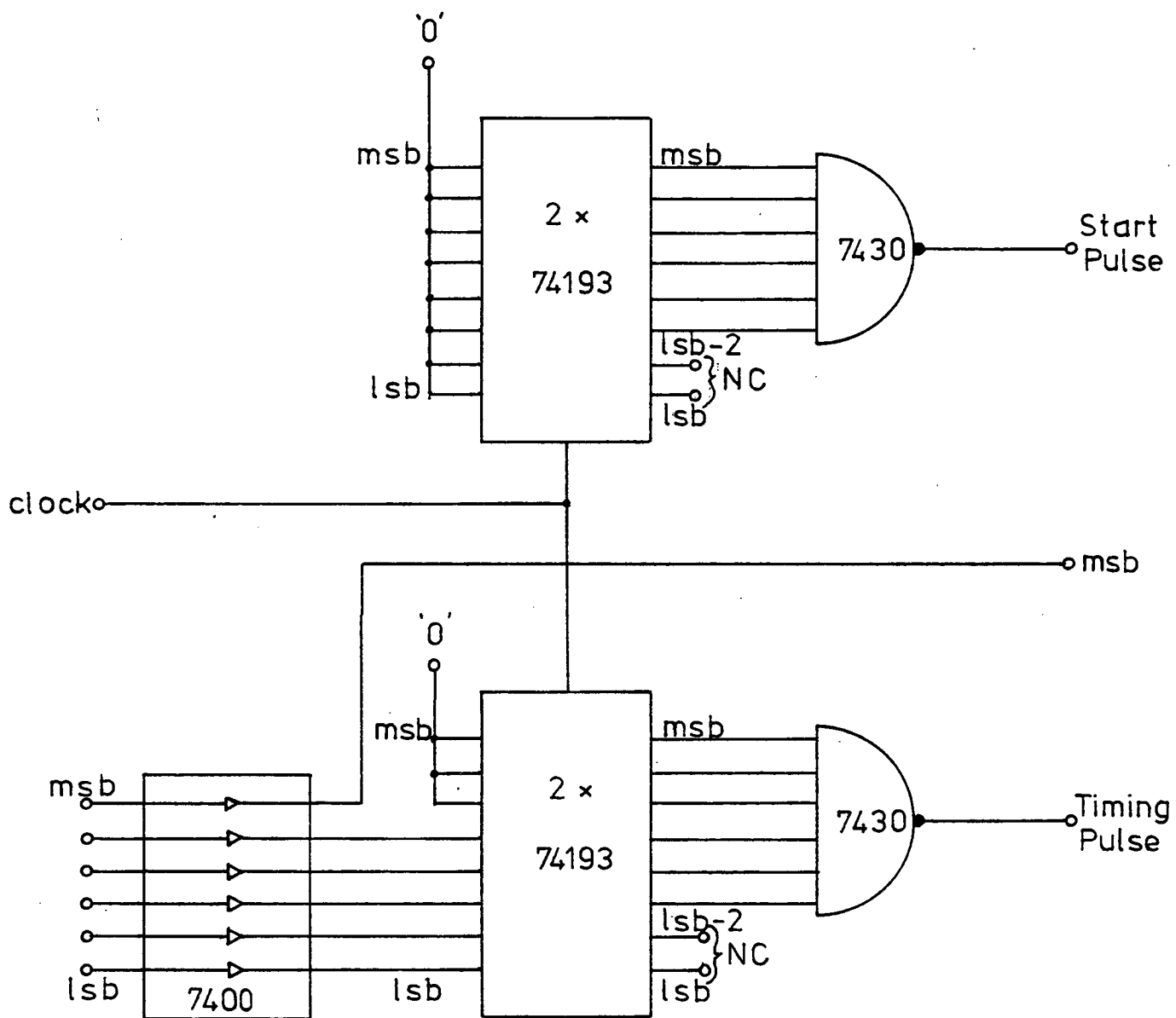


Figure 4.6 Programmable Pulse Generator Board Schematic





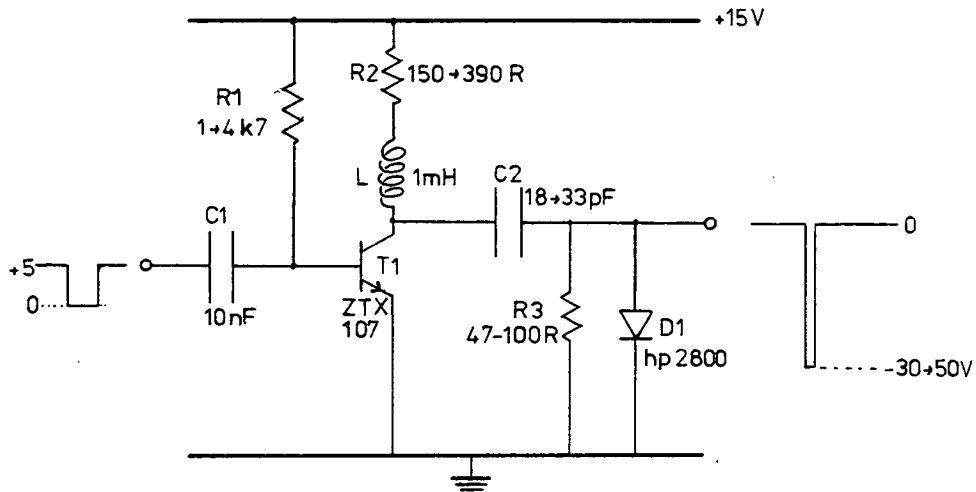


Figure 4.9 Impulse Generator Circuit Diagram

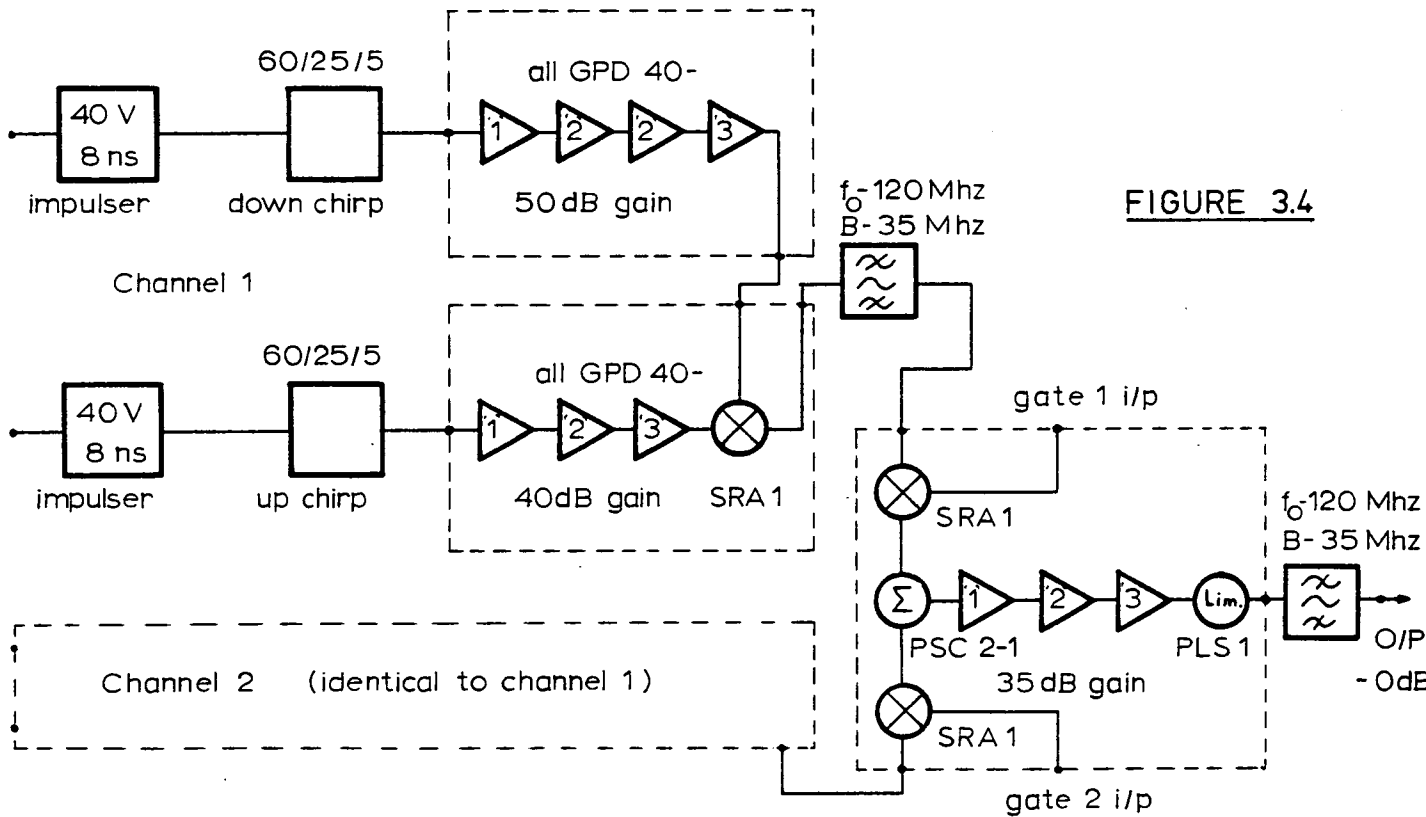
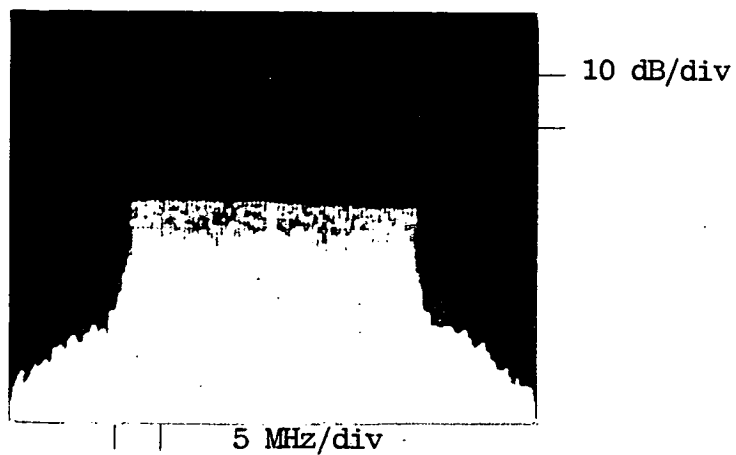


FIGURE 3.4

### Synthesiser RF Section

Figure 4.10 Synthesiser RF Section



63 hops, over a 25 MHz bandwidth, centred on 120 MHz

Figure 4.11 Comb Spectrum Produced by a PN Code Controlled FH Synthesiser

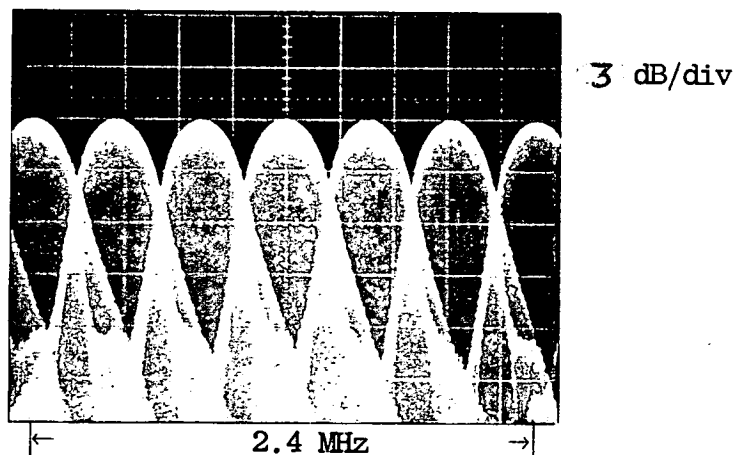
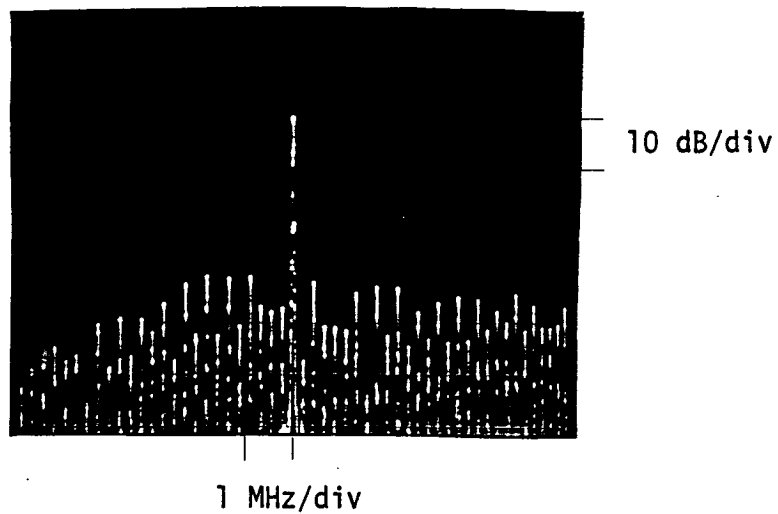


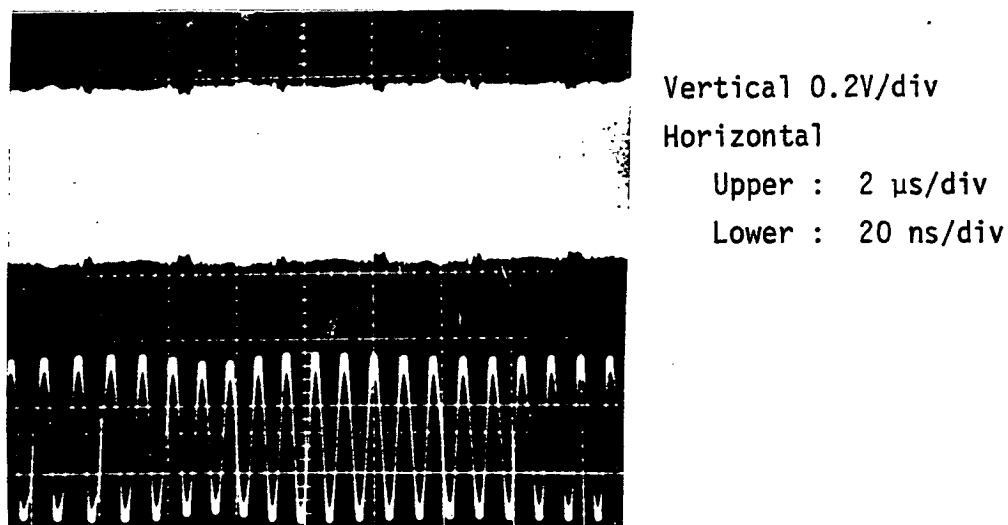
Figure 4.12 Expanded Detail of Trace in Figure 4.11



(a) CW Frequency Spectrum

Centre Frequency 1 MHz

Maximum Spurious Level -32 dBc



(b) CW Time Domain Waveform

Figure 4.13 CW Performance of a Chirp Mixing Synthesiser

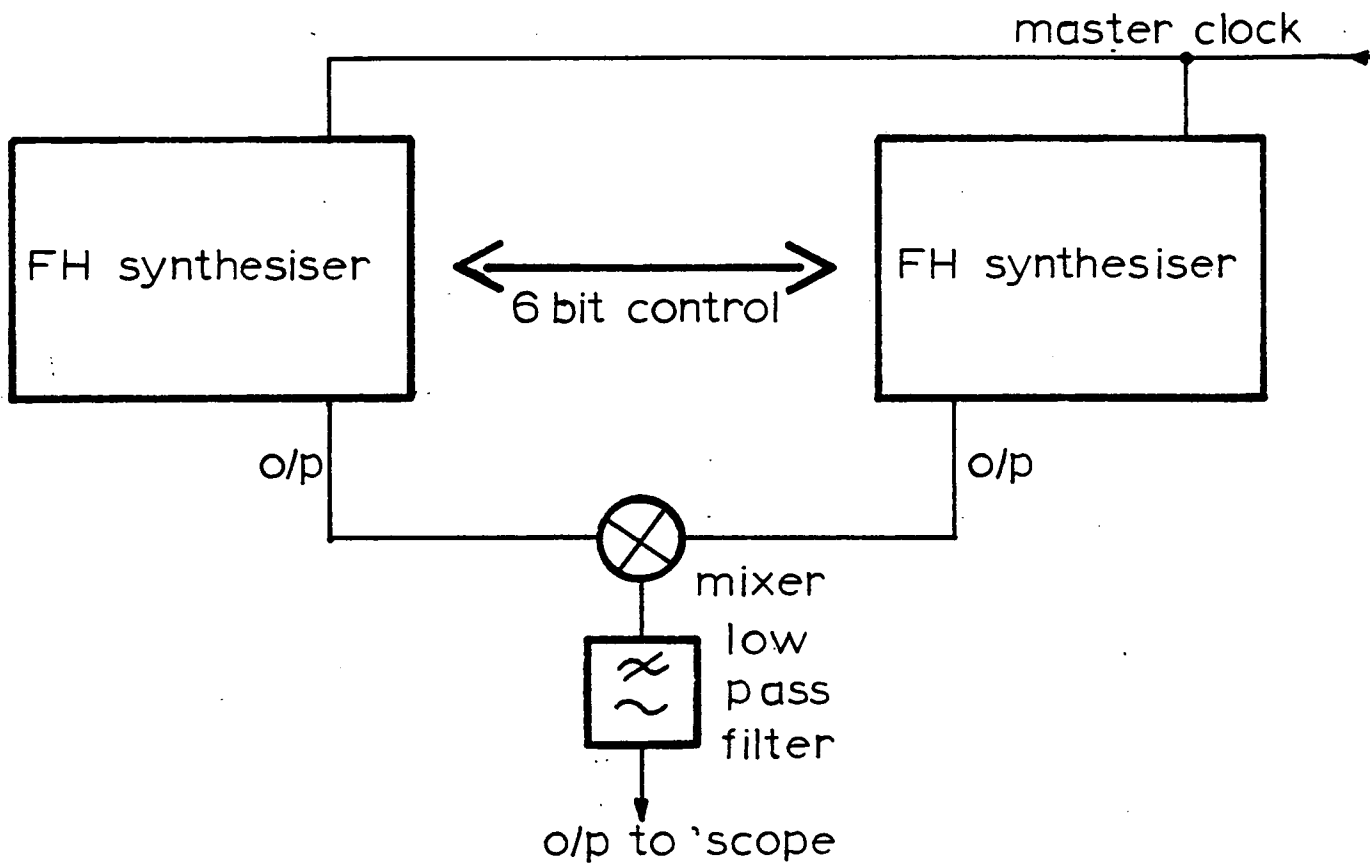
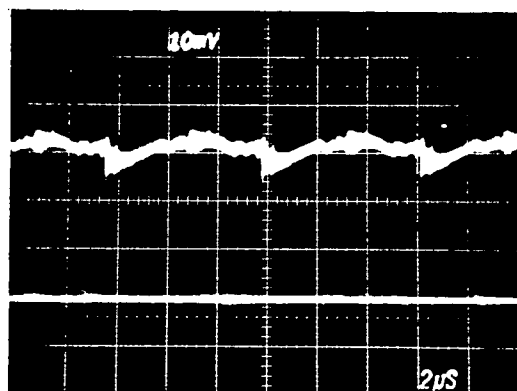


FIGURE 4.14      Coherence measurement circuit



Vertical    10mV/div.

Horizontal    2μs/div.

ZERO LEVEL

### Phase Coherence Between Synthesisers

FIGURE 4.15

## CHAPTER 5 : EVALUATION OF SYNTHESISER DESIGN AND PERFORMANCE

### 5.1 WAVEFORM ANALYSIS AND ERROR SOURCES

Chapter 3 presented a review of frequency synthesis techniques and discussed the associated performance bounds and criteria. Ideally a frequency synthesiser should be capable of generating a perfect, stable sinusoid, with a signal to noise ratio determined by the system noise floor and the peak linear output level. For fast frequency hopping applications this performance should be repeatable at a large number of frequencies over a wide bandwidth and with instantaneous switching between frequencies. Viewed on a spectrum analyser, such a synthesiser would generate a single spectral line when operating in CW mode, and an orthogonal set of  $\sin x/x$  responses when operating in FH mode.

In practice, this performance is difficult to achieve as the CW waveform is generally distorted by noise or modulation generated in the synthesis process or the surrounding electronics and the FH waveform is additionally distorted by the finite rise, fall and settling times for each hop which contribute to the degradation of the ideal  $\sin x/x$  spectrum.

The overall effect of these imperfections on system performance is highly dependent on the modulation technique and the full system requirements and in practice, it is not essential that both synthesisers produce ideal waveforms, but rather that a high degree of match is provided between transmitter and receiver.

Figure 4.12 illustrates an expanded trace of a practical chirp mixing synthesiser output when operating in FH mode. This waveform exhibits a first order match with theory, but due to the inherent overlap associated with a number of orthogonal  $\sin x/x$  responses, it is difficult to analyse each constituent waveform. A measure of the system performance can be achieved by back-to-back modem operation, but this is only a valid measurement for the particular modulation technique selected. In addition, this type of measurement provides no information as to the mechanisms within each synthesiser which cause the signal distortion, hence precluding any assessment of the ultimate limitations on the equipment usage.

Experimental measurement of the phase coherence between two synthesisers was made (Figure 4.14) but this was restricted to CW operation as difficulty was experienced in maintaining reliable operation of both the constructed synthesisers over the full FH bandwidth for an extended period of time. Figure 4.13 shows the synthesiser output operating in CW mode. The high spurious content (approximately -30 dB with respect to the peak output) indicates that there is distortion present in the signal and more important that this distortion is both clearly visible and precisely defined. For this reason, the remainder of the Chapter is dedicated to analysis of the chirp mixing synthesiser operating in CW mode such that each individual error mechanism can be identified and quantified separately. As these mechanisms can be attributed to component tolerancing, system design parameters and constructional details, the following subsection contains a description of the potential error sources and their ultimate significance to SAW chirp mixing synthesis.

### 5.1.1 Error Sources

The theoretical expression of Equation (4.3) describes the process of chirp mixing under ideal conditions. Careful examination of this equation<sup>134</sup> shows that errors in the start frequencies ( $\omega_1, \omega_2$ ), dispersive slopes ( $\mu_1, \mu_2$ ) or the chirp timing ( $\tau$ ) can all lead to unwanted phase or frequency offset terms in the synthesised output. For FH operation, these errors result in correlation mismatch loss<sup>134</sup> which degrades the SNR improvement offered by coherent predetection integration. In the CW mode, errors in each hop destroy the phase coherence criteria of Equations (4.13) and (4.14) resulting in a complicated periodic modulation of the signal which produces high spurious levels (spurs) in the output spectrum.

Based on these observations, the synthesiser performance can be characterised by identifying all potential error sources which result from component tolerancing, system design and construction. These include :

- (1) Relative amplitude ( $\Delta A$ ) and phase ( $\Delta \theta$ ) imbalance between channels which results in spurious modulation of the carrier.
- (2) Impulse timing errors ( $\Delta \tau$ ) leading to interchannel frequency imbalance arising through fixed time offsets, clock instability and impulse jitter.
- (3) Gate edge timing errors ( $\Delta t_g$ ) which directly influence spurious levels.
- (4) Chirp centre frequency errors ( $\Delta f_{1,2}$ ) which result in inter-channel frequency imbalance as (2).

- (5) Chirp slope mismatch ( $\Delta\mu$ ) which results in a residual linear FM term.
- (6) Chirp phase ripple ( $\Delta\phi$ ) which gives rise to a variable FM term depending on  $\tau$ .
- (7) Temperature dependence of system components (in particular the SAW devices) which leads to frequency offset of the synthesised frequency envelope.
- (8) Mixer spuri which arise through harmonic generation and result in increased 'background' spurious level.

Items (1), (3), (4), (5) and (6) arise directly as a result of the chirp mixing technique whereas aspects of items (2) and (8) are applicable to all direct synthesisers. Item (7) applies to all synthesis techniques and in particular, the effects of SAW device temperature dependence are applicable to all SAW based synthesisers. Schematic illustrations of these error mechanisms are given in Figures 5.1, 5.2 and 5.3.

Impulse timing errors and chirp centre frequency errors not only result in frequency imbalance between channels, but contradict the phase coherence criteria of Equations (4.13) and (4.14). Fixed time offsets in the impulse path can arise from delay offsets in logic components, impulser circuits, group delay difference between SAW devices and group delay differences in amplifier chains. Careful circuit design, layout and matching between channels can reduce these effects to a minimum.



One source of error not considered during the implementation of the hardware described in Chapter 4 was that of mixer spurs. In particular, the highest spurious term generated in a double balanced mixer (3 times the local oscillator (LO) frequency minus the input RF frequency) occurs at  $\sim -15$  dB with respect to the desired sum or difference product. When sum frequency operation is employed, this term occurs with a frequency  $3\omega_1 - \omega_2 + 4\mu\tau$  in comparison to the desired sum product at  $\omega_1 + \omega_2 - \mu\tau$ , and as both terms exist for time  $(T_0 - \tau)$  it is possible that they will both appear in the desired output band (B). To avoid this occurrence, a simple analysis shows that  $\omega_1$  and  $\omega_2$  should be selected such that

$$|\omega_1 - \omega_2| > 1.25 B$$

This criteria was not applied in the constructed hardware due to use of available components, but it would in fact be possible to use spectral inversion to provide an upchirp signal spaced  $\pm 1.25 B$  from the centre frequency of the down chirp and this may have other attractions in terms of cancelling phase ripple and slope mismatch between devices.<sup>134</sup>

Temperature dependence deserves special mention, as the mechanism involved includes the effect of two separate components, namely the hopping rate and the spectral envelope of the synthesised frequency. This topic is discussed in more detail in Section 5.4 following an analysis of the synthesised waveform in Section 5.2 which provides relevant information towards the understanding and assessment of temperature effects.

The main source of error in the SAW chirp mixing synthesiser is the fidelity and reproducibility of the SAW chirp filter. Items (4), (5), (6) and (7) are all error mechanisms attributable to practical SAW device tolerancing, typical figures for which are given in Table 5.1. Although group delay, temperature and frequency offsets can be reduced by careful matching, compensation and receiver tracking loops, the residual FH term due to slope mismatch and phase ripple provides a fundamental limitation to the fidelity of the synthesised hop. To assess the effect of individual error mechanisms on the synthesiser performance, analytical and computer aided techniques were used to simulate CW chirp mixing synthesis under the distortions described in Items (1) – (6). Temperature effects (Item (7)) are discussed in Section 5.4, but mixer spurs are omitted from further study as they can be designed out of band as described above.

### 5.1.2 Analysis Technique

The techniques used to analyse the synthesiser performance include both analytical and computer aided methods, but all rely heavily on Fourier transform theory.<sup>137</sup>

The Fourier transform pair (Equations (5.1) and (5.2)) enable conversion of any general time domain waveform to the frequency domain and vice versa.

$$F(\omega) = \int_{-\infty}^{\infty} f(t)e^{-j\omega t} dt = \mathcal{F}\{f(t)\} \quad \dots (5.1)$$

$$f(t) = \frac{1}{2\pi} \int_{-\infty}^{\infty} F(\omega)e^{j\omega t} d\omega = \mathcal{F}^{-1}\{F(\omega)\} \quad \dots (5.2)$$

This transform pair is an essential tool for communication engineering and tables of standard transform pairs and identities can be found in most communications texts<sup>8</sup> and mathematical tables.<sup>137</sup> Wherever possible, use has been made of standard results to reduce the amount of mathematical derivation required.

The most important transform pairs used are those of the eternal cosine waveform,  $\cos(\omega_k t)$ , and the rectangular pulse,  $\text{rect}(t)$ , where

$$\text{rect}(t) = \begin{cases} 1, & |t| < \frac{1}{2} \\ 0, & |t| > \frac{1}{2} \end{cases}$$

These are given in Equations (5.3) and (5.4) using the notation  $\mathcal{F}$  to represent forward Fourier transformation (ie, from time to frequency domain).

$$\mathcal{F}(\cos(\omega_k t)) = \pi\delta(\omega - \omega_k) + \pi\delta(\omega + \omega_k) \quad \dots (5.3)$$

$$\mathcal{F}(\text{rect}(t)) = \frac{\sin(\omega/2)}{\omega/2} = \text{Sa}(\omega/2) \quad \dots (5.4)$$

$$\delta(\lambda) \equiv \text{impulse function}$$

where  $\int_a^b \delta(\lambda - \lambda_k) d\lambda = 1, a < \lambda_k < b$

Similarly, the most important identities used are those of superposition (linearity), time shift (delay), frequency shift (modulation) and convolution/multiplication. These results are listed below for convenience.<sup>8,137</sup>

(1) Superposition :

$$\{a_1 f_1(t) + a_2 f_2(t)\} = a_1 F_1(\omega) + a_2 F_2(\omega) \quad \dots (5.5)$$

(2) Time Shift :

$$\{f(t - t_s)\} = F(\omega)e^{-j\omega t_s} \quad \dots (5.6)$$

(3) Frequency Shift :

$$\{f(t)e^{j\omega_m t}\} = F(\omega - \omega_m) \quad \dots (5.7)$$

(4) Convolution (\*) / Multiplication (x) :

$$\{f(t) * h(t)\} = F(\omega) \times H(\omega) \quad \dots (5.8)$$

$$\{f(t) \times h(t)\} = \frac{1}{2\pi} [F(\omega) * H(\omega)] \quad \dots (5.9)$$

The identities of Equations (5.8) and (5.9) are particularly important for graphical analysis and describe the relationship between convolution and multiplication as follows :

- Convolution in the time domain is equivalent to multiplication in the frequency domain,

and conversely,

- Multiplication in the time domain is equivalent to convolution in the frequency domain.

In all these expressions, angular frequency ( $\omega$  = radians per second) has been used, and will be used throughout the analytical and computational work. Where specific results have been calculated

relating to practice, these are represented in terms of inverse time ( $f = \omega/2\pi$ , ie, Hz).

By nature, the FH waveform is periodic and thus lends itself to Fourier series analysis.<sup>8</sup> A periodic time domain waveform has a frequency spectrum which comprises discrete components ( $F_n$ ), known as the Fourier or harmonic components, which are spaced in frequency by the inverse of the time domain period. Mathematically, these components can be derived in a number of ways, but in this case it is convenient to express them as

$$F_n = \frac{1}{T_r} \cdot F(\omega) \Big|_{\omega = n\omega_r} \quad \dots (5.10)$$

where

$$\omega_r = \frac{2\pi}{T_r}$$

$$T_r = \text{time domain periodicity}$$

$$F(\omega) = \mathcal{F}(f(t))$$

The following sections make use of the above theory to predict the synthesiser output under the error conditions stated in Section 5.1.1. Section 5.2 analyses the waveform theoretically and presents a graphical approach for prediction of the synthesised amplitude spectrum. A discussion of the synthesised waveform and results of numerical computation based on Fourier series analysis are presented for amplitude, frequency and phase errors.

For situations where more complex errors occur, such as phase ripple and residual chirp signals, analytical analysis become unwieldy. In that case, simulation of these effects was achieved using

fast Fourier transform (FFT) computation techniques.<sup>138</sup> This is described in Section 5.3 along with a summary of results relating to the synthesiser performance.

Finally, Section 5.4 investigates the effects of temperature on the output waveform.

## 5.2 FOURIER SERIES ANALYSIS

The analysis, results and graphical presentation described in this section serve as a convenient tool for quantifying the spectral distortion present in a CW chirp mixing synthesiser due to fundamental frequency, amplitude and phase errors. Due to the mathematical simplicity of the error signals, this also provides a convenient basis for understanding the more complex error mechanisms due to chirp filter imperfections and simultaneously provides a means of verifying the results obtained in more complex FFT computer aided analyses of Section 5.3. In particular, the graphical approach of Section 5.2.2 is particularly useful in this respect.

The mathematical derivation is applicable to any practical situation, but where specific examples are given, these have been chosen (where possible) to coincide with the experimental synthesiser performance and reflect the level of error signal likely to occur.

### 5.2.1 Mathematical Derivation

The waveform illustrated in Figure 5.4(a) can be represented mathematically by

$$\begin{aligned}
 f_k(t) &= A_k \cos(\omega_k t + \theta_k) & 0 \leq t \leq t_k \\
 &= 0 & t < 0, t > t_k
 \end{aligned}$$

where  $A_k$  is the peak amplitude

$\omega_k = 2\pi \cdot f_k$ , and  $f_k$  is the sinusoidal frequency

$\theta_k$  = the phase at  $t = 0$ .

The true Fourier spectrum of this waveform can be obtained using Equation (5.1) to give

$$\begin{aligned}
 F_k(\omega) &= \frac{A_k t_k}{2} \text{Sa}(\omega_k - \omega) \frac{t_k}{2} \cdot e^{j\left[(\omega_k - \omega)\frac{t_k}{2} + \theta_k\right]} \\
 &\quad + \frac{A_k t_k}{2} \text{Sa}(\omega_k + \omega) \frac{t_k}{2} \cdot e^{-j\left[(\omega_k + \omega)\frac{t_k}{2} + \theta_k\right]} \\
 &= F_{k+}(\omega) + F_{k-}(\omega) \quad \dots (5.12)
 \end{aligned}$$

The two terms,  $F_{k+}(\omega)$  and  $F_{k-}(\omega)$ , in Equation (5.12) have identical amplitude spectra (Figure 5.4(b)) centred on frequency  $+\omega_k$  and  $-\omega_k$  respectively. Provided  $\omega_k$  is large in comparison to  $\frac{1}{t_k}$  (ie, there is small percentage bandwidth), there should be negligible interaction between the positive and negative responses. In FH mode, the chirp mixing synthesiser described in Chapter 4 is designed to operate over a 21% bandwidth, but each individual hop has a main lobe bandwidth of 800 kHz <sup>between</sup> the first nulls which corresponds to <1% bandwidth. In this analysis the waveform is a CW signal which is modulated to varying degrees at a rate dictated by the hop period, ( $t_k = T_H$ ).

For relatively small error signals (<1%) the associated noise spectrum should be relatively narrow band. For the remainder of the analysis, the positive response  $F_{k+}(\omega)$  alone will be considered for the sake of clarity.

To achieve the waveform of Figure 5.4(c), the rectangular cosine burst must be forced to repeat with period  $T_r$ , and the resultant line spectrum (Figure 5.4(d)) is derived by Fourier series analysis. In this case it is convenient to perform this analysis through use of the identity in Equation (5.10), where  $F(\omega)$  is replaced by  $F_{k+}(\omega)$  of Equation (5.12),  $\omega_r = 2\pi/T_r$  and  $F_n$  becomes  $F_{nk+}$  referring to the harmonic components of the positive frequency response. The line spectrum can now be represented by

$$F_{nk+} = \frac{A_k}{2} \cdot \frac{t_k}{T_r} \text{Sa}(\omega_k - n\omega_r) \frac{t_k}{2} \cdot e^{j\left[(\omega_k - n\omega_r) \frac{t_k}{2} + \theta_k\right]} \quad \dots (5.13)$$

This waveform contains separate amplitude and phase terms, each of which has been graphed against frequency in Figures 5.4(d) and (e).

The expression for  $F_{nk+}$  in Equation (5.13) is a general expression defining the spectral components of a sinusoidal signal of frequency  $f_k = \frac{\omega_k}{2\pi}$ , duration  $t_k$ , phase offset  $\theta_k$  and repetition period  $T_k$ . It should be noted that  $t_k \times f_k$  and  $T_k \times f_k$  need not be integral implying that this waveform could not be simplified to 100% amplitude modulation of an eternal sinusoid by a rectangular waveform. This point is significant when error effects are concerned and will be discussed with the aid of an illustrative example in Section 5.2.2.



For ideal CW synthesis, Equation (5.13) represents the output from Channel 1 of the chirp mixing synthesiser. To be consistent with the system design and nomenclature of Chapter 4, this requires that

$$t_k = \frac{T_k}{2}$$

where  $t_k \equiv T_H$ , hop duration

and  $T_k \equiv T_0$ , chirp duration and channel hop repetition period.

The terms  $A_k$ ,  $\omega_k$ ,  $\omega_r$  and  $\theta_k$  can also be replaced by  $A_1$ ,  $\omega_1$ ,  $\omega_0 (= 2\pi/T_0)$  and  $\theta_1$ , and  $F_{nk+}$  then becomes

$$F_{n1+} = \frac{A_1}{4} \text{Sa}(\omega_1 - n\omega_0) \frac{T_0}{4} e^{j\left[(\omega_1 - n\omega_0) \frac{T_0}{4} + \theta_1\right]} \quad \dots (5.14)$$

The output from Channel 2 is identical to this but is delayed by one hop period as illustrated in Figure 5.5 (a) and (c), to allow time interlace of the two channels. Making use of the Fourier time shift identity (Equation (5.6)) where  $t_s$  in this case is  $\frac{T_0}{2}$ , the positive line spectrum associated with Channel 2 can be written as

$$F_{n2+} = \frac{A_2}{4} \text{Sa}(\omega_2 - n\omega_0) \frac{T_0}{4} \cdot e^{j\left[(\omega_2 - n\omega_0) \frac{T_0}{4} + \theta_2 - n\omega_0 \frac{T_0}{2}\right]} \quad \dots (5.15)$$

where  $A_2$ ,  $\omega_2$  and  $\theta_2$  represent the amplitude, angular frequency and phase offset for this channel, and the term  $e^{-jn\omega_0 \frac{T_0}{2}}$  represents the

desired delay. Comparison of Equations (5.14) and (5.15) illustrates that this delay term introduces an additional offset in the phase spectrum of Channel 2 but has no effect on the amplitude spectrum (Figure 5.4 and 5.5).

A continuous output signal can now be obtained by complex addition of these two equations, and once again, this can be simplified for the ideal case of CW synthesis by applying the following conditions :

$$\omega_1 = \omega_2 = \omega$$

$$A_1 = A_2 = A$$

$$\theta_1 = \theta_2 = 0$$

$$\omega = 2\ell\omega_0 \quad \text{where } \ell \text{ is an integer in the set } 0, 1, 2, \dots$$

$$\omega_0 = 2\pi/T_0$$

The combined synthesiser output signal is now written as

$$\begin{aligned} F_{n0+} &= F_{n1+} + F_{n2+} \\ &= \frac{A}{4} \text{Sa}(2\ell - n) \frac{\pi}{2} \cdot e^{j(2\ell - n)\frac{\pi}{2}} \left[ 1 - e^{-jn\pi} \right] \\ n &= 0, \pm 1, \pm 2, \dots \quad \dots (5.16) \end{aligned}$$

The term  $e^{-jn\pi}$  assumes the values  $\pm 1$  for even and odd values of  $n$  respectively. This reduces all terms where  $n$  is odd to zero by phase cancellation. All even values of  $n$  coincide with null points in the

Sa( $\omega$ ) waveform excepting where  $n = 2\ell$  and  $\text{Sa}(2\ell - n) \Big|_{n = 2\ell} = 1$  resulting in

$$F_{n0+} \Big|_{n = 2\ell} = \frac{A}{2} \quad \dots(5.17)$$

This is illustrated graphically in Figure 5.6.

A similar analysis of the negative frequency spectrum yields an identical result: ( $F_{n0-} \Big|_{n = -2\ell} = \frac{A}{2}$ ) at frequency  $\omega = -2\ell\omega_0$  and the combination of these two spectra yields a spectrum identical to the theoretical integral transform of a cosine waveform.<sup>137</sup>

By this simple Fourier series analysis, the generation of a CW signal has been shown to be dependent on the phase, frequency and amplitude match of the two constituent waveforms. The extent of this dependence in relation to the error mechanisms described in Section 5.1 is the subject of the remainder of the chapter. With knowledge of these relationships, estimation of practical distortion levels is possible, and conversely, working from this knowledge, a modulated CW spectrum can provide an indication of the type if not the source of error involved.

### 5.2.2 Graphical Interpretation

An estimate of the previous result can be achieved graphically following a technique described by Brigham,<sup>138</sup> for the analysis of DFT and FFT calculations. This technique makes use of standard Fourier transform pairs and identities, and providing the time domain waveform can be built up from a number of standard functions, the frequency spectrum can be predicted without recourse to rigorous mathematics.

As an illustrative example, the output from a single channel of the synthesiser operating in CW mode is described graphically in Figure 5.7. The following paragraph describes the graphical analysis, and the way in which the time domain waveform is derived from knowledge of the synthesiser operation.

(During the analysis the bracketed letters will refer to sub-sections of Figure 5.7.)

The spectrum (f) of a single hop generated by the synthesiser can be derived from an eternal sinusoid (a) at the centre frequency,  $f_1$ , truncated by a rectangular pulse (c) of duration  $T_0/2$ . The truncation is achieved by multiplication of the two time domain waveforms (a) and (c) which corresponds to convolution of their spectra resulting in (f). This waveform was the basis of the Fourier series analysis of Section 5.2.1. For ideal CW operation, the channel must generate this hop with a 50% duty cycle, and hence must be triggered by an impulse train (g) with period  $T_0$ . This impulse train has an equivalent frequency domain response (h) comprising a line spectrum with spacing  $1/T_0$ . The final channel output (i) can now be derived by convolving the time domain waveforms of (e) and (g), and the equivalent frequency spectrum (j) is the result of multiplying (f) and (h). This latter effect is often described as frequency sampling.

Thus by a process of multiplication and convolution, the amplitude spectrum of Figure 5.7(j) illustrates a  $\text{Sa}(\omega)$  function with peak response at  $f_1$ , sidelobe null spacing  $2/T_0$ , sampled at frequency intervals which are integral multiples of  $1/T_0$ . In this case,  $f_1 = N/T_0$  where  $N$  is an integer, and the waveform is identical to that predicted by Equation (5.13).

The above analysis can be repeated for the other synthesiser channel which is identical but time shifted by  $T_0/2$ . Figure 5.8 illustrates the resultant waveforms, and as predicted by Section 5.2.1, the amplitude spectrum is identical. However, this does illustrate one disadvantage of the graphical technique, namely that no phase information is presented, which prevents combination of the waveforms to achieve the true CW output.

From this latter result, it would appear that the graphical analysis is only valid for multiplication and convolution operations, and hence should only be used as a guide to more rigorous analysis. The technique does provide a useful insight into the synthesiser operation, and combined with the knowledge of the phase spectra obtained in Section 5.2.1 can be used to predict the spectra obtained when frequency, phase or amplitude errors are present in either or both channels.

### 5.2.3 Discussion of the Synthesised Waveform

Ideal CW operation requires that each channel generates a 50% duty cycle waveform, with an identical frequency, start phase and amplitude in each hop. To achieve ideal match of the two channels, each hop should also contain an integral number of hops per channel. This in fact is a special case of Equation (5.13), where  $t_k = \frac{T_k}{2} = \frac{T_0}{2}$  and  $(\frac{\omega_k}{2\pi} \cdot T_k) = (\frac{\omega_1}{2\pi} \cdot T_0)$  is an integer, and represents the 100% amplitude modulation of a sinusoid (frequency  $f_1$ ) by a square wave (period  $T_0$ ). In general, this latter waveform and the synthesiser output described by Equation (5.13) are quite different. To illustrate this point, a graphical analysis of the

square wave modulated waveform is given in Figure 5.9. Comparison of this with Figure 5.7 illustrates an identical end result, but also shows that the 3rd and 4th steps in the process have been reversed. Thus the spectrum of the square wave modulated sinusoid is achieved by frequency domain convolution (of Figures 5.9(b) and 5.9(h)) whilst the synthesised waveform is achieved by frequency domain multiplication (of Figures 5.7(f) and 5.7(h)).

The implications of this statement can best be illustrated by considering the effect of a frequency shift ( $\Delta f$ ) on each waveform. For the square wave modulation case, the spectral line of Figure 5.9(b) is shifted by  $\Delta f$ . The modulating square wave is unaffected and hence the convolution of Figures 5.9(b) and 5.9(h) result in an identical modulation pattern centred on ( $f_1 + \Delta f$ ) as shown in Figure 5.10(a). For the synthesised waveform, the frequency shift moves the peak response of the  $S_a(\omega)$  function in Figure 5.7(f) by  $\Delta f$ . The frequency sampling waveform of Figure 5.7(h) is left unaffected as the master clock frequency within the synthesiser remains invariant so that when these two waveforms are multiplied, the frequency samples no longer occur at the peak and nulls of the  $S_a(\omega)$  waveform, as shown in Figure 5.10(b).

This demonstrates two fundamental effects in the synthesis process :

1. The hop duration and timing are directly dependent on the master clock, and hence the  $S_a(\omega)$  spectral shape (but not necessarily position) and the Fourier components in the output signal will remain invariant and defined within the limits of the master clock stability.

2. Although the hop selection is controlled by the master clock, the absolute frequency within each hop is a function of the chirp filter characteristics, hence the position of the  $S_a(\omega)$  spectrum can vary in relation to the Fourier component sampling frequencies.

The above analyses have been carried out with respect to single channel operation. However, with the knowledge of the phase spectra given in Section 5.2.1, it is possible to predict the effect the frequency shift ( $\Delta f$ ) will have on the CW spectrum. In fact, a frequency shift has no relative effect on the phase spectra of the two channels, so the odd harmonics around the centre frequency ( $f_1$ ), still cancel. However, due to shift in the  $S_a(\omega)$  amplitude spectrum, the even harmonics no longer coincide with the null points in the response, and add constructively to give an asymmetric spectrum in this case. The time domain waveform is now a series of frequency hops duration  $T_0/2$ , with a phase jump between each hop. When  $\Delta f$  is increased to  $1/T_0$ , the highest spur assumes a value equal to that associated with  $f_1$ , and eventually if  $\Delta f$  is increased to  $2/T_0$ , the CW condition is again achieved, but at a new centre frequency of  $f_1 + \Delta f$ .

#### 5.2.4 Calculated Error Levels

Equations (5.14) and (5.15) were programmed into an Apple microcomputer to calculate the Fourier components of a CW waveform synthesised from two time interlaced repetitive sinusoidal burst waveforms with burst duration  $T_0/2$  and repetition period  $T_0$ . It was assumed that perfect time interlacing between channels would take place.

Individual variation of the channel amplitudes ( $A_1$ ,  $A_2$ ), frequencies ( $f_1$ ,  $f_2$ ) and start phases ( $\theta_1$ ,  $\theta_2$ ) was possible, and nominal parameters of 120 MHz centre frequency and 2.5  $\mu$ s hop duration ( $T_0/2$ ) were selected to simulate the parameters of the experimental equipment. Simulation was carried out using the positive Fourier spectrum initially but subsequently both positive and negative terms were used.

The error mechanisms simulated were :

1. Amplitude imbalance  $20 \log_{10}(\Delta A) - \text{dB}$   
 $(\Delta A = A_1 - A_2)$
2. Frequency imbalance  $\Delta f - \text{kHz}$   
 $(f_1 = 120 \text{ MHz})$   
 $(f_2 = 120 + \Delta f)$
3. Frequency error  $\Delta f_p - \text{kHz}$   
 $(f_1 = f_2 = 120 + \Delta f_p)$
4. Phase imbalance  $\Delta \theta - \text{degrees}$   
 $(\Delta \theta = \theta_2 - \theta_1)$

and the values used are listed in Table 5.2.

To facilitate graphical output of these results, the same equations were programmed into an ICL 2972 mainframe computer. Each calculation provided amplitude and phase spectra for each individual channel plus the combined output. Examples of all



four error types simulated are presented in Figures 5.11 and 5.12. A summary of the results for the various error magnitudes is shown in Figure 5.13 where the highest spurious level (with respect to theoretical peak output) is graphed for the four error mechanisms. In addition, a graph of the zero error ideal CW spectrum is contained in this figure. Close examination of these results shows the maximum error magnitude for a -60 dB spur level to be  $\Delta A = .03$  dB,  $\Delta f = .35$  kHz,  $\Delta f_p = .4$  kHz, and  $\Delta\theta = 0.2^\circ$ . Table 5.3 presents these results along with the error levels permissible for -50, -40, and -30 dB spurious.

The spectra of Figure 5.13(b) agrees with the analytical results for ideal CW operation described in Section 5.2.1. Similarly, the graphical method of Section 5.2.3 can be used to predict the results illustrated in Figures 5.11 and 5.12. Three distinct spectra arise from the error simulations 2, 3 and 4 above. These represent : (a) a constant frequency shift in both channels resulting in a phase jump between hops, (b) a frequency shift in one channel resulting in a phase jump between every second hop and a frequency difference between channels, and (c) a simple phase offset between otherwise ideal channel operation.

Error (a) results in an asymmetric amplitude spectrum occurring at all even Fourier components surrounding the original centre frequency. This is due to the relative movement of the  $\sin x/x$  envelope (associated with both hops) with respect to the invariant spectral lines. Phase cancellation of all odd harmonics still occurs because  $f_1 = f_2$ , but the even harmonics, previously suppressed by the nulls in the  $\sin x/x$  response, now assume values proportional

to the  $\sin x/x$  envelope. Error (b) results in an asymmetric spectrum occurring at all the Fourier components, as both phase cancellation and null suppression have been lost. Error (c) results in an odd harmonic spectrum as the even harmonics appear at null points in the  $\sin x/x$  but the odd harmonics no longer cancel due to the phase imbalance between channels.

### 5.3 COMPUTER SIMULATION

#### 5.3.1 Difference Frequency Simulation

Chronologically, the first simulated results of the synthesiser performance were carried out on the Edinburgh Multi Access mainframe computer System (EMAS). Within the limits of computing time and capacity, the objective of this exercise was to obtain the maximum amount of information regarding the spectral content of the hopper waveform.

A nominal resolution of 1 kHz was assumed and the values shown in Table 5.4 calculated to determine the number of FFT points required for operation at a range of frequencies from 0.4 MHz to 132.5 MHz. In tandem, a sample program was run to investigate the computing time required for various numbers of FFT points. Based on the approximate rule that computing time doubles with the number of FFT points used, Table 5.5 was constructed. From these two tables, it becomes apparent that operation close to DC was advantageous to reduce computing time and cost, so it was decided to carry out the simulation based on the difference frequency mode of operation, under the assumption that the results would be directly applicable to sum frequency operation.

An IF frequency of 800 kHz was chosen, with data generated from 512 frequency hops each of 2.5  $\mu$ s duration, providing a resolution of 781.25 Hz. The minimum Nyquist sampling rate for this waveform is 1.6 MHz (equivalent to 2048 FFT points), so a sample rate of 3.2 MHz was selected which required 4096 FFT points. Table 5.6 summarises the parameters of interest for the computation. Results were calculated for frequency ( $\Delta f$ ) and phase ( $\Delta \theta$ ) errors as before and in addition inter-channel phase ripple ( $\Delta \phi$  - assumed to be a one cycle sinusoid departure from the expected time domain quadratic phase response) and inter-channel chirp mismatch ( $\Delta \mu / 2\pi$ , MHz/ $\mu$ s) were simulated. Table 5.7 lists the magnitude of error simulated in each case.

The results obtained are graphed in Figure 5.14 showing the decibel value of the highest spurious level compared to that of the desired output frequency level. Comparable levels for amplitude modulation and time gating errors (calculated from 100% rectangular wave amplitude modulation theory<sup>139</sup>) are shown for comparison. Sample graphs for each case are shown in Figure 5.15 - 5.18. These graphs noticeably all illustrate an asymmetry around the centre frequency which with reference to Figures 5.11 and 5.12 is expected under certain circumstance but noticeably should not occur for the case of  $\Delta \theta$  where a symmetrical output is predicted.

Careful consideration of the FFT process shows that this effect can be attributed to contributions from the negative image frequency (ignored in the previous theoretical sum frequency analysis as having negligible contribution to positive frequencies due to the small fractional bandwidths involved), and a positive "alias"

frequency image centred on 3.2 MHz - the FFT sample rate ( $F_s$ ). The latter of these effects can be removed by greatly increasing the sampling rate so that the alias occurs at a much higher frequency and provides no contribution at 800 kHz (ie,  $N = 512 \times 4096 = 2097152 \Rightarrow F_s = 1.6384$  GHz). The former however, is a real effect and reflects the asymmetry associated with modulating a waveform at a rate of 50% of its absolute value.

These results have been recorded here mainly to illustrate the effects of the negative image frequency and its resultant limitation on difference frequency operation when a very short hop period (in relation to the hop frequency) is used. To illustrate the improvement available by carrying out the simulation at a higher centre frequency, and without severe aliasing, results were obtained for a phase error of  $\Delta\theta = 1.0^\circ$  at an IF of 8 MHz. This is shown in Figure 5.19, and the results obtained correlate to within 0.001 dB with the theoretical calculation of Section 5.2.4. However, based on the number of FFT points (2097152) required to reduce aliasing, this technique would appear unwieldy even by mainframe computer standards. The problem can in fact be circumvented by reducing the FFT resolution, which is possible due to the discrete line spectra involved.

As the theoretical analysis described in the previous section was carried out in parallel and in some cases subsequent to this computing, it became apparent that the waveform would in fact be a line spectrum with a line spacing dictated by the inverse of the hop period, so that providing the FFT routine sampled on these points the resolution was uncritical. This enabled the data to be created

from 2 hop periods (one for each channel) which results in a resolution of 200 kHz, and a sample rate of 819.2 MHz for 4096 FFT points. The results shown in Figure 5.19 for an 8 MHz centre frequency were calculated in this way.

The result of this simplification of the FFT process implied that true system simulation based on the operational centre frequency of 120 MHz was now possible. This is described in the following subsection.

A flow diagram and computer listing of the difference frequency computer program can be found in Appendix 3, along with a sample print out of results.

### 5.3.2 Sum Frequency Simulation

Sum frequency simulation was based on the experience gained in the difference frequency work. An FFT was performed on data representing two hop periods, each of 2.5  $\mu$ s duration containing a nominal centre frequency of 120 MHz. The maximum number of points acceptable to the FFT subroutine (16384) was used to minimise the aliasing effect. This provided a sampling rate of 3.2768 GHz and a resolution of 200 kHz.

The results of Section 5.2.4 and 5.3.1 were recalculated for similar values of  $\Delta A$ ,  $\Delta f$ ,  $\Delta f_p$ ,  $\Delta \theta$ ,  $\Delta \phi$  and  $\Delta \mu/2\pi$  as detailed in Tables 5.2 and 5.7. The peak spur levels are graphed in Figure 5.20. Comparison of results for  $\Delta A$ ,  $\Delta f$  and  $\Delta \theta$  with those of the theoretical analysis in Section 5.2.4 shows a high degree of correlation, which provides a degree of confidence in the results for  $\Delta \phi$  and  $\Delta \mu/2\pi$

which are not easily calculated by analytical methods. It was noted that some asymmetry still existed in the case of  $\Delta\theta$  (approximately 0.01 dB) but recalculation of the theoretical analysis including the negative frequency image (at -120 MHz) produced similar results, illustrating that it was in fact a real effect. Sample graphical outputs are illustrated in Figures 5.21 - 5.24.

Comparison of the peak spur levels for difference and sum frequency operation shown in Figures 5.14 and 5.20 illustrates a peak signal to spur improvement of between 2 and 5 dB for sum frequency operation. Taken in conjunction with the high degree of correlation with the theoretical calculations, these results can be taken as representative of projected synthesiser operation. Examination of the  $\Delta\phi$  and  $\Delta\mu/2\pi$  curves in Figure 5.20 illustrate that spurious levels of -60 dB with respect to the peak output would require  $<0.2^\circ$  phase ripple and  $<0.0005$  MHz/ $\mu$ s dispersive slope mismatch. Both of these figures are currently outside available SAW device performance bounds where typical values would be  $\Delta\phi = 5^\circ$ , and  $\Delta\mu/2\pi = 0.05$  MHz/ $\mu$ s. In practice, experimental work<sup>134</sup> has shown that minimum slope mismatch is likely to occur if the two chirp responses are generated from one filter using spectral inversion techniques.

Based on measured results for the prototype synthesiser SAW devices, two simulations were performed with the following values of dispersive slope:

SIMULATION				1	2
				$\mu$	$\mu$
Channel 1	Filter 1	=	.	4.98	4.98
	Filter 2	=		4.93	4.93
Channel 2	Filter 3	=		4.98	4.98
	Filter 4	=		4.93	4.95

TABLE of Dispersive Slope Values ( $\frac{\mu}{2\pi}$ ), (MHz/ $\mu$ s)  
[based on experimental data]

The resultant peak spurious levels were : (1) -14.7 dB and (2) -16.8 dB, and the simulation output is shown in Figure 5.25. Notably for the second simulation, the asymmetry between channels results in spurs every 200 kHz as opposed to 400 kHz for simulation (1). The experimental results illustrated in Figure 4.13 do not correlate with these calculated values. This can be attributed to fortuitous phase cancellation between a number of error mechanisms achieved through careful tuning of the master clock frequency. Following random switch-on the prototype performance could easily match that calculated.

A listing of the program used for sum frequency simulation is contained in Appendix 4 along with a sample print out of results. Subsequently an interactive program was generated with user notes and a variety of input/output facilities to allow easy selection of individual parameters for simulation. A listing and sample print out are contained in Appendix 5.

#### 5.4 TEMPERATURE DEPENDENCE OF SYNTHESISER OPERATION

Previous sections have shown that the spectral line spacing in the synthesiser output is a function of the hop period only and is referenced through digital division to the stable master oscillator. It has also been shown that a frequency offset in the output hop leads to a shift in the associated  $\sin x/x$  envelope resulting in the generation of spurious levels in CW operation. If an ovened crystal source is used as the master clock, the absolute position of these spurs would be expected to remain constant, but the relative

magnitude of each one (including the desired output) would vary according to the position of the  $\sin x/x$  envelope associated with each channel. In a practical synthesiser, one potential source of frequency error is that due to temperature variation of component parameters.

Measurement of the prototype synthesiser operating in sum CW mode verified this theory. Using an ovened crystal source as a reference, the output at 120 MHz was measured against a reference signal on a Hewlett Packard spectrum analyser with a resolution of 10 Hz. No perceptible frequency offset was noted over a temperature range of 20°C to 70°C but variation of the amplitude level occurred. It was initially thought that spurious reduction could be achieved by temperature compensation through adjustment of the master clock frequency. Although this is theoretically possible, it does not represent a viable solution as adjustment of the master clock changes the gating period and hence the position of each spectral component. Spurious reduction is therefore only achieved at the expense of an absolute frequency offset given by

$$\Delta f_n = \frac{\Delta f_c n}{63}$$

where  $\Delta f_n$  represents the change in the  $n^{\text{th}}$  spectral line due to  $\Delta f_c$ , the master clock frequency shift required to reduce the spurious level and 63 is the division factor used in the prototype equipment.

A number of factors could contribute to changes in the output spectrum as the temperature varies, but in a well-designed synthesiser, the limiting factor is likely to be the temperature characteristics of



the SAW chirp filters. In practice, these devices are normally fabricated on ST-cut quartz to obtain the best available temperature stability.

Experimental results obtained by Schulz and Holland<sup>98</sup> indicate that the variation of phase delay with temperature is primarily parabolic, and can be expressed by

$$T = T_0(1 + \alpha(\delta - \delta_0)^2)$$

where

$T$  = delay between any two points on the surface

$T_0$  = delay at a temperature  $\delta_0$

$\delta$  = temperature,  $\delta_0$  is the turn over temperature

$\alpha$  =  $\sim 32 \times 10^{-9} \text{ } ^\circ\text{C}^{-2}$  (experimental data)<sup>98</sup>

This delay change will cause a resultant frequency change since

$$f_0 = \frac{1}{t_0}$$

where  $f_0$  is the output frequency at room temperature and  $t_0$  is the delay per wavelength at room temperature, and hence

$$\begin{aligned} f(\delta) &= \frac{1}{t_0(1 + \alpha(\delta - \delta_0)^2)} \\ &= \frac{f_0}{\beta} \end{aligned}$$

where  $\beta = 1 + \alpha(\delta - \delta_0)^2$ .

Adopting the terminology of Equation (4.6), the output from an ideal synthesiser with temperature can be written as

$$\omega_{\delta} = \frac{1}{\beta} (\omega_{1_{\delta_0}} + \omega_{2_{\delta_0}}) - \frac{1}{\beta_2} (\mu_{\delta_0} \tau)$$

The first term of this expression is dominant as  $\omega_1 + \omega_2 \gg \mu\tau$  for a sum frequency synthesiser. The frequency shift in ppm versus temperature for various values of  $\tau$  is graphed in Figure 5.26. The values chosen are representative of the prototype synthesiser.

As the primary effect on the output waveform is a frequency offset in each hop, the effect on the CW synthesised spectrum can be calculated theoretically as in Section 5.2.4 and the resulting spurious level taken from the graph in Figure 5.13. To illustrate the potential spurious level over a range from  $-20^{\circ}$  to  $+70^{\circ}\text{C}$ , Figures 5.26 and 5.13 have been combined for a frequency in the centre of the output band (ie,  $\tau = 0$ ) and are graphed in Figure 5.27.

From this analysis it is apparent that major degradation of the synthesiser output can be expected if CW operation is required over a wide temperature range without ovening the SAW devices. It can also be seen that compensation by master clock adjustment is possible, but ineffective due to the resultant change in output frequency.

Temperature effects do not provide the same problem for FH applications, as the frequency error can be small in comparison to the hop bandwidth, and since the start phase in both transmit and receive synthesisers should remain constant, the error due to temperature variations will result in a small correlation loss in the receiver.

## 5.5 DISCUSSION OF RESULTS

An analysis of the CW chirp mixing waveform has been presented in this Chapter, and the effects of tolerancing in the constructed equipment quantified. A number of error mechanisms have been described which led to amplitude, frequency and phase mismatch between synthesiser channels. The most significant error sources were shown to be SAW chirp slope mismatch, phase ripple and temperature dependence.

Simulation of the effects of chirp slope mismatch and phase ripple have shown that current device repeatability and linearity are unlikely to yield better than 40 dB spurious suppression for CW synthesis. Using typical experimental data, the performance of the constructed equipment (30 dB suppression) was shown to be considerably better than predicted (~15-17 dB suppression) but this was attributed to fortuitous cancellation achieved by careful master clock tuning.

Temperature effects on synthesiser performance result in increased spurious signal level. This effect can only be minimised by temperature control of the SAW devices. For FH applications the frequency drift due to temperature is small in comparison to the hop bandwidth, and as each synthesiser in a link should maintain the same start phase, only a small correlation loss should occur in the receiver.

The devices used to construct the prototype equipment were currently available components which had not been optimised or selected to provide closely matched responses. The results of this Chapter show that considerable importance lies in the design and manufacture of the SAW devices if acceptable CW or slow FH signal generation is required.

The results of computer simulation of the system performance are presented in Figures 5.11 to 5.27, where typical error magnitudes have been selected. A summary of the results obtained for the complete range of error mechanisms (over a range of magnitudes) is presented in Figure 5.20. These represent the performance available from a sum frequency synthesiser generating a CW signal. Comparative results carried out for difference frequency operation are presented in Figure 5.14.

The results presented in this Chapter have concentrated on the limitations of the SAW chirp mixing synthesiser when used for generating CW signals. The degradations which apply in that situation do not necessarily effect the FH performance of the system. The primary error for FH operation is due to correlation mismatch loss attributable to residual chirp signals. Recent work<sup>134</sup> has shown this to be less than 1 dB for hardware and experimental link operation has been demonstrated<sup>140, 141</sup>.

	ST-X Quartz		Y-Z LiNbO <sub>3</sub>	
Mechanism	Tolerance	Cause	Tolerance	Cause
Substrate manufacture and orientation	$\pm 10\text{ppm}$	ST-angle	$\pm 200\text{ppm}$	Structure variations
Metal film thickness	$\pm 20\text{ppm}$	$\pm 2.5\%$ in Al. at $2000\text{\AA}$	$\pm 20\text{ppm}$	$\pm 2.5\%$ in Al. at $2000\text{\AA}$
Mark to Space ratio	$\pm 10\text{ppm}$	$\pm 5\%$	$\pm 300\text{ppm}$	$\pm 5\%$
Substrate Flatness	$\pm 20\text{ppm}$	$\pm 10$ fringes of sodium light	$\pm 20\text{ppm}$	$\pm 10$ fringes of sodium light
Total velocity tolerance	$\pm 60\text{ppm}$		$\pm 540\text{ppm}$	

Table 5.1 Velocity Tolerance in ST-X Quartz and Y-Z LiNbO<sub>3</sub> at 50 to 100 MHz

ERROR MECHANISM	SYMBOL	SIMULATION RANGE
Amplitude Imbalance	$\Delta A$ (dB)	0.0 - 0.9
Frequency Imbalance	$\Delta f$ (kHz)	0.0 - 100
Frequency Error	$\Delta f_p$ (kHz)	0.0 - 100
Phase Imbalance	$\Delta \theta$ (degrees)	0.0 - 10

Table 5.2 Range of Error Mechanisms Simulated by Fourier Series Analysis

Maximum Spurious Levels Error Mechanism	-30	-40	-50	-60	Fractional Error Multiplier
$\Delta A$	89	19.4	10.3	3.4	$\times 10^{-3}$
$\Delta t_g$	32	11.2	3.2	0.88	$\times 10^{-3}$
$\Delta f_p$	85	35	11	3.3	$\times 10^{-6}$
$\Delta f$	84	27	9.1	3.0	$\times 10^{-6}$
$\Delta \theta$	15	4.7	1.6	0.47	$\times 10^{-3}$
$\Delta \phi$	11.4	3.6	1.6	0.36	$\times 10^{-3}$
$\frac{\Delta \mu}{2\pi}$	18.8	5.6	1.96	0.6	$\times 10^{-4}$

**Table 5.3** Maximum Fractional Error for -30, -40, -50, -60 dB Spurious Level w.r.t. Peak Theoretical Output

Maximum Analysis Frequency (MHz)	Minimum Nyquist Sampling Rate (MHz)	Required Resolution (kHz)	Number of Sample Points N	Nearest Radix-2 Number $\geq N$	Equivalent Exponent of 2
0.4	0.8	1	800	1,024	10
0.8	1.6	1	1,600	2,048	11
1.2	2.4	1	2,400	4,096	12
107.5	215.0	1	215,000	262,144	18
120.0	240.0	1	240,000	262,144	18
132.5	265.0	1	265,000	524,288	19

**Table 5.4** Minimum FFT Sampling Rate and Number of Points for Sum and Difference Frequency Simulation

Number of FFT Samples  (N)	Equivalent Exponent of 2  (NU : $2^{NU} = N$ )	Approximate Computing Time  (minutes)
8,192	13	0.5
16,384	14	1.0
32,768	15	2.0
65,536	16	4.0
131,072	17	8.0
262,144	18	16.0
524,288	19	32.0

Table 5.5 Computing Time Required for N-Point FFT Execution

Value Parameter	Difference Frequency Simulation	Sum Frequency Simulation
FFT time window ( $\mu$ s)	1280	5
No of hops in window	512	2
No of samples	4096	8192 or 16384
Sample rate (MHz)	3.2	1638.4 or 3276.8
FFT resolution (kHz)	.78125	200
IF frequency (MHz)	.8	120

Table 5.6 FFT Parameters Applicable to Difference and Sum Frequency Simulation

ERROR MECHANISM	SYMBOL	SIMULATION RANGE
Frequency Imbalance	$\Delta f$ (kHz)	0.0 - 100
Phase Imbalance	$\Delta \theta$ (degrees)	0.0 - 10.0
Chirp Phase Ripple	$\Delta \phi$ (degrees)	0.0 - 10.0
Chirp Slope Mismatch	$\frac{\Delta \nu}{2\pi}$ (MHz/ $\mu$ s)	0.0 - 0.01

Table 5.7 Range of Error Mechanisms Simulated by Difference Frequency FFT Analysis



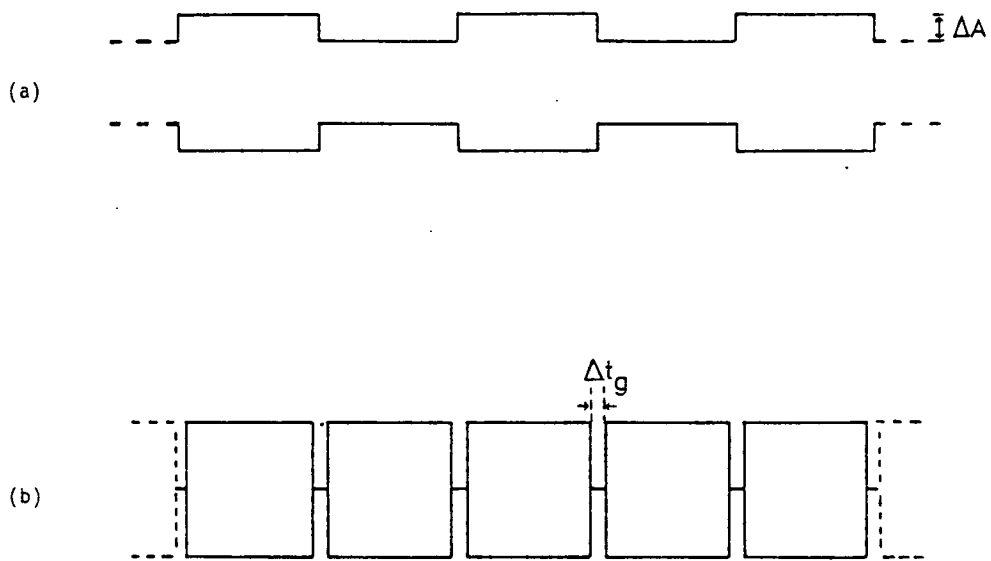
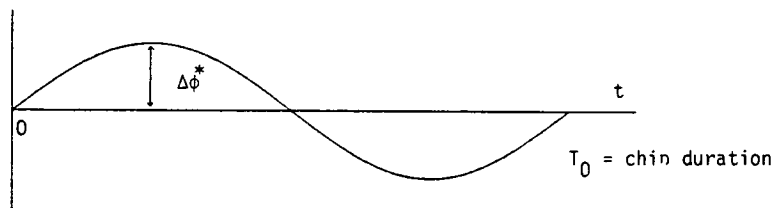
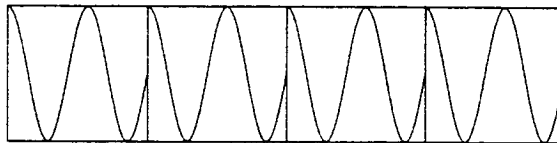


Figure 5.1 Amplitude (a) and Timing (b) Error Mechanisms

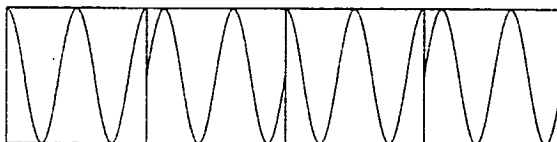


- (a) Chirp Phase Ripple ( $\Delta\phi$ ) (defined \* cycle sinusoidal departure for ideal quadratic phase)

\*  $\Delta\phi_{200} = 1$  cycle sinusoidal departure  
 $\Delta\phi_{400} = 2$  cycle sinusoidal departure



- (b) Frequency Error ( $\Delta f_p$ ) in Both Channels (leading to phase jumps between hops)



- (c) Inter-Channel Phase Error ( $\Delta\theta$ )

Figure 5.2 Phase Ripple, Frequency and Phase Offset Error Mechanisms

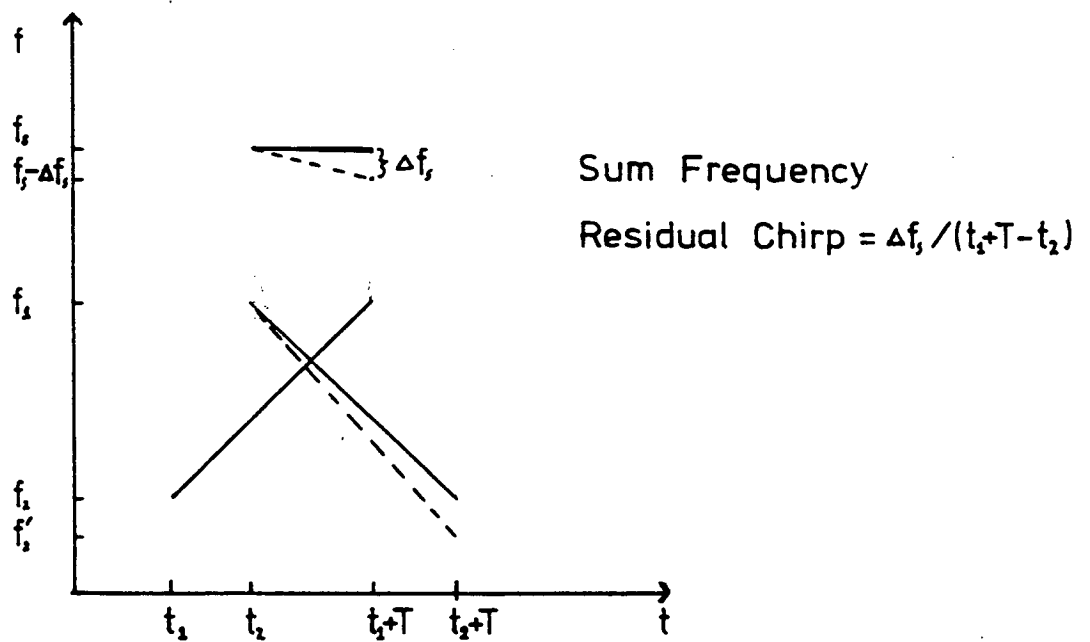
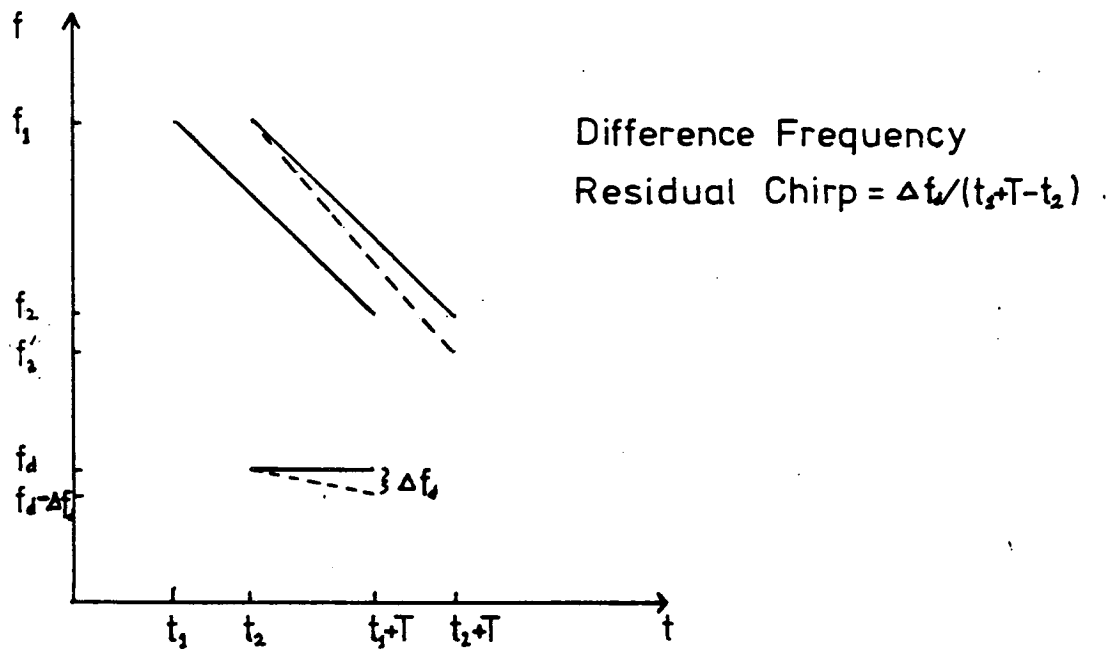
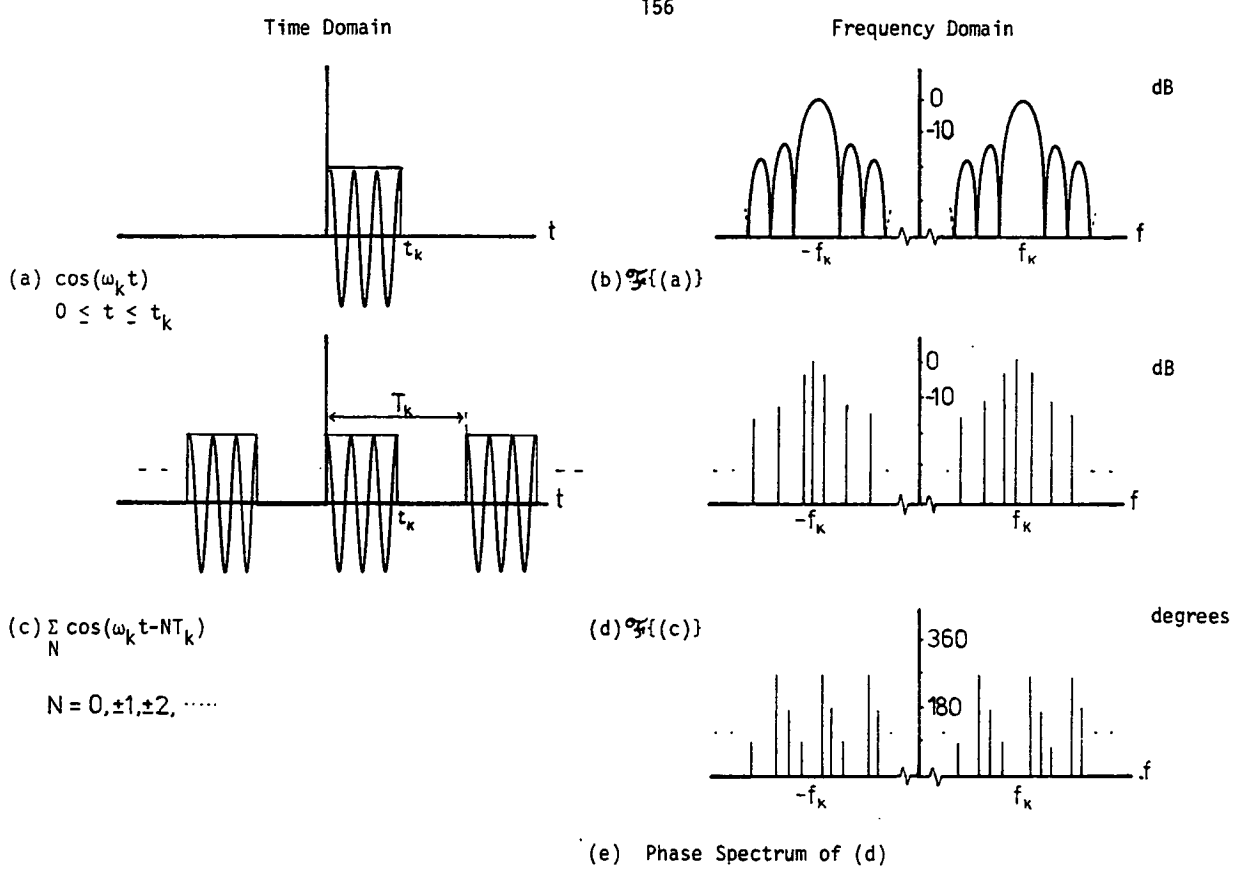
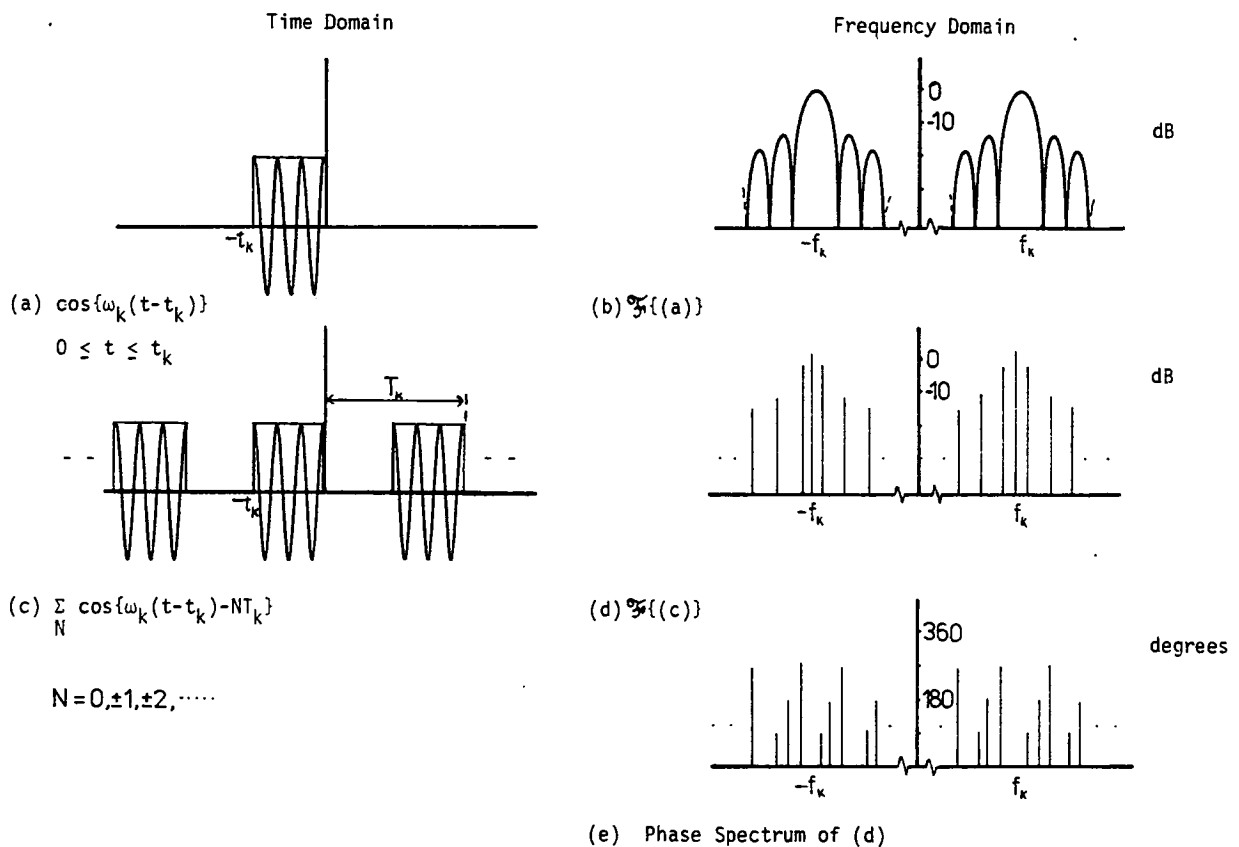


Figure 5.3 Chirp Slope Mismatch Error Mechanism



**Figure 5.4** Amplitude and Phase Spectra of a Repetitive Cosine Burst Waveform



**Figure 5.5** Amplitude and Phase Spectra of a Delayed Repetitive Cosine Burst Waveform

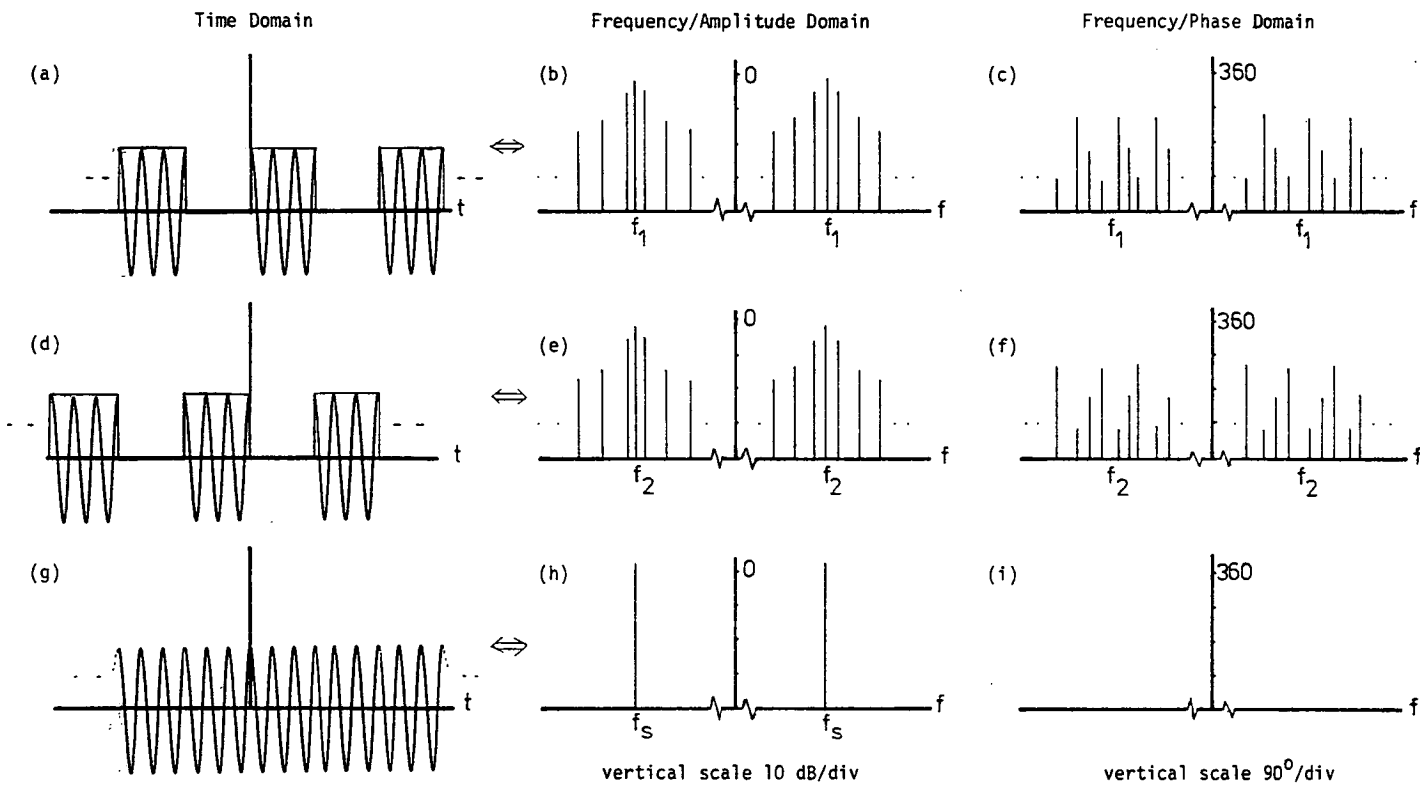


**Figure 5.6** Amplitude and Phase Spectra : Illustrating CW Frequency Synthesis from Two Repetitive Burst Cosine Waveforms  
 (a), (b), (c) - Channel 1; (d), (e), (f) - Channel 2; (g), (h), (i) - Ideal Synthesiser Output

⇔ Forward/Reverse Fourier Transformation

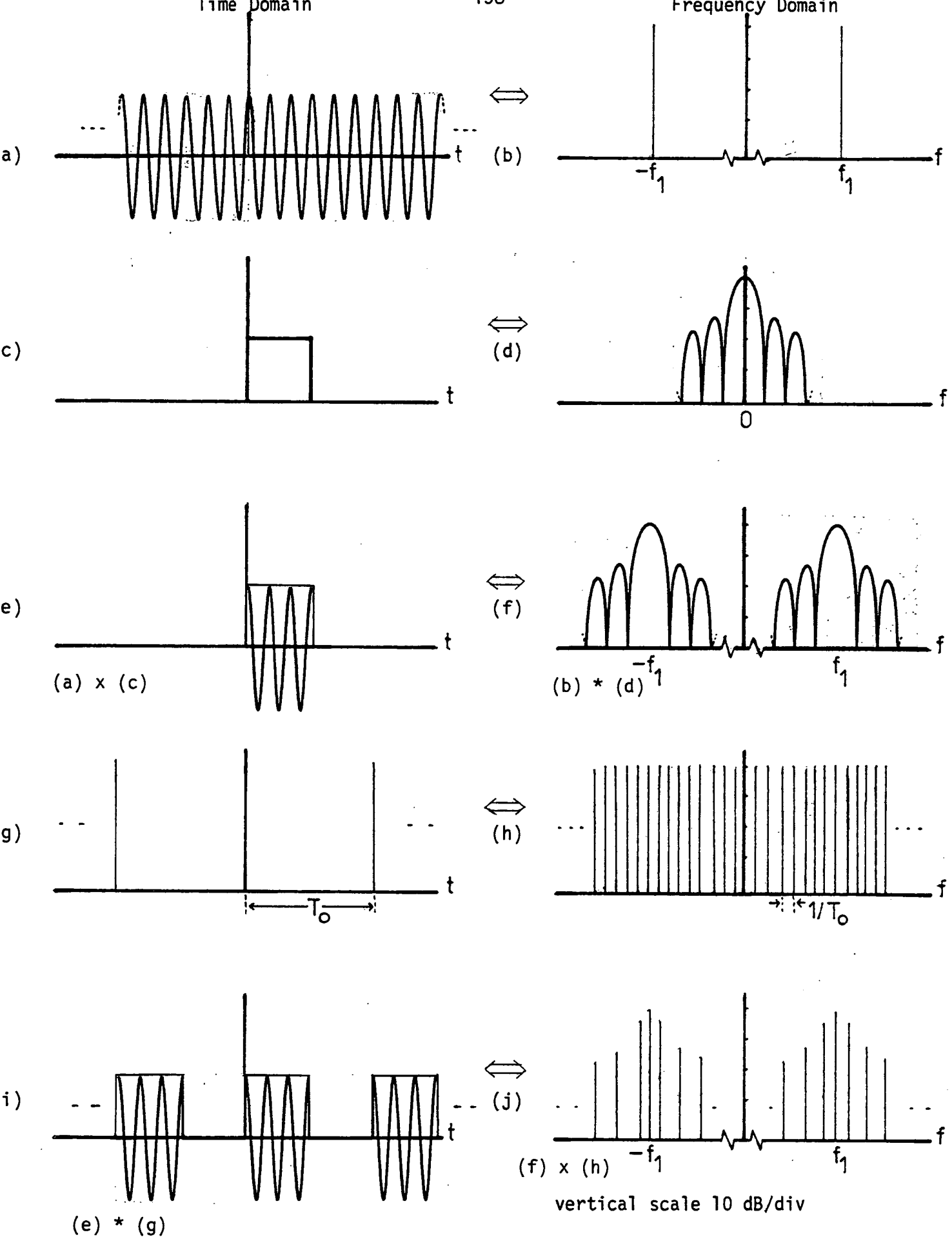


**Figure 5.7** Graphical Derivation of the Amplitude Spectrum for Channel 1

$\Leftrightarrow$  Forward/Reverse Fourier Transformation

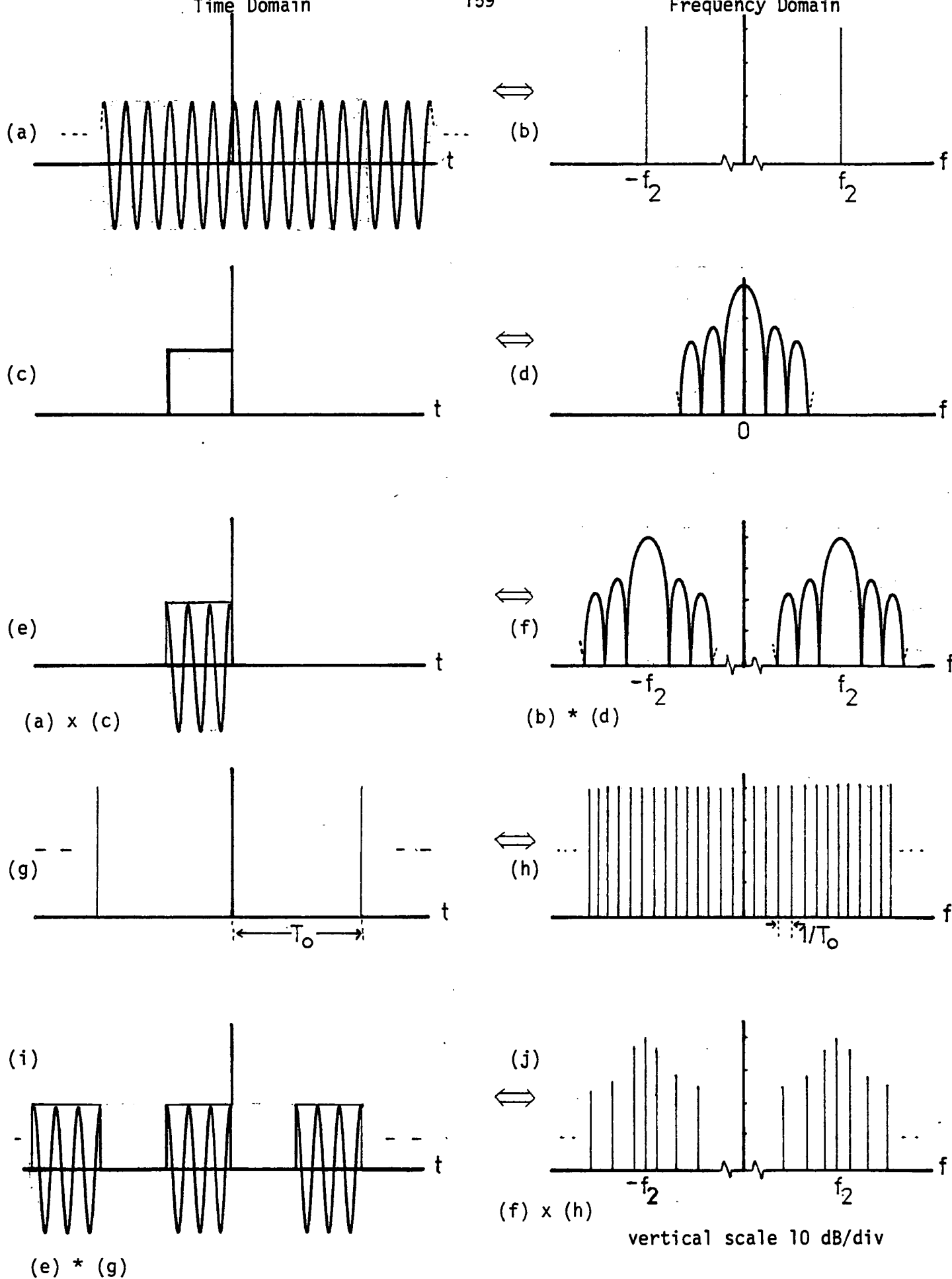


**Figure 5.8** Graphical Derivation of the Amplitude Spectrum for Channel 2

$\rightleftharpoons$  Forward/Reverse Fourier Transformation

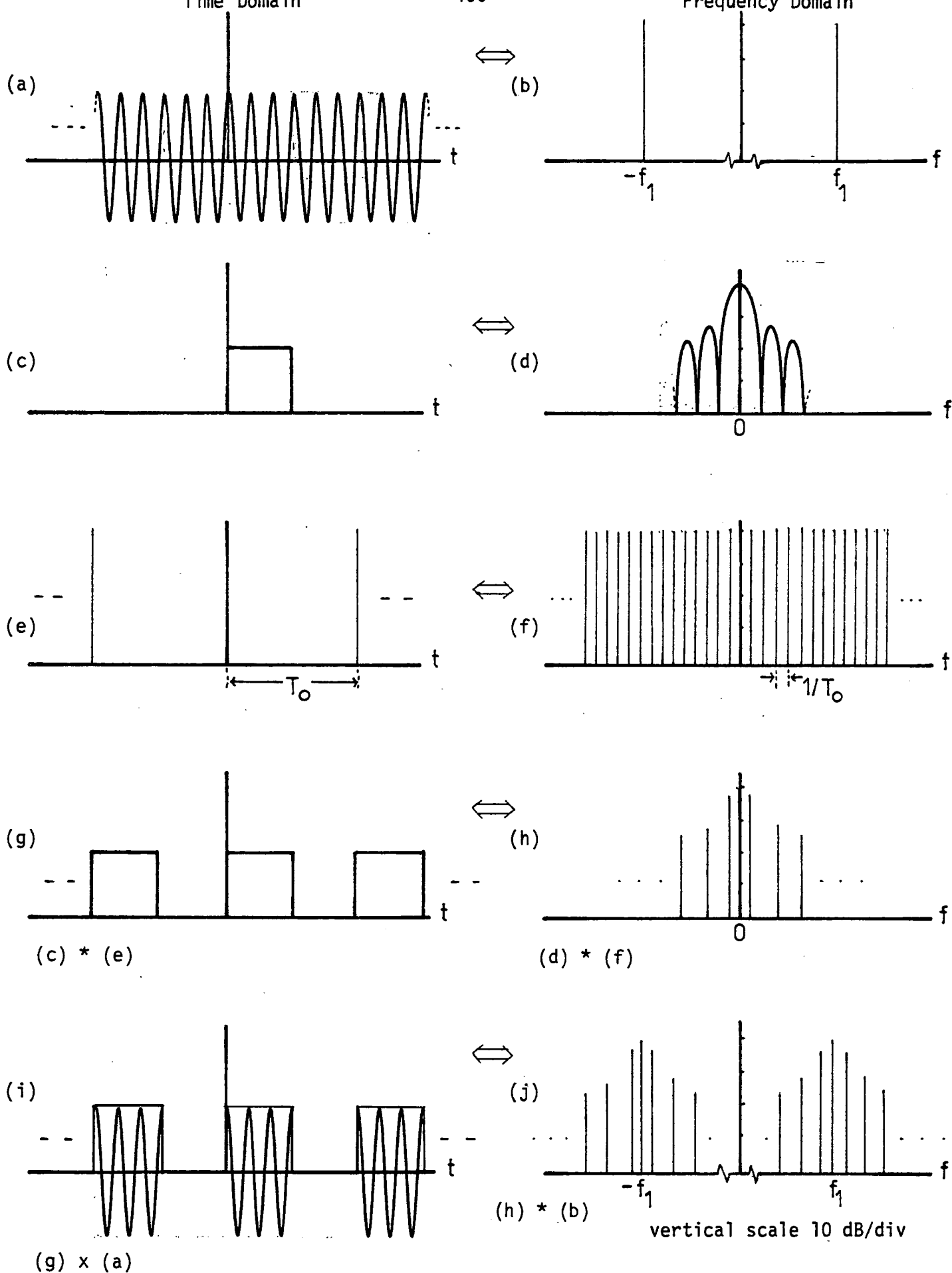
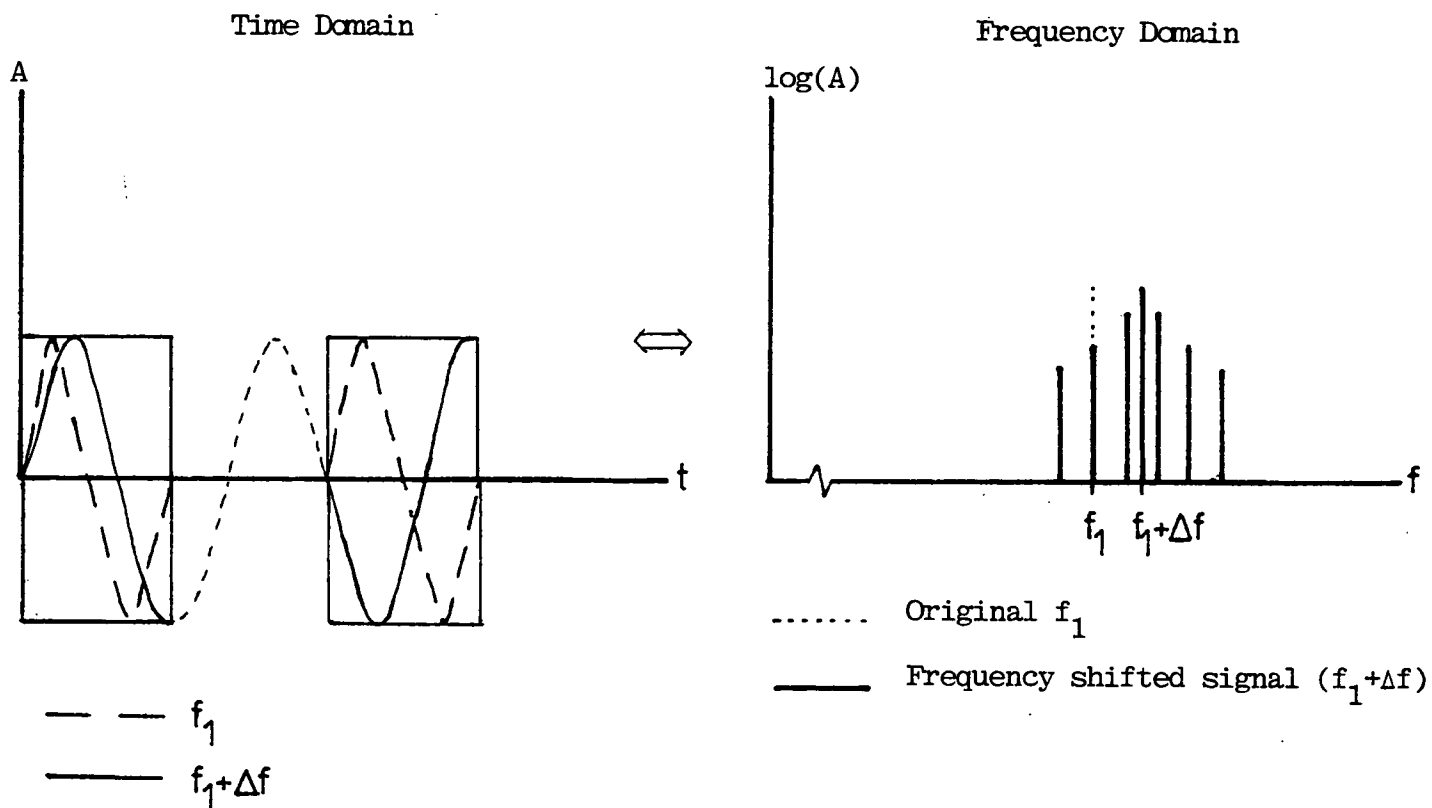


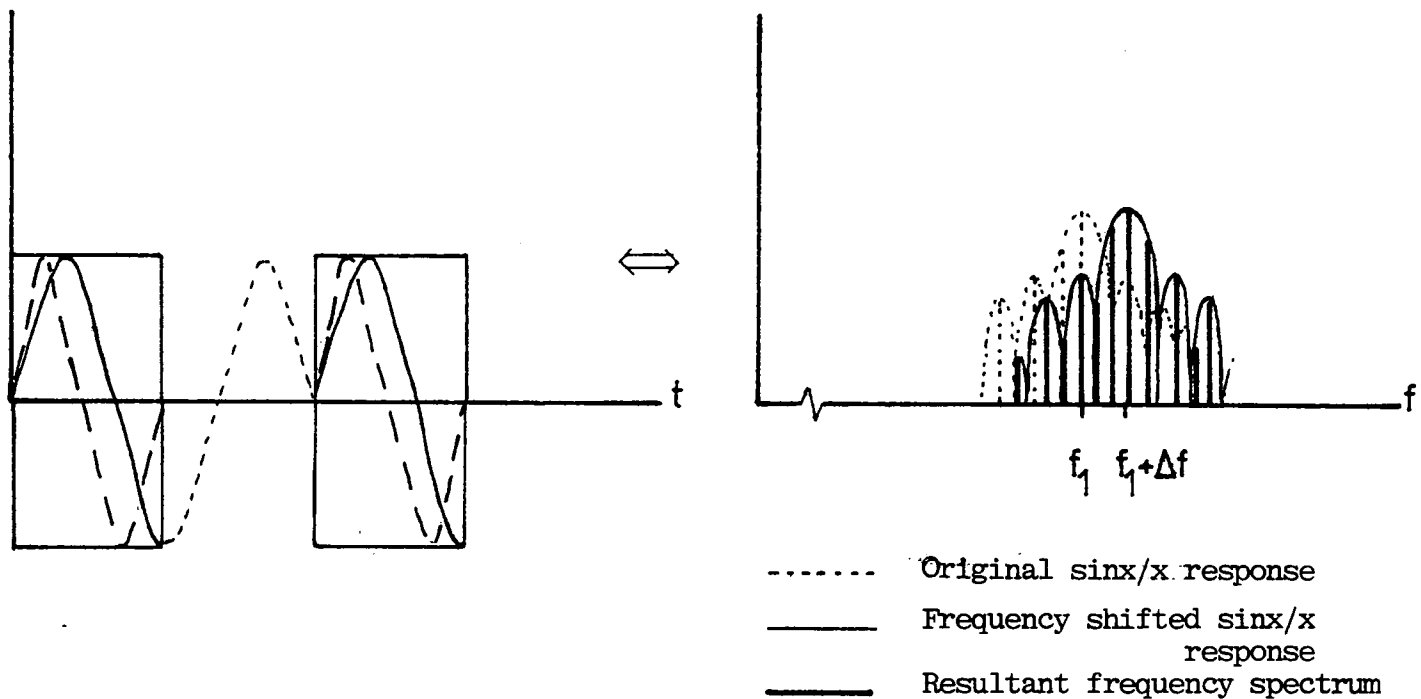
**Figure 5.9**

Graphical Derivation of the Amplitude Spectrum of a 100% Amplitude Modulated Cosine Waveform

$\Leftrightarrow$  Forward/Reverse Fourier Transformation



(a) Amplitude modulated cosine waveform - non integral no. of cycles/burst

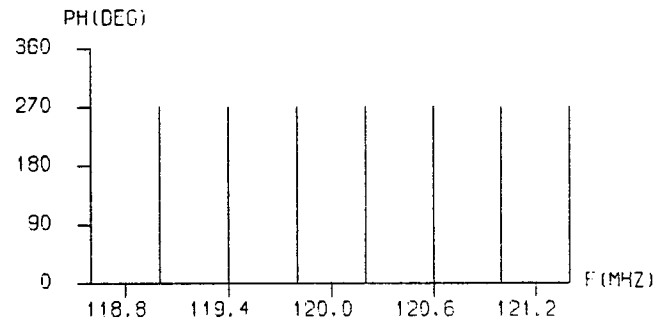
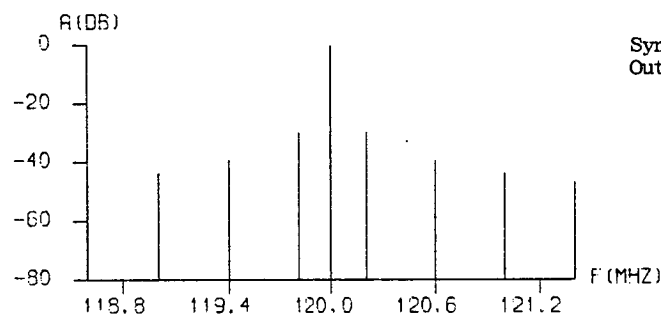
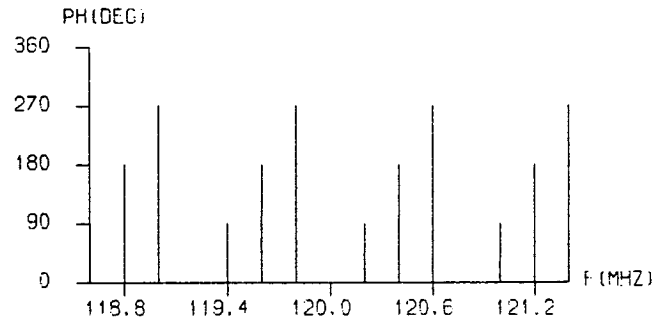
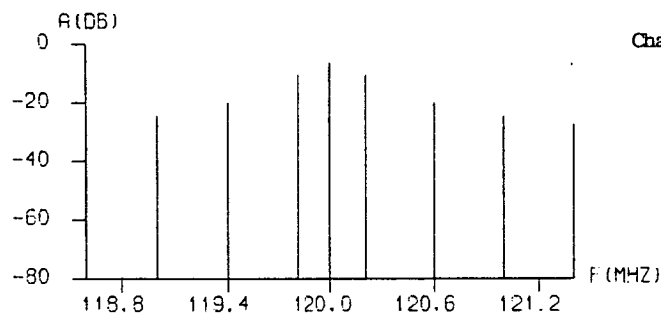
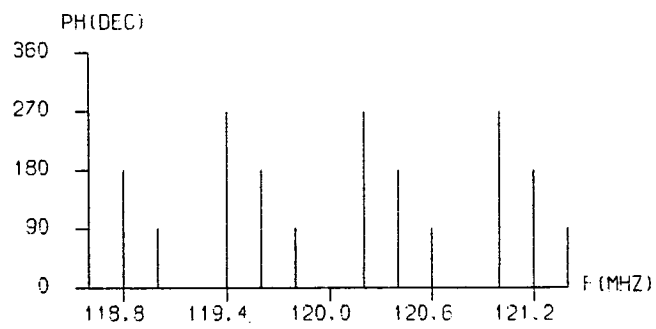
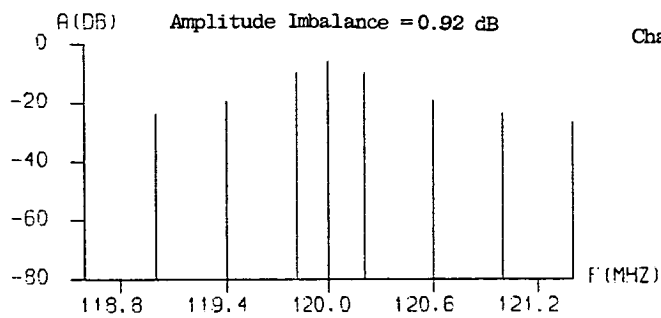


(b) FH channel output - non integral no. of cycles/hop

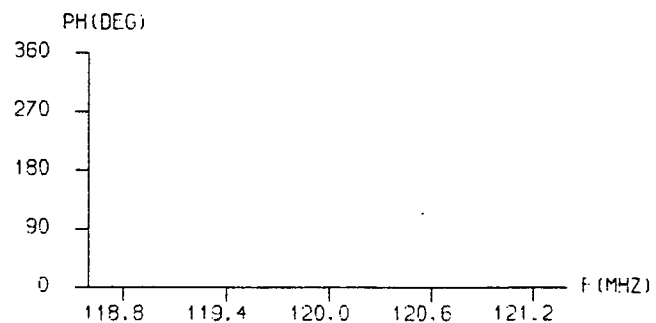
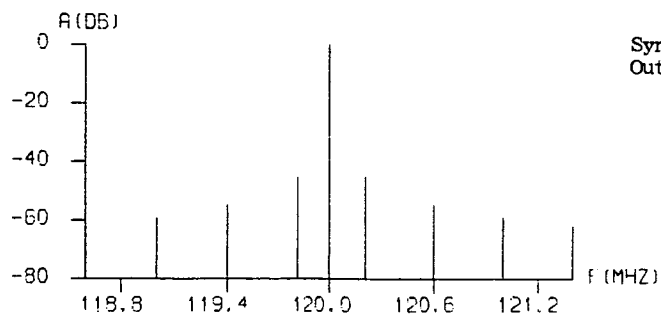
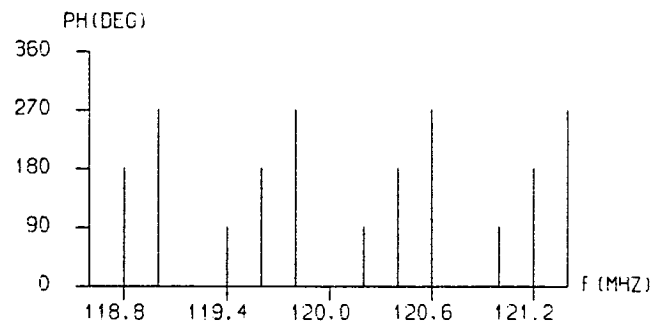
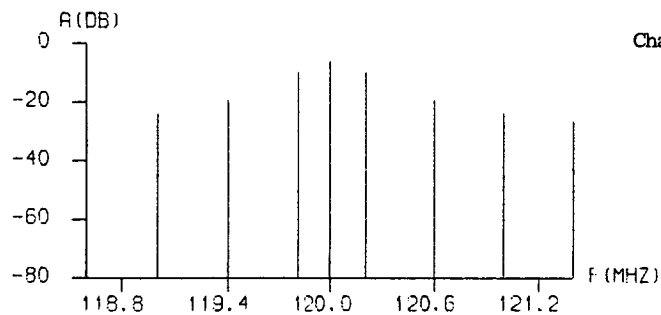
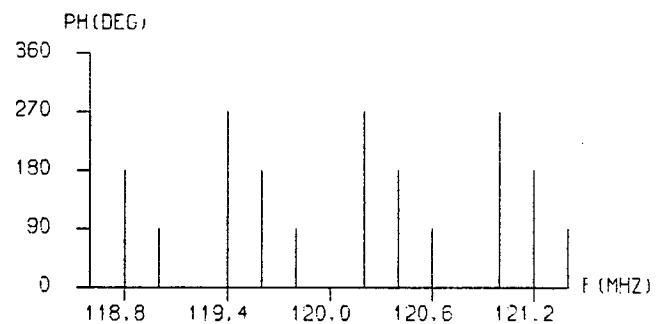
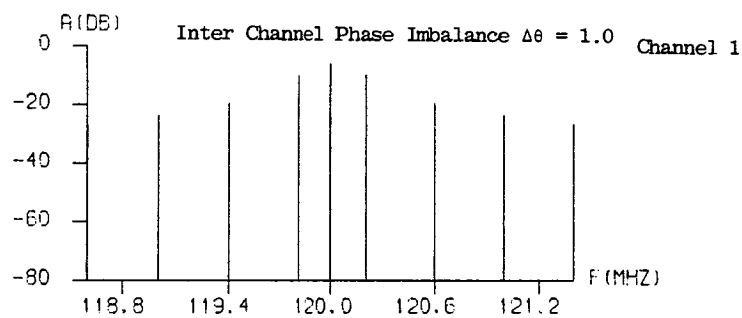
**Figure 5.10** Comparison of FH and Square Wave Amplitude Modulated Waveforms, with a Frequency Shifted Output Signal.

$\Longleftrightarrow$  Forward/Reverse Fourier Transformation



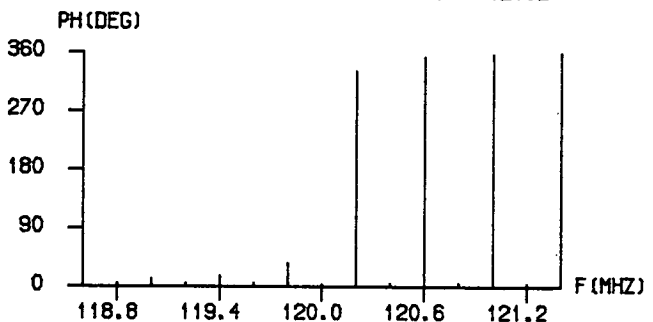
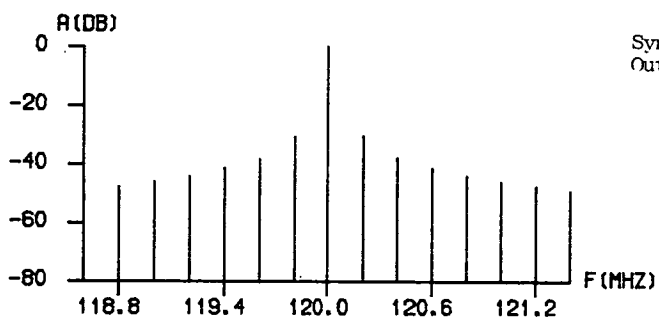
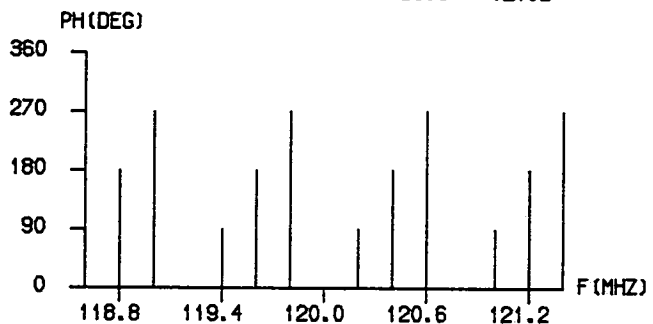
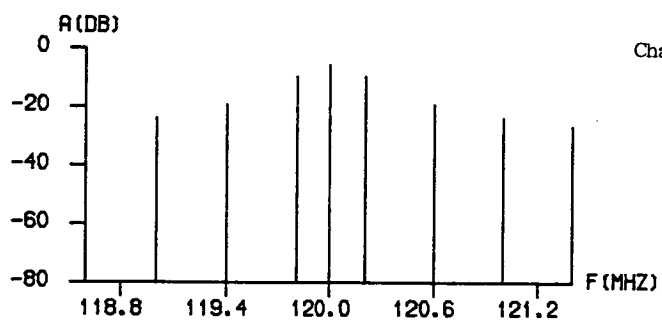
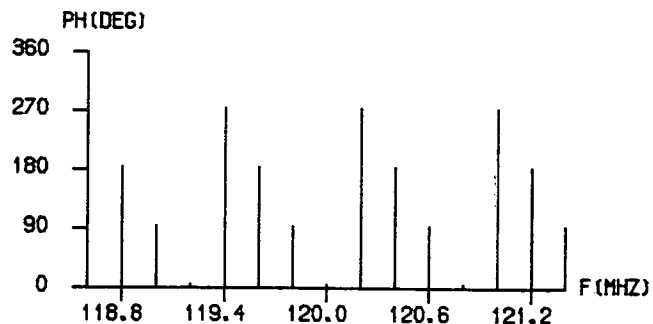
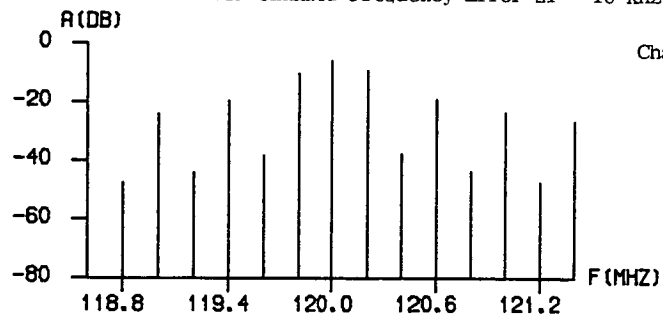


(a) Amplitude Imbalance Error

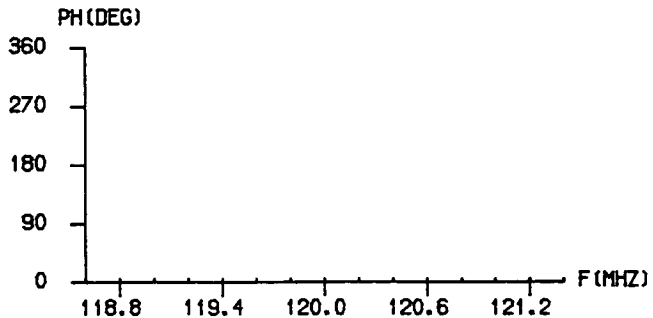
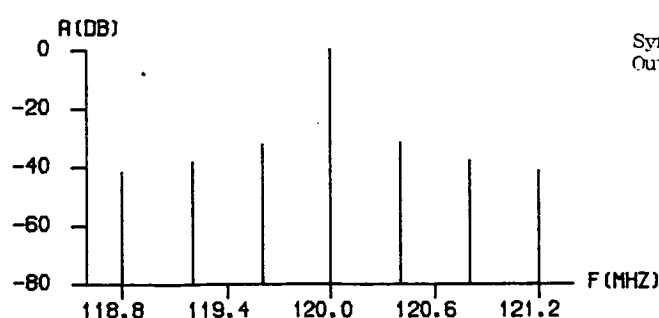
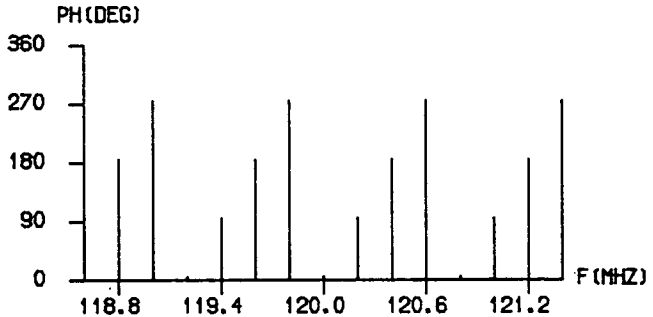
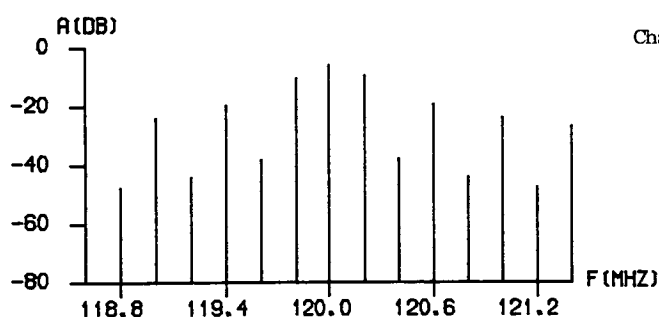
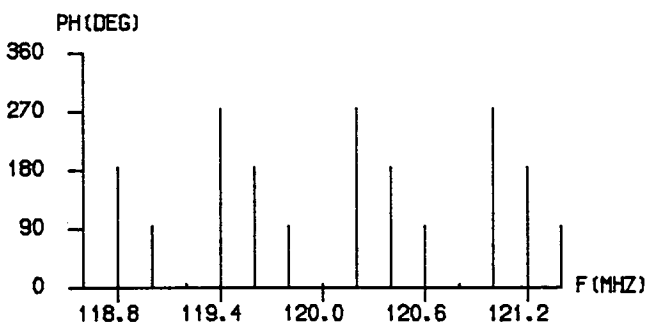
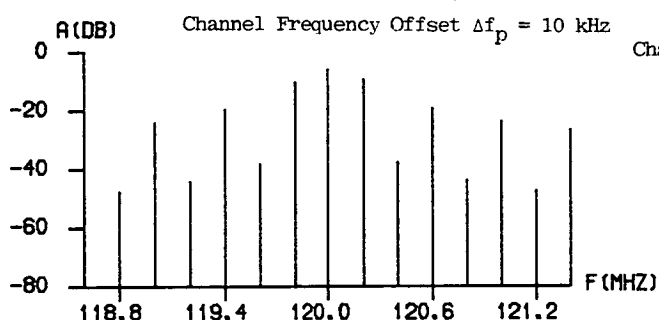


(b) Inter Channel Phase Imbalance

Figure 5.11 Synthesiser Error Simulation. Extrinsic Sounding



(a) Inter Channel Frequency Error



(b) Channel Frequency Offset

Figure 5.12 Synthesiser Error - Fourier Series Program

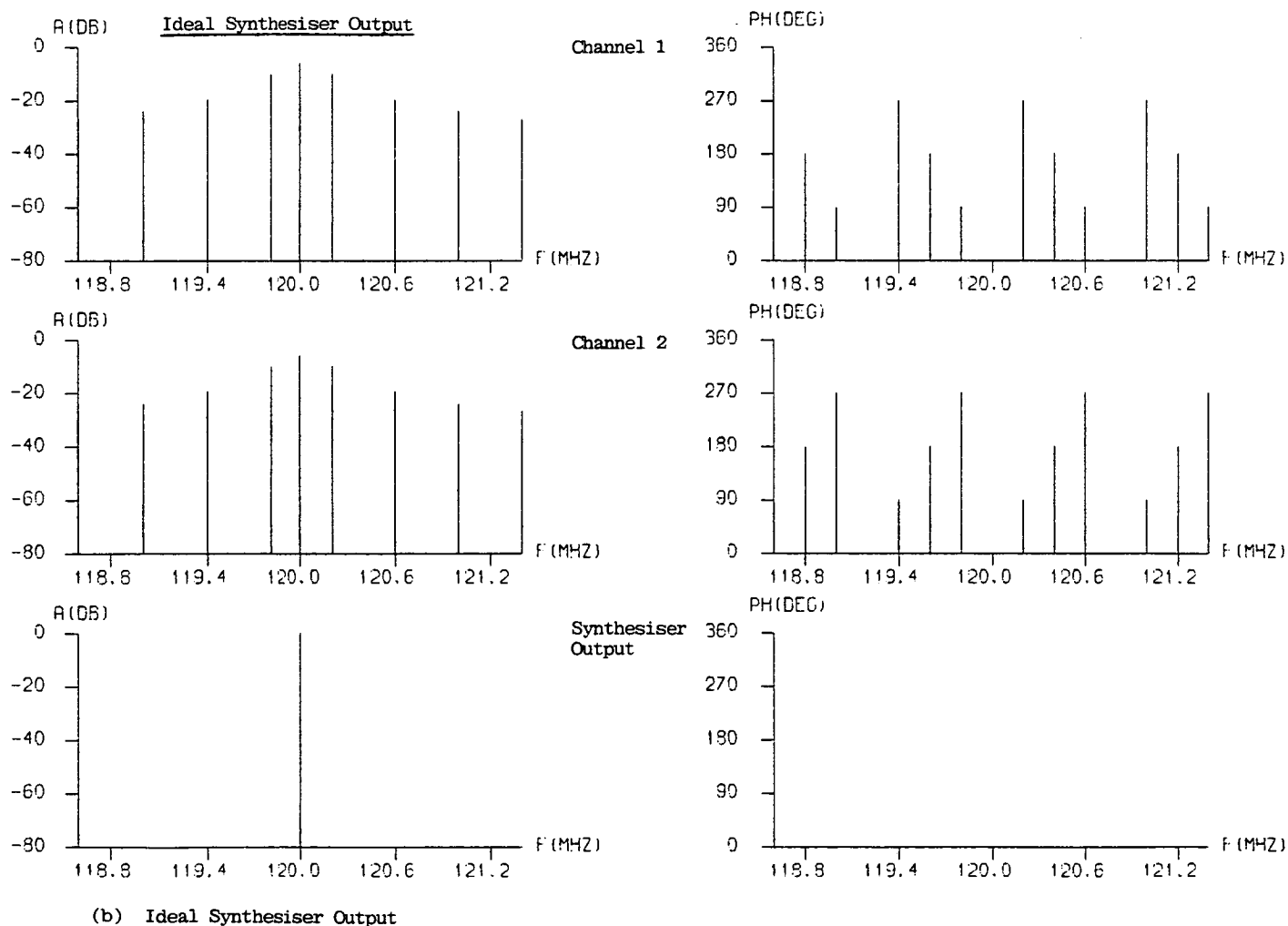
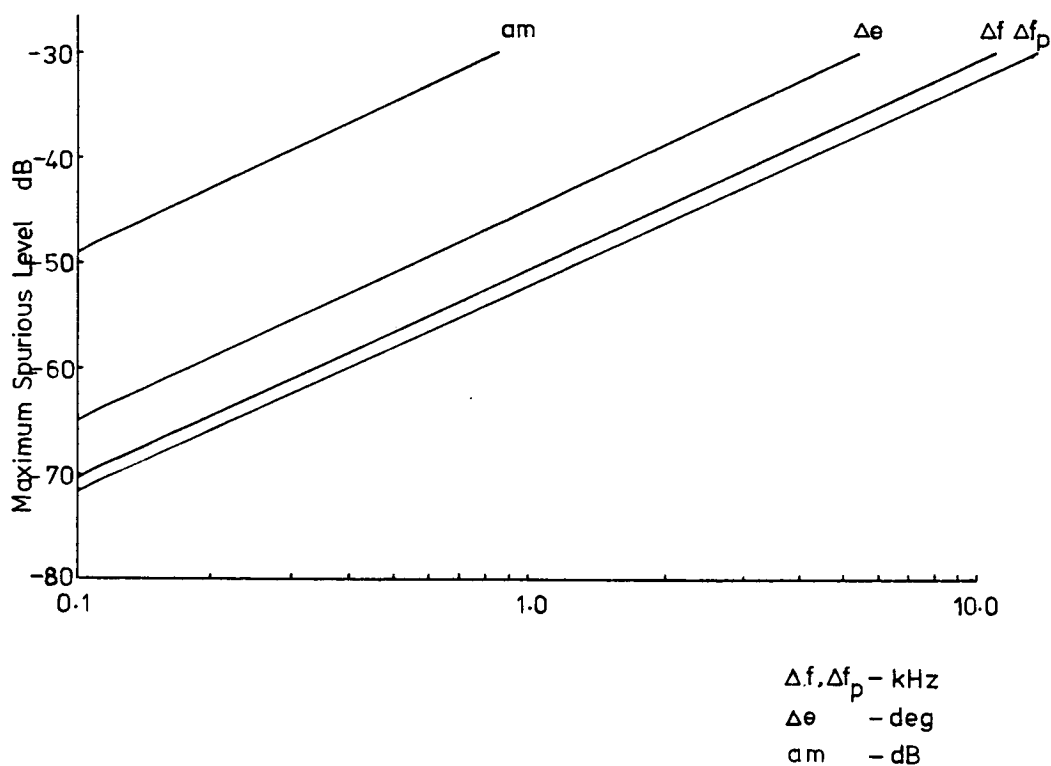


**Figure 5.13** (a) Maximum Spurious Level vs. Synthesiser Error Mechanisms -  $\Delta A$ ,  $\Delta \theta$ ,  $\Delta f$ ,  $\Delta f_p$   
 (b) Ideal Synthesiser Output - Fourier Series Simulation

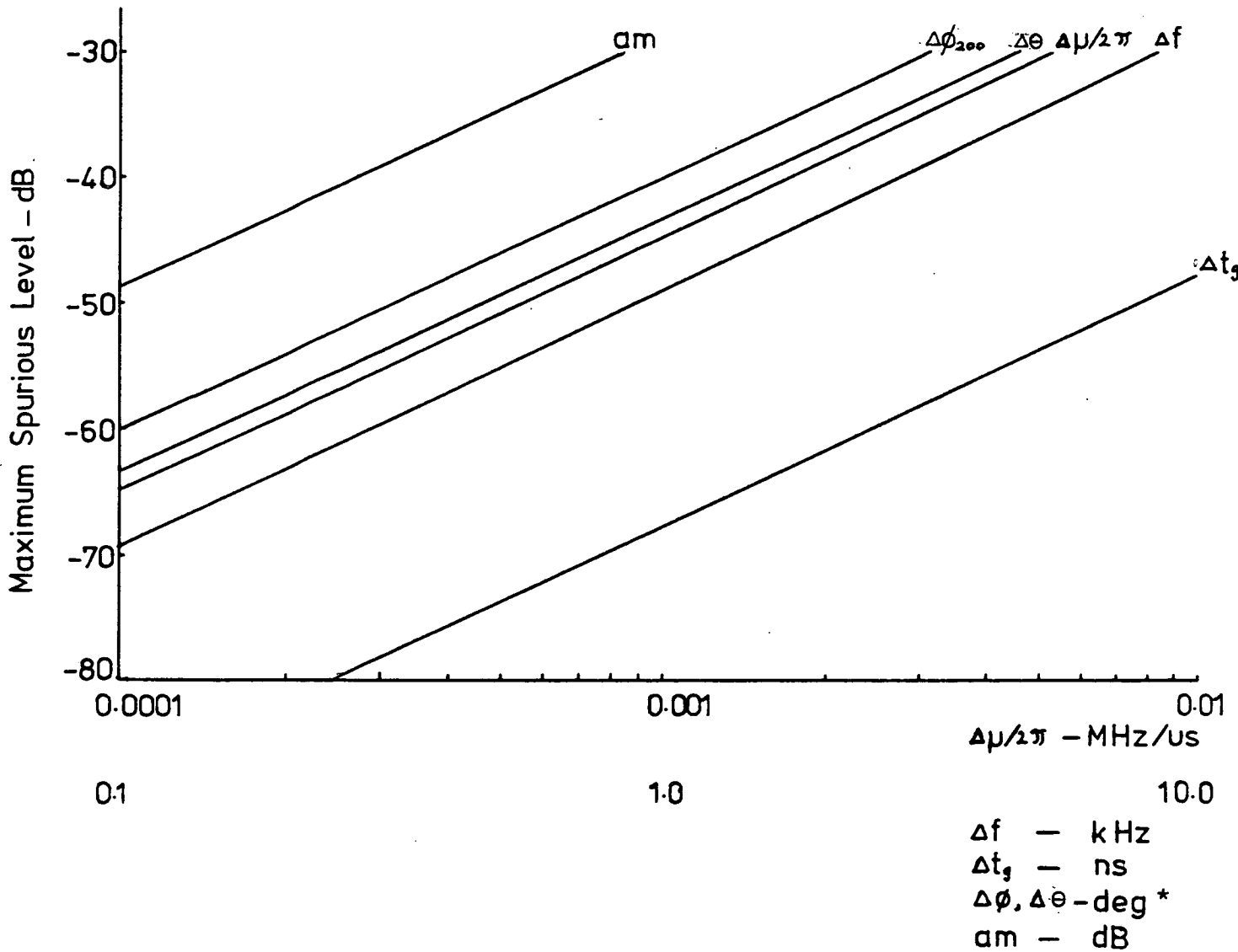


**Figure 5.14** Maximum Spurious Level w.r.t. Theoretical Peak Output  
vs Error Mechanisms

(Difference Frequency FFT Simulation)

\* $\Delta\phi_{200}$  refers to 200 kHz chirp phase ripple

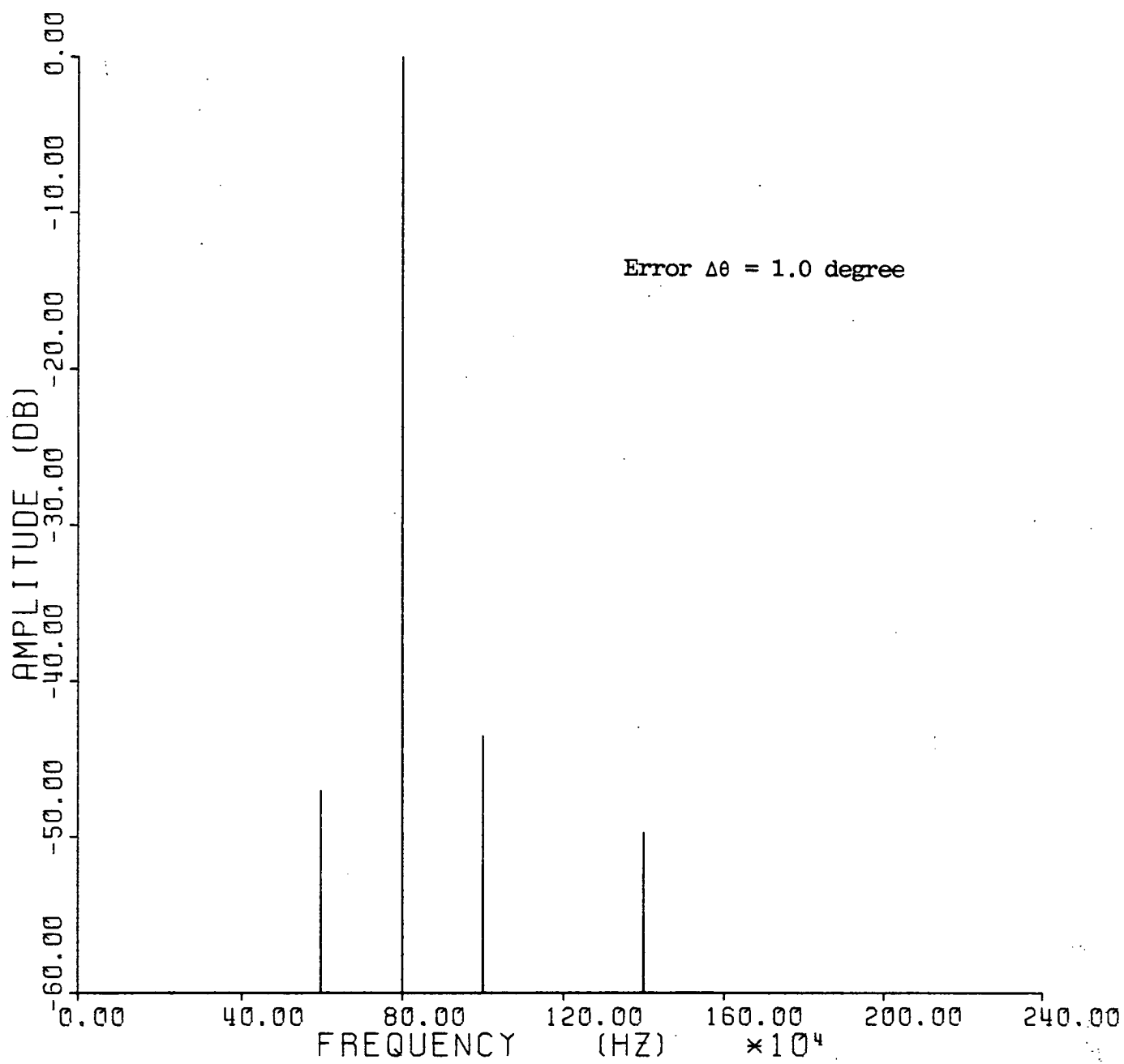


Figure 5.15 Synthesiser Error Simulation  
Difference Frequency FFT Program

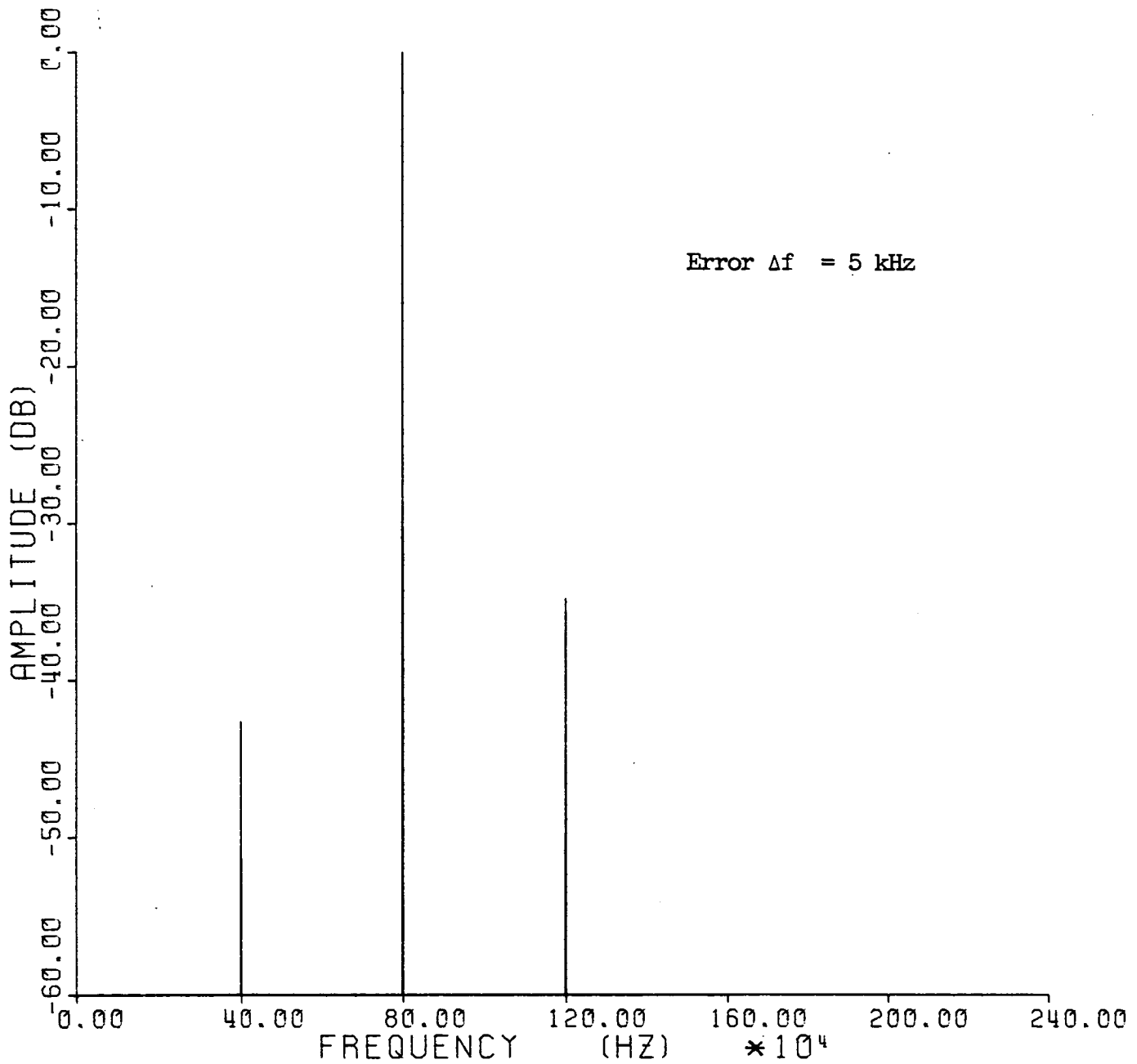


Figure 5.16 Synthesiser Error Simulation  
Difference Frequency FFT Program

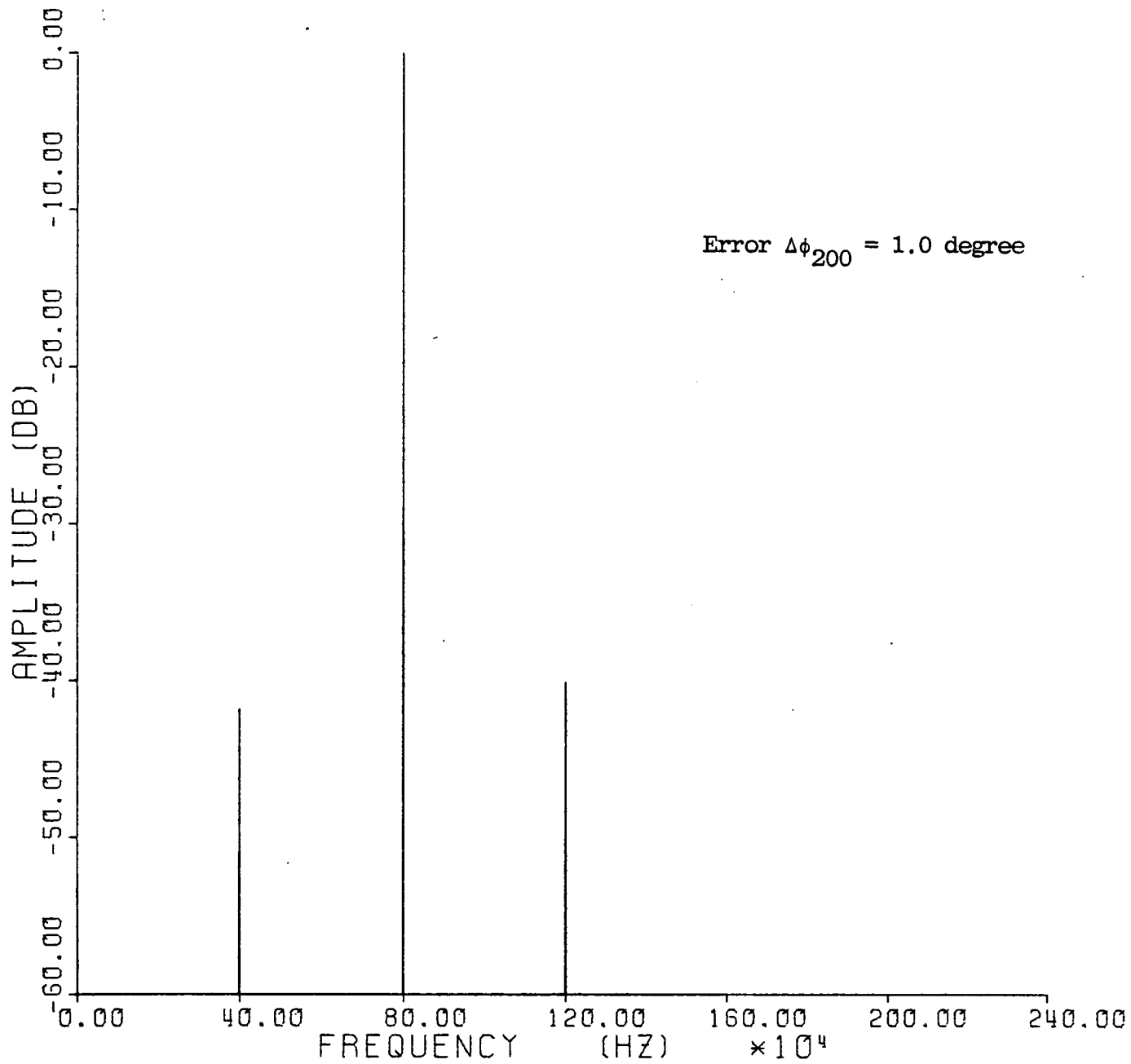


Figure 5.17 Synthesiser Error Simulation  
Difference Frequency FFT Program

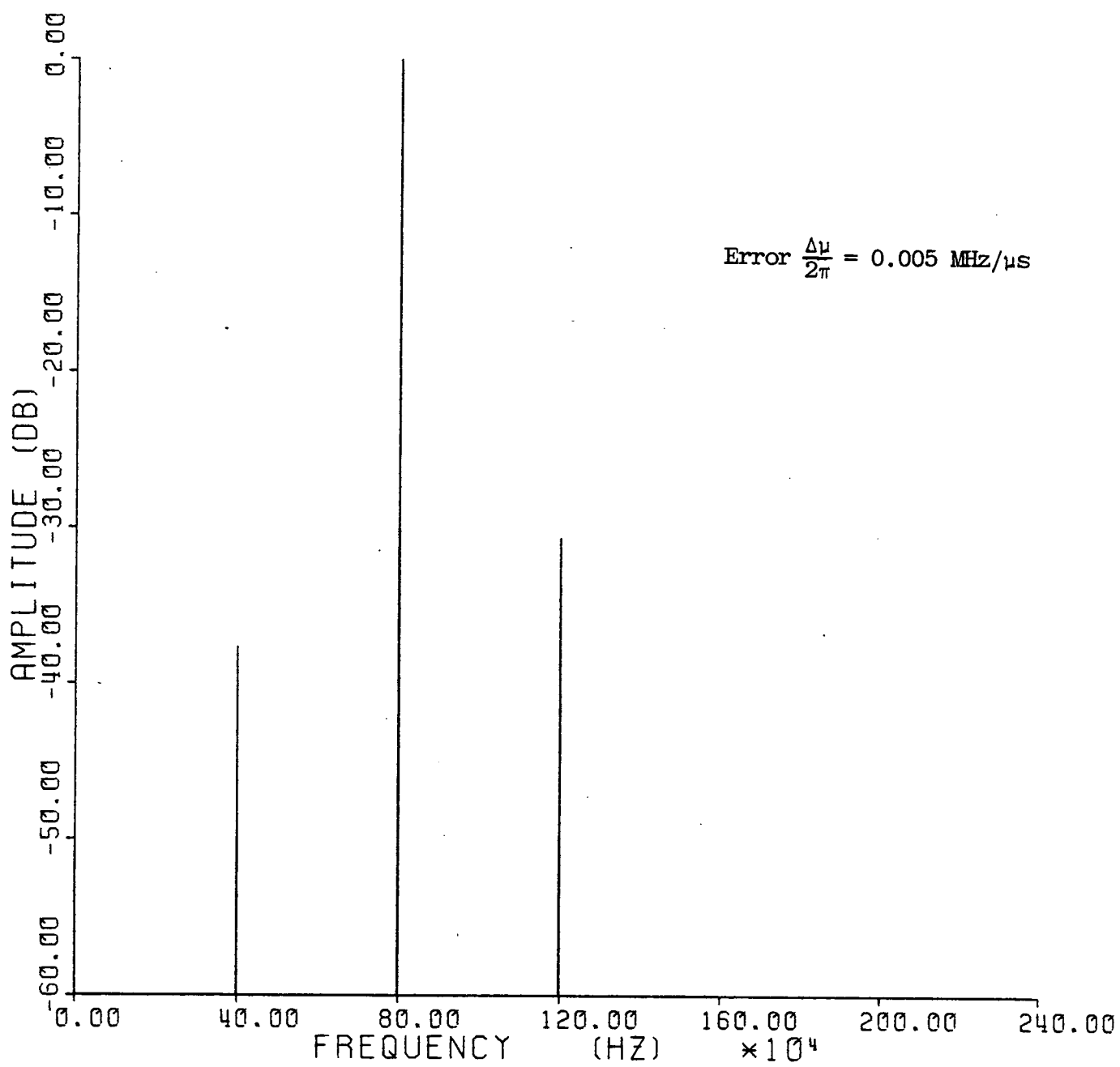
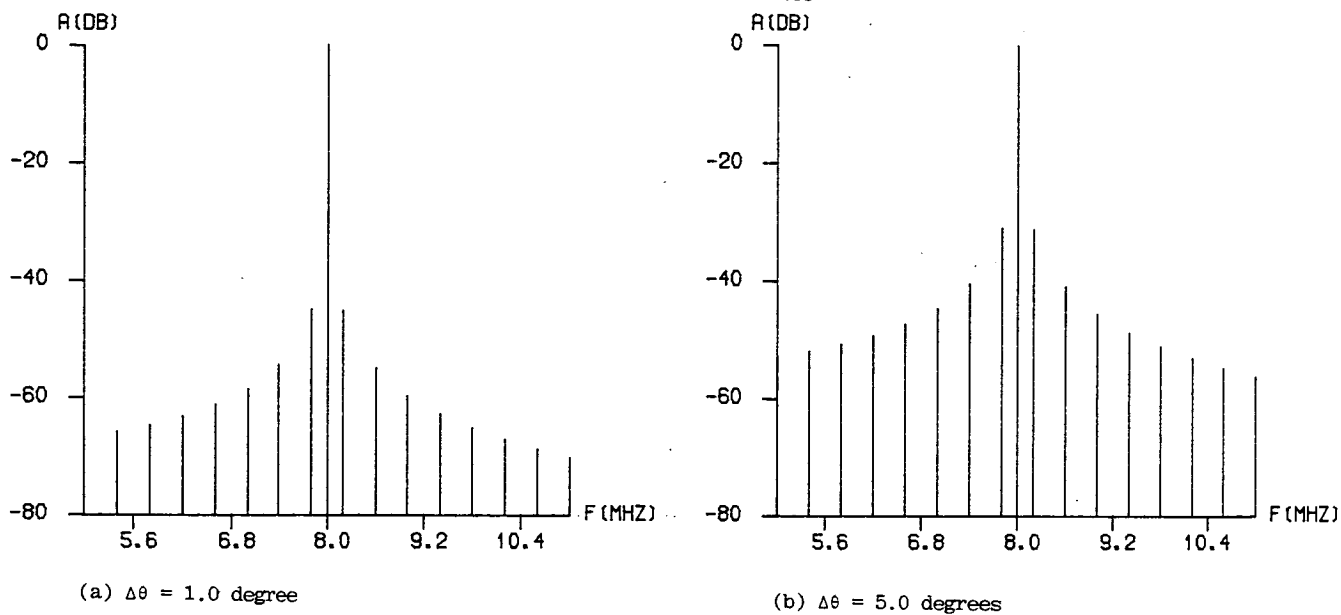


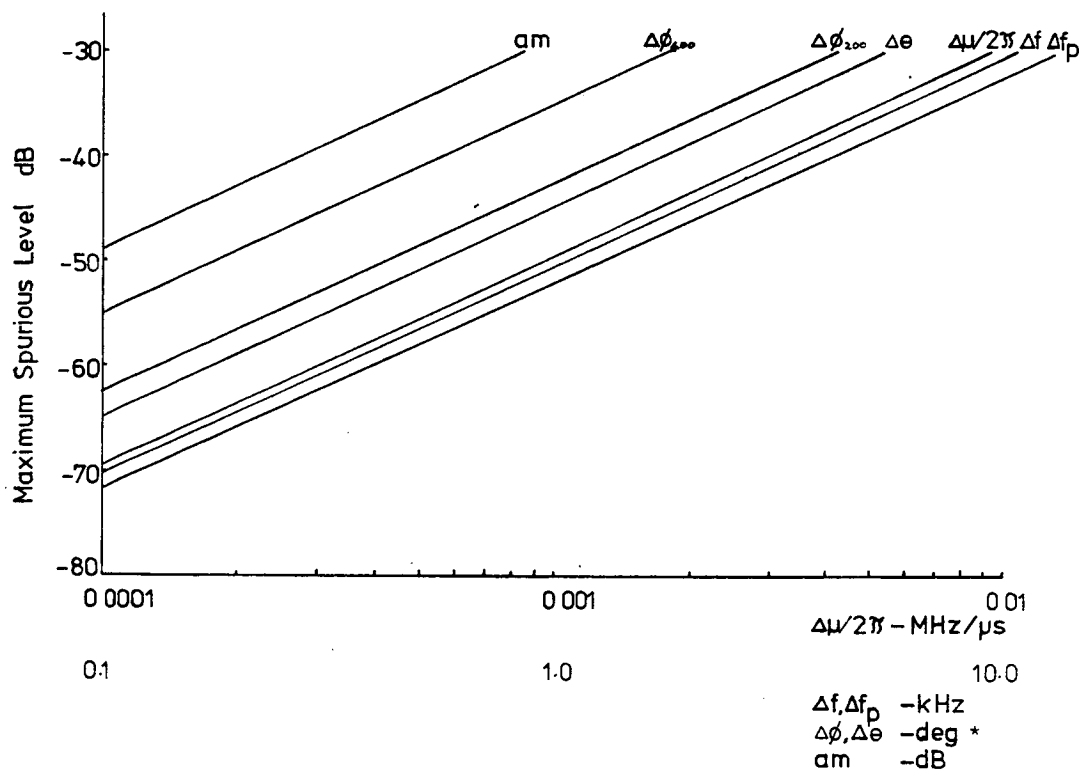
Figure 5.18 Synthesiser Error Simulation  
Difference Frequency FFT Program



## Inter Channel Phase Imbalance



**Figure 5.19** Synthesiser Error Simulation  
Inter Channel Phase Imbalance, Simulated at 8 MHz Centre Frequency  
Difference Frequency FFT Program (modified for 200 kHz sampling rate)

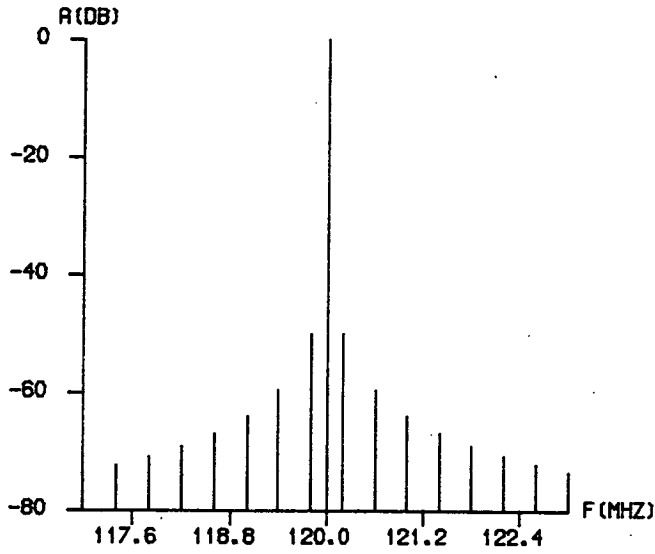
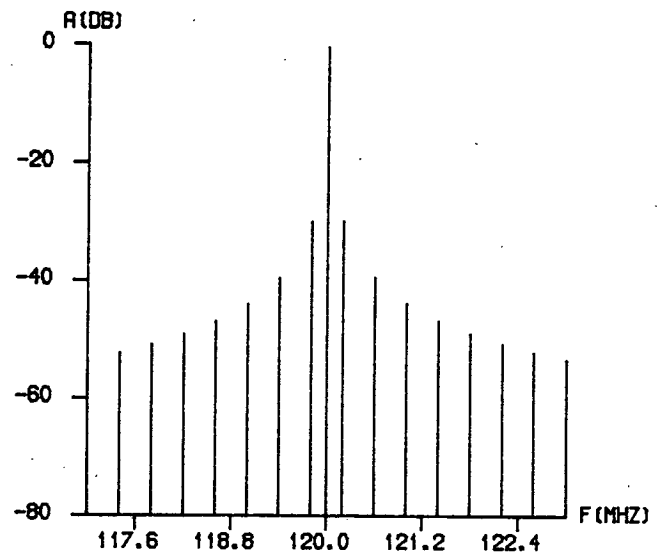


**Figure 5.20** Maximum Spurious Level w.r.t. Theoretical Peak Output  
vs Error Mechanisms  
(Sum Frequency FFT Simulation)

\* $\Delta\phi_{200}$  refers to 200 kHz chirp phase ripple

$\Delta\phi_{400}$  refers to 400 kHz chirp phase ripple

## Inter Channel Amplitude Error

(a)  $\Delta A = 0.087$  dB(b)  $\Delta A = .92$  dB

## Inter Channel Phase Imbalance

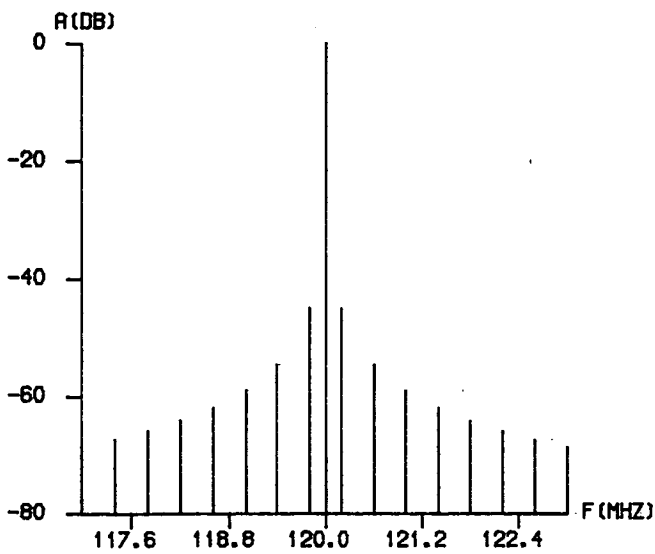
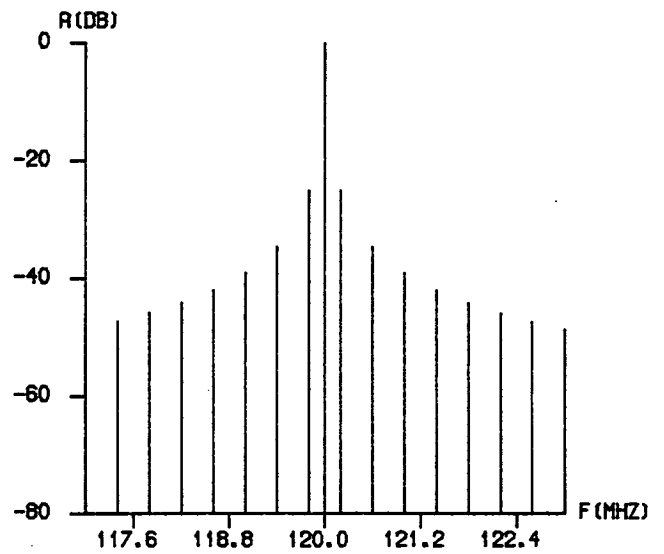
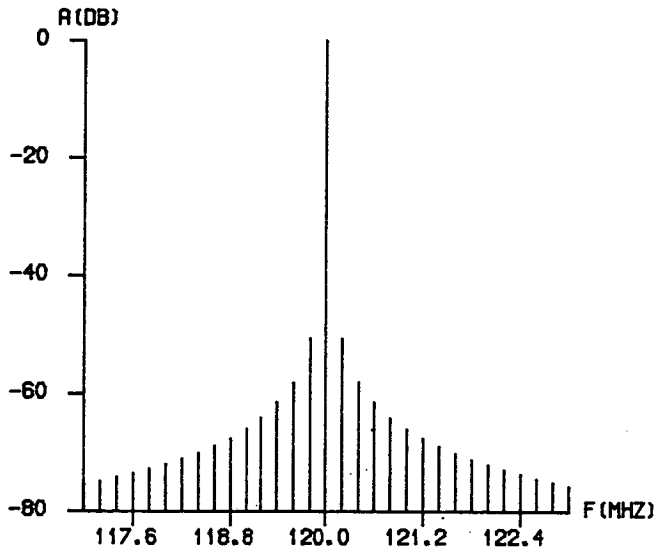
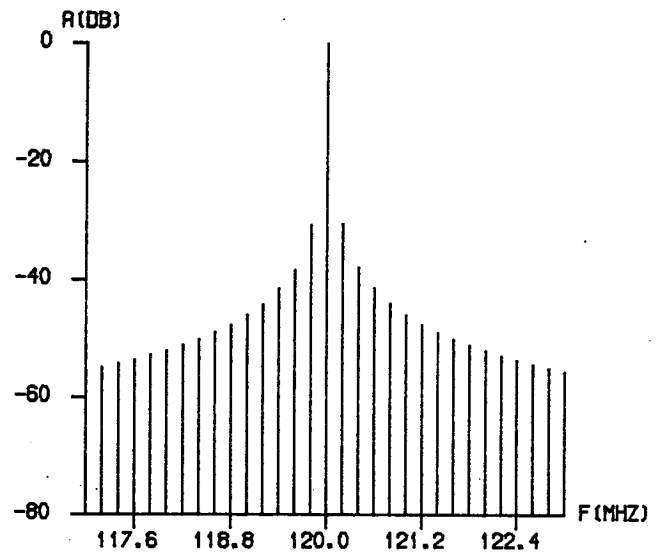
(c)  $\Delta \theta = 1.0$  degree(d)  $\Delta \theta = 10.0$  degrees

Figure 5.21 Synthesiser Error Simulation  
Sum Frequency FFT Program

## Inter Channel Frequency Imbalance

(a)  $\Delta f = 1$  kHz(b)  $\Delta f = 10$  kHz

## Channel Frequency Offset

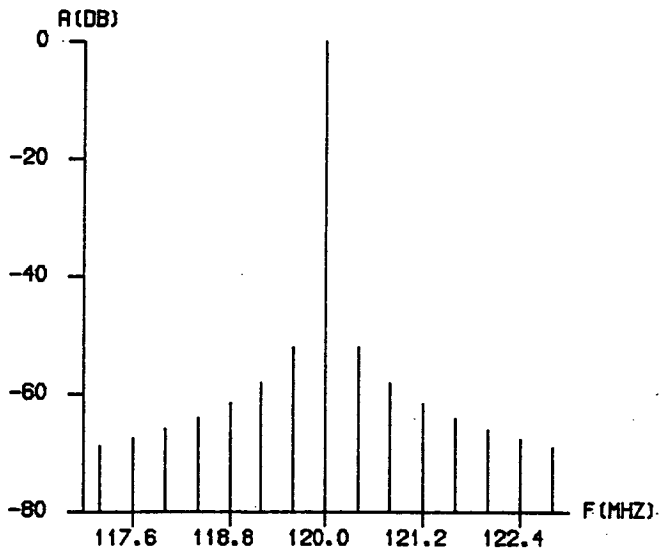
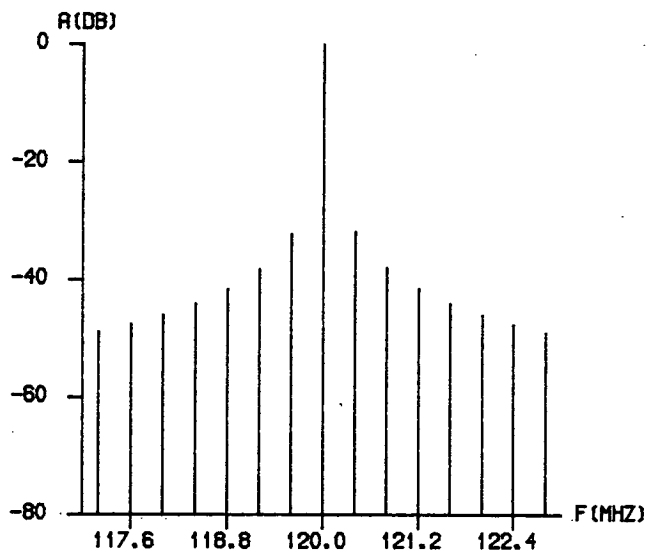
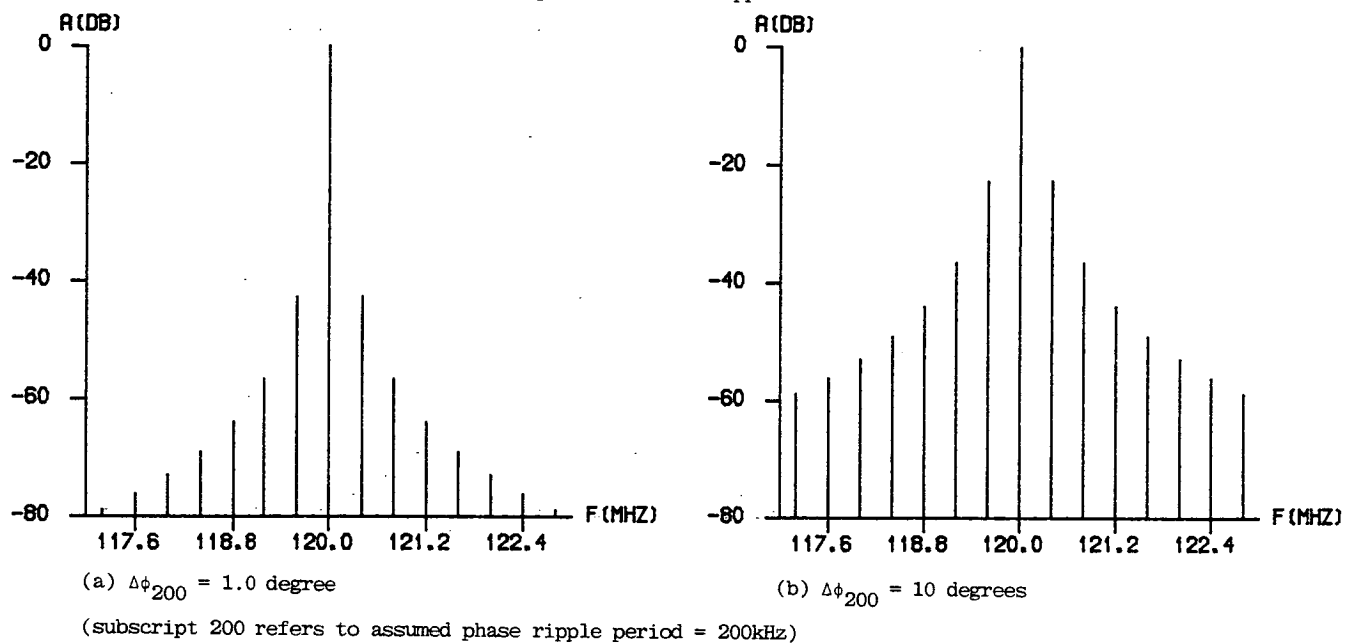
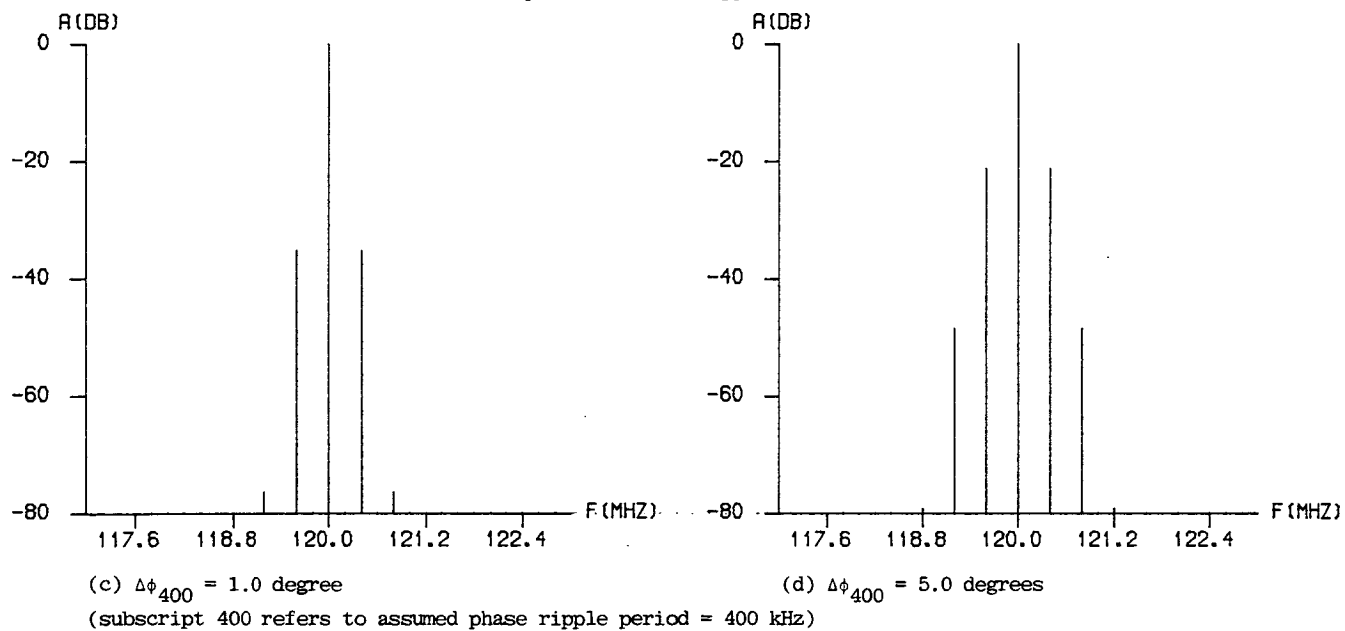
(c)  $\Delta f_p = 1$  kHz(d)  $\Delta f_p = 10$  kHz

Figure 5.22 Synthesiser Error Simulation  
Sum Frequency FFT Program

Chirp Filter Phase Ripple



Chirp Filter Phase Ripple



**Figure 5.23** Synthesiser Error Simulation  
Sum Frequency FFT Program

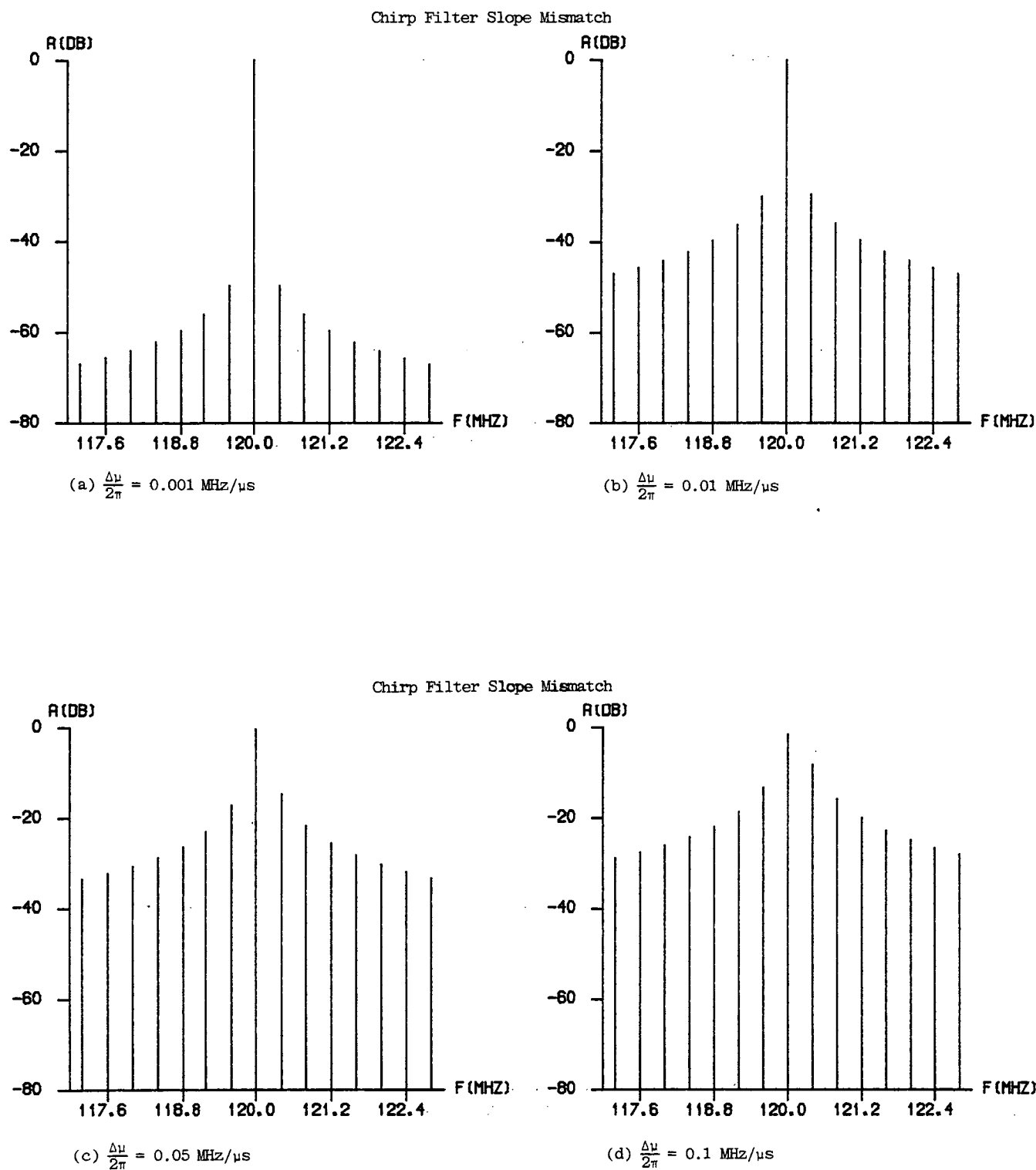
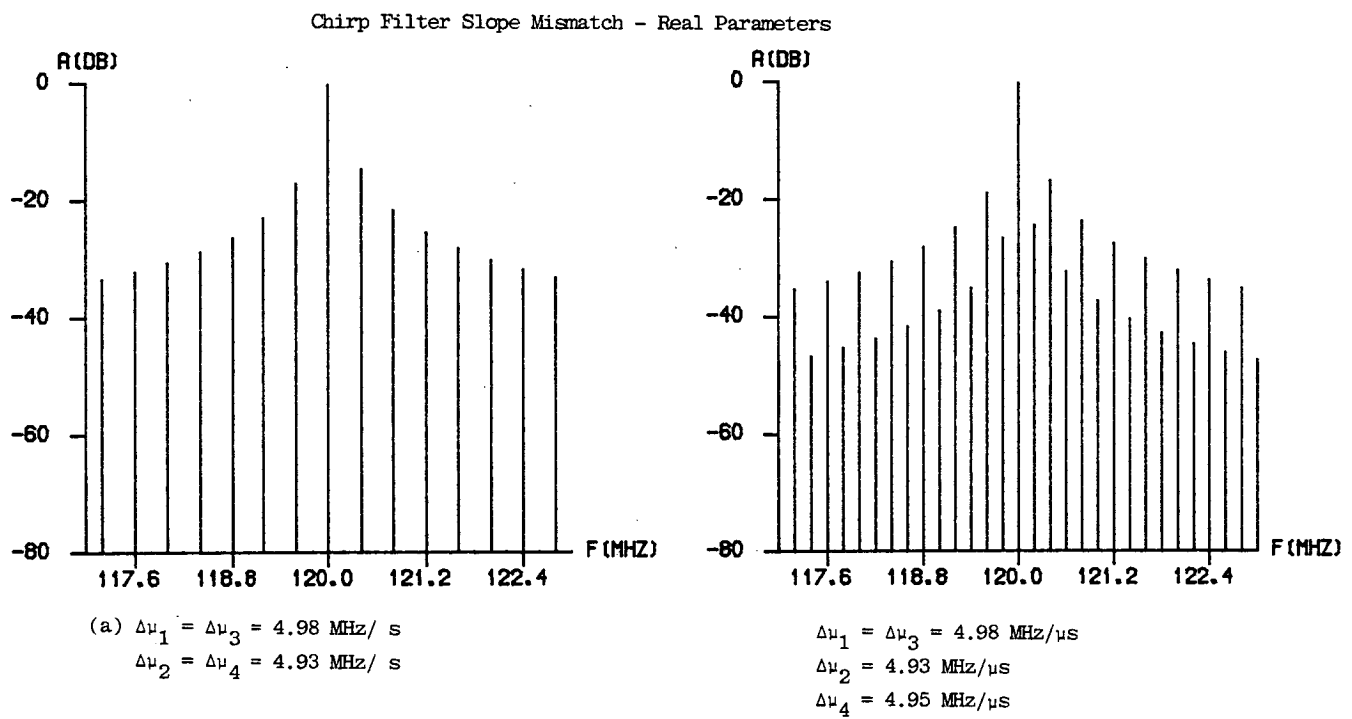


Figure 5.24 Synthesiser Error Simulation  
Sum Frequency FFT Program



**Figure 5.25** Synthesiser Error Simulation  
 Chirp Filter Slope Mismatch, based on Measured Parameters  
 Sum Frequency FFT Program

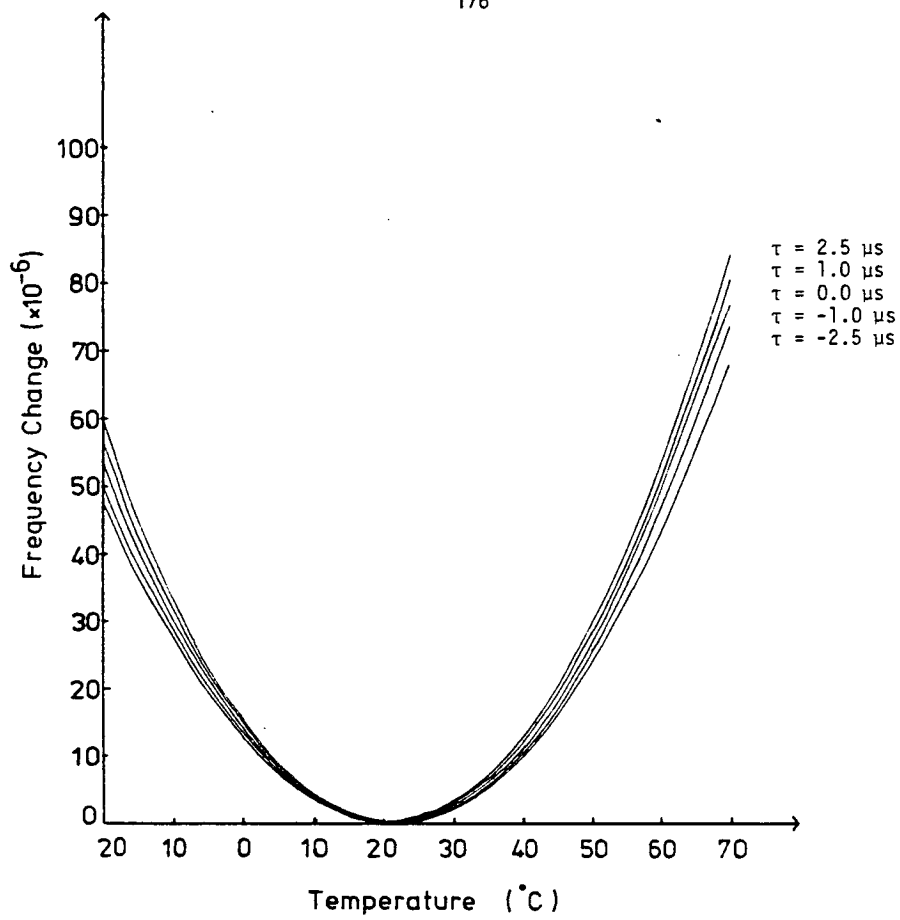


Figure 5.26 Frequency Change vs Temperature for  $-2.5 \mu\text{s} < \tau < 2.5 \mu\text{s}$

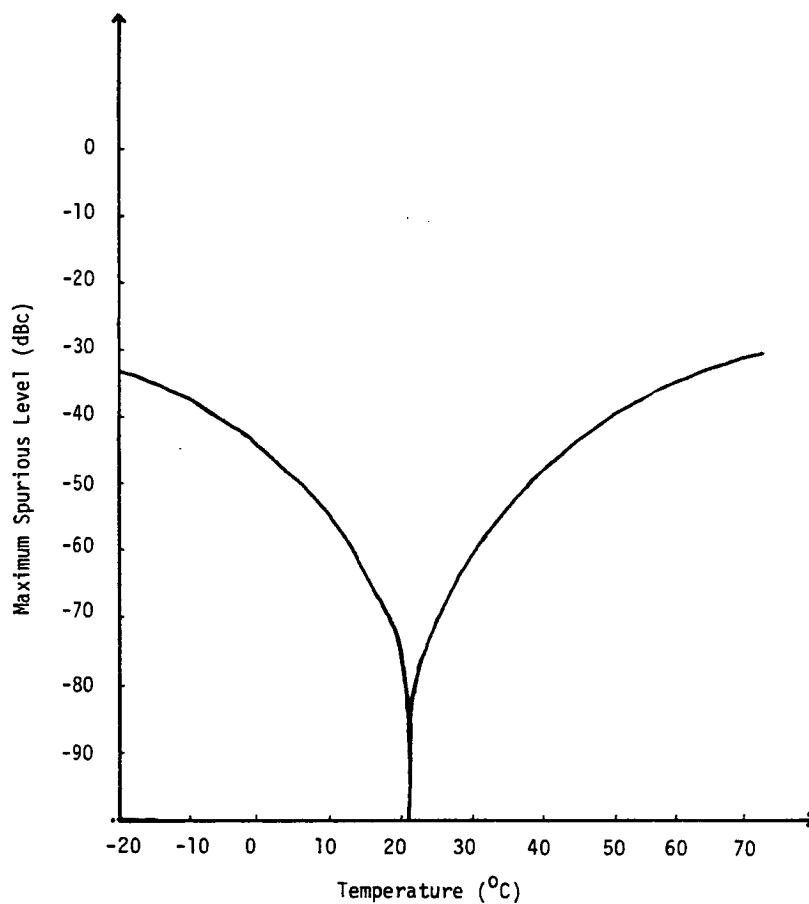


Figure 5.27 Maximum Spurious Level vs Temperature (for  $\tau = 0$ )

## CHAPTER 6 : SUMMARY AND CONCLUDING REMARKS

The work detailed in this thesis has been concerned with techniques for SAW chirp mixing frequency synthesis for fast FHSS applications. An introduction to this work and the contents of the thesis were presented in Chapter 1.

Current techniques for SS modulation were reviewed in Chapter 2 along with the principal methods for information transmission, PN code generation and synchronisation, carrier and code tracking and information demodulation. SS systems were shown to be more complex than conventional FDM equipment and hence are primarily used in applications where they provide more efficient multiple access capability, improved multipath interference rejection or inherent message privacy through low density coded transmission. Discussion of the two favoured spreading techniques, FH and DS, showed that DS is inherently simpler but suffers from unacceptably long synchronisation delays. FH systems employ a wideband frequency synthesiser to provide comparable processing gain at much reduced code rate, resulting in reduced synchronisation delay at the expense of increased hardware complexity. In practice, the optimum solution for many applications is a combination of DS, FH and TH where each technique contributes a portion of the overall system processing gain.

Chapter 3 presented a review of conventional techniques for frequency synthesis based on direct or indirect methods. These have limited application in fast FHSS due to the size, weight and power consumption associated with direct synthesis and the slow switching speeds inherent in indirect equipments. The digital



"look-up" synthesiser was shown to provide a novel technique based on the selection of sinusoidal data stored in read-only-memory. A review of SAW technology was presented in Section 3.3 as an introduction to frequency synthesis techniques based on SAW components. The capability of this technology to provide complex amplitude and phase functions over a wide IF frequency range (10 MHz - 1 GHz) was stressed and applications in radar, communications and signal processing reported. In particular, the development of high fidelity linear FM (chirp) filters for radar pulse compression was discussed due to the importance of these components in SAW chirp mixing frequency synthesis.

The principal methods discussed for SAW based frequency synthesis were filter bank, oscillator and chirp mixing techniques. Of these three, the multimode oscillator potentially presents the simplest solution for wideband synthesis. However, reliable mode selection and coherent operation are difficult to achieve in practice, and frequency switching is relatively slow implying parallel operation for fast FH applications. The filter bank technique provides a fast switching, high purity output signal, but the number of available frequencies is limited to less than 20 by the complexity of the SAW device and RF switching network. Through the use of a number of parallel units and conventional direct synthesis techniques, both filter bank and oscillator techniques can produce up to 500 hops over a 500 MHz bandwidth, at the expense of increasing system complexity. For coherent, wideband, fast switching, multifrequency operation, the SAW chirp mixing synthesiser provides the most attractive option with the potential capacity for 4000 hops, 50 kHz resolution, 500 MHz bandwidth and 10 ns switching speed.

A theoretical analysis of the chirp mixing process was presented in Chapter 4. Details of sum and difference frequency operation were provided along with a set of design rules defining synthesiser performance in terms of the constituent chirp parameters. Expressions were derived for optimum hop duration ( $T_0/2$ ), maximum number of hops was ( $T_0B/2$ ) and maximum bandwidth ( $B$ ). Sum frequency operation was stated to provide the more useful output range for practical applications. The design and construction of a prototype synthesiser were described in Section 4.2 and 4.3 respectively. A two channel configuration was employed to produce a continuous sum frequency output of either FH or CW form. Available chirp filters were used with centre frequency 60 MHz, bandwidth 25 MHz and time dispersion 5  $\mu$ s. FH performance under PN code control demonstrated a contiguous frequency spectrum containing 63 hops of 2.5  $\mu$ s duration in the range 107.5 to 132.5 MHz. CW operation was achieved by manual frequency selection, and performance at 122 MHz demonstrated a peak signal to spurious level of >30 dB. Phase coherence measurement between two prototype synthesisers operating in CW mode illustrated  $<2^\circ$  offset. Comparison of this prototype with a similar unit constructed in parallel illustrated a high degree of correlation in experimental results. From this experimental work, it was concluded that the synthesiser was capable of producing a continuous fast FH output, but that the CW performance would be unacceptable for most applications without additional filtering to reduce the high spurious signal level.

Chapter 5 presented a detailed analysis of the chirp mixing waveform and investigated potential sources of performance degradation in the synthesiser design. The major error mechanisms

identified were impulse timing offsets, chirp filter tolerances, interchannel phase or frequency imbalance, temperature effects and mixer spuri. The most critical of these were shown to be chirp slope mismatch, phase ripple and temperature drift. With these exceptions, careful system design and circuit layout can be used to minimise performance degradation.

To fully demonstrate the effects of individual error mechanisms, analysis of the CW synthesised output was performed. Fourier series analysis of the ideal chirp mixing waveform provided a basic understanding of the synthesis process, and demonstrated the importance of phase and frequency matching between channels. A graphical analysis of the process was presented as a shorthand method for predicting the amplitude spectra of synthesised waveforms. Quantitative results for the degradation associated with individual errors were obtained by computer simulation. Fourier series analysis was used to calculate amplitude, frequency and phase errors, and FFT analysis was used for chirp phase ripple and slope mismatch error assessment. From these results, it was shown that the level of SAW chirp filter reproducibility required to achieve -60 dBc spurious suppression was at least an order of magnitude better than currently available. This demonstrated the current limitations on synthesiser performance and suggested that future work should be directed towards techniques for providing high fidelity chirp waveforms

The effects of temperature variation on the synthesiser output were discussed in Section 5.4. An analysis of frequency errors in the generated waveform due to temperature drift of SAW chirp filters

was presented. It was shown that the output frequency does not vary with temperature, but that the amplitude and spurious signal levels do vary. Results were presented which quantify the increase in spurious signal level with temperature. This analysis implied that temperature compensation by master clock tuning was ineffective and that ovened SAW devices were required for high purity CW operation. In the case of FH operation, the frequency error due to temperature can be small in comparison to the hop bandwidth resulting in a small mismatch loss in the receiver.

The work presented in this thesis described the performance of a prototype SAW chirp mixing synthesiser and presented an analysis of the fundamental limitations associated with this technique. A number of areas remain which require further study and a certain amount of this work has been carried out in the period following completion of this work but prior to submission of this document. A summary of this work is described in the following paragraphs.

Darby<sup>134</sup> reported the performance of a similar equipment producing 127 hops with 2.5  $\mu$ s duration in the frequency range 335 to 385 MHz. He also presented an analysis of the performance bounds of FH links due to mismatch loss resulting from residual FM components in each hop. Results showed that a maximum chirp TB product of 3500 was possible for a 1 dB correlation loss based on replication accuracies of 2 parts in  $10^4$ . Subsequent work by Eustace, Bale and Darby<sup>140</sup> demonstrated the performance of a third prototype unit producing 480 hops with 5  $\mu$ s duration covering 96 MHz in two separate bands from 306 - 354 MHz and 356 - 404 MHz. This paper describes FH modem operation using binary FSK data and

employing a delay locked tracking loop in the receiver. High accuracy between synthesisers was measured in a back to back configuration, with errors of less than 20 kHz measured at spot frequencies.

Further details of this equipment were published by Darby and Hannah<sup>141</sup>. Preliminary bit error rate measurements were reported for FH modem operation including upconversion to a microwave carrier. From these results, it was estimated that the implementation loss due to the SAW synthesiser and correlator amount to 2 dB in total. Additional information is presented in this paper concerning the reduction of spurious signals in the CW mode by use of a narrow-band tracking filter. Experimental work carried out by Hannah and Reid<sup>85</sup> demonstrated the use of a phase locked loop to track the FH synthesiser output. Improvement of spurious suppression from -32 dBc to < -60 dBc was demonstrated using the synthesiser described in Chapter 4. The switching time of the loop for a full band (25 MHz) jump was shown to be 2 ms.

A number of areas concerning SAW chirp mixing synthesis still exist which could usefully be explored. For existing designs, hardware miniaturisation, and reduction of power consumption are important. Fuller investigation of spectral inversion techniques merit consideration in the search for optimally matched chirp waveforms. Due to the ultimate dependence of the equipment on chirp reproducibility, current work<sup>142,143</sup> on digitally generated chirp waveforms provides a technique for generating long, high accuracy chirp signals with the added advantage of programmability. This would need to be considered in light of digital "look-up" synthesis

techniques. Finally, a full characterisation of FH performance is required with consideration given to optimum hop rates, modulation techniques and minimisation of spectral spreading associated with individual hops.

This thesis has discussed a potentially attractive technique for fast FH waveform synthesis. It is hoped that in the future, SS systems designers can usefully employ this equipment to achieve effective communication under a variety of channel conditions.

## REFERENCES

1. Dixon, R C : Spread Spectrum Systems, John Wiley & Sons, New York, 1976, ISBN 0-471-21629-1.
2. AGARD Lecture Series No 58 on Spread Spectrum Communications, Technical Editing and Reproduction Ltd, Hartford House, 7-9 Charlotte Street, London, July 1973.
3. Gorski-Popiel, J (Ed) : Frequency Synthesis : Techniques and Applications, IEEE Press, 1975.
4. Morgan, D P (Ed) : Key Papers on Surface-Acoustic-Wave Passive Interdigital Devices, IEE Reprint Series 2, Peter Peregrinus Ltd, 1976, ISBN : 0901223 824.
5. Walther, F G, Budreau, A J, Carr, P H : "Multiple VHF frequency generation using acoustic surface-wave filters", Proc IEEE, Vol 61, pp 1162-1163, 1973.
6. Bale, R A, Maines, J D, Palmer, K J : "Frequency hopping using SAW oscillators", Proc IEEE Ultrasonics Symp, IEEE Cat No 75 CH0994-4SU, pp 248-250, 1975.
7. Atzeni, C, Manes, G, Masotti, L : "Programmable signal processing by analogue chirp-transformation using SAW devices", Proc IEEE Ultrasonics Symp, IEEE Cat No 75 CH0994-4SU, pp 371-376, 1975.
8. Stremier, F G : Introduction to Communications Systems, Addison-Wesley Publishing Company Inc, Phillipines, 1977, ISBN 0-201-07244-0.
9. Costas, J P : "Poisson, Shannon and the radio amateur", Proc IRE, No 47, pp 2058-2068, Dec 1959.
10. Shannon, C E : "Communication in the presence of noise", Proc IRE, Vol 37, pp 10-21, Jan 1959.
11. Harris, R L : "Introduction to spread spectrum techniques", AGARD Lecture Series No 58, Ref 3, July 1973.
12. Cahn, C R : "Spread spectrum applications and state of the art equipments", AGARD Lecture Series No 58, Ref 5, July 1973.
13. Cook, C E, Bernfeld, M : Radar Signals - An Introduction to Theory and Application, Academic Press, New York and London, 1967.
14. Golomb, S W (Ed) : Digital Communications with Space Applications, Prentice Hall, New Jersey, 1964.
15. Peterson, W W : Error Correcting Codes, MIT Press and John Wiley, 1961.

16. Gold, R : "Optimal binary sequences for spread spectrum multiplexing", IEEE Trans Inform Theory, Vol IT-13, pp 619-621, Oct 1967.
17. Craigie, J H et al : "The application of satellites to communications navigation and surveillance", TRW Report No 14671-60-R0-00, Dec 1970.
18. Schwartz, J W, Aein, J M, Kaiser, J : "Modulation technique for multiple access to a hard limiting satellite repeater", Proc IEEE, Vol 54, No 5, pp 763-777, May 1966.
19. Huth, G K : "Optimisation of coded spread spectrum system performance", IEEE Trans Commun, Vol COM-25, No 8, pp 763-770, Aug 1977.
20. Viterbi, A J : "On coded phase-coherent communications", IRE Trans Space Electron Telem, Vol SET-7, pp 3-14, March 1961.
21. Barker, R H : "Group synchronisation of binary digital systems" in Communications Theory, Butterworth, London, 1953.
22. Reed, I S, Solomon, G : "Polynomial codes over certain finite fields", Journal SIAM, 8, No 2, pp 300-304, June 1960.
23. IEEE Conference Proceedings No 63, SKYNET, 1970.
24. Sudworth, J P : "A simple NAVSTAR receiver", IEE Conference Proceedings 180, pp 85-89, September 1979.
25. Smith, W R : "SAW filters for CPSM spread spectrum communication" Proc IEEE Ultrasonics Symp, IEEE Cat No 77 CH1264-1SU, pp 524-528, 1977.
26. Mitchell, R F : "Surface acoustic wave devices and applications : 4. Bandpass filters", Ultrasonics, Vol 12, pp 29-35.
27. Turin, G L : "An introduction to matched filters", IRE Trans Inform Theory, Vol IT-6, pp 311-329, June 1960.
28. Stiglitz, I G : "Multiple access considerations", IEEE Trans Commun, Vol COM-21, No 5, pp 577-582, May 1973.
29. Bell, D T, Holmes, J D, Ridings, R V : "Application of acoustic surface-wave technology to spread spectrum communications", IEEE Trans Microwave Theory and Techniques, Vol MTT-21, pp 263-271, April 1973.
30. Grieco, D M : "The application of CCD's to spread spectrum systems", IEEE Trans Commun, Vol COM-28, No 9, pp 1693-1705, September 1980.
31. Hartmann, C S, Claiborne, L T, Buss, D D, Staple, E J : "Programmable transversal filters using surface waves, charge transfer devices and conventional digital approaches", IEE Conference Proceedings No 109, pp 102-114, September 1973.



32. Grant, P M : "Application of analogue signal processors to matched and adaptive filters for spread spectrum communications", in "Digital processing of signals in communications", IERE Conference Proceedings, 6-10 April 1981.
33. Davies, N G : "Performance and synchronisation considerations", AGARD Lecture Series No 58, Ref 4, July 1973.
34. Painter, J H : "Designing pseudorandom coded ranging systems", IEEE Trans Aerosp Electron Sys, Vol AES-3, pp 14-27, Jan 1967
35. Haggarty, R D, Key, E L, Kramer, J D R, Palo, E H : "Spread spectrum communications and signal processing requirements", IEE Conference Proceedings No 180, pp 76-84, September 1979.
36. Geraniotis, E A, Pursley, M H : "Performance analysis for fast frequency-hopped spread spectrum multiple-access communications", IEEE 1980 National Telecommun Conf, Houston, December 1980.
37. Johnson, G R : "Understanding low power spread spectrum radars", Electronic Warfare, pp 75-77, November 1978.
38. Heighway, J, Thompson, A : "SAW devices and their potential implication for novel radar systems design", IEE Conference Proceedings No 109, pp 212-221, September 1973.
39. Otto, J : "Chirping RPV-data links for ECM protection", Microwaves, pp 54-60, December 1974.
40. Whittman, J H : "Analysis of a hybrid frequency-time hopping random access satellite communication system", IEEE Int Conv Rec, pt 2, pp 61-68, March 1967.
41. Agardograph, No 245, Part 3, "JTIDS" Papers 25-40, July 1979.
42. Scholtz, R A : "Spread spectrum concept", IEEE Trans Commun, Vol COM-25, No 8, August 1977.
43. Didday, R L, Lindsey, W C : "Subcarrier tracking methods and communication system design", IEEE Trans on Communication Technology, Vol COM-16, pp 541-550, August 1968.
44. Lindsey, W C : Synchronisation Systems in Communications and Control, Prentice-Hall Inc, New Jersey, 1972.
45. Schrieber, H H : "Self-noise of frequency hopping signals", IEEE Trans Commun Technol, Vol COM-17, pp 588-590, October 1969.
46. Malm, R, Schreder, K : "Fast frequency hopping techniques", Proc Symp Spread Spectrum Commun, March 1973.
47. Ward, R B : "Digital communications on a pseudo-noise tracking link using sequence inversion modulation", IEEE Trans Commun Technol, Vol COM-15, pp 69-78, February 1967.

48. Sage, G F : "Serial synchronisation of pseudonoise systems", IEEE Trans on Commun Technol, Vol CS-12, No 4, p 123, December 1964.
49. Ward, R B : "Acquisition of pseudo noise signals by sequential estimation", IEEE Trans on Commun Technol, Vol COM-13, No 4, pp 475-483, December 1965.
50. Ward, R B, Yiu, K P : "Acquisition of pseudo noise signals by recursion-aided sequential estimation", IEEE Trans on Commun, Vol COM-25, No 8, pp 784-794, August 1977.
51. Hunsinger, B J, Franck, A R : "Programmable surface-wave tapped delay line", IEEE Trans Sonics Ultrasonics, Vol SU-18, pp 152-154.
52. Staples, E J, Claiborne, L T : "A review of device technology for programmable surface wave filters", IEEE Trans Microwave Theory Tech, Vol MTT-21, p 279, 1973.
53. Reeder, T M : "Electronically programmable convolution and correlation using nonlinear delay line filters", IEE Conference Publication No 109, pp 73-84, September 1973.
54. Kino, G S, Ludvik, S, Shaw, H J, Shrewe, W R, White, J M, Winslow, D K : "Signal processing by parametric interactions in delay line devices", IEEE Trans Microwave Theory Tech, Vol MTT-21, pp 244-255, 1973.
55. Tuan, H C, Grant, P M, Kino, G S : "The theory and application of ZnO on Si monolithic storage correlators", Proc IEEE Ultrasonics Symp, IEEE Cat No 78 CH1344-1SU, pp 38-43, 1978.
56. Morgan, D P, Hannah, J M, Collins, J H : "Spread spectrum synchroniser using a SAW convolver and recirculating loop", Proc IEEE, Vol 64, No 5, pp 751-754, May 1976.
57. Spilker, J J(Jr), Magill, D T : "The delay-lock discriminator - an optimum tracking device", Proc IRE, Vol 49, pp 1403-1416, September 1961.
58. Hartmann, H P : "Analysis of a dithering loop for PN code tracking", IEEE Trans Aeorsp Electron Syst, Vol AES-10, pp 2-9, January 1974.
59. Cahn, C R, Leimer, D K, Marsh, C L, Huntowski, F J, La Rue, C L : "Software implementation of a PN spread spectrum receiver to accommodate dynamics", IEEE Trans on Commun, Vol COM-25, No 8, pp 832-840, August 1977.
60. Pinches, M C, Munday, P J : "Jaguar V FH Radio", Proc IEE, Vol 129, Part F, No 3, June 1982 (to be published).
61. Pawula, R F : "Effects of quadratic AM-PM conversion in frequency division multiple-access communications satellite systems", IEEE Trans Commun Tech, Vol COM-19, No 3, pp 345-349, June 1971.

62. Mohanty, N C : "Spread spectrum and time division multiple access satellite communications", IEEE Trans Commun, Vol COM-25, No 8, pp 810-815, August 1977.
63. Huang, R Y, Hooten, P : "Communication satellite processing repeaters", Proc IEEE, Vol 59, pp 238-252, February 1971.
64. Drouilhet, P R (Jr), Bernstein, S L : "TATS - a bandspread modulation-demodulation system for multiple access tactical satellite communications", IEEE Electron Aerosp Syst Conv Rec, pp 126-132, October 1969.
65. Lebow, I L, Jordan, K L, Drouilhet, P R (Jr) : "Satellite communications to mobile platforms", Proc IEEE, Vol 59, No 2, pp 139-159, February 1971.
66. Dixon, R C : "A spread spectrum ranging technique for aerospace vehicles", 20th Annual South-Western IEEE Conf and Exhib Rec, April 1968, reprinted in Spread Spectrum Techniques, edited by R C Dixon, IEEE Press, New York, 1976.
67. McCalmont, A M : "Multiple access, discrete address communications systems", IEEE Spectrum, Vol 4, No 8, pp 87-94, August 1967.
68. Cooper, G R, Nettleton, R W : "A spread spectrum technique for high capacity mobile communications", Proc IEEE 27th Annual Vehicle Technology Conf, Orlando, 1977.
69. Eckert, R P, Kelly, P M : "Implementing spread spectrum technology in the land mobile radio services", IEEE Trans Commun, Vol COM-25, No 8, pp 867-869, August 1977.
70. Matthews, P A, Drury, D A : "Direct sequence spread spectrum system analysis for land mobile radio communication", IEE Conference Publication No 184, pp 187-191, 1980.
71. Shipton, M S, Ormondroyd, R F : "Improvements in use of congested spectrum for land mobile radio service by adoption of bandsharing spread spectrum systems with TV broadcast channels", IEE Proc, Vol 128, Part F, No 5, October 1981.
72. Fawcette, J : "Mystic link revealed", Microwave Syst News, Vol 7, No 9, pp 81-94, September 1977.
73. Van Duzer, W E : "A 0-50 MHz frequency synthesiser with excellent stability, fast switching and fine resolution", Hewlett-Packard Journal, Vol 15, pp 1-8, May 1964.
74. Tierney, J, Rader, C M, Gold, B : "A digital frequency synthesiser", IEEE Trans Audio Electroacoustics, Vol AU-19, pp 48-56, March 1971.
75. Noyes, A, Jr : "Coherent decade frequency synthesisers", The Experimenter, Vol 38, No 9, September 1964.

76. Meyer, D G : "An ultra-low noise direct frequency synthesiser", 24th Annual Frequency Control Symposium, April 1970.
77. Noordanus, J : "Frequency synthesisers - a survey of techniques", IEEE Trans Commun Technol, Vol COM-17, No 2, pp 257-271, April 1969.
78. Gardener, F M : Phaselock Techniques, John Wiley & Sons Inc, New York, 1966.
79. Lindsey, W C, Simon, M K : Telecommunication Systems Engineering, Prentice-Hall Inc, New Jersey, 1973.
80. Kroupa, V F : Frequency Synthesis, Charles Griffin & Co Ltd, 42 Drury Lane, London, 1973.
81. Nash, G : "Phase-locked loop design fundamentals", Application Note AN-535, Motorola Semiconductor Products Inc, pp 1-12, 1971.
82. Brubaker, R, Nash, G : "A new generation of integrated avionics synthesisers", Application Note AN-553, Motorola Semiconductor Products Inc, pp 1-10, 1971.
83. Delaune, J : "MTTL and MECL avionics digital frequency synthesisers", Application Note AN-532 A, Motorola Semiconductor Products Inc, pp 1-11, 1971.
84. Atkinson, P, Allen, A J : "Design of type-2 digital phase-locked loops", Radio and Electronic Engineer, Vol 45, No 11, pp 657-666, November 1975.
85. Hannah, J M, Reid, J R C : "Frequency hopper with improved performance", Wolfson Microelectronics Institute, King's Buildings, Edinburgh, Final Report on MOD Contract A72A/432/CBA72A, September 1979 (unpublished).
86. Stokes, V O : "Techniques for frequency synthesis", Proc IEE, Vol 120, No 10R, pp 1057-1077, October 1973, (IEE Reviews).
87. Guest, D H : "Simplified data-transmission channel measurements", Hewlett-Packard Journal, Vol 26, No 3, pp 15-24, November 1974.
88. Lord Rayleigh : "On waves propagated along the plane surface of an elastic solid", Proc London Math Soc, Vol 17, pp 4-11, 1885.
89. Smith, W R, Gerard, H M, Collins, J H, Reeder, T M and Shaw, H J : "Analysis of interdigital surface wave transducers by use of an equivalent circuit model", IEEE Trans Microwave Theory Tech, Vol MTT-17, No 11, pp 856-864, November 1969, and "Design of surface wave delay line with interdigital transducers", same Journal, pp 865-873, November 1969.
90. Marshall, F G, Newton, C O, Paige, E G S : "Surface acoustic wave multistrip components and their applications", IEEE Trans Microwave Theory Tech, Vol MTT-21, pp 216-225, April 1973.

91. Lewis, M F : "Triple transit suppression in surface-acoustic-wave devices", Electronics Letters, No 8, pp 553-554, October 1972.
92. Rosenfeld, R C, Brown, R B, Hartman, C S : "Unidirectional acoustic surface wave filters with 2 dB insertion loss", Proc IEEE Ultrasonics Symp, IEEE Cat No 74 CH0896-1SU, pp 425-428, 1974.
93. Mitchell, R F, Read, E : "Suppression of bulk wave radiation from surface acoustic wave devices", IEEE Trans Sonics Ultrasonics, Vol SU-22, pp 264-270, 1975.
94. Matthews, H (Ed) : Surface Wave Filters : Design, Construction and Use, John Wiley & Sons, New York, 1977, ISBN 0-471-58030-9.
95. Butler, M B N : "SAW devices for signal processing", IEE Conference Proceedings No 180, pp 21-33, September 1979.
96. Bristol, T W : "Analysis and design of surface acoustic wave transducers", IEE Conference Publication No 109, pp 115-129, September 1973.
97. Kallmann, H E : "Transversal Filters", Proc IRE, Vol 28, pp 302-310, July 1940.
98. Schulz, M B, Holland, M G : "Materials for surface acoustic wave components", IEE Conference Publication No 109, Peter Peregrinus Ltd, pp 1-10, September 1973.
99. Armstrong, G A, Butler, M B N : "Engineering design and evaluation of SAW pulse compression filters with low time sidelobes", Radio and Electronic Engineer, Vol 46, No 5, pp 221-228, May 1976.
100. Williamson, R C, Smith, H I : "Large time-bandwidth-product pulse compressor employing reflective gratings", Electronics Letters, No 8, pp 401-402, August 1972.
101. Martin, T A : "The IMCON pulse compression filter and its applications", IEEE Trans Sonics Ultrasonics, Vol SU-20, pp 104-112, April 1973.
102. Brewer, G R : "The application of electron/ion beam technology to microelectronics", IEEE Spectrum, Vol 8, pp 23-27, January 1971.
103. Maines, J D : "Applications of surface wave devices", IEE Conference Publications No 109, pp 191-201, September 1973.
104. De Vries, A J, Sreenivasan, T, Subramanian, S, Wojick, T J : "Detailed description of a commercial surface-wave TV IF filter", Proc IEEE Ultrasonics Symp, IEEE Cat No 74 CH0896-1SU, pp 147-152, 1974.

105. Harrington, J B, Nelson, R B : "Compressive intercept receiver uses SAW devices", Microwave Journal, pp 57-62, September 1974.
106. Millet, R E : "A matched-filter pulse-compression system using a nonlinear FM waveform", IEEE Trans Aerosp and Electron Syst, Vol AES-6, pp 73-78, Jan 1970.
107. Butler, M B N : "Radar applications of SAW dispersive filters", Proc IEEE, Vol 127, part F, No 2, pp 118-124, 1980.
108. Paige, E G S : "Dispersive filters : their design and application to pulse compression and temporal transformation", IEE Conference Publication No 109, pp 167-180, September 1973.
109. Jack, M A, Grant, P M, Collins, J H : "The theory, design, and applications of surface acoustic wave Fourier-transform processors", Proc IEEE, Vol 68, No 4, pp 450-468, April 1980.
110. Racal MESL Microwave Ltd, SAW Data Sheets 507 and 512, Lochend Industrial Estate, Newbridge, Scotland, 1979.
111. Jacobs, W W : "W1801 SAW analogue variable delay line", Racal MESL Microwave Publication, Case Study 5, 1979.
112. Golden, L A, Rosenburgh, R L : "SAW resonator filter overview : design and performance tradeoffs", Proc IEEE Ultrasonics Symp, IEEE Cat No 78 CH1344-1SU, pp 422-432, 1978.
113. Lewis, M F : "The design, performance and limitations of SAW oscillators", IEE Conference Publication No 109, Peter Peregrinus Ltd, pp 63-72, September 1973.
114. Robinson, M J, Butler, M B N : "13 bit Barker code correlator", Racal MESL Microwave Publication, Case Study 9, 1979.
115. Hickernell, F S, Kline, A J, Allen, D E, Brown, W C : "Surface elastic wave bandpass filters for frequency synthesis", IEEE Trans Microwave Theory Tech, MTT-21, pp 300-302, April 1973.
116. Hunsinger, B J, Burke, A G, Bush, H J, Richards, W L, Entzminger, J N : "Coherent FH/PN synthesiser using surface wave techniques", IEEE Trans Sonics Ultrasonics, Vol SU-21, No 4, pp 289-293, October 1974.
117. Budreau, A J, Carr, P H, Laker, K R : "Multiple channel UHF frequency synthesiser using acoustic surface-wave filters", Proc IEEE Ultrasonics Symp, IEEE Cat No 73 CH0807-8SU, pp 464-467, 1973.
118. Budreau, A J, Carr, P H, Laker, K R : "Frequency synthesiser using acoustic surface wave filters", Microwave Journal, 17, pp 65-66, and 68-69, March 1974.
119. Laker, K R, Budreau, A J, Carr, P H : "Interconnecting SAW filters for low loss frequency multiplexers and frequency synthesisers", Proc IEEE Ultrasonics Symp, IEEE Cat No 74 CH0896-1SU, pp 161-163, 1974.

120. Laker, K R, Budreau, A J, Carr, P H : "A circuit approach to SAW filterbanks for frequency synthesis", Proc IEEE, Vol 64, No 5, pp 692-695, May 1976.
121. Slobodnik, A J (Jr), Budreau, A J, Kearns, W J, Szabo, T L, Roberts, G A : "SAW filters for frequency synthesis applications", Proc IEEE Ultrasonics Symp, IEEE Cat No 76 CH1120-5SU, pp 432-435, 1976.
122. Budreau, A J, Carr, P H : "Direct SAW frequency synthesiser", Proc IEEE Ultrasonics Symp, IEEE Cat No 77 CH1264-1SU, pp 511-513, 1977.
123. Slobodnik, A (Jr), Roberts, G, Silva, J, Kearns, W, Sethares, J, Szabo, T : "UHF switchable SAW filterbanks", Proc IEEE Ultrasonics Symp, IEEE Cat No 78 CH1 344-1SU, pp 486-489, 1978.
124. Zaken, M B, Silberman, N, Kogan, E, Romik, P, Sofer, E : "A UHF fast frequency synthesiser using SAW filters", Proc IEEE Ultrasonics Symp, IEEE Cat No 80 CH1602-2, pp 230-234, 1980.
125. Browning, I, Lewis, M F : "Theory of multimoding in SAW oscillators", Proc IEEE Ultrasonics Symp, IEEE Cat No 76 CH1120-5SU, pp 256-259, 1976.
126. Browning, I, Crabb, J, Lewis, M F : "A SAW frequency synthesiser", Proc IEEE Ultrasonics Symp, IEEE Cat No CH0994-4SU, pp 345-247, 1975.
127. Young, J C T : "An L-band SAW discriminator stabilised oscillator", Racal MESL Microwave Publication, Case Study 7, 1979.
128. Gilden, M, Reeder, T M, DeMarcia, A J : "The mode-locked SAW oscillator", Proc IEEE Ultrasonics Symp, IEEE Cat No CH0994-4SU, pp 251-254, 1975.
129. Lee, L L, Hunsinger, B J, Cho, F Y : "A SAW stabilised pulse generator", IEEE Trans Sonics Ultrasonics, SU-22, pp 141-142, March 1975.
130. Adkins, L R : "Fast frequency hopping with surface acoustic wave (SAW) frequency synthesisers", Proc 30th Annual Symp on Frequency Control, US Army Electronics Command, Fort Monmouth, NJ, 1976.
131. Grant, P M, Morgan, D P, Collins, J H : "Generation and correlation of digitally controlled coherent frequency-hopped waveforms using surface acoustic wave devices", Proc IEEE, 64, pp 826-828, May 1976.
132. Hannah, J H, Grant, P M, Collins, J H : "Fast coherent frequency hopped waveform synthesis using SAW devices", Proc IEEE Ultrasonics Symp, IEEE Cat No 76 CH1120-5SU, October 1976.

133. Patterson, E W, Dods, A S M, Hannah, J M : "Frequency-hopped waveform synthesis by using SAW chirp filters", Electronics Letters, Vol 13, No 21, pp 633-635, 13 October 1977.
134. Darby, B J, Bale, R A, Eustace, C T, Hannah, J M, Patterson, E : "Performance of frequency hop synthesisers based on chirp mixing", Proc IEEE Ultrasonics Symp, IEEE Cat No 77 CH1264-1SU, pp 514-523, 1977.
135. Alsup, J M, Whitehouse, H J : "Frequency synthesis via the discrete chirp and prime sequence ROM's", Proc IEEE, Vol 64, No 5, pp 721-723, May 1976.
136. Manes, G, Grant, P : "Frequency-hopped-waveform synthesis with a surface-acoustic-wave tapped delay line", Electronics Letters, Vol 12, No 2, 22 January 1976.
137. Bracewell, R : The Fourier Transform and Its Applications, McGraw-Hill Book Company, New York, 1965.
138. Brigham, E O : The Fast Fourier Transform, Prentice-Hall Inc, New Jersey, 1974.
139. Connor, F R : Introducing Topics in Electronics and Telecommunications : Modulation, Edward Arnold Ltd, London, ISBN 07131 33031, 1973.
140. Eustace, C T, Bale, R A, Darby, B J : "An improved frequency hop modem based on chirp mixing", Proc IEEE Ultrasonics Symp, IEEE Cat No 78 CH1344-1SU, pp 553-556, 1978.
141. Darby, B J, Hannah, J M : "Programmable frequency hop synthesisers based on chirp mixing", IEEE Trans Microwave Theory Tech, Vol MTT-29, No 5, pp 456-463, May 1981.
142. Roy, R, Lowenschuss, O : "Chirp waveform generation using digital samples", IEEE Trans Aerosp Electron Syst, Vol AES-10, No 1, pp 10-16, January 1974.
143. Iglehart, S C : "Some results on digital chirp", IEEE Trans Aerosp Electron Syst, Vol AES-14, No 4, pp 118-127, January 1978.



APPENDIX 1 : RELEVANT PUBLICATION

Patterson, E W, Dods, A S M, Hannah, J M :  
"Frequency-hopped waveform synthesis by using  
SAW chirp filters", Electronics Letters, Vol 13,  
No 21, pp 633-635, 13 October 1977.

# FREQUENCY-HOPPED WAVEFORM SYNTHESIS BY USING S.A.W. CHIRP FILTERS

*Indexing terms: Frequency synthesis, Surface-acoustic-wave devices*

The design and construction of a surface-acoustic-wave (s.a.w.) pseudonoise (p.n.) code controlled frequency-hopping (f.h.) synthesiser for spread-spectrum (s.s.) communication is reported. The prototype synthesiser uses s.a.w. chirp filters with 60 MHz centre frequency, 5 MHz/ $\mu$ s dispersive slope and 25 MHz bandwidth, and operates in both continuous-wave and f.h. modes. Experimental results show an output centred on 120 MHz, electronically programmable over a 25 MHz bandwidth in 63 discrete hops.

**Introduction:** Wideband (10-500 MHz) synthesisers are employed in spread-spectrum communication transmitters to spread narrowband subscriber information into a common wideband communication channel.<sup>1</sup> Two spreading techniques, frequency hopping and phase-shift keying (p.s.k.), are employed, with p.s.k. systems at present predominating, owing to the technological difficulties in producing a fast-switching phase-coherent wideband f.h. synthesiser. However, the advent of surface-acoustic-wave technology has revived interest in f.h.-s.s. communication, and various approaches have been reported.<sup>2-6</sup>

This letter describes the design and construction of an f.h. synthesiser based on impulsing s.a.w. linear frequency-modulated (f.m.) 'chirp' filters. Results are presented which demonstrate this synthesiser operating in continuous-wave (c.w.) and f.h. modes.

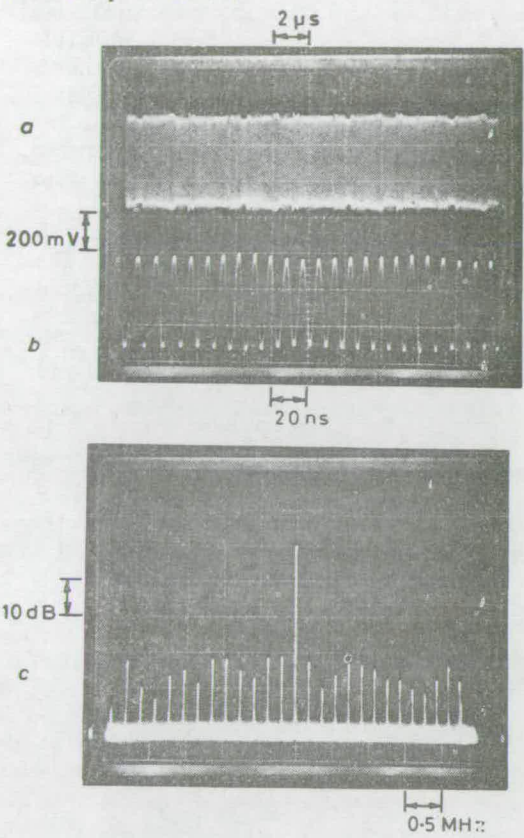
**Synthesiser principle:** The operation of this synthesiser relies on the 'mixing' of two linear f.m. waveforms of form  $\cos(\omega t + \frac{1}{2}\mu t^2)$ , where  $\omega$  represents the starting frequency and  $\mu$  the dispersive slope. The introduction of a time delay between the start of two such waveforms with parameters  $\omega_1, \mu$  and  $\omega_2, -\mu$  yields a sum-product after mixing of the form

$$\frac{1}{2} \cos \{(\omega_1 + \omega_2 + \mu\tau) t - \omega_2\tau - \frac{1}{2}\mu\tau^2\} \quad (1)$$

This is a pulse of frequency  $\omega_1 + \omega_2 + \mu\tau$  which exists for  $\tau \leq t \leq T$ , where  $T$  is the duration of the chirp waveforms. Other configurations are possible by using waveforms with different parameters, where the difference frequency<sup>5</sup> is selected.

Eqn. 1 shows that the synthesised frequency depends on  $\tau$ , which is the relative timing of the chirp waveforms. By varying  $\tau$ , pulses of minimum length  $T - |\tau_{max}|$  can be generated over

a frequency range of  $2\mu|\tau_{max}|$ . F.H. applications normally require orthogonal frequency spacing where the slot separation is the reciprocal of the pulse length. Thus the number of frequencies, which is given by  $2\mu|\tau_{max}|(T - |\tau_{max}|)$ , is maximised when  $|\tau_{max}| = \frac{1}{2}T$ . The bandwidth cover is  $\mu T$ , which is the chirp bandwidth.



centre frequency=122.85MHz 513/2

**Fig. 2** Sum-frequency synthesiser producing c.w. output  
a Time domain  
b Time domain expand  
c Frequency domain

In practice, the time-delayed chirp waveforms can be generated by impulsing s.a.w. chirp filters. When the impulse timing is derived from a stable master clock, the synthesised output frequencies will be phase coherent from hop to hop, and, by interlacing two channels, it is possible to produce a continuous output.

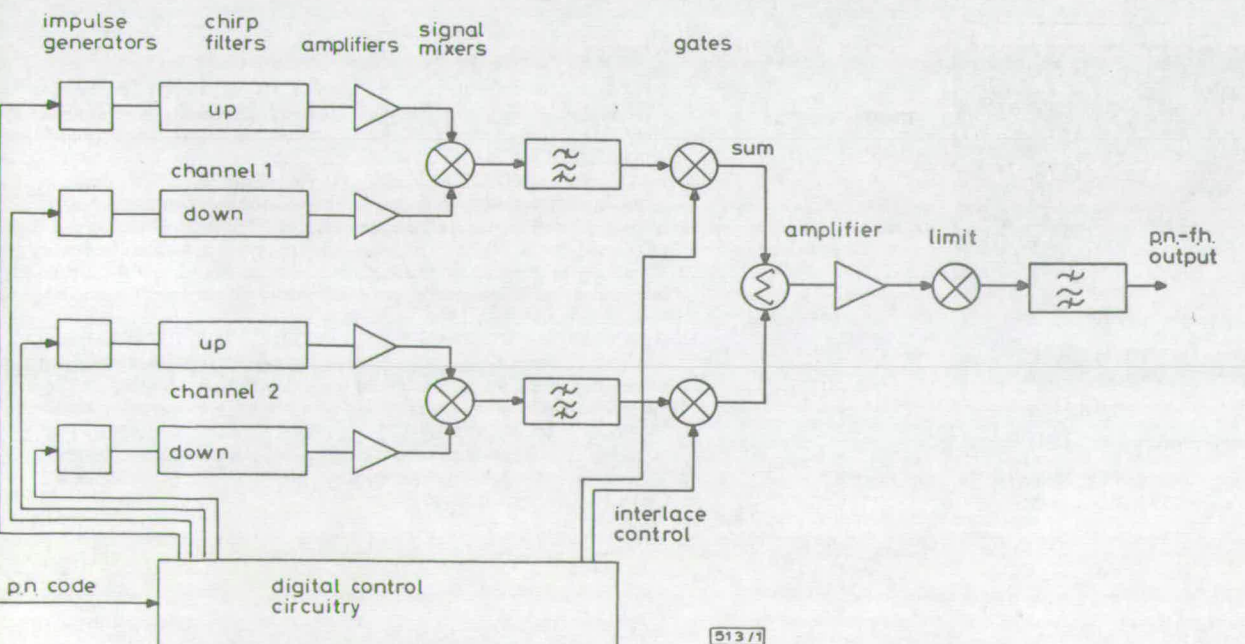


**Fig. 1** P.N.-F.H. (sum frequency) synthesiser employing s.a.w. chirp filters



**Synthesiser operation:** The synthesiser was designed around available double-dispersive s.a.w. chirp filters with 60 MHz centre frequency, 5 MHz/ $\mu$ s dispersive slope and 25 MHz bandwidth. This allowed generation of 63 hops,  $\sim$  400 kHz apart, centred on 120 MHz.

Fig. 1 illustrates a block diagram of our prototype synthesiser, which uses four chirp filters to produce two time-interlaced channels, giving a continuous output. A stable master clock drives separate programmable pulse generators in each channel. These generate pulse trains, with the required time delay  $\tau$ , which are then input to the impulse generators to produce accurately timed 40 V 8 ns-wide pulses. The chirp-filter outputs are amplified and drive a double balanced mixer which generates sum-and-difference products.

The sum product is selected in a bandpass filter with 120 MHz centre frequency and 35 MHz bandwidth. The generated frequency burst is gated in a second double balanced mixer operating as an r.f. switch, to give a fixed-duration output, irrespective of hop frequency. This output is subsequently summed with the second channel, amplified and

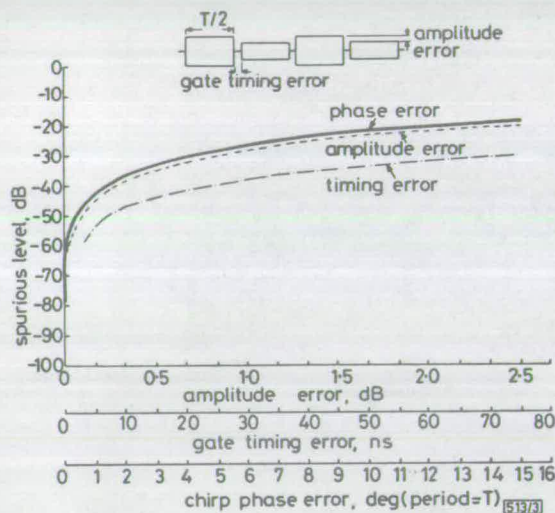


Fig. 3 Highest spurious for difference-frequency c.w. synthesis

Computer-simulation studies of the factors affecting spurious levels in generating c.w. signals have been carried out. Fig. 3 shows results which illustrate separately the effect of amplitude imbalance between channels, timing error in the gating circuits and chirp phase errors. Careful design should permit a spurious level of  $\sim$  40 dB to be achieved with available high-performance chirp-filter designs.

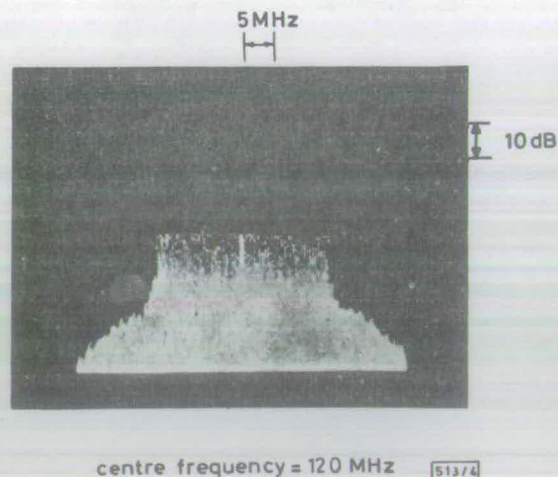


Fig. 4 Sum-frequency synthesiser operating in fast hopping mode, producing 63 hops over 26 MHz bandwidth

limited to remove amplitude ripple and imbalance between the two channels. Finally, the output is again bandpass filtered to remove any unwanted signals produced by the gating and limiting processes. The synthesised frequency is selected by a 6 bit digital input to the programmable pulse generators. This can be applied from manual switches or a p.n. code generator.

**Experimental results:** Fig. 2a illustrates the time-domain response for a c.w. output. The master-clock rate was 11.218 MHz, giving a hop duration of 2.81  $\mu$ s and a frequency spacing of 356.127 kHz. This is shown in expanded form in Fig. 2b. The eighth hop above the centre frequency of 120 MHz was selected, producing a frequency of 122.85 MHz, and the spectrum of this signal is shown in Fig. 2c. The spurious level is 30 dB down on the generated frequency. Measurement of the performance of the gating circuitry has indicated that this is currently limiting the spurious level attainable.

Fig. 4 illustrates the synthesiser operating in f.h. mode, producing 63 hops over a bandwidth of 26 MHz. Here, the absolute spurious level produced by one hop is not crucial, as the receiver hops in synchronism with the transmitter following an identical pattern of frequency hops. Interference protection in this case is provided by the crosscorrelation properties of the p.n. control code.

**Conclusions:** The coherent s.a.w.-f.h. synthesiser reported here offers rapid hopping with many hops over a wide bandwidth, all under the control of an external digital code. It offers high-speed switching without the complexity, size and cost penalties associated with conventional direct synthesisers. Compared to other s.a.w.-f.h. approaches, this system can produce a large number of hops over a wide bandwidth without multiplexing a number of individual synthesisers. With present s.a.w. chirp filters, synthesisers could be designed to produce 100s of hops over bandwidths up to 500 MHz. It therefore has potential applications in f.h. systems operating in the v.h.f./u.h.f. and low microwave range.

**Acknowledgments:** The authors thank B. J. Darby and P. M. Grant for helpful discussions. This work was supported by the Procurement Executive of the UK Ministry of Defence and the UK Science Research Council.

E. W. PATTERSON  
A. S. M. DODS  
J. M. HANNAH

8th September 1977

Department of Electrical Engineering  
University of Edinburgh  
King's Buildings, Mayfield Road, Edinburgh EH9 3JL, Scotland

## References

- 1 DIXON, R. C.: 'Spread spectrum systems' (Wiley, New York, 1976)
- 2 WALTHER, F. G., BUDREAU, A. J., and CARR, P. H.: 'Multiple UHF frequency generation using acoustic surface wave filters', *Proc. IEEE*, 1973, 61, pp. 1162-1163
- 3 BALE, R. A., MAINES, J. D., and PALMER, K. J.: 'Frequency hopping using SAW oscillators'. Proceedings of ultrasonics symposium, 1975 (IEEE catalogue 75 CH0994-SU), pp. 248-250
- 4 ADKINS, L. R.: 'Fast frequency hopping with surface acoustic wave (SAW) frequency synthesisers'. Proceedings of 30th annual symposium on frequency control, US Army Electronics Command, Fort Monmouth, NJ, 1976
- 5 GRANT, P. M., MORGAN, D. P., and COLLINS, J. H.: 'Generation and correlation of digitally controlled coherent frequency-hopped waveforms using surface acoustic wave devices', *Proc. IEEE*, 1976, 64, pp. 826-828
- 6 HANNAH, J. M., GRANT, P. M., and COLLINS, J. H.: 'Fast coherent frequency hopped waveform synthesis using SAW devices'. Ultrasonics symposium, Annapolis, 1976 (IEEE catalogue 76 CH1120-SSU), pp. 428-431



APPENDIX 2 : COMPUTER PROGRAM LISTING AND SAMPLE RESULT PRINT OUT  
(FOURIER SERIES SIMULATION)

A2.2            Main Program : Fourser  
                 Sample Print Out

```

C PROGRAM FOURSER.
C PROGRAM TO CALCULATE THE FOURIER COMPONENTS OF
C TWO TIME INTERLACED SQUAREWAVES, WHERE THE CONTENT OF
C EACH SQUAREWAVE BURST IS SINUSOIDAL SIGNAL WITH
C AMPLITUDEA1,A2;FREQUENCY F1,F2; PHASES P1,P2;
C AND HOP PERIOD T.
C THE OUTPUT IS FREQUENCY,AMPLITUDE AND
C PHASE DATA, WITH 15 POINTS IN EACH OF THREE ARRAYS.

```

```

IMPLICIT REAL*8(A-H,O-Z)
DIMENSION A(3,15),P(3,15),FREQ(15)
PI2 = 8.0*DATAN(1.0D00)
WRITE(6,1)
1 FORMAT(/1HX,'FOURIER SERIES PROGRAM'/1HX,
C/SPECIFY AMPLITUDES,PHASES,FREQUENCIES&HOP PERIOD./)
CALL FPRMPT('A1:',3)
READ*,A1
CALL FPRMPT('A2:',3)
READ*,A2
CALL FPRMPT('PH1:',4)
READ*,PH1
PH1 = PH1*PI2/360.
CALL FPRMPT('PH2:',4)
READ*,PH2
PH2 = PH2*PI2/360.
CALL FPRMPT('F1:',3)
READ*,W1
W1 = W1*PI2
CALL FPRMPT('F2:',3)
READ*,W2
W2 = W2*PI2
CALL FPRMPT('T-HOP:',6)
READ*,TH
W0 = PI2/TH
NC = INT(W1/W0)+1
N1 = NC-9
DO 2 I = 1,15
  WA = (W1-(N1+I)*W0)*TH/4.
  WB = (W2-(N1+I)*W0)*TH/4.
  IF(WA.EQ.0.) GOTO 7
  A(1,I) = A1/4.*(DSIN(WA)/WA)
  GOTO 8
7 A(1,I) = A1/4.
8 P(1,I) = WA+PH1
  X1 = A(1,I)*DCOS(P(1,I))
  Y1 = A(1,I)*DSIN(P(1,I))
  A(1,I) = DSQRT(X1*X1+Y1*Y1)
  P(1,I) = (P(1,I)/PI2-DINT(P(1,I)/PI2))*360
  IF(WB.EQ.0.) GOTO 9
  A(2,I) = A2/4.*(DSIN(WB)/WB)
  GOTO 10
9 A(2,I) = A2/4.
10 P(2,I) = WB-(N1+I)*PI2/2.+PH2
  X2 = A(2,I)*DCOS(P(2,I))
  Y2 = A(2,I)*DSIN(P(2,I))
  A(2,I) = DSQRT(X2*X2+Y2*Y2)
  P(2,I) = (P(2,I)/PI2-DINT(P(2,I)/PI2))*360
  AX = X1+X2
  AY = Y1+Y2
  A(3,I) = DSQRT(AX*AX+AY*AY)
  P(3,I) = DATAN(AY/(AX+0.1D-20))
  P(1,I) = P(1,I)*360./PI2
  P(2,I) = P(2,I)*360./PI2
  P(3,I) = P(3,I)*360./PI2
2 CONTINUE
DO 13 I = 1,15
DO 14 J = 1,3
  IF(P(J,I).GT.180.0) P(J,I) = -(360.-P(J,I))
  IF(P(J,I).LT.0.00000) P(J,I) = 360+P(J,I)
  IF(P(J,I).GT.359.999) P(J,I) = 0.000
14 CONTINUE
13 CONTINUE
IF(A2.GT.A1) GOTO 4
AM = A1
GOTO 5
4 AM = A2
AM = 0.5
5 DO 3 I = 1,15
  FREQ(I) = (N1+I)*W0/PI2
  A(1,I) = 20.*DLOG10(2.*A(1,I)/AM+1.0D-50)
  IF(A(1,I).LT.-80.) A(1,I) = -80.
  A(2,I) = 20.*DLOG10(2.*A(2,I)/AM+1.0D-50)
  IF(A(2,I).LT.-80.) A(2,I) = -80.
  A(3,I) = 20.*DLOG10(2.*A(3,I)/AM+1.0D-50)
  IF(A(3,I).LT.-80.) A(3,I) = -80.
3 CONTINUE
CALL FPRMPT('IOP?:',5)
READ*,IOP
WRITE(IOP,6) ((FREQ(J),A(I,J),P(I,J),J=1,15),I=1,3)
6 FORMAT(D14.8,F13.4,F13.4)
END

```

Command:RUN(FOUR0)

FOURIER SERIES PROGRAM  
SPECIFY AMPLITUDES,PHASES,FREQUENCIES&HOP PERIOD.

A1:1.0  
A2:1.0  
PH1:1.0  
PH2:0.0  
F1:120.0D06  
F2:120.0D06  
T-HOP:5.0D-06  
IOP?:50

STOP

Command:LIST(INFO,.OUT)

0.11860000D 09	-26.8450	271.0000
0.11880000D 09	-80.0000	181.0000
0.11900000D 09	-23.9224	91.0000
0.11920000D 09	-80.0000	1.0000
0.11940000D 09	-19.4854	271.0000
0.11960000D 09	-80.0000	181.0000
0.11980000D 09	-9.9430	91.0000
0.12000000D 09	-6.0206	1.0000
0.12020000D 09	-9.9430	271.0000
0.12040000D 09	-80.0000	181.0000
0.12060000D 09	-19.4854	91.0000
0.12080000D 09	-80.0000	1.0000
0.12100000D 09	-23.9224	271.0000
0.12120000D 09	-80.0000	181.0000
0.12140000D 09	-26.8450	91.0000
0.11860000D 09	-26.8450	90.0000
0.11880000D 09	-80.0000	180.0000
0.11900000D 09	-23.9224	270.0000
0.11920000D 09	-80.0000	0.0000
0.11940000D 09	-19.4854	90.0000
0.11960000D 09	-80.0000	180.0000
0.11980000D 09	-9.9430	270.0000
0.12000000D 09	-6.0206	0.0000
0.12020000D 09	-9.9430	90.0000
0.12040000D 09	-80.0000	180.0000
0.12060000D 09	-19.4854	270.0000
0.12080000D 09	-80.0000	0.0000
0.12100000D 09	-23.9224	90.0000
0.12120000D 09	-80.0000	180.0000
0.12140000D 09	-26.8450	270.0000
0.11860000D 09	-62.0075	0.5000
0.11880000D 09	-80.0000	0.5000
0.11900000D 09	-59.0850	0.5000
0.11920000D 09	-80.0000	0.5000
0.11940000D 09	-54.6480	0.5000
0.11960000D 09	-80.0000	0.5000
0.11980000D 09	-45.1056	0.5000
0.12000000D 09	-0.0000	0.5000
0.12020000D 09	-45.1056	0.5000
0.12040000D 09	-80.0000	0.5000
0.12060000D 09	-54.6480	0.5000
0.12080000D 09	-80.0000	0.5000
0.12100000D 09	-59.0850	0.5000
0.12120000D 09	-80.0000	0.5000
0.12140000D 09	-62.0075	0.5000

Command:



APPENDIX 3 : COMPUTER PROGRAM LISTING AND SAMPLE PRINT OUT  
(DIFFERENCE FREQUENCY FFT SIMULATION)

A3.2            Main Program : D2 Prog  
                 Sample Print Out

A3.3            Data Creation Routine : Flow Diagram

A3.4            Data Creation Routine : DCRT  
                 Data Manipulation Routines : DMRTS

```

C      PROGRAM D2PROG
C      MAIN PROGRAM FOR COMPUTING FFT SIMULATION OF
C      DIFFERENCE FREQUENCY CHIRP MIXING SYNTHESIS.
C      DATA CREATION ROUTINE DFS PROVIDES THE WAVEFORM
C      REQUIRED. FFT DATA IS READ FROM FT09,KDATA.

```

```

      IMPLICIT REAL*8 (A-H,O-Z)
      REAL*4 X(4096),Y(4096)
      COMMON /BLK2/ FT
      DIMENSION XDAT(4096),XIDAT(4096),FREQ(4096)
      DIMENSION XDAT2(4096),XIDAT2(4096)
      DIMENSION FT(32768)
      DIMENSION NX(5),NA(5),NY(5)
      DATA NX,NA/' FREQUENCY (HZ) ', 'AMPLITUDE (DB)'/
      DATA NY/'PHASE (DEGREES)'/
      PI = 4.*DATAN(1.0D00)
      CALL EMASFC('DEFINE',6,'FT09,KDATA',10)
      READ(9,99) KP,KU,K
99  FORMAT(I5)
      CALL DFS(XDAT,XIDAT,FREQ,K)
      K0 = 2*K
      CALL DF0URT(XDAT,XIDAT,K,KU,K0,-1.0D00)
      CALL DSWITCH(XDAT,K)
      CALL DSWITCH(XIDAT,K)
      K1 = K/2+1
      K2 = K
      CALL DZOOM(XDAT,XIDAT,FREQ,K,K1,K2)
      K = K1
      CALL DXNP(XDAT,XIDAT,K)
      CALL DMAXAMP(XDAT,K,K3)
      Z = 2.*KU/2
      CALL DLOGAMP(XDAT,K,Z)
      Z = -60.0
      CALL DCUTOFF(XDAT,K,Z)
      K1 = 1
      K2 = K
      IF(K1.LT.0) K1 = 1
      IF(K2.GT.K) K2 = K
      CALL DZOOM(XDAT,XIDAT,FREQ,K,K1,K2)
      K = K1
      CALL DPRNT3(FREQ,XDAT,XIDAT,K,50)
      DO 1 I = 1,2048,256
      WRITE(51,100) FREQ(I),XDAT(I)
100  FORMAT(D16.9,F13.5)
1  CONTINUE
      IF(KP.LT.0) GOTO 11
      CALL SINGLE(FREQ,XDAT,X,Y,K)
      CALL EDPLT1(X,Y,K,K+2,1.,1.)
11  CONTINUE
      END

```

Command:RUN(D2PROG0)

FFT ANALYSIS OF ANALYTICAL CHIRP MIXING CW FREQUENCY SYNTHESIS

```

4096
0.200000000D 06
0.200000000D 06
0.126000000D 08
0.100000000D 01
0.100000000D 01
0.000000000D 00
0.000000000D 00
0.000000000D 00
0.000000000D 00
0.000000000D 00
0.000000000D 00
0.100000000D 01
0.800000000D 06
0.800000000D 06
0.800000000D 06
0.800000000D 06
0.500000000D 13
0.500000000D 13
0.500000000D 13
0.500000000D 13

```

STOP

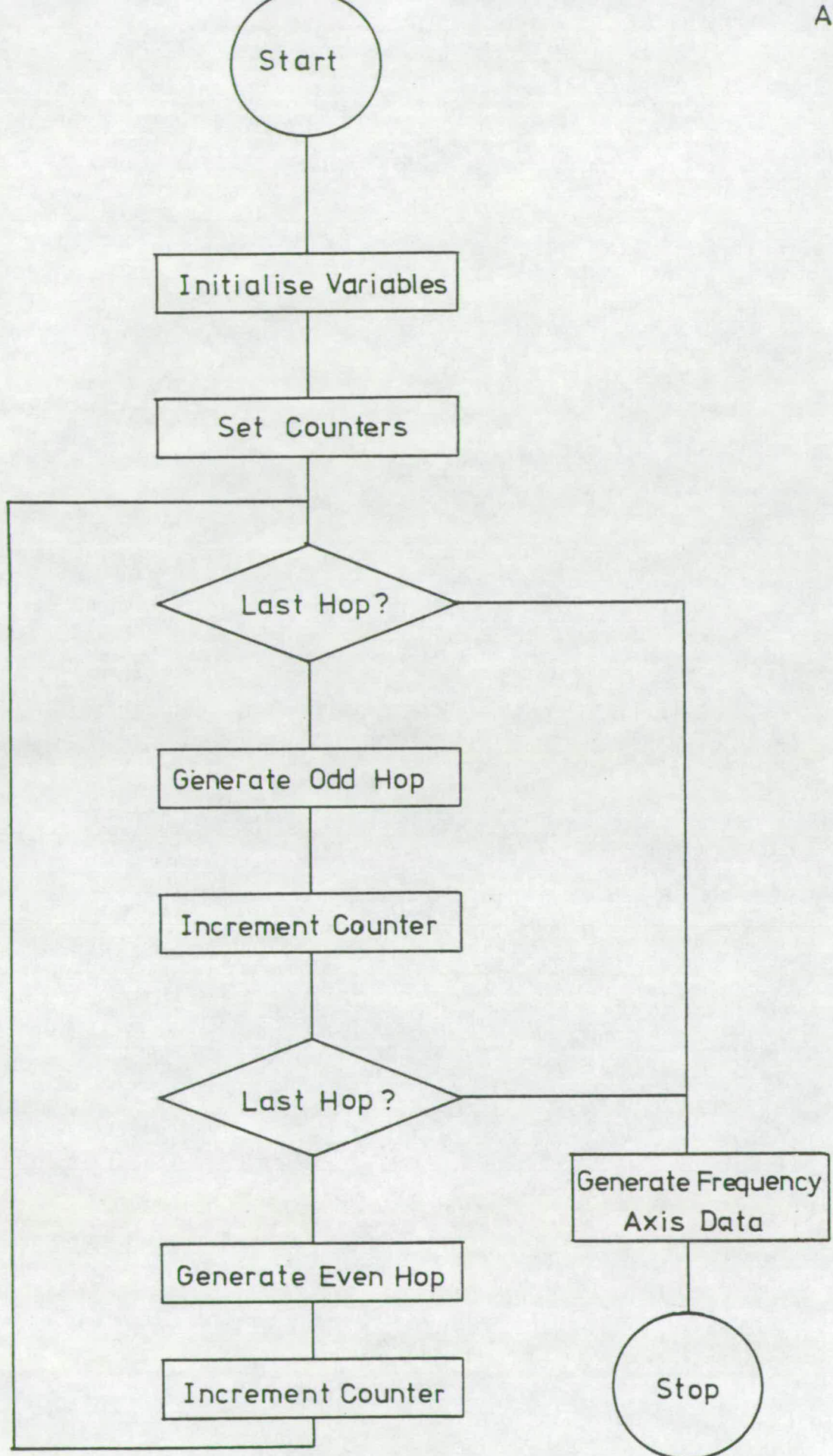
Command:LIST(INFO2,.OUT)

```

0.000000000D 00 -60.00000
0.200000000D 06 -52.46721
0.400000000D 06 -60.00000
0.600000000D 06 -44.85225
0.800000000D 06 -0.00033
0.100000000D 07 -44.91026
0.120000000D 07 -60.00000
0.140000000D 07 -52.60726

```





Data Creation Routine : Flow Diagram



```

C PROGRAM DCRT.
C PROGRAM DCRT CONTAINS ROUTINE DFS - DIFFERENCE
C FREQUENCY SIMULATION OF SAW CHIRP MIXING SYNTHESIS.
C THE DATA CREATED HAS 512 HOPS, 2.5 MICRO SEC IN
C DURATION, OPERATING AT AN IF FREQUENCY OF 800 KHZ.
C THE NUMBER OF FFT POINTS IS 4096, AND THE RESOLUTION
C IS 781.25 HZ.
C DATA IS READ IN FROM FT11, DATA1, AND IS READ OUT INTO
C FT50, INFO.

```

```

SUBROUTINE DFS(XREAL,XIMAG,XFREQ,N)
IMPLICIT REAL*8(A-H,O-Z)
DIMENSION XREAL(N),XIMAG(N),XFREQ(N)
PI = 4.0*ATAN(1.0)
CALL EMASFC('DEFINE',6,'FT11,DATA1',10)
CALL EMASFC('DEFINE',6,'FT50,INFO',F80',14)
READ(11,101) WA,WB,XF,A1,A2,XTAU1,XTAU2,PCNT,PCNT2,THETA1,THETA2,
CXU1,XU2,XU3,XU4,XU1,XU2,XU3,XU4
WRITE(6,102)
WRITE(6,201) N,WA,WB,XF,A1,A2,XTAU1,XTAU2,PCNT,PCNT2,THETA1,
CTHETA2,XU1,XU2,XU3,XU4,XU1,XU2,XU3,XU4
101 FORMAT(19(D16.9//))
102 FORMAT(///',',FFT ANALYSIS OF ANALYTICAL CHIRP MIXING ',
'C'CW FREQUENCY SYNTHESIS'///)
201 FORMAT(15/,19(D16.9//))
XW1 = XU1*2*PI
XW2 = XU2*2*PI
XW3 = XU3*2*PI
XW4 = XU4*2*PI
XU1 = XU1*2*PI
XU2 = XU2*2*PI
XU3 = XU3*2*PI
XU4 = XU4*2*PI
WA = 2.*PI*WA
WB = 2.*PI*WB
THETA1 = THETA1*2*PI/360
THETA2 = THETA2*2*PI/360
XTG = 2.5D-06
DT = XTG/8
WIF = 800000*2.0*PI
J = 0
L = 0
M = 1
90 IF (J.GE.N) GO TO 92
J = J+1
T = (L*DT)+XTAU1-(M-1)*XTG
XTHI1 = PCNT*2.0*PI/360*DSIN(WA*T)
XTHI2 = PCNT*2.0*PI/360*DSIN((WA*T)+PI)
XREAL(J) = A1*DCOS((XW1-XW2+WIF+XU2*XTAU1)*T+XW2*XTAU1-0.5*XU2
C*XTAU1*2+XTHI1-XTHI2+0.5*(XU1-XU2)*T+THETA1)
XIMAG(J) = 0
L = L+1
IF (L*DT.LT.M*XTG) GO TO 90
M = M+1
91 IF (J.GE.N) GO TO 92
J = J+1
T = (L*DT)+XTAU2-(M-1)*XTG
XTHI3 = PCNT2*2.0*PI/360*DSIN(WB*T)
XTHI4 = PCNT2*2.0*PI/360*DSIN((WB*T)+PI)
XREAL(J) = A2*DCOS((XW3-XW4+WIF+XU4*XTAU2)*T+XW4*XTAU2-0.5*XU4
C*XTAU2*2+XTHI3-XTHI4+0.5*(XU3-XU4)*T+THETA2)
XIMAG(J) = 0
L = L+1
IF (L*DT.LT.M*XTG) GO TO 91
M = M+1
IF (J.LT.N) GO TO 90
92 M = J+1
N = N/2
T = N*DT
T = 1/781.25
DO 452 J = 1,M
XFREQ(J) = -(M-J+1)/T
L = M+J
XFREQ(L) = (J-1)/T
452 CONTINUE
RETURN
END

```

```

C PROGRAM DMRTS.
C DMRTS CONTAINS A SET OF DATA MANIPULATION ROUTINES.
C THESE ARE USED FOR CONVERTING TO LOG AMPLITUDES, SELECTING
C THE LARGEST DATA POINT, AND ZOOMING IN ON SECTIONS OF THE
C GENERATED DATA. ROUTINES INCLUDE;
C DSWITCH; DXMP; DMAXAMP; DLOGAMP; DZOOM; &DCUTOFF.

```

```

SUBROUTINE DSWITCH(Z,N)
IMPLICIT REAL*8 (Z)
DIMENSION Z(N)
N2 = N/2
DO 26 J = 1,N2
Z1 = Z(J)
Z(J) = Z(N2+J)
Z(N2+J) = Z1
26 CONTINUE
RETURN
END

```

```

SUBROUTINE DXMP(XREAL,XIMAG,N)
IMPLICIT REAL*8 (A-H,O-Z)
DIMENSION XREAL(N),XIMAG(N)
PI = 4.0*ATAN(1.0D00)
DO 27 I = 1,N
A = XREAL(I)+0.1E-70
B = XIMAG(I)
XREAL(I) = DSQRT(A*A+B*B)
C = DATAN(B/A)/PI
XIMAG(I) = (C-IDINT(C))*180
27 CONTINUE
RETURN
END

```

```

SUBROUTINE DMAXAMP(XREAL,N,N1)
IMPLICIT REAL*8 (A-H,O-Z)
DIMENSION XREAL(N)
R = XREAL(1)
N1 = 1
DO 28 I = 2,N
IF (XREAL(I).GT.R) N1 = I
R = XREAL(N1)
28 CONTINUE
RETURN
END

```

```

SUBROUTINE DLOGAMP(XREAL,N,Z)
IMPLICIT REAL*8 (A-H,O-Z)
DIMENSION XREAL(N)
DO 100 I = 1,N
XREAL(I) = 20*DLOG10(XREAL(I)/Z+0.1E-70)
100 CONTINUE
RETURN
END

```

```

SUBROUTINE DZOOM(XREAL,XIMAG,XFREQ,N,N1,N2)
IMPLICIT REAL*8 (A-H,O-Z)
DIMENSION XREAL(N),XIMAG(N),XFREQ(N)
DO 310 J = N1,N2
L = (J+1-N1)
XREAL(L) = XREAL(J)
XIMAG(L) = XIMAG(J)
XFREQ(L) = XFREQ(J)
310 CONTINUE
N1 = N2-N1+1
RETURN
END

```

```

SUBROUTINE DCUTOFF(XREAL,N,XR)
IMPLICIT REAL*8 (A-H,O-Z)
DIMENSION XREAL(N)
DO 400 J = 1,N
IF (XREAL(J).LT.XR) XREAL(J) = XR
400 CONTINUE
RETURN
END

```

APPENDIX 4 : COMPUTER PROGRAM LISTING AND SAMPLE RESULT PRINT OUT  
(SUM FREQUENCY FFT SIMULATION)

A4.2            Main Program : D3 PROG  
                 Sample Print Out

A4.3            Data Creation Routine : SCRT  
                 (Data Manipulation Routines as per Appendix 3)



```

C PROGRAM D3PROG
C PROGRAM TO CARRY OUT SUM FREQUENCY FFT ANALYSIS OF
C SAW CHIRP MIXING FREQUENCY SYNTHESISER.
C FFT INFORMATION IS READ FROM FT09,KDATA.
C SIMULATION DATA IS READ FROM WITHIN THE DATA CREATION
C PROGRAM-SFS.
C THE FIRST TERM IN FT09,KP, IS +1 FOR GRAPHICAL OUTPUT,
C AND IS -1 FOR DATA OUTPUT ONLY. DATA IS OUTPUT TO FT50,INFO.

```

FFT ANALYSIS OF ANALYTICAL CHIRP MIXING CW FREQUENCY SYNTHESIS

DOUBLE PRECISION PROGRAM

```

IMPLICIT REAL*8 (A-H,O-Z)
REAL*4 X(16386),Y(16386)
COMMON /BLK2/ FT
DIMENSION XDAT(16386),XIDAT(16386),FREQ(16386)
DIMENSION FT(32768)
DIMENSION NX(5),NA(5),NY(5)
DATA NX,NA// FREQUENCY (HZ) ', 'AMPLITUDE (DB)'/
DATA NY// PHASE (DEGREES)'/
PI = 4.0*DATAN(1.0D00)
CALL ENASFC('DEFINE',6,'FT09,KDATA',10)
102 FORMAT('1///', 'FFT ANALYSIS OF ANALYTICAL CHIRP',
C MIXING CW FREQUENCY SYNTHESIS')
103 FORMAT('///', 'DOUBLE PRECISION PROGRAM'//)
WRITE(6,102)
WRITE(6,103)
READ(9,99) KP,KU,K
99 FORMAT(I5)
CALL SFS(FREQ,K)
CALL DFCOOL(KU,-1.0D00)
DO 10 I = 1,K
XDAT(I) = FT(2*I-1)
XIDAT(I) = FT(2*I)
10 CONTINUE
CALL DSWITCH(XDAT,K)
CALL DSWITCH(XIDAT,K)
K1 = K/2+1
K2 = K
CALL DZOOM(XDAT,XIDAT,FREQ,K,K1,K2)
K = K1
CALL DXMP(XDAT,XIDAT,K)
CALL DMAXAMP(XDAT,K,K3)
Z = 2*KU/2
CALL DLOGAMP(XDAT,K,Z)
Z = -80.0
CALL DCUTOFF(XDAT,K,Z)
K1 = K3-15
K2 = K3+15
CALL DZOOM(XDAT,XIDAT,FREQ,K,K1,K2)
K = K1
CALL DPRNT2(FREQ,XDAT,K,50)
IF(KP.LT.0) GOTO 11
CALL FPRMPT('PLT O/P: ',9)
READ*,IPLT
CALL PLTPRT(FREQ,XDAT,K,IPLT)
11 CONTINUE
END

```

```

FFT POINTS : 16384
CLOCK FREQUENCY : 0.126000000D 08
PHASE RIPPLE FREQUENCY 1: 0.200000000D 06
2: 0.200000000D 06
AMPLITUDE 1 : 0.100000000D 01
2 : 0.100000000D 01
TIME DELAY 1 : 0.000000000D 00
2 : 0.000000000D 00
PHASE RIPPLE AMP. 1 : 0.000000000D 00
2 : 0.000000000D 00
PHASE OFFSET 1 : 0.000000000D 00
2 : 0.100000000D 01
START FREQUENCY 1 : 0.475000000D 08
2 : 0.725000000D 08
3 : 0.475000000D 08
4 : 0.725000000D 08
CHIRP SLOPE 1 : 0.500000000D 13
2 : -0.500000000D 13
3 : 0.500000000D 13
4 : -0.500000000D 13

```

FREQUENCY	AMPLITUDE
117.00000D 06	-68.51961
117.20000D 06	-80.00000
117.40000D 06	-67.29111
117.60000D 06	-80.00000
117.80000D 06	-65.85452
118.00000D 06	-80.00000
118.20000D 06	-64.12592
118.40000D 06	-80.00000
118.60000D 06	-61.95740
118.80000D 06	-80.00000
119.00000D 06	-59.04919
119.20000D 06	-80.00000
119.40000D 06	-54.62654
119.60000D 06	-80.00000
119.80000D 06	-45.09842
120.00000D 06	-0.00033
120.20000D 06	-45.11270
120.40000D 06	-80.00000
120.60000D 06	-54.66937
120.80000D 06	-80.00000
121.00000D 06	-59.12057
121.20000D 06	-80.00000
121.40000D 06	-62.05734
121.60000D 06	-80.00000
121.80000D 06	-64.25440
122.00000D 06	-80.00000
122.20000D 06	-66.01156
122.40000D 06	-80.00000
122.60000D 06	-67.47670
122.80000D 06	-80.00000
123.00000D 06	-68.73376



```

C   PROGRAM SCRT
C   PROGRAM CONTAINS ROUTINE SFS - SUM
C   FREQUENCY SIMULATION DATA CREATION.
C   DATA IS READ IN FROM FT11,DATA1,
C   AND IS OUTPUT TO FT50,INFO ALONG WITH
C   TITLE INFORMATION.
C   THE ROUTINE CREATES TWO HOPS REPRESENTING
C   EACH CHANNEL IN THE SYNTHESIZER. ERRORS OF
C   AMPLITUDE,FREQUENCY,PHASE,PHASE RIPPLE, AND
C   DISPERSIVE SLOPE CAN BE INTRODUCED.

```

```

SUBROUTINE SFS(FREQ,N)
IMPLICIT REAL*8 (A-H,O-Z)
COMMON /BLK2/ FT
DIMENSION FT(32770)
DIMENSION FREQ(N)
PI = 4.0*DATAN(1.0D00)
CALL EMASFC('DEFINE',6,'FT11,DATA1',10)
CALL EMASFC('DEFINE',6,'FT50,INFO,,F80',14)
READ(11,101) WA,WB,XF,A1,A2,XTAU1,XTAU2,PCNT,PCNT2,THETA1,THETA2,
CXW1,XW2,XW3,XW4,XU1,XU2,XU3,XU4
C   CALL FPRMPT('KNOCK OUT: ',11)
C   READ*,KNO
C   WRITE(50,102)
C   WRITE(50,103)
101 FORMAT(D16.9)
102 FORMAT('FFT ANALYSIS OF ANALYTICAL CHIRP MIXING CW ',
C'FREQUENCY SYNTHESIS')
103 FORMAT(' ', 'DOUBLE PRECISION PROGRAM' ///)
201 FORMAT(I5)
300 FORMAT('FFT POINTS : ',I5)
301 FORMAT('CLOCK FREQUENCY : ',D16.9)
302 FORMAT('PHASE RIPPLE FREQUENCY 1: ',D16.9)
303 FORMAT(' ',D16.9)
304 FORMAT('AMPLITUDE 1 : ',D16.9)
305 FORMAT(' ',D16.9)
306 FORMAT('TIME DELAY 1 : ',D16.9)
307 FORMAT(' ',D16.9)
308 FORMAT('PHASE RIPPLE AMP. 1 : ',D16.9)
309 FORMAT(' ',D16.9)
310 FORMAT('PHASE OFFSET 1 : ',D16.9)
311 FORMAT(' ',D16.9)
312 FORMAT('START FREQUENCY 1 : ',D16.9)
313 FORMAT(' ',D16.9)
314 FORMAT(' ',D16.9)
315 FORMAT(' ',D16.9)
316 FORMAT('CHIRP SLOPE 1 : ',D16.9)
317 FORMAT(' ',D16.9)
318 FORMAT(' ',D16.9)
319 FORMAT(' ',D16.9)
320 FORMAT(' ',D16.9)
C 321 FORMAT('ZERO SAMPLES IN HOP 1 : ',I5)
WRITE(50,300) N
WRITE(50,301) XF
WRITE(50,302) WA
WRITE(50,303) WB
WRITE(50,304) A1
WRITE(50,305) A2
WRITE(50,306) XTAU1
WRITE(50,307) XTAU2
WRITE(50,308) PCNT
WRITE(50,309) PCNT2
WRITE(50,310) THETA1
WRITE(50,311) THETA2
WRITE(50,312) XW1
WRITE(50,313) XW2
WRITE(50,314) XW3
WRITE(50,315) XW4
WRITE(50,316) XU1
WRITE(50,317) XU2
WRITE(50,318) XU3
WRITE(50,319) XU4
C   WRITE(50,321) KNO
C   WRITE(50,320)
XW1 = XW1*2*PI
XW2 = XW2*2*PI
XW3 = XW3*2*PI
XW4 = XW4*2*PI
XU1 = XU1*2*PI
XU2 = XU2*2*PI
XU3 = XU3*2*PI
XU4 = XU4*2*PI
WA = 2.*PI*WA
WB = 2.*PI*WB
THETA1 = THETA1*2*PI/360
THETA2 = THETA2*2*PI/360
DT = 63/(XF*N)
N2 = N/2
DO 10 I = 1,N2
T = (I-1)*DT
XTHI1 = 2.0*PCNT*2.0*PI/360*DSIN(WA*T)
FT(2*I-1) = A1*DCOS((XW1+XW2-XU2*XTAU1)*T-XW2*XTAU1+0.5*XU2*XTAU1
C**2+XTHI1+0.5*(XU1+XU2)*T+THETA1)
FT(2*I) = 0.0D00
J = I+N2
XTHI3 = 2.0*PCNT2*2.0*PI/360*DSIN(WB*T)
FT(2*J-1) = A2*DCOS((XW3+XW4-XU4*XTAU2)*T-XW4*XTAU2+0.5*XU4*XTAU2
C**2+XTHI3+0.5*(XU3+XU4)*T+THETA2)
FT(2*J) = 0.0D00
10 CONTINUE
M = N/2
MI = (M-KNO)+1
DO 12 I = MI,M
C   FT(2*I-1) = 0.0D00
C 12 CONTINUE
T = N*DT
DO 11 I = 1,M
FREQ(I) = -(M-I+1)/T
L = M+I
FREQ(L) = (I-1)/T
11 CONTINUE
RETURN
END

```

APPENDIX 5 : COMPUTER PROGRAM LISTING AND SAMPLE PRINT OUT  
(INTERACTIVE SUM FREQUENCY FFT SIMULATION)

A5.2            Main Program : Interact

A5.4            Data Creation Routine : DTS  
(Data Manipulation Routines as per Appendix 3)

A5.5            Sample Print Out



```

C
C INTERACTIVE PROGRAM FOR ANALYSING THE SPECTRAL OUTPUT
C OF A CW FH CHIRP MIXING FREQUENCY SYNTHESISER
C

IMPLICIT REAL*8 (A-H,O-Z)
COMMON /BLK1/ FC,A1,A2,A3,A4,U1,U2,U3,U4,U1,U2,U3,U4,TAU1,TAU2,
CTAU3,TAU4,THI1,THI2,THI3,THI4,KU,K
COMMON /BLK2/ FT
DATA IN/'NO '/
DATA IY/'YES '/
DIMENSION FT(32770)
DIMENSION NX(5),NA(5),NY(5)
DATA NX,NA/' FREQUENCY (HZ) ','AMPLITUDE (DB)'/
DATA NY/'PHASE (DEGREES)'/
PI = 4.*ATAN(1.0D00)
CALL EMASFC('DEFINE',6,'FT13,DATA3',10)
CALL EMASFC('DEFINE',6,'FIS0,INFO,F00',9)
IEXEC = 1

C
C TITLE PRINTOUT
C
WRITE(6,230)
230 FORMAT('/// ','70('*')/' ','70('*')/' ','8('*')/' SURFACE ACOUSTI',
C'C WAVE CHIRP MIXING FREQUENCY SYNTHESIS ','6('*')/' ','8('*')/' CO',
C'MPUTER SIMULATION OF SUM FREQUENCY SYNTHESIS '8(' ')',6('*')/'
C' ','70('*')/' ','70('*')/'//)

C
C EXPLANATORY INFORMATION IS AVAILABLE IF REQUIRED (REPLY YES OR NO)
C
WRITE(6,235)
235 FORMAT('/// ','IS EXPLANATORY INFORMATION REQUIRED? (YES OR NO)'/)
CALL FPRMPT('INFO:',5)
READ(5,210) IYN
IF(IYN.EQ.IN) GOTO 1

C
C EXPLANATORY INFORMATION
C
WRITE(6,231)
231 FORMAT('T7, 'SIMULATION IS BY DIRECT MULTIPLICATION',
C' OF THE CHIRP WAVEFORMS 'T7, 'FOLLOWED BY FOURIER TRANSFORMA',
C'TION OF THE RESULTANT DATA. 'T7, 'DATA CAN BE INPUT TO THE ',
C'PROGRAM FROM THE TELETYPE',
C'T7, 'OR BY SPECIFYING AN INPUT DATA STREAM. 'T7, '
C'THE VARIABLES REQUIRED IN THE INPUT DATA ARE: '//)
WRITE(6,232)
232 FORMAT('T25, 'K - THE NUMBER OF FFT POINTS, 'T25,
C'KU - WHERE KU=2**K, 'T25, 'KP - A GRAPH PLOTTER CONTROL CHARACTER'
C'T31, '(+1 FOR PLOT; -1 FOR NO PLOT), 'T25,
C'FC - THE SYSTEM MASTER CLOCK FREQUENCY, 'T25,
C'A1->A4 - THE CHIRP AMPLITUDES, 'T25,
C'F1->F4 - THE CHIRP START FREQUENCIES, 'T25,
C'U1->U4 - THE CHIRP DISPERSIVE SLOPES, 'T25,
C'TAU1->TAU4 - THE CHIRP DELAY TERMS, 'T25,
C'THI1->THI4 - THE CHIRP START PHASE OFFSETS. '//)
WRITE(6,234)
234 FORMAT('T7, 'REAL DATA IS IN DOUBLE PRECISION FORMAT:D16.9'/
CT7, 'INTEGER DATA IS IN I6 FORMAT. '//)
WRITE(6,233)
233 FORMAT('T7, 'THE NOMINAL DEFAULT INPUT DATA FILE IS DATA3: ST13.'
CT7, 'THE NOMINAL OUTPUT DATA FILE IS INFO: ST50. 'T7, '70('*')')

C
C THE DIFFERENT DATA INPUT OPTIONS FOLLOW
C
C THE OPTIONS ARE:1) INPUT THE NO OF FFT POINTS FROM THE TTY,
C THEN INPUT THE OTHER DATA FROM A DATA FILE
C 2) INPUT ALL THE DATA FROM THE DATA FILE
C 3) INPUT ALL THE DATA FROM THE TTY.
C
1 WRITE(6,250)
250 FORMAT('/// ','TELETYPE OR FULL DEFAULT FILE INPUT?',
C'(1 FOR TTY; 0 FOR ST:X)'/)
CALL FPRMPT('DATA TYPE:',10)
READ*,ID
IF(ID.EQ.0) GOTO 32

C
C INPUT FFT POINTS & PLOTTER INFO
C
WRITE(6,251)
251 FORMAT('/// ','FFT POINTS - 2**KU=K; KU=1->14'/)
CALL FPRMPT('KU:',3)
READ*,KU
K = 2**KU
WRITE(6,248)
248 FORMAT('/// ','GRAPH PLOTTER OUTPUT?(YES OR NO)'/)
CALL FPRMPT('GRAPH PLOT:',11)

```

```

① READ(5,210) IYN
210 FORMAT(A4)
IF(IYN.EQ.IY) GOTO 30
KP = -1
GOTO 31
30 KP = 1
31 CONTINUE

C
C CHOOSE WHERE REMAINING DATA COMES FROM (TTY OR FILE)
C
WRITE(6,249)
249 FORMAT('/// ','REMAINING DATA FROM TELETYPE OR DATA FILE?',
C'(1 FOR TTY, 0 FOR DATA FILE)'/)
CALL FPRMPT('DATA TYPE:',10)
READ*,ID2
IF(ID2.EQ.0) GOTO 32

C
C TTY INPUT SECTION
C
300 WRITE(6,252)
252 FORMAT('/// ','MASTER CLOCK FREQUENCY?'/)
CALL FPRMPT('FC:',3)
READ*,FC
IF(IEXEC.GT.1) GOTO 2
301 WRITE(6,253)
253 FORMAT('/// ','CHIRP AMPLITUDES? (1->4)'/)
CALL FPRMPT('A1:',3)
READ*,A1
CALL FPRMPT('A2:',3)
READ*,A2
CALL FPRMPT('A3:',3)
READ*,A3
CALL FPRMPT('A4:',3)
READ*,A4
IF(IEXEC.GT.1) GOTO 2
302 WRITE(6,254)
254 FORMAT('/// ','CHIRP START FREQUENCIES? (1->4)'/)
CALL FPRMPT('F1:',3)
READ*,F1
CALL FPRMPT('F2:',3)
READ*,F2
CALL FPRMPT('F3:',3)
READ*,F3
CALL FPRMPT('F4:',3)
READ*,F4
IF(IEXEC.GT.1) GOTO 3
303 WRITE(6,255)
255 FORMAT('/// ','CHIRP DISPERSIVE SLOPES? (1->4)'/)
CALL FPRMPT('U1:',3)
READ*,U1
CALL FPRMPT('U2:',3)
READ*,U2
CALL FPRMPT('U3:',3)
READ*,U3
CALL FPRMPT('U4:',3)
READ*,U4
IF(IEXEC.GT.1) GOTO 4
304 WRITE(6,256)
256 FORMAT('/// ','CHIRP TIME DELAYS? (1->4)'/)
CALL FPRMPT('TAU1:',5)
READ*,TAU1
CALL FPRMPT('TAU2:',5)
READ*,TAU2
CALL FPRMPT('TAU3:',5)
READ*,TAU3
CALL FPRMPT('TAU4:',5)
READ*,TAU4
IF(IEXEC.GT.1) GOTO 2
305 WRITE(6,257)
257 FORMAT('/// ','CHIRP PHASE OFFSETS? (1->4)'/)
CALL FPRMPT('THI1:',5)
READ*,THI1
CALL FPRMPT('THI2:',5)
READ*,THI2
CALL FPRMPT('THI3:',5)
READ*,THI3
CALL FPRMPT('THI4:',5)
READ*,THI4
IF(IEXEC.GT.1) GOTO 5
GOTO 35

C
C DEFINE INPUT STREAM & INPUT DATA FROM THEREFROM
C
32 WRITE(6,258)
258 FORMAT('/// ','NOMINAL DEFAULT INPUT STREAM IS 13'/)
CALL FPRMPT('I/P-STREAM:',11)
READ*,IIP
IF(ID2.EQ.0) GOTO 33
READ(IIP,99) KP,KU,K
99 FORMAT(I6)
GOTO 34

C
C DUMMY READ IN FOR OPTION 1
C
33 READ(IIP,99) ID1,ID2,ID3
34 READ(IIP,100) FC,A1,A2,A3,A4,F1,F2,F3,F4,U1,U2,U3,U4, ②

```



```

②→ CTAU1,TAU2,TAU3,TAU4,TH11,TH12,TH13,TH14
100 FORMAT(D16.9)
35 CONTINUE

C
C   DEFINE OUTPUT STREAM
C
WRITE(6,259)
259 FORMAT(' ', 'NOMINAL OUTPUT STREAM IS DATA FILE INFO-ST50')
CALL FPRMPT('0/P-STREAM:',11)
READ*,IOP

C
C   PRINT OUT INPUT DATA
C
WRITE(6,229)
229 FORMAT(' ')
CALL FPRMPT('PRINT OUT ? ',12)
READ(5,210) IYN
IF(IYN.EQ.1N) GOTO 7
WRITE(IOP,230)
WRITE(IOP,260) K
260 FORMAT(' ', 'NO. OF FFT POINTS = ',I6)
WRITE(IOP,261) FC
261 FORMAT(' ', 'MASTER CLOCK FREQUENCY = ',2PD16.9)
WRITE(IOP,262) A1,A2,A3,A4
262 FORMAT(' ', 'CHIRP AMPLITUDES A1->A4:',4(T29,1PD16.9))
WRITE(IOP,263) F1,F2,F3,F4
263 FORMAT(' ', 'CHIRP START FREQUENCIES F1->F4:',4(T36,2PD16.9))
WRITE(IOP,264) U1,U2,U3,U4
264 FORMAT(' ', 'CHIRP DISPERSIVE SLOPES U1->U4:',4(T36,1PD16.9))
WRITE(IOP,265) TAU1,TAU2,TAU3,TAU4
265 FORMAT(' ', 'CHIRP TIME DELAYS TAU1->TAU4:',4(T36,1PD16.9))
WRITE(IOP,266) TH11,TH12,TH13,TH14
266 FORMAT(' ', 'CHIRP PHASE OFFSETS TH11->TH14:',4(T36,1PD16.9))
7 CONTINUE
3 U1 = 2*PI*F1
U2 = 2*PI*F2
U3 = 2*PI*F3
U4 = 2*PI*F4
IF(IEEXEC.GT.1) GOTO 2
4 U1 = 2*PI*U1
U2 = 2*PI*U2
U3 = 2*PI*U3
U4 = 2*PI*U4
IF(IEEXEC.GT.1) GOTO 2
5 TH11 = TH11*2*PI/360
TH12 = TH12*2*PI/360
TH13 = TH13*2*PI/360
TH14 = TH14*2*PI/360

C
C   START PROGRAM COMPUTATION
C
IF(IEEXEC.EQ.1) GOTO 6
2 CALL FPRMPT('MORE DATA?:',11)
READ(5,210) IYN
IF(IYN.EQ.1N) GOTO 6
IEEXEC = IEEXEC-1
GOTO 278
6 CONTINUE
K = 2**KU
T = 63/FC
CALL DMLTCD

C
C   IS A LIMITING FUNCTION REQUIRED PRIOR TO THE FFT?
C
WRITE(6,280)
280 FORMAT(' ', 'IS LIMITING REQUIRED? (YES OR NO)')
CALL FPRMPT('LIMIT?:',7)
READ(5,210) IYN
IF(IYN.EQ.1N) GOTO 281
WRITE(6,282)
282 FORMAT(' ', 'WHAT LEVEL OF CLIPPING IS REQUIRED? (ALPHA:0->1)')
CALL FPRMPT('ALPHA?:',7)
READ*,ALPHA
CALL HLIMIT(K,ALPHA)
281 CONTINUE

C
C   IS A HAMMING WEIGHTING FUNCTION REQUIRED
C
K0 = 2*K
WRITE(6,400)
400 FORMAT(' ', 'IS HAMMING WEIGHTING REQUIRED? (YES OR NO)')
CALL FPRMPT('HAMM?:',6)
READ(5,210) IYN
IF(IYN.EQ.1N) GOTO 401
CALL HANN(K)
401 CALL DFCOOL(KU,-1.0D00)
FCOUNT = 1
K = K/2
CALL DXMP(K)
CALL DMAXAMP(K,K3)
CF = K3+FCOUNT-2
FREQ = CF/T
WRITE(6,283) FT(2*K3-1),FREQ

```

```

③→283 FORMAT(' ', 'MAX. OUTPUT OF',F10.2,' AT A ',
C'FREQUENCY OF',3PD13.2)
A5.3
C
Z = FT(2*K3-1)
Z = (2**KU)/4
CALL DLOGAMP(K,Z)
Z = -80.0
CALL DCUTOFF(K,Z)

C
C   CHOOSE BETWEEN A FULL OR PART PRINTOUT
C
WRITE(6,284)
284 FORMAT(' ', 'IS A FULL PRINTOUT REQUIRED? (YES OR NO)')
CALL FPRMPT('FULL PRINT?:',12)
READ(5,210) IYN
IF(IYN.EQ.1Y) GOTO 285
WRITE(6,286)
286 FORMAT(' ', 'NUMBER OF POINTS REQUIRED? (EACH SIDE OF CENTRE',
C'FREQUENCY)')
CALL FPRMPT('NO OF POINTS:',13)
READ*,KPTS
K1 = K3-KPTS
K2 = K3+KPTS
IF(K1.LE.0) K1=1
IF(K2.GE.K) K2=K
WRITE(6,287)
287 FORMAT(' ', 'INTERVAL BETWEEN POINTS?')
CALL FPRMPT('INT:',4)
READ*,KINT
290 DO 291 I = K1,K2,KINT
FREQ = (1+FCOUNT-2)/T
WRITE(IOP,288) FREQ,FT(2*I-1)
288 FORMAT(3PD16.5,8PF14.5)
291 CONTINUE
GOTO 289

C
285 CONTINUE
C
K1 = 1
K2 = K
KINT = 1
GOTO 290

C
289 CONTINUE
C
IF(IEEXEC.GT.1) GOTO 276
IF(KP.LT.0) GOTO 11
K1 = K+2
WRITE(6,270)
270 FORMAT(' ', 'IS PLOTTER INFO. REQUIRED (YES OR NO)')
CALL FPRMPT('INFO:',5)
READ(5,210) IYN
IF(IYN.EQ.1N) GOTO 40
WRITE(6,271)
271 FORMAT(' ', 'THERE ARE TWO PLOTTER FORMATS AVAILABLE',
C' 1) 1 SINGLE GRAPH ON A4 FORMAT',
C' 2) 6 IDENTICAL SETS OF AXES ON A3 FORMAT.')
WRITE(6,272)
272 FORMAT(' ', 'OPTION 1 REQUIRES CONLIB.CLCMPLIB TO BE CONNECTED,
CAND REQUIRES THE INPUT DATA IN ALTERNATE LOCATIONS OF ARRAY FT
C(I.E. X-AXIS AND Y-AXIS DATA).',
C'OPTION 2 REQUIRES CONLIB.GRAPHLIB TO BE CONNECTED,AND REQUIRES
CTWO',
C' ARRAYS WITH 6 SETS OF X AND Y DATA, WITH ALL THE X-DATA
C SEQUENTIALLY',
C' PLACED IN ONE ARRAY, AND ALL THE Y-DATA
C SIMILARLY IN ANOTHER.')
40 WRITE(6,273)
273 FORMAT(' ', 'WHICH OPTION IS REQUIRED? (1 OR 2)')
CALL FPRMPT('OPTION:',7)
READ*,OPT
IF(OPT.EQ.2) GOTO 41
42 CONTINUE
CALL EDPLT1(K1,1.,1.,T,CF)
GOTO 11
41 IE = 6 - IEEXEC
WRITE(6,274) IE
274 FORMAT(' ', 'YOU HAVE SELECTED PLOTTER OPTION 2!!',
C'THIS REQUIRES 6 RUNS OF THE BASIC PROGRAM PRESENTLY UNDER
CEXECUTION.',
C'AT PRESENT YOU REQUIRE',I2,' MORE RUNS
C BEFORE YOU CAN USE THE PLOTTING ',
C'ROUTINE!')
C'IF YOU WISH TO TERMINATE OR MAKE ANY DATA CHANGES BEFORE THE
C NEXT RUN,',
C' SELECT THE APPROPRIATE NUMBER FROM THE
CMENU.',
C'IF MORE THAN ONE DATA CHANGE IS REQUIRED, THE
C MENU WILL BE REPRINTED.',
C' AFTER EACH SUBSEQUENT RUN,
CTHE REMAINING RUNS REQUIRED WILL BE PRINTED, AND THE MENU
C AGAIN PRINTED.')
GOTO 276
278 WRITE(6,275)
275 FORMAT(' ', 'T7,0 - TERMINATE PROGRAM'
C' ,T7,1 - SELECT OPTION 1'
C' ,T7,2 - CHANGE FC'
C' ,T7,3 - CHANGE A1->A4'
C' ,T7,4 - CHANGE F1->F4'
C' ,T7,5 - CHANGE U1->U4'
C' ,T7,6 - CHANGE TAU1->TAU4'
C' ,T7,7 - CHANGE TH11->TH14')
CALL FPRMPT('SELECT:',7)
READ*,ISLECT

```



```

④→ IF(ISLECT.EQ.0) STOP
   IF(ISLECT.EQ.1) GOTO 42
   ISLECT = ISLECT-1
   IEXEC = IEXEC+1
   GOTO (300,301,302,303,304,305), ISLECT
276 CALL EMASFC('DBEYFILE',8,'CFILE,.NULL',11)
   IF(IEXEC.EQ.6) STOP
   IE = 6-IEXEC
   WRITE(6,277) IE
277 FORMAT('/// ', 'THE REMAINING NUMBER OF RUNS IS', I2, '.'/)
   GOTO 278
11 CONTINUE
   WRITE(6,229)
END

```

```

C PROGRAM DTS.
C PROGRAM DTS CONTAINS SUBROUTINE DMLTCD.
C THIS ROUTINE MULTIPLIES TWO CHIRP WAVEFORMS
C FOR USE IN INTERACTIVE FH-FFT SIMULATION
C PROGRAM 'INTERACT'.
C DATA IS INPUT VIA COMMON BLOCKS 1&2, WHICH
C ARE SPECIFIED IN THE MAIN PROGRAM.

```

```

SUBROUTINE DMLTCD
  IMPLICIT REAL*8 (A-H,O-Z)
  COMMON /BLK1/ FC,A1,A2,A3,A4,U1,U2,U3,U4,TAU1,TAU2,
  CTAU3,TAU4,THI1,THI2,THI3,THI4,KU,K
  COMMON /BLK2/ FT
  DIMENSION FT(32768)
  PI = 4.0*DATAN(1.0D00)
  WRITE(6,102)
  WRITE(6,103)
102 FORMAT('1/// ', 'FFT ANALYSIS OF TWO CHIRP ',
  C' WAVEFORMS MULTIPLIED TOGETHER')
103 FORMAT('/// ', 'DOUBLE PRECISION PROGRAM')

  T = 63/FC
  DT = T/K
  K2 = K/2

  DO 10 I = 1,K2
    TI = (I-1)*DT
    FT(2*I-1) = A1*DCOS(W1*(TI-TAU1)+0.5*U1*(TI-TAU1)**2+THI1)*
  CA2*DCOS(W2*(TI-TAU2)+0.5*U2*(TI-TAU2)**2+THI2)
    FT(2*I) = 0.
    J = K2+I
    TJ = (J-1)*DT
    FT(2*J-1) = A3*DCOS(W3*(TJ-TAU3)+0.5*U3*(TJ-TAU3)**2+THI3)*
  CA4*DCOS(W4*(TJ-TAU4)+0.5*U4*(TJ-TAU4)**2+THI4)
    FT(2*J) = 0.
10 CONTINUE
  RETURN
END

```



IS EXPLANATORY INFORMATION REQUIRED? (YES OR NO)

INFO: YES

SIMULATION IS BY DIRECT MULTIPLICATION OF THE CHIRP WAVEFORMS  
FOLLOWED BY FOURIER TRANSFORMATION OF THE RESULTANT DATA.

DATA CAN BE INPUT TO THE PROGRAM FROM THE TELETYPE  
OR BY SPECIFYING AN INPUT DATA STREAM.

THE VARIABLES REQUIRED IN THE INPUT DATA ARE:

K - THE NUMBER OF FFT POINTS,  
KU - WHERE  $KU=2**K$ ,  
KP - A GRAPH PLOTTER CONTROL CHARACTER  
(+1 FOR PLOT; -1 FOR NO PLOT),  
FC - THE SYSTEM MASTER CLOCK FREQUENCY,  
A1->A4 - THE CHIRP AMPLITUDES,  
F1->F4 - THE CHIRP START FREQUENCIES,  
U1->U4 - THE CHIRP DISPERSIVE SLOPES,  
TAU1->TAU4 - THE CHIRP DELAY TERMS,  
THI1->THI4 - THE CHIRP START PHASE OFFSETS.

REAL DATA IS IN DOUBLE PRECISION FORMAT: D16.9  
INTEGER DATA IS IN I6 FORMAT.

THE NOMINAL DEFAULT INPUT DATA FILE IS DATA3: ST13.  
THE NOMINAL OUTPUT DATA FILE IS INFO: ST50.

\*\*\*\*\*

TELETYPE OR FULL DEFAULT FILE INPUT? (1 FOR TTY; 0 FOR ST: X)

DATA TYPE: 1

FFT POINTS -  $2**KU=K; KU=1->14$

KU: 14

GRAPH PLOTTER OUTPUT? (YES OR NO)

GRAPH PLOT: NO

REMAINING DATA FROM TELETYPE OR DATA FILE? (1 FOR TTY, 0 FOR DATA FILE)

DATA TYPE: 0

NOMINAL DEFAULT INPUT STREAM IS 13

I/P-STREAM: 13

NOMINAL OUTPUT STREAM IS DATA FILE INFO-ST50

O/P-STREAM: 50

PRINT OUT ? YES

FFT ANALYSIS OF TWO CHIRP WAVEFORMS MULTIPLIED TOGETHER

DOUBLE PRECISION PROGRAM

IS LIMITING REQUIRED? (YES OR NO)

LIMIT?: NO

IS HANNING WEIGHTING REQUIRED? (YES OR NO)

HANN?: NO

MAX. OUTPUT OF 4095.00 AT A FREQUENCY OF 120.000 06

IS A FULL PRINTOUT REQUIRED? (YES OR NO)

FULL PRINT?:NO

NUMBER OF POINTS REQUIRED? (EACH SIDE OF CENTRE FREQUENCY!)

NO OF POINTS:15

INTERVAL BETWEEN POINTS?

INT:1

STOP

Command:LIST(INFO,.OUT)

```

*****
***** SURFACE ACOUSTIC WAVE CHIRP MIXING FREQUENCY SYNTHESIS *****
***** COMPUTER SIMULATION OF SUM FREQUENCY SYNTHESIS *****
*****

```

NO. OF FFT POINTS = 16384

MASTER CLOCK FREQUENCY = 12.60000000D #6

CHIRP AMPLITUDES A1->A4; 1.00000000D #0  
1.00000000D #0  
1.00000000D #0  
1.00000000D #0

CHIRP START FREQUENCIES F1->F4; 47.50000000D #6  
72.50000000D #6  
47.50000000D #6  
72.50000000D #6

CHIRP DISPERSIVE SLOPES U1->U4; 5.00000000D 12  
-5.00000000D 12  
5.00000000D 12  
-5.00000000D 12

CHIRP TIME DELAYS TAU1->TAU4; 0.00000000D #0  
0.00000000D #0  
2.50000000D-06  
2.50000000D-06

CHIRP PHASE OFFSETS TH1->TH4; 1.00000000D #0  
1.00000000D #0  
0.00000000D #0  
0.00000000D #0

117.00000D #6	-62.49896
117.20000D #6	-58.85975
117.40000D #6	-61.27050
117.60000D #6	-58.89204
117.80000D #6	-59.83397
118.00000D #6	-58.92420
118.20000D #6	-58.10542
118.40000D #6	-58.95623
118.60000D #6	-55.93695
118.80000D #6	-58.98813
119.00000D #6	-53.02879
119.20000D #6	-59.01990
119.40000D #6	-48.60620
119.60000D #6	-59.05155
119.80000D #6	-39.07812
120.00000D #6	-0.00042
120.20000D #6	-39.09245
120.40000D #6	-59.11446
120.60000D #6	-48.64918
120.80000D #6	-59.14574
121.00000D #6	-53.10043
121.20000D #6	-59.17689
121.40000D #6	-56.03725
121.60000D #6	-59.20792
121.80000D #6	-58.23437
122.00000D #6	-59.23883
122.20000D #6	-59.99158
122.40000D #6	-59.26963
122.60000D #6	-61.45677
122.80000D #6	-59.30030
123.00000D #6	-62.71389